# UNIVERSITY OF LONDON THESIS

Degree phil Year 2007 Name of Author SEBASTIAN FLEIRE

# Recognition of membrane ligands by lymphocytes

Sebastian Fleire

**University College London**





ProQuest LLC
789 East Eisenhower Parkway
P.O. Box 1346
Ann Arbor, MI 48106-1346

## Declaration

I, Sebastian Fleire, confirm that the work presented in this thesis is my own. Where information has been derived from other sources, I confirm that this has been indicated in the thesis.

## Abstract

Recognition of membrane-bound ligands is a fundamental event that determines the fate of lymphocytes during immune responses. Extensive studies have been performed in order to understand the recognition of soluble ligands, however very little is known of the parameters that determine the interaction of membrane-bound ligand/receptors. In my PhD thesis I have studied how lymphocytes interact with membrane-bound ligands.

I initially characterise how B cells recognise membrane-ligands by expressing GFP-tagged antigens on the surface of target cells. To further dissect this process, I have set-up a system of artificial lipid bilayers that allows a quantitative analysis. Fluorescently labelled antigen molecules of varying affinities are displayed at a range of densities on glass-supported bilayers. The interaction of transgenic B cells with them can then be followed by different microscopy techniques in real time.

I have described a dynamic cellular response in the early stages of the recognition process in which B cells spread and contract on the antigen bearing membranes to collect the bound molecules in a central cluster to later extract it. This response is triggered by signals delivered through the BCR and is an active process guided by actin polymerisation. The extent of the spreading response is dependent on both the antigen density and its affinity for the BCR and it determines the amount of antigen accumulated. I have also set-up a technique to analyse at the molecular level the differential dynamics of reorganisation of key co-receptor molecules involved in triggering B cell activation.

Finally, I extended the bilayers system to characterise the interaction of human NK T cells with a set of specific ligands of different affinities for the T cell receptor (TCR). I have determined the thresholds for the formation of the immunological synapse.

In summary, I have characterised the early events triggered upon membrane-antigen recognition and elucidated a novel mechanism by which B cells are able to gather antigen and therefore perform their biological function.

## Acknowledgements

I thank all the people that directly or indirectly helped me in many ways during the course of my studies that are many at Cancer Research UK. I want to thank particularly my supervisor, Facundo Batista, for all the opportunities that he gave me and still does, and all the people at the Lymphocyte Interaction Lab: Yoli, Anne, Kathy, Elo, Michele, Julia, Bebhinn and David. I enjoyed very much sharing my time with all of them. I want also to thank Caetano for being my second supervisor and pushing me to think harder on my research.

Last but not least, I want to thank my family and friends for their unconditional support in all my choices and decisions. And finally I want to dedicate this Thesis to two very important persons in my life: Maria and Violeta.

# TABLE OF CONTENTS

## Chapter 6: Recognition of lipidic antigens by natural killer T cells



## Chapter 7: Molecular events during B cell activation



## Chapter 8: Discussion

# List of Figures and Tables

## Figures

## Tables

# Chapter 1: Introduction

## Aims

Interactions between ligands and receptors are crucial events that determine the outcome of a large variety of processes in biology. In the immune system, the recognition of antigens by lymphocytes is a key event in the initiation of the immune response.

The main focus of this study is to understand the process of membrane antigen recognition by lymphocytes, particularly B cells and a subset of T cells: natural killer T cells (NK T cells).

In this Chapter, we will give an overview of basic lymphocyte biology and we will describe recent updates on membrane antigen/receptor interactions and how these determine the lymphocyte activation and function of lymphocytes.

## 1.1 Lymphocytes: key players of the adaptive immune response

The immune system consists of a complex network of specialised cells, organs and tissues that act in a coordinated fashion to defend the body against invading foreign pathogens. The adaptive immunity is the arm of the immune system that confers the remarkable capacity to respond to a large variety of antigens.

B and T lymphocytes are the main players of the adaptive immune response. They are able to respond to almost any antigen due to the expression of prototypical antigen receptors on their plasma membrane, the T cell receptor (TCR) and the B cell receptor (BCR), through which they sense antigens in their environment with a very high specificity (**Janeway, 2005**).

Therefore, understanding how lymphocytes recognise and respond to antigens is a fundamental issue in immunology.

Lymphocytes are continuously generated from the hematopoietic stem cells (HSC) that reside in the bone marrow niche. During the process of lymphopoiesis HSC give rise to immature T and B cells that develop into mature naïve T and B cells (see details in Figure 1.1) (**Janeway, 2005**). While development of B cells occurs in the bone marrow, the development of T cells takes place in the thymus (**Janeway, 2005**). At the end of this process, each lymphocyte will express on its cell surface a unique antigen receptor that confers its antigen specificity.

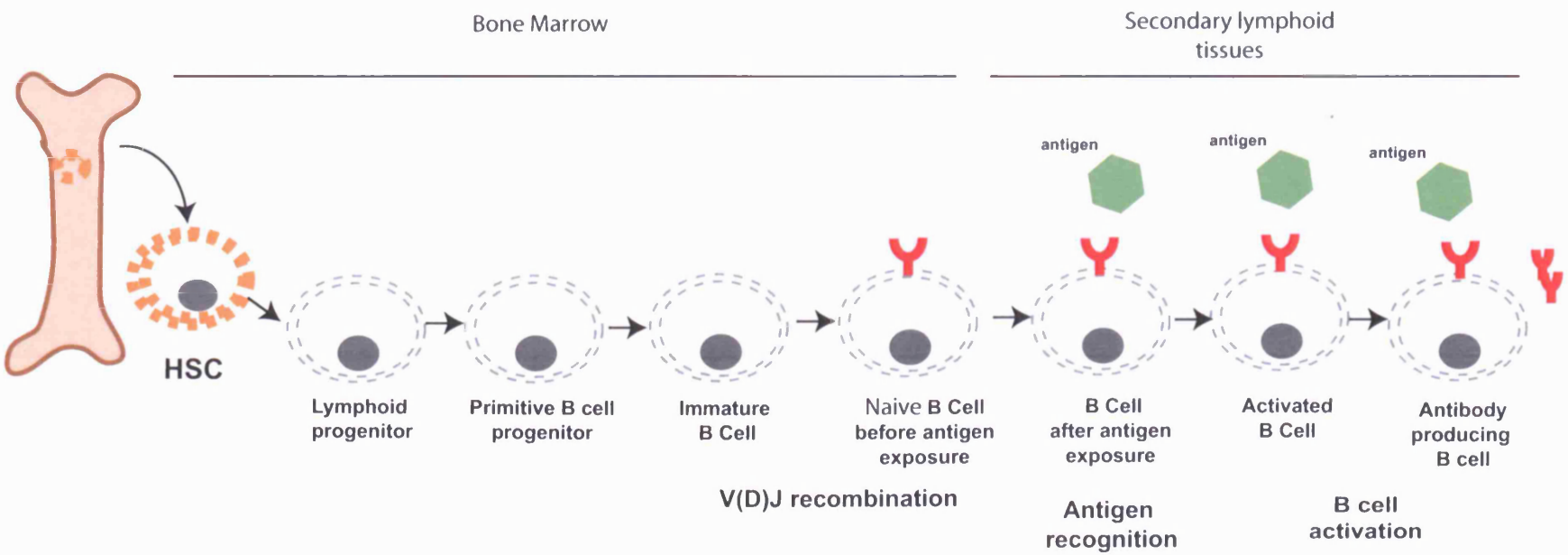


**Figure 1.1. B cell development and maturation.**
B cell development begins in the fetal liver and continues in the bone marrow throughout our lives. This diagram illustrates the main stages of B cell development. After several rounds of differentiation the hematopoietic stem cell (HSC) generates a B cell. Lymphoid progenitor cells receive signals from bone marrow stromal cells to begin B cell development. The cells undergo D-J joining on the H chain chromosome to become early pro-B cells and also begin expressing CD45 (B220) and Class II MHC. Joining of a V segment to the D-JH completes the late pro-B cell stage. At this stage a B cell can express both H and L chains on its membrane. However, it is still immature and can be easily killed by contact with self antigens until it also expressed membrane IgD. This is achieved after the Ig genes are rearranged in a process known as V(D)J recombination. The mature B cell that moves into the periphery can be activated by antigen and become an antibody-secreting plasma cell or a memory B cell which will respond more quickly to a second exposure to antigen. B cells which fail to successfully complete B cell development undergo apoptosis (Adapted from Immunobiology, 2005).

Antigen receptors consist of multi-protein complexes characterised by two distinct components: a variant antigen-binding component and an invariant signalling component (Figure 1.2) (Janeway, 2005). In the case of T cells the antigen-binding component is composed of two chains, being either alpha and beta, or gamma and delta (Figure 1.2 A). Whereas, the BCR consists of a membrane immunoglobulin, characterised by two heavy chains and two light chains (Figure 1.2 B) (Hombach et al., 1990). As a result of this structure, the BCR is a divalent receptor while the TCR is monovalent (Figure 1.2).

The invariant components perform the signalling function of the receptors. In the case of B cells, these are composed of two transmembrane proteins, the Igα and Igβ, which form a heterodimer that associates with the BCR (Schamel and Reth, 2000).

In the case of T cells, the CD3 invariant accessory chains form the signalling complex together with the ζ chain. The CD3 complex includes CD3γ, CD3ε and CD3δ (Janeway, 2005).

Signals through the antigen receptors are initiated by the phosphorylation of tyrosines included in a target amino acid sequence known as immunoreceptor tyrosine-based activation motifs (ITAMs) (Reth, 1989). These sequences are contained in the cytoplasmic domains of the invariant signalling components of the antigen receptors.

## 1.2 V(D)J recombination: a first round to generate antigen receptor diversity

The variant antigen-binding components of the TCR and BCR are generated by gene recombination during lymphocyte development. This coordinated process give rise to polyclonal populations of T and B cells, responsible of the characteristic diversity of the adaptive immune system (see details in Figure 1.1 and Figure 1.3).

The variable regions of the variant antigen-binding components of the TCR and BCR are known as complementary determining regions (CDRs) (Figure 1.3). The CDRs are generated through a complex genetic mechanism known as V(D)J

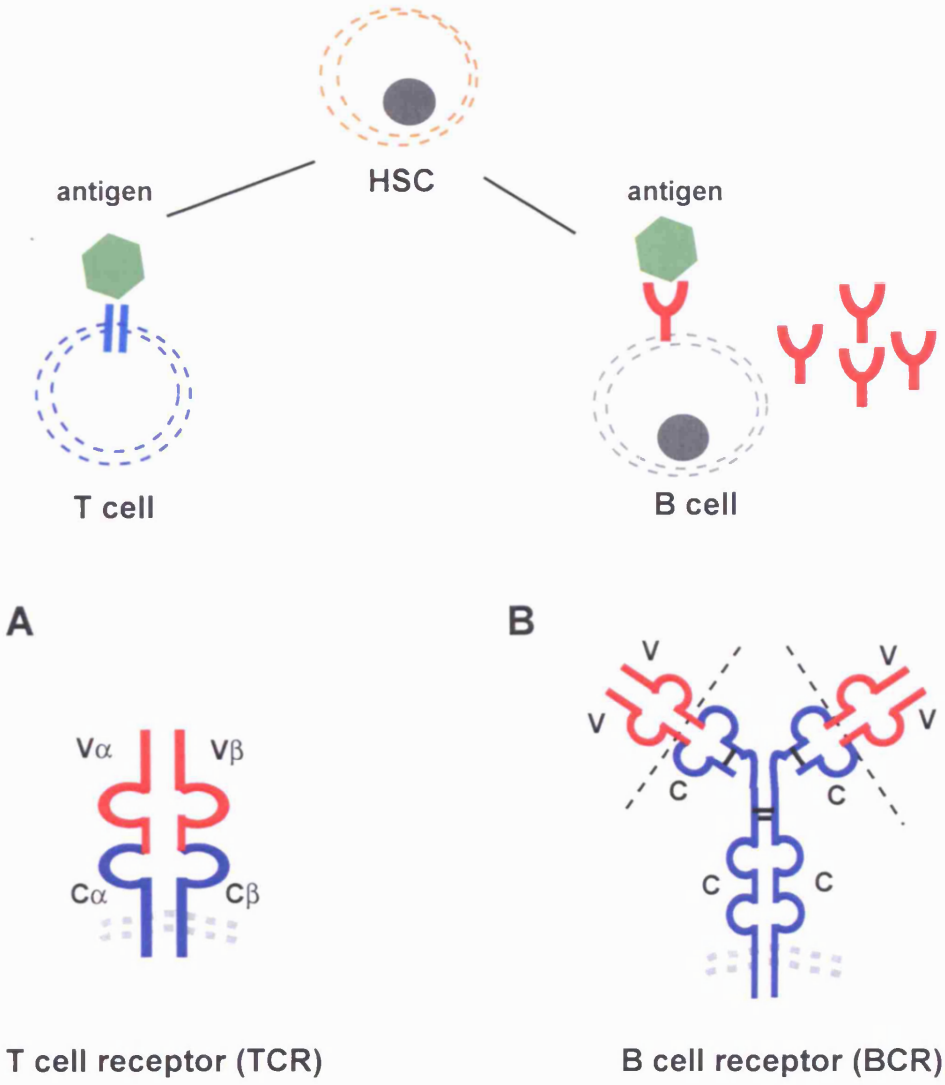


**Figure 1.2. Lymphocytes and their antigen receptors.**
This diagram shows the lymphocyte antigen receptors that recognise the antigen (green). **(A)** T cells express a clonal antigen-specific receptor. The T cell receptor (TCR) has two paired polypeptide chains both of which have constant and variable portions and both of which are composed of immunoglobulin-like domains. It exists only as a cell surface receptor and has no counterpart to secreted antibody. **(B)** The B cell receptor (BCR) is also a clonal antigen-specific receptor. It is made up of a dimer of two polypeptide chains linked by disulfide bonds, the heavy chain (H) and the light chain (L). Both chains have a constant (C; in blue) and a variable (V; in red) domain. The variable regions form the antigen binding domain. The BCR exists as a cell surface receptor and has a counterpart secreted antibody. The TCR is monovalent, whereas the BCR is divalent.

recombination that takes place during early lymphocyte development (Figure 1.3;(Bassing et al., 2002). During this process different gene segments known as variable (V), diversity (D) and joining (J) gene segments are randomly recombined, therefore generating a combinatorial diversity (Figure 1.2).

In the case of B cells, the heavy chain is recombined from V, D and J segments, and is initially associated with a surrogate light chain. Later in development the light chain is generated through a recombination of V and J segments (Figure 1.2). Thus, from a limited number of genes, the V(D)J recombination process gives rise to a combinatorial diversity of polyclonal population of B and T cells. This diversity is increased by several orders of magnitude by the addition or subtraction of nucleotides at the junction of gene segments in a process known as junctional diversity mechanism.

Within this diversity T cells and B cells that express antigen receptors that recognise self-antigens are generated. Stringent selection processes ensure their elimination from the repertoire (Figure 1.1). If cells that recognise self-antigens are not deleted from the repertoire, autoimmune events may take place later.

## 1.3 Antigen recognition and lymphocyte activation

Once the development process is completed, mature lymphocytes that have passed the selection process migrate through the bloodstream to the peripheral secondary lymphoid organs (lymph nodes, Peyer's patches, tonsils, etc), where they will encounter their specific antigens for the first time (Figure 1.4). Recognition of antigen through the antigen receptor initiates an intracellular signalling cascade that leads to cell proliferation and differentiation and the execution of lymphocytes' effector functions (Figure 1.4).

Antigen engagement through the TCR triggers the differentiation of CD8 T cells into cytotoxic T cells that kill cells that present the specific antigen on the surface. CD4 T cells differentiate into helper T cells that have a coordinating function by secreting cytokines that regulate and direct the immune response to specific antigens. Due to these effector functions, T cells are responsible of the cell-mediated response of the adaptive immunity.

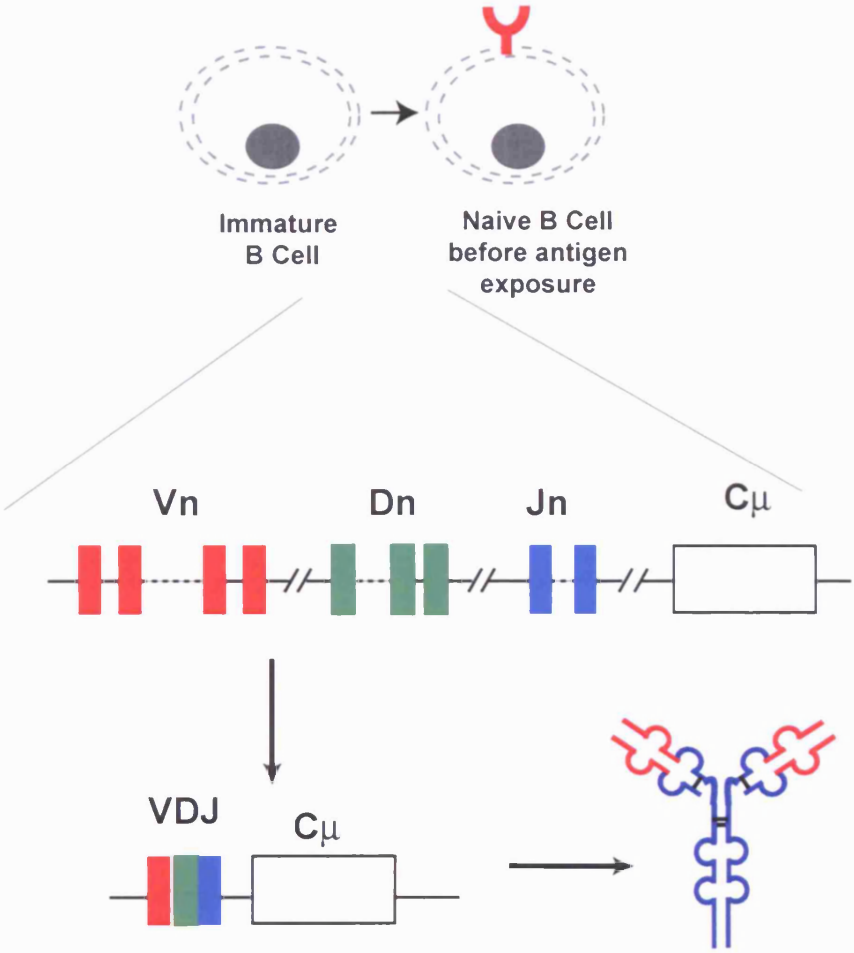


**Figure 1.3. V(D)J recombination confers BCR diversity.**
During B cell development, immature B cells undergo a series of gene rearrangements. The V, D and J gene segments are recombined to generate the complementary determining regions (CDRs) responsible for the antigen binding site.

Antigen engagement through the BCR triggers two events that will lead to B cell activation (Figure 1.4). On one hand, it triggers series of intracellular signalling cascades, and on the other hand it internalises the antigen (Niiro and Clark, 2002). The internalised antigen is then degraded to peptides and presented to T cells in the context of MHC molecules (Figure 1.4; (Rock et al., 1984)). When these two events converge, B cells proliferate and differentiate into plasma cells that produce and secrete antibodies, a soluble form of the B cell receptor, that bind an neutralise specific antigens (Figure 1.4). This effector function defines B cells as part of the humoral immune response.

Some B cells do not need the help of T cells to elicit a humoral immune response. B cells that recognize antigens with repetitive epitopes such as polysaccharides can elicit a humoral immune response, however they cannot undergo an affinity maturation of the immune response.

Therefore, antigens are classified as T-dependent or T-independent based on their necessity of T cell help to elicit a humoral immune response.

## 1.4 Affinity maturation: a second round to generate BCR diversity

B cells must be able to sense a wide range of affinities to assure an adequate immune response and their activation must be tightly regulated. This is of great importance, as activation by self-antigens could lead to an autoimmune event.

When B cells migrate to peripheral tissues they might encounter their cognate antigens. A subpopulation of these activated B cells are recruited to the germinal centres (GCs) (Figure 1.5). In these structures, they undergo two distinct immunoglobulin gene diversification processes, the process of class switch recombination and somatic hypermutation. The first one involves the recombination between the switch (S) regions leading to the modification of the C region of the IgH and thus changing the effector function of the immunoglobulin molecules. This process has no impact on changing the affinity of the BCR for its cognate antigen (Odegard and Schatz, 2006).

During the process of somatic hypermutation, random mutations are introduced at a rate of $10^{-3}$ mutations per base pair per cell division in the variable region of rearranged immunoglobulin heavy and light chain genes (Odegard and Schatz,

2006). This process is the basis of the process of affinity maturation, which results in the preferential outgrowth of B cells expressing an immunoglobulin that have high affinity for their cognate antigen (See Figure 1.5).

Affinity maturation is a term that describes the increment of the affinity of the antibodies secreted during the time course of an immune response (Figure 1.5 B; (Tarlinton and Smith, 2000). B cells in the GC continue to proliferate extensively and downregulate their BCRs to differentiate into centroblasts. Centroblasts undergo somatic hypermutation of the genes coding for the variable domains of their BCRs (Figure 1.2; Figure 1.5; (Tarlinton and Smith, 2000). Once the cell cycle is completed, the centroblasts re-express the newly mutated BCRs to become centrocytes. Centrocytes are then subject to a selection process based on antigen affinity: centrocytes that express BCRs with an improved affinity for the antigen are selected and expanded at the expenses of low affinity binders (Figure 1.5).

After successive rounds of somatic hypermutation and affinity-based selection, the affinity of the specific antibodies secreted during the immune response increases over the time (Foote and Milstein, 1991). Typically, the affinity will increase 100-1000 times (Eisen and Siskind, 1964; Foote and Milstein, 1991).

While the precise mechanism of the affinity maturation process is not fully understood, it is clear that the selection process is dependent on competition for limiting amounts of antigen, presumably displayed on the surface of follicular dendritic cells (Haberman and Shlomchik, 2003); Figure 1.5).

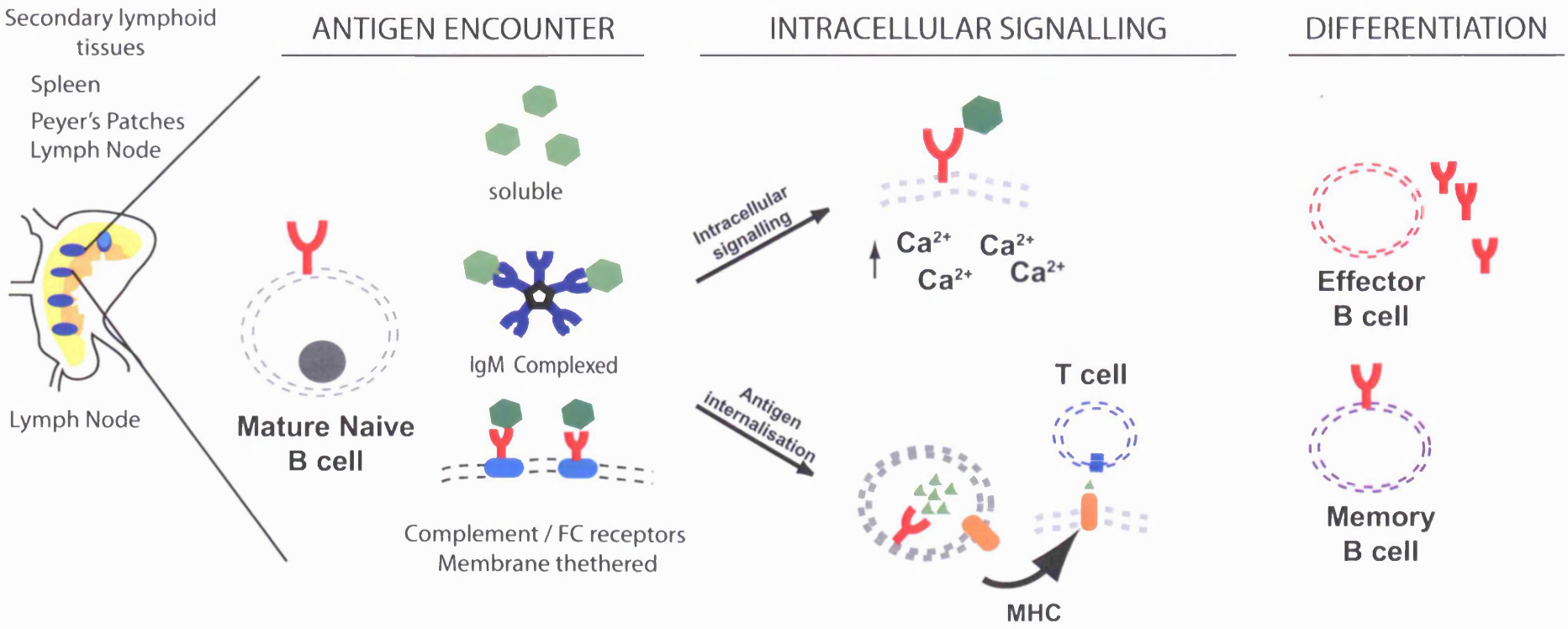


**Figure 1.4. The process of antigen encounter and B cell activation.**
This diagram illustrates the different stages that lead to B cell activation. Mature naive B cells migrate to secondary lymphoid tissues in the periphery, including the lymph nodes, in which they will encounter specific antigens and become activated. Naive B cells recognise antigens in a variety of forms such as soluble antigens, immunocomplexes or membrane thethered antigens. Antigen engagement through the BCR leads to an intracellular signalling cascade and to antigen internalisation, processing and presentation to T cells in the context of MHC molecules. B cells that encounter specific antigens and receive appropriate T cell help, proliferate and form germinal centers in the follicles. These activated B cells divide rapidly and differentiate into antibody-secreting plasma cells or memory B cells that will respond more quickly to a second antigen exposure (Adapted from Immunobiology, 2005).

## 1.5 Types of antigens that interact with lymphocytes

T cells recognize antigens in the context of MHC molecules.

Cells of the immune system (dendritic cells, macrophages, B cells) are able to internalize and degrade proteins to peptides and present them on the cell surface in the context of MHC molecules to T cells (Itano and Jenkins, 2003; Lanzavecchia, 1985). Cells that have this capacity are known as antigen presenting cells (APCs).

Therefore, T cells require that APCs present MHC-peptide complexes expressed on the surface in order for them to get activated. The situation for B cells is not so clear.

In vitro studies have shown that B cells are sensitive to intact, soluble antigens (Batista and Neuberger, 1998; Kouskoff et al., 1998); Figure 1.4). However, in vivo studies have shown that during the course of an immune response, follicular dendritic cells (FDC) retain on their surfaces a large proportion of the available intact antigen through low affinity antibodies or complement Fc receptors (Haberman and Shlomchik, 2003; Kosco-Vilbois, 2003); Figure 1.4).

More recently, Wykes and co-workers have shown that dendritic cells (DCs) are able to retain and present intact antigens to B cells in vitro and in vivo (Wykes et al., 1998). In these experiments they also showed that the contact between a dendritic cell and a B cell is necessary to trigger the activation of B cells. These observations are further supported by experiments that demonstrated that antigen-pulsed DCs are able to stimulate B cells when they are transferred into unimmunized recipients (Balazs et al., 2002; Berney et al., 1999; Colino et al., 2002; Wykes et al., 1998). While the mechanism of presentation is not fully understood, a recent study suggests that the process by which DCs present intact antigen to B cells differs from the normal FDC presentation via Fc or complement receptors, and it appears to be more complex. It has been suggested that it might involve initial antigen internalisation and then recycling to the cell surface (Bergtold et al., 2005); Figure 1.7). The mechanism of this type of presentation has not been demonstrated yet but it is likely to involve a specific set of receptors to contributing to the DC function (Carrasco and Batista, 2006a). In addition, the immunoreceptor tyrosine-based inhibitory motif-bearing FcγRIIb has been

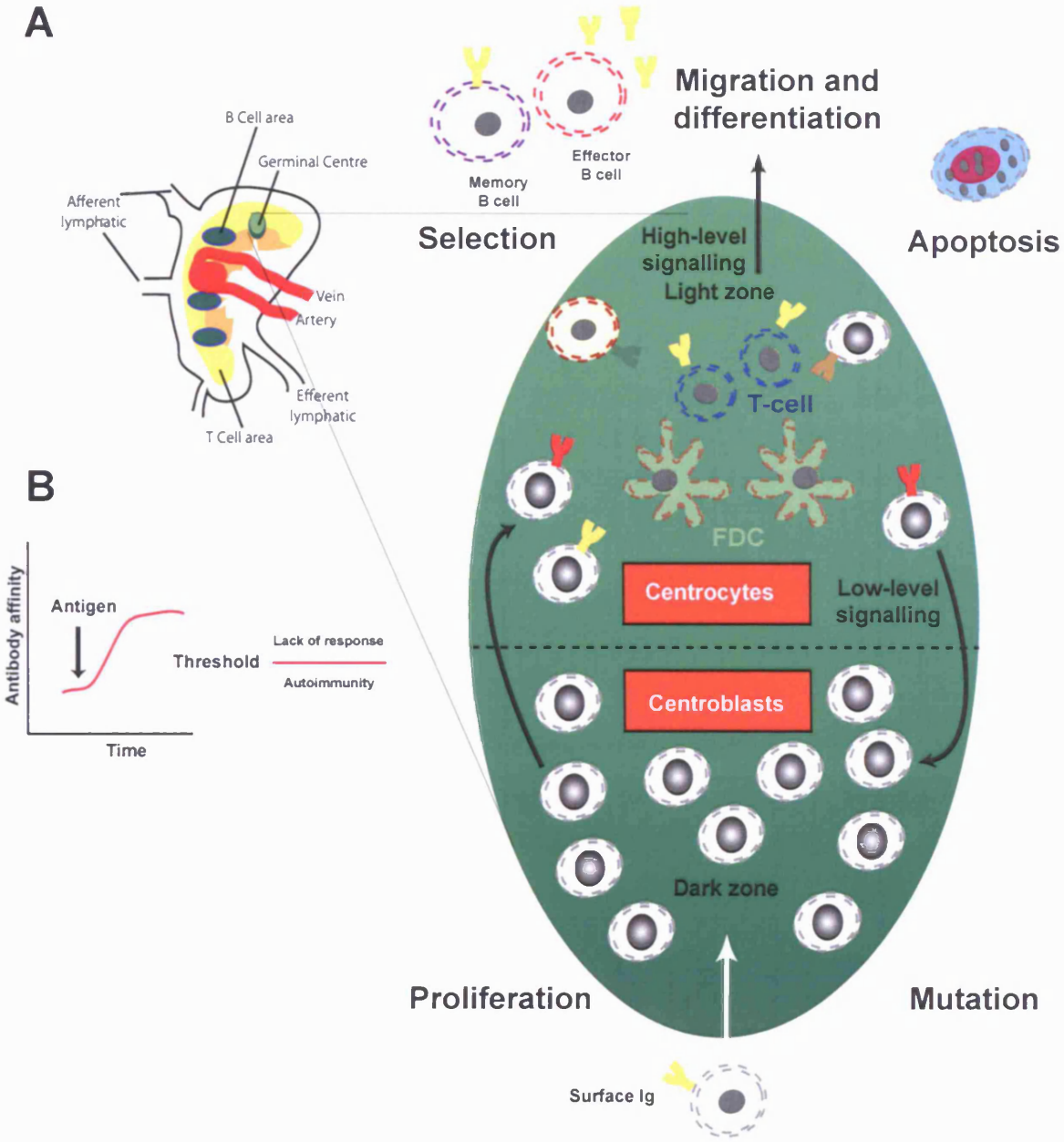


**Figure 1.5. Affinity maturation.**
**(A)** B cells encountering antigen and receiving appropriate T cell help, divide rapidly and undergo somatic hypermutation of their Ig gene segments. In this process random mutations are introduced in rearranged V regions. Cells that express mutated BCRs with an improved antigen binding affinity are favoured in terms of activation and co-operation with T cells, and therefore are selected as antibody producing cells. **(B)** The affinity of the antibodies secreted during an immune response increases over time. Taken and adapted from Tarlinton and Smith, 2000.

implicated as one of the possible molecules that facilitates the presentation of intact antigen to B cells (Bergtold et al., 2005). Thus, it is likely that membrane antigens are the main form of B lymphocyte stimulation in vivo during the adaptive immune response. Although this concept has been proposed for almost 10 years, only very recently it started to be addressed.

## 1.6 Recognition of membrane antigens: its importance in immune recognition

### 1.6.1 The immunological synapse (IS)

In the cell membrane of B lymphocytes, a large array of proteins coexist, including the BCR, the FCγRII, the integrins, LFA1 and VLA4, and the co-receptors CD45 and CD19. These molecules are randomly distributed at the membrane interface (See Figure 1.7A). The recognition of antigens displayed on the surface of an APC leads to the formation of a specialised junction between the lymphocyte and the target cell known as the immunological synapse (IS) (Batista et al., 2001; Grakoui et al., 1999; Monks et al., 1998); Figure 1.7 A and B).

The IS was first described in T cells, and since then the T cell/APC immunological synapse has been extensively characterised (Grakoui et al., 1999; Wulfing et al., 2002b). Later studies by Batista et al have shown that the IS formation upon membrane antigen recognition is a general phenomenon of lymphocytes as B cells also form a IS (Batista et al., 2001; Carrasco et al., 2004). The B cell synapse shares the basic features of the T cell IS (Figure 1.7). B cell recognition of membrane-bound antigens leads to the formation of an immunological synapse and efficient B cell activation.

When B cells and APC make contact a series of events follow to facilitate the encounter of antigen. The APC presents either intact antigen tethered by FcγRII or complement receptors (CD21) via complement fragment 3b (C3b). It has been shown that the BCR encounter of antigen molecules is facilitated by the integrins VLA-4 and its ligand VCAM-1 (Carrasco and Batista, 2006b); see Figure 1.7). It is likely that other receptors might also be involved in this process. When the BCR engages antigen, the adhesion of the B cell to the APC is enhanced via integrins,

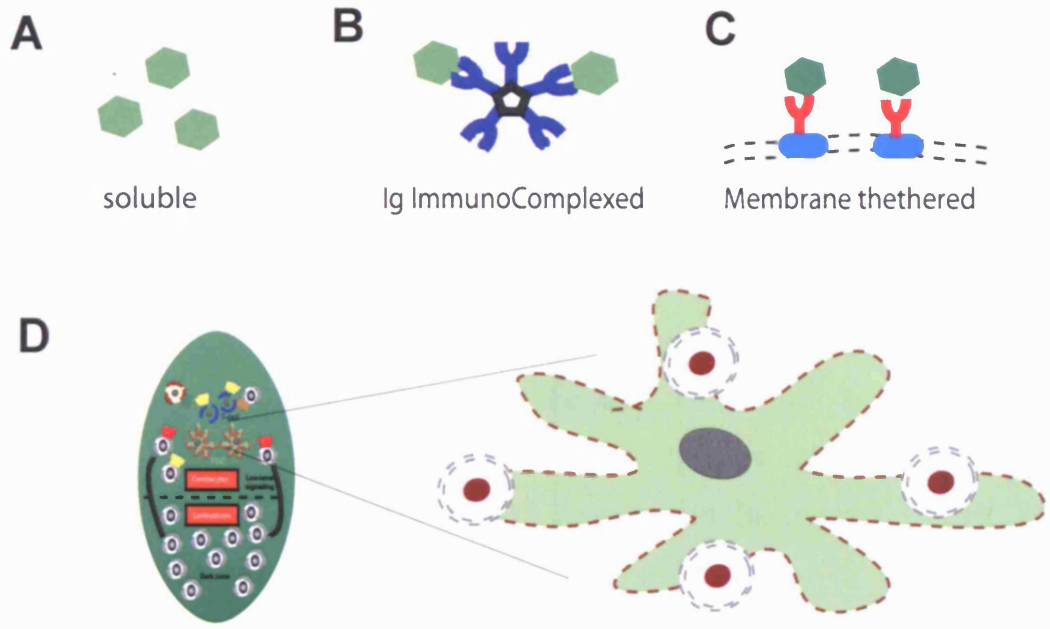


**Figure 1.6. Type of antigen encountered by B cells.**
B cells can encounter antigens in several forms **(A)** soluble, **(B)** complexed with IgM, or **(C)** membrane tehthered through Fc receptors or complement receptors. **(D)** Membrane bound antigens have been shown to be very effective in activating B cells. It is thought that in vivo B cells encounter antigen that is retained on the surface of FDCs in germinal centers (Carrasco and Batista, 2006).

including LFA-1 and VLA-4 (Carrasco and Batista, 2006b). This increment in adhesion facilitates the formation of the IS and therefore promotes B cell activation.

As it can be appreciated from the diagram shown in Figure 1.7, during the process of IS formation, the receptors in the membrane are reorganised and segregated into supramolecular activation complexes (SMACs). Then the BCR gathers antigen into a central cluster (cSMAC), which is surrounded by a peripheral ring of adhesion molecules (pSMAC). The phosphatase CD45 is excluded, probably forming a distal SMAC (dSMAC). In addition, PLCγ2 and Ganglioside GM1 (GM1) also get recruited to the cSMAC (Batista et al., 2001; Cheng et al., 2001).

The co-receptors, CD19–CD21 and FcγRII are recruited to the IS and are able to modulate the signalling triggered by the BCR (these will be discussed more extensively in later sections). Finally, the antigen is internalised in specific compartments and later processed and presented in the context of MHC class II molecules to T cells (See Figures 1.4 and 1.7).

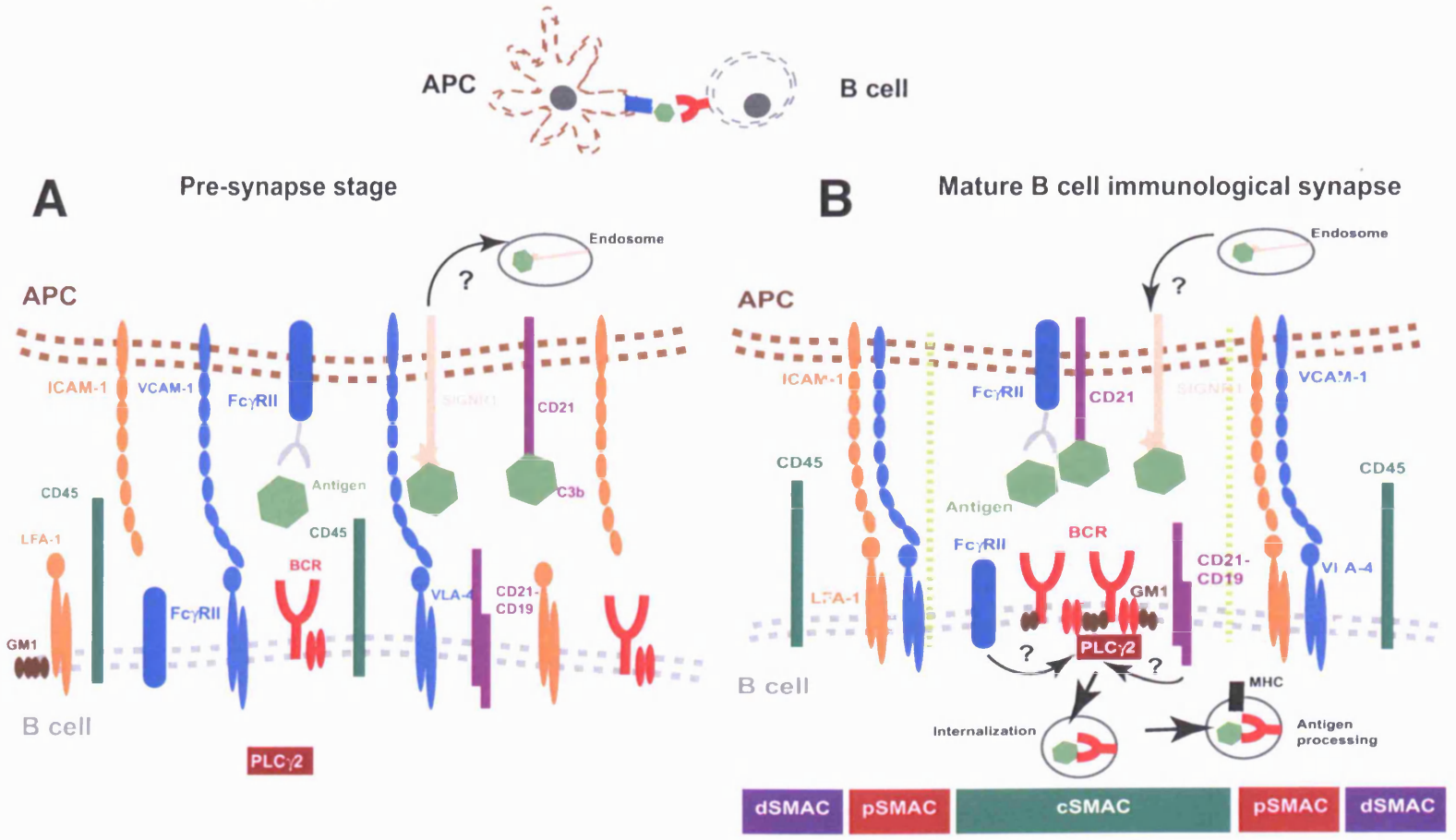


**Figure 1.7. The B cell immunological synapse formation.**
This diagram illustrates the different stages that lead to the formation of a B cell immunological synapse. **(A)** Illustrates the distribution of co-receptors in the cell membrane during early stages of antigen recognition before the IS is formed. **(B)** The membrane proteins surrounding the BCR are differentially sorted during the formation of the IS leading to the formation of an organized structure consisting of a central cluster of receptor/antigen complexes known as cSMAC (central supramolecular activation complex), surrounded by a peripheral ring of ICAM-1/LFA-1 adhesion molecules known as pSMAC (peripheral supramolecular activation complex). Other cell membrane proteins are also differentially sorted during the formation of the IS. See main text for more details. (Adapted from Carrasco and Batista, 2006).

## 1.7 Ligand/receptor interactions in solution vs membrane ligand/receptor interactions

When studying ligand/receptor interactions it is important to define the parameters that determine this interaction and also to adapt these parameters to the environment in which this interaction take place.

When ligands and receptors encounter each other in solution, they associate in a complex (Figure 1.8 A). The rate at which these complexes are formed is known as the association rate constant or $k_{on}$ and the rate at which they dissociate is known as the dissociation rate constant or $k_{off}$ (Figure 1.8 A). A more intuitive parameter is defined by the dissociation half-life ($t_{1/2}$) that expresses the time that it will take for 50% of the complexes to dissociate. At equilibrium, complexes will form and dissociate constantly at exactly the same rate in a steady state condition (Figure 1.8 B). The association constant, $K_a$, is the parameter that characterizes this steady state equilibrium, and is a measurement of the strength of the interaction (Figure 1.8 C).

Binding properties in solution are related to three-dimensional parameters (3D), and therefore they are expressed in terms of molar concentrations of reactants.

The case of membrane-bound receptors and ligands is far more complex. Their interaction is restricted to a two-dimensional (2D) space, and therefore we need to consider this when defining the parameters of this interaction (Bell, 1978).

For instance, the concentration of membrane proteins cannot be expressed as a solution concentration but it can be expressed as surface density, a measure of the number of molecules per unit area. Thus, in the same line, the affinity can be expressed as a 2D $K_a$ (Bell, 1978; Shaw and Dustin, 1997).

This has proved to be a very difficult experimental task and only a few measurements of 2D $K_a$ have been obtained from experimental data (Dustin et al., 1996; Dustin et al., 1997; Shaw and Dustin, 1997).

The interaction of membrane ligands and receptors will also be affected by different factors as they are tethered on a membrane. These would include, the diffusion of molecules on the bilayer, the mechanical properties of the membrane, the presence of other molecules and cytoskeletal dynamics adds up to the complexity of the recognition process.

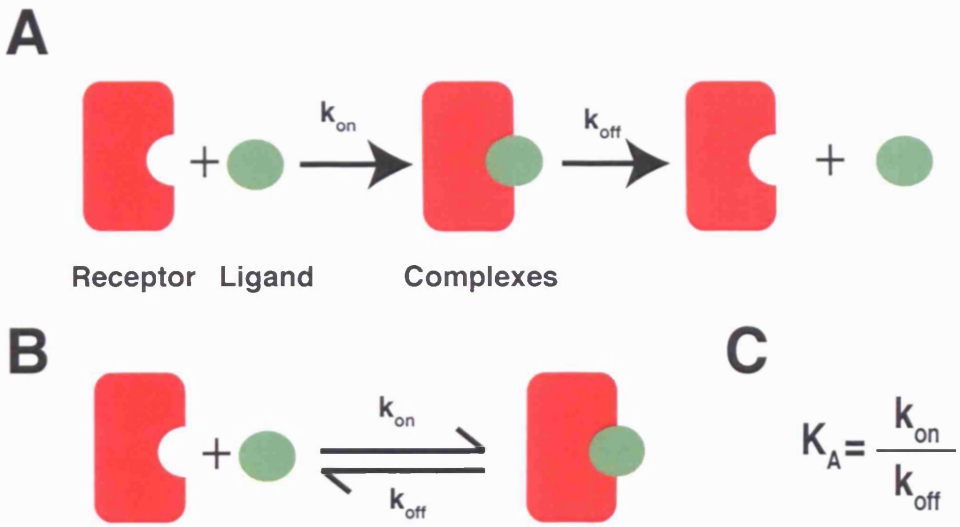


**Figure 1.8. Kinetic parameters of ligand-receptor binding interaction.**
**(A)** Ligands and receptor associate according to the association rate constant ( $k_{on}$), and dissociate according the dissociation rate constant ($k_{off}$). **(B)** At equilibrium the association is equaled by the dissociation of complexes. This steady-state is characterised by the association constant ($K_a$), a measurement of the affinity of the interaction. **(C)** The association constant is defined by the ratio of the two rate constants.

### 1.7.1 T cells recognise antigens of a narrow range of affinities

The first quantitative studies of the IS aimed to define the thresholds of recognition of MHC-peptide complexes by T cells and to unveil the parameters that govern the formation of the IS.

Based on kinetic studies on glass-supported lipid bilayers, Grakoui et al. suggested that the accumulation of the TCR/MHC-peptide complexes is dependent on the dissociation rate constant ($k_{off}$) of this interaction (Grakoui et al., 1999).

From these experiments, several mathematical models have been proposed to explain the parameters that drive the differential segregation of receptors in the cell surface leading to the formation of the IS (Burroughs and Wulfing, 2002; Lee et al., 2002a; Lee et al., 2002b; Qi et al., 2001).

These models explain the differential segregation of ligand/receptor pairs based on the equilibrium thermodynamics of relevant physicochemical parameters (protein binding/dissociation parameters, physical properties of the membranes and bond lengths between molecule pairs) (Burroughs and Wulfing, 2002; Lee et al., 2002a; Lee et al., 2002b; Qi et al., 2001).

Furthermore, they stress the importance of the $k_{off}$ in the MHC-peptide/TCR interaction and the cytoskeletal involvement in synapse formation (Lee et al., 2002b; Wulfing and Davis, 1998). Finally, Lee et al also predicted the kinetic values of TCR/MHC-peptide interaction necessary to promote the accumulation of antigen and the formation of a T cell immunological synapse (Lee et al., 2002b).

While these studies have stressed the importance of the affinity and the density of specific ligands in the recognition process, recent publications suggest that also endogenous peptides play an important role during antigen recognition (Krogsgaard et al., 2005; Stefanova et al., 2002; Wulfing et al., 2002a). Different studies indicate that the presence of MHC-endogenous peptides on the surface of an APC contribute to T cell recognition (Krogsgaard et al., 2005; Stefanova et al., 2002; Wulfing et al., 2002a).

In a combined experimental and computational approach, Chakraborty and colleagues suggested that CD4 may enhance T cell sensitivity by recruiting Lck Src kinase to the IS upon MHC-peptide recognition that would promiscuously phosphorylate MHC-endogenous peptides (Li et al., 2004). From the proposed

mathematical model, the authors also predicted that the thresholds of T cell activation are determined by a precise combination of the dissociation half-lives of the two complexes (Li et al., 2004).

In this line, Krogsgaard et al have shown in an elegant study that pre-existing MHC-agonist/endogenous peptide heterodimers may drive T cell activation and sensitivity (Krogsgaard et al., 2005).

The so called 'pseudodimer theory' was extended also to CD8 T cells. In a recent report, Zal and colleagues showed that the interaction of CD8 with an MHC-endogenous peptide enhances the recognition of antigen (Yachi et al., 2005).

In conclusion, the extensive literature available supports the notion that the dissociation half-life is the key parameter determining the recognition of antigens by T cells.

### 1.7.2 B cells recognise antigens of a wide range of affinities

Contrary to T cells, the interaction of B cell with membrane antigens remains largely unexplored. In vitro studies performed with soluble antigens have shown that the affinity of the B cell receptor (BCR) for the antigen is a critical parameter that determines the thresholds of B cell activation (Batista and Neuberger, 1998; Kouskoff et al., 1998). Moreover, Batista and colleagues suggested that the dissociation half-life of the antigen/BCR interaction is important in the response of a B cell to soluble antigens (Batista and Neuberger 1998). In this line, Foote and Milstein demonstrated in an elegant study the importance of the binding kinetics in the affinity maturation of antibodies (Foote and Milstein, 1991). This crucial process in the life of B lymphocytes will be discussed in detail in the last section.

Different groups have shown that membrane antigens are particularly effective at triggering B cell activation in vivo (Hartley et al., 1991; Nemazee and Burki, 1989). B cells that express a BCR that recognises a self-antigen are eliminated from the repertoire only if the antigen is expressed on a membrane, while if the antigen is in solution B cells become anergic (Goodnow et al., 1988; Hartley et al., 1991; Nemazee and Burki, 1989). In this line, Batista and colleagues have shown that the way in which antigens are presented to B cells have a critical impact on the activation process (Batista and Neuberger, 1998; Batista and

Neuberger, 2000). However, the parameters that determine the kinetics of interaction of B cells with membrane-bound antigens are not known.

Furthermore, during the course of an immune response B cells encounter antigens of a much wider range of affinity than T cells. In addition, unlike T cells, B cells are capable to effectively recognize antigens in the absence of ICAM-1 or any accessory molecule (Carrasco et al., 2004). Thus, the models available for T cells cannot predict the kinetics of interaction of B cells with membrane-bound antigens, as they are limited to the narrow range of affinities of the TCR/MHC peptide interactions.

## 1.8 Events triggered by the B cell receptor upon membrane antigen recognition

Antigen engagement by the BCR initiates a signalling cascade mediated by the CD79α and CD79β chains of the antigen receptor complex (Niiro and Clark, 2002). Initial signals involve the activation of src kinases (including Lyn, Fyn, Blk, kinase) by dephosphorylation of its negative regulatory site by CD45 (Niiro and Clark, 2002). In turn, this event triggers the phosphorylation of the ITAM motifs of the signalling components of the BCR and facilitates the recruitment of Syk and Btk tyrosine kinases (Niiro and Clark, 2002). Syk and Btk kinases then activate downstream cascades including phospholipase Cγ2 (PLCγ2) and PI3 kinase. Both enzymes participate in the metabolism of phosphoinositides to generate key second messengers in BCR signalling (Niiro and Clark, 2002).

PI3 kinase phosphorylates phosphatidylinositol-4,5-biphosphate to produce phosphatidylinositol-3,4,5-triphosphate ($PIP_3$), and PLCγ2 degrades the same substrate into inositol-1,4,5-triphosphate ($IP_3$) and diacylglycerol (DAG). These molecules serve as second messengers that ultimately lead to the transcription of genes important for survival and proliferation of B cells (Niiro and Clark, 2002).

## 1.9 General aims

Given the importance of the recognition of membrane antigens by B cells and how little is known, in this Thesis we set out to understand the interaction of lymphocytes with membrane antigens. We focused on the interaction of B cells and NKT cells with their respective antigens.

We have set up a system of artificial lipid bilayers that allow quantitative analysis of the membrane antigen recognition process. We took advantage of this system to characterise in detail the interaction of B cells and NKT cells with their respective antigens and define the parameters that define this process. Furthermore, we dissected the early molecular events that take place in B cells upon membrane antigen recognition.

Since B cells recognise antigens of a wide range of affinities that include all possible interactions, we hope that the findings of this study will be extended to other ligand-receptor pairs.

# Chapter 2: Materials and Methods

## 2.1 Mice

### 2.1.1 Animal care and breeding

All animal care and breeding was carried out by the Clare Hall Animal Unit (Cancer Research UK). MD4, D1.3 and HSμ trasngenic mice were maintained as heterozygous on a C57BL/6 background. 3-83 transgenic mice were maintained as heterozygous on a Balb/c background.

Mice were killed according to humane killing practices approved by the Home Office.

### 2.1.2 Genotyping

Genotyping of the MD4, 3-83 and HSμ transgenic mice was performed by detecting antigen-specific antibodies in the serums of the mice with a capture ELISA. Briefly, 96-well immunoplates (Maxisorp Immuno Plate, Nunc) were coated with the specific antigens (HEL for MD4, p31 for 3-83, and NIP-ovoalbumin for HSμ) for 1 hr at 37 °C. Then the plates were blocked by adding 200 μl/well of blocking buffer (PBS, 2% BSA, 0.01% Tween-20, 0.1% $NaN_3$) and incubating for 1 hr at room temperature. Then, dilutions of the serums were incubated in the plates for 1 hr at RT.

Specific antibodies captured in the plates were detected by incubating sequentially with a biotinylated anti-mouse $IgM^a$ antibody (BD Pharmingen), streptavidin-alkaline phosphatase conjugate (Extravidin-AP, Sigma), and the corresponding substrate (alkaline phosphatase yellow (pNPP) substrate tablets, Sigma).

D1.3 transgenic mice were screened by FACS analysis of peripheral blood lymphocytes. Heparinized blood samples (2-3 drops) were first incubated for 5 minutes with 1 ml of Tris-ammonium buffer (0.75% Tris, 0.2% $NH_4Cl$, pH=7.2) to lyse the erytrocytes, and the white blood cells were then isolated by centrifugation.

D1.3 positive transgenic B cells, labelled with $HEL^{WT}$-Alexa Fluor 488 and anti-B220-PE-Cy5 (BD Pharmingen), were detected by FACS.

This transgenic line was a kind gift from Dr Michael Neuberger (LMB, Cambridge).

## 2.1 Cell culture

All the solutions and reagents were purchased from GIBCO, except where indicated.

### 2.2.1 Cell culture

Primary naïve B cells, A20 B cell line (Kim et al., 1979), COS-7 (Gluzman, 1981), L-cells, J558L (Weigert et al., 1970), Sp2/0 (Shulman et al., 1978) and LG2 cells were cultured in RPMI medium containing 10% fetal calf serum (FCS), 10 mM HEPES, 10 IU/ml penicillin/streptomycin antibiotics and 50 μM 2-mercaptoethanol (Sigma).

Human NKT cells were cultured in RPMI medium containing 5% human serum (Cambrex), 2 mM glutamine, 1 mM non-essential amino acids, 1 mM sodium pyruvate, 10 IU/ml penicillin and streptomycin antibiotics and 50 μM 2-mercaptoethanol (Sigma).

### 2.2.2 Naïve B cells isolation

Naïve B cells were isolated by negative selection from the spleens of transgenic mice (2-3 months old) on the day of the experiment. Total splenocytes were prepared by disrupting the spleen on a cell strainer (70 μm, BD Falcon) with a syringe plunger and washing with PBS (three washes of 3 ml each). After a Lympholyte (Cedarlane Laboratories) step and red blood cells lysis in Tris-ammonium buffer (0.75% Tris, 0.2% $NH_4Cl$, pH=7.2), T cells were depleted by incubation with Dynabeads mouse pan-T (Dynal Biotech ASA, Oslo, Norway) for 30 minutes at 4 °C. The cells were then incubated in 10 ml of RPMI medium in 10 mm round plates (BD Falcon) for 1 hr at 37 °C to allow the macrophages to stick to the plastic. The population obtained had 95-98% B cells as assessed by FACS using anti-B220 and anti-IgM specific antibodies.

### 2.2.3 NKT cells culture

NKT cell lines from human origin were stimulated once every 20 days to promote their growth. For the stimulation 4 x $10^6$ peripheral blood mononucleated cells (from human donors) and 4 x $10^5$ LG2 cells were irradiated (5000 Rads) in 2 ml of

culture medium supplemented with 1 μg/ml PHA and 500 IU/ml IL-2 (Cambrex). NKT cells (1 x $10^6$) were then cultured with the feeders for stimulation.
The medium was replaced with fresh medium containing IL-2 (500 IU/ml) every 3-4 days.

### 2.2.4 Cell transfection

For cell-to-cell interaction studies, COS-7 cells were transfected with a $HEL^{WT}$-GFP construct using the Superfect reagent according to manufacturer's instructions (Gibco) (Batista and Neuberger, 2000).
Cells were plated on clean and sterile glass coverslips (Bioptechs, Inc.) at 80% of confluence 24 hours before transfection. On the day of transfection they were treated with 5-10 μg of the $HEL^{WT}$-GFP coding vector dissolved in 100 μl of Superfect reagent and 1 ml of RPMI medium without serum. After 2.5 hours of incubation at 37 °C, the cells were washed and kept in RPMI 10% medium until experiments were performed 24 hours later.
On the day of the experiment unbound cells were washed away with chamber buffer and the coverslip was assembled on the FCS2 closed chamber system according to manufacturer's instructions (Bioptechs, Inc.). The interaction of MD4 or WT B cells with transfected COS-7 cells was visualised immediately.
For protein production J558L cells were transfected by electroporation. J558L cells (5 x $10^6$) were mixed with 10-20 μg of plasmid in 500 μl of RPMI culture medium and electroporated at 0.26 V and 960 μF (BioRad Gene Pulser). Stable clones were then obtained by limiting dilution and selection in medium containing G-418 (1 mg/ml).

### 2.2.5 Fluorescence Activated Cell Sorting (FACS) analysis

Cell stainings for FACS analysis were performed with the indicated antibodies and concentrations in FACS buffer (PBS, 2% fetal calf serum, 0.1% $NaN_3$). Cells were incubated at 4 °C for 20 minutes and washed once with FACS buffer. Samples were analysed with a FACS Calibur cytometer (Becton, Dickinson and Company) and the Cellquest software (Becton, Dickinson and Company).

## 2.3 Artificial membranes technology

### 2.3.1 Liposomes preparation

Liposomes were prepared by detergent dialysis (Brian and McConnell, 1984; Mimms et al., 1981). Lipid stocks were purchased dissolved in chloroform from Avanti Polar Lipids. The following lipids were used in the preparation of liposomes: 1,2-dioleoyl-sn-glycero-3-phosphocholine (DOPC), 1,2-dioleoyl-sn-glycero-3-phosphoethanolamine-NBD (PE-NBD), 1,2-dioleoyl-sn-glycero-3-phosphoethanolamine-N-(Cap Biotinyl) (N-biotinyl Cap-PE), 1,2-distearoyl-sn-glycero-3-phosphocholine (DSPC).

The chloroform in the lipids was first evaporated under a $N_2$ stream and solvent traces were removed by high vacuum for 2 hs. The thin film of dry lipids was then resuspended in buffer (25 mM Tris, 150 mM NaCl, 2% octylglucoside, pH=8.00) to obtain a 2 mM solution (10 x stock), and sonicated until clear.

PE-NBD and N-biotinyl Cap-PE solutions were mixed with DOPC in a 1:50 molar ratio. The solutions were then diluted 1:10 (2% octylglucoside buffer), filtered (0.22 μm, Millipore) and dialysed against octylglucoside-free buffer (25 mM Tris, 150 mM NaCl, pH=8.00) for 36 hs with buffer exchange every 12 hs to remove the detergent and generate the liposomes.

### 2.3.2 Expression and purification of the GPI-linked HyHel5 Fab fragment protein

The HyHel5 Fab fragment was produced as a GPI-linked protein on the cell membranes of transfected cells and purified by affinity chromatography. The constructs coding for the Fab fragment (the kappa light chain and heavy chain fused to EGFP) of the HyHel5 antibody (Yolanda Carrasco & Facundo Batista, unpublished results) were co-transfected in a 1:5 ratio in Sp2/0 cell line, a cell line deficient in the expression of light chains (Shulman et al., 1978). Positive clones were selected in the presence of geneticin (0.5 mg/ml) and screened by FACS analysis (Yolanda Carrasco).

The GPI-linked fusion protein was then purified by affinity chromatography as previously described (Bromley et al., 2001). Cell membranes containing the GPI-linked Fab were solubilised in lysis buffer (25 mM Tris, 150 mM NaCl, 0.1% $NaN_3$, 1% Triton X-100, pH=8.00) in the presence of protease inhibitors (Complete EDTA-free tablets, Roche Diagnostics). A ratio of 20 ml of buffer / 1 gram of cell pellet was used, and approximately 4 grams of cells (5 liters) were

used in each purification. The solution was incubated with mild agitation for 1 hr at 4 °C; nuclei were eliminated by centrifugation at 1000 x g for 10 min. The supernatant was then incubated for an additional hour at 4 °C in the presence of 0.5% DOC, and finally clarified by ultracentrifugation at 100000 x g for 45min. After filtering the supernatant through a 0.22 μm filter, the protein was loaded on a hen egg lysozyme (HEL)-coupled Sepharose column (1-2 mg of HEL were coupled in an NHS-activated HiTrap 1 ml column according to manufacturer's instructions, Amersham). The column was then washed with lysis buffer containing 0.5% DOC (15 column volumes) and equilibrated with labelling buffer (100 mM $NaHCO_3$, 150 mM NaCl, 1% Triton X-100, pH=8.4). After that the column was injected with 200-400 μg of Alexa Fluor 488 succinimidyl ester (Molecular Probes, Invitrogen) to increase the specific labelling due to the EGFP and incubated for 30 min at RT with occasional mixing. The protein-labelling reagent was then washed out with labelling buffer and then the column was equilibrated with pre-elution buffer (25 mM Tris, 150 mM NaCl, 2% octylglucoside, pH=8.00) in order to replace the Triton X-100 with the octylglucoside (OG). Elution was performed with an acidic buffer (100 mM Gly, 150 mM NaCl, 2%OG, pH=2.5) and the fractions (8 x 1 ml each) were collected in 1 M Tris (pH=8.00) to neutralise the pH.

Protein purification was assessed by FACS analysis and SDS-PAGE (Silver staining).

For FACS analysis dilutions 1:50 of the eluted fractions (100 μl, in FACS buffer) were mixed with 1 μl of streptavidin-coated beads loaded with biotin-$HEL^{WT}$ and incubated for 20 minutes at RT with agitation to avoid the beads from settling (Thermomixer, Eppendorf). After washing once with buffer, the beads were incubated for 20 min at RT with an anti-kappa-PE antibody (1:400), and then analysed.

Fractions containing the pure and active protein were pooled and reconstituted into DOPC liposomes by detergent dialysis (see previous section).

### 2.3.3 Monobiotinylation of the tethering antibody

The monobiotinylated F10 anti-HEL monoclonal antibody was prepared by incubation with limiting concentrations of the EZ-Link sulfo-NHS-LC-LC-biotin reagent (Pierce).

The antibody was first dialyzed against PBS to eliminate any traces of amine-containing buffer (final antibody concentration ≈ 1 mg/ml). Then it was mixed with varying concentrations of the sulfo-NHS-biotin reagent (200 mg/ml stock solution in DMSO). Usually, final concentrations of 0.1 - 0.01 μg/ml yielded monobiotinylated species of antibody.

The mixture was left to react for 30 minutes at room temperature, and then dialysed against phosphate buffer saline (PBS) with several changes of buffer to remove the excess reagent (biotin).

The degree of biotinylation of the antibody was evaluated by FACS with streptavidin-coated beads (Bangs Laboratories, Inc.) as described below.

1 μl of beads were mixed with 100 μl of a dilution 1:50 (in FACS buffer) of the biotinylated antibody. The mixture was incubated for 20 minutes at room temperature with agitation (to prevent the beads from settling in the bottom of the tube) and then washed once.

The beads were then incubated with 100 μl of streptavidin-Alexa Fluor 633 (1:400 dilution) and an anti-mouse Ig-FITC antibody (BD Pharmingen) for 20 minutes at room temperature with agitation. After washing, the beads were analysed by FACS. The monobiotinylated antibody can be distinguished from a polybiotinylated one by the levels of streptavidin-Alexa Fluor 633 staining.

### 2.3.4 Planar lipid bilayers preparation

Planar lipid bilayers were prepared in FCS2 chambers (Bioptechs Inc.) by liposomes spreading as previously described (Brian and McConnell, 1984; Dustin et al., 1996). Glass coverslips were treated with sulphochromic solution over night, and rinsed with distilled water and acetone; the excess acetone was removed by aspirating it.

Liposomes containing functionalized N-biotinyl Cap-PE or the labelled GPI-linked HyHel5 Fab fragment were mixed at different ratios with 1,2-dioleoyl-*sn*-glycero-3-phosphocholine (DOPC, Avanti Polar Lipids, Inc.) liposomes to get the required molecular densities. Then, liposome drops (0.8 μl per membrane) were deposited

on the glass coverslips, and the FCS2 chambers were assembled following the manufacturer's instructions. After 20 minutes of incubation, the chambers were flushed with blocking buffer (PBS 2% FCS) and incubated for at least 1 hour.

Hen egg lysozyme (HELs) antigens were tether directly on lipid bilayers containing the GPI-linked Fab fragment by incubating the chambers with the antigen (1 ml, concentration ≈ 200 ng/ml).

In the case of lipid bilayers containing biotinylated lipids, the chambers were successively incubated with 1 ml of fluorescently labelled avidin (concentration ≈ 1 µg/ml), 1 ml of monobiotinylated F10 antibody (concentration ≈ 50 µg/ml), and 1 ml of the HEL antigen (concentration ≈ 200 ng/ml), or incubated with 1 ml of the monobiotinylated antigens after the avidin step.

All the incubations were performed at room temperature for 10-15 minutes in chamber buffer (PBS 0.5% FCS, 2 mM $Mg^{2+}$, 0.5 mM $Ca^{2+}$, 1 g/l D-glucose, pH=7.4). The chambers were washed between incubations with at least 5 ml of chamber buffer to eliminate the excess of reagents.

In all the cases, the excess antigen was washed out of the chambers with 5-10 ml of chamber buffer right before injection of the cells. Assays were performed in chamber buffer using the FCS2 closed system temperature controller set at 37 °C.

### 2.3.5 Determination of molecular densities

#### 2.3.5.1 Bilayers containing the GPI-linked Fab fragment protein

The density was estimated with an enzyme-linked immunosorbent assay (ELISA).

Bilayers were prepared on glass coverslips (Culturewell, Grace Bio-Labs) according to the *Lipid bilayers* section; these coverslips have 8 round wells with a defined surface area of 20 x $10^6$ $\mu m^2$. Then the bilayers were resuspended in a fixed volume of detergent buffer (PBS, 0.2% Tween-20, 1% Triton X-100), and the amount of recovered Fab fragment was estimated with a capture ELISA.

For the ELISA, 96-well immunoplates (Maxisorp Immuno Plate, Nunc) were coated with a rat anti-mouse kappa light chain antibody (20 µg/ml, 80 µl/well) for 1 hr at 37 °C. Then, they were blocked for 1 hr by adding 200 µl/well of blocking buffer (PBS, 2% bovine serum albumine, 0.01% Tween-20, 0.1% $NaN_3$).

The samples (100 µl/well, diluted 1:3 in blocking buffer) were incubated for 1 hr at room temperature. A calibration curve was obtained with Fab fragments prepared from the HyHel5 antibody (see *Fab preparation* section).

After the incubation period, the plates were loaded with biotinylated $HEL^{WT}$ (300 ng/ml, 100 µl/well) for 1 hr at room temperature. Finally, the ELISA was developed by incubating sequentially with streptavidin-alkaline phosphatase (Extravidin-AP, Sigma), and its substrate (alkaline phosphatase yellow (pNPP) susbstrate tablets, Sigma) according to manufacturer's instructions. The developed color was read at 450 nm.

The calibration curve was converted to density of molecules with the surface area of the coverslips, and the densities of the samples were derived from it.

#### 2.3.5.2 Bilayers containing biotinylated lipids

The density of antigen was estimated as the density of monobiotinylated F10 antibody on the surface of the artificial lipid bilayers. This was determined with a fluorometric assay using calibrated beads (Bangs Laboratories).

These beads consist of five populations of beads that have different antibody binding capacities (ABC, 4 plus the negative control); this value represents the number of molecules of mouse IgG that each population binds.

To estimate the density, the beads were incubated in FACS buffer with saturating concentrations of the F10 monoclonal antibody (20 µg of antibody/drop of beads, final volume = 100 µl) for 20 minutes. The beads were then washed and incubated with an anti-kappa-PE antibody (10 µg of antibody, final volume = 100 µl).

In parallel, lipid bilayers containing biotinylated lipids were prepared and loaded with Alexa Fluor 488-avidin and monobiotinylated F10 antibody according to *Planar lipid bilayers preparation*. Then the F10 tethered on the bilayers was labelled with the same anti-kappa antibody for 20 minutes and then washed out.

The fluorescence intensity of the beads and the artificial bilayers were then measured by confocal microscopy. The density was then estimated as explained in Chapter 3.

## 2.4 Antigens

All the purifications described were performed with an Akta purifier FPLC system using the indicated columns (Amersham).

### 2.4.1 Recombinant lysozymes

The mutant lysozymes were obtained by genetic modification of the wild-type hen egg white lysozyme ($HEL^{WT}$). The following residues were converted to alanine: $HEL^{RD}$, aa 21, 101; $HEL^{RDGN}$, aa 21, 101, 102, 103; $HEL^{K}$, with aa 97; $HEL^{KD}$, aa 97, 101; $HEL^{RK}$, aa 21, 97; $HEL^{RKD}$, aa 21, 97, 101; $HEL^{KK}$, aa 21, 97; $HEL^{V}$, a 120; and $HEL^{D}$, a 35 (Batista and Neuberger, 1998). The different HEL mutants were expressed as His-tagged proteins in the J558L B cell line and purified from the supernatant by $Ni^{2+}$-NTA agarose columns (HisTrap HP 1 ml, Amersham) according to the manufacturer's protocol.

$HEL^{V}$ and $HEL^{D}$ were purified by cation exchange chromatography on a CM-Sepharose column (1 ml, Amersham). Protein purification was assessed by SDS-PAGE (4-20%) and Coomassie blue staining (Pierce). Both procedures yielded 0.5-2 mg of recombinant protein of high purity (90%) per litre of supernatant. Antigens were used without any further purification.

### 2.4.2 Peptides recognised by the 3-83 BCR

The p0, p5, p7, p11 and p31 monobiotinylated peptides were synthesised by the Peptide Synthesis Laboratory at Cancer Research UK. The sequences of the peptides were (from N-terminal to C-terminal):

p0: SGSGPRLDSAKEIMASGSC

p5: SGSGLMNTGGYQSLLPSGS

p7: SGSGVLTPQDYRWFLDSGSC

p11: SGSGGMNWNWLQAHTSGSC

p31: SGSGHDWRSGFGGFQHLCCSGS

The peptides were dissolved in deionised water at a concentration of 0.5 mg/ml, aliquoted and stored at -20 °C.

### 2.4.3 Expression, purification and biotinylation of H-2K monomers

Dr Ton Schumacher (The Netherlands Cancer Institute, Netherlands) and Dr Dirk Busch (Institute of Microbiology, Immunology and Hygiene, Munich Technical

University, Germany) provided us with the vectors coding for the H2-$K^k$ and H2-$K^b$ heavy chains, and the β2-microglobulin to generate the MHC class I molecules. The vectors coding for the heavy chain molecules contain the extracellular domain fused to a target site for the biotin ligase (BirA). This enzyme catalyses the transfer of a biotin molecule to a lysine contained in a short amino acidic sequence (O'Callaghan C et al., 1999).

H-2K proteins (heavy chain and β2-microglobulin) were produced in bacteria and purified from inclusion bodies following a protocol provided by Dr Dirk Busch.

The vectors coding for the different proteins were transfected by electroporation into the BL21 ($RecA^-$) pLysS Escherichia coli strain (kind gift of Dr Neil McDonald, Cancer Research UK). After selection of positive transfectants in LB agarose plates containing carbenicillin (Sigma, 100 μg/ml), colonies were picked and grown in LB medium until the $OD_{600}$ reached 0.7-0.75. Protein production was then induced by treatment with IPTG (Sigma, 0.4 mM).

After 3 hours, the production of protein was checked by SDS-PAGE. The bacteria were then pelleted by centrifugation, resuspended in lysis buffer (50 mM Tris, 100 mM NaCl, 0.5% Triton X-100, 0.1% $NaN_3$, 1 mM DTT, pH=8.00) and lysed by sonication (probe sonicator). Inclusion bodies were recovered by centrifugation (11000 x g, 20 minutes), and cleared with three cycles of washing (50 mM Tris, 100 mM NaCl, 1 mM EDTA, 0.1% $NaN_3$, 1 mM DTT, pH=8.00) and centrifugation. The pellets looked white after this procedure.

Proteins in the inclusion bodies were then dissolved in 1 ml of urea solution (50 mM Tris, 100 mM NaCl, 8 M urea, 10 mM EDTA, 0.1 mM DTT, pH=8.00). Precipitated material was removed by ultracentrifugation (100000 x g, 20 minutes at 4 °C) and the purity of the supernatant checked by SDS-PAGE and Coomassie blue staining (approximately 90% of purity). Protein concentration (molarity) was determined by measuring the absorbance at 280 nm using the following extinction coefficient and molecular weights:

| Protein | ε ($cm^{-1}$ $mg^{-1}$ ml) | MW (Da) |
|---|---|---|
| **H-2K$^b$** | 79800 | 34739 |
| **H-2K$^k$** | 89600 | 34990 |
| **β2-microglobulin** | 18200 | 11679 |

The resuspended proteins were stored at -80 °C until further use.

H2-K monomers were refolded by gradual removal of the urea by dialysis. The heavy chain and the β2-microglobulin were mixed in a 1:2 molar ratio and diluted in urea solution (with 1 tablet of Complete protease inhibitor cocktail tablet per 50 ml of buffer) to a final protein concentration of ≈ 0.4 mg/ml. The refolding mixture was then slowly dialysed against solutions of decreasing urea concentration for two days (2-fold reduction of urea concentration every 12 hours).

After dialysis, the sample was centrifuged to remove precipitated protein and concentrated to a final volume of 200 µl (Centricon 0.5 ml concentrator, MWCO = 10 kDa). The H-2K complexes were purified from the single chains by size exclusion chromatography on a Superose 12 HR10/30 column (Amersham) using PBS as eluent. Fractions were analysed by SDS-PAGE and those containing the monomer were pooled and concentrated (Centricon 0.5 ml concentrator, MWCO = 10 kDa).

Monobiotinylation of the monomers was achieved by using the biotin ligase enzyme (BirA). Monomers were incubated in buffer with the BirA (1:25 enzyme/protein ratio) in the presence of biotin (100 µM), ATP (10 mM) and $MgCl_2$ (5 mM) for 16 hs at RT. The excess biotin was removed by dialysis against PBS (Pierce dialysis cassettes, MWCO = 10 kDa). The biotinylation efficiency was tested by FACS using streptavidin-coated beads and fluorescently-labelled anti-H-2K molecules antibodies.

### 2.4.4 Expression and purification of the biotin ligase enzyme (BirA)

The biotin ligase enzyme (BirA) was produced in bacteria and purified from the periplasmic fraction by affinity chromatography (His-tagged) through a $Ni^{2+}$-NTA column (HisTrap HP 1 ml, Amersham).

The vector coding for a His-tagged version of the BirA enzyme was transfected by electroporation into the BL21 ($RecA^-$) pLysS Escherichia coli strain. Selection of transfected colonies and production of protein was performed with the same protocol used for the H-2K monomers.

After 3 hours, the production of protein was checked by SDS-PAGE. The bacteria were then pelleted by centrifugation (6000 RPM, 20 min), resuspended in lysis buffer (50 mM Tris, 100 mM NaCl, 0.5% Triton X-100, 0.1% $NaN_3$, 1 mM DTT, pH=8.00) and lysed by sonication (probe sonicator). The protein was then purified through a HisTrap HP 1 ml column according to the manufacturer's protocol (Amersham). Further purification was achieved by size exclusion chromatography through a Superdex column.

### 2.4.5 Expression and purification of HEL-peptide fusion proteins

The plasmid coding for the $HEL^{RD}$ mutant was used as the backbone to generate a fusion protein with the p11 and p31 peptides. This vector contains the $HEL^{RD}$ mutant and a 6 x histidine tag to facilitate the purification process (F.D. Batista, personal communication).

The plasmid was initially digested with the restriction enzymes Bam HI and XhoI (New England Biolabs). The peptides were then introduced into the construct by PCR with the following primers:

p11: CCGCTCGAGTATGAACTGGAATTGGCTACA

p31: AGAGGCTGCCGGCTGTGG

The cloned products were transfected by electroporation. J558L cells ($5 \times 10^6$) were mixed with 10-20 µg of plasmid in 500 µl of RPMI culture medium and electroporated at 0.26 V and 960 µF. Stable clones were then obtained by limiting dilution and selection in medium containing G-418 (1 mg/ml).

The protein was then purified from the supernatant by affinity chromatography (His-tagged) through a $Ni^{2+}$-NTA column (HiTrap 1 ml, Amersham) according to the manufacturer's instructions. The purification process was assessed by SDS-PAGE and Coomassie blue staining (Pierce).

### 2.4.6 Measurements of affinity and binding kinetics

The affinity and binding kinetic parameters for specific monoclonal antibodies (mAbs)/antigens interactions were measured by surface plasmon resonance (SPR) on a BIAcore 3000 biosensor system (BIAcore, Uppsala, Sweden).

Interactions between hen egg lysozyme mutants and the HyHel10, D1.3 and HyHel5 monoclonal antibodies (mAbs) were analysed by immobilizing the biotinylated mAbs on an SA sensor chip. Then, various concentrations of the different mutants were injected at a flow rate of 10 µl/min.

Interactions between p11 and p31 peptides and the 3-83 monoclonal antibody (mAbs) were analysed by immobilising the monobiotinylated peptides on an SA sensor chip. Then, various concentrations of the antibody were injected at a flow rate of 10 µl/min.

In both cases, the sensorgram of the negative control (unrelated biotinylated antibody or peptide) was subtracted from the interactions of the different antigens and the specific mAb.

All binding assays were performed in HEPES-buffered saline (Biacore, pH = 7.4).

### 2.4.7 CD1d molecules

The CD1d molecules loaded with the antigenic lipids were kindly provided by Dr Vincenzo Cerundolo (Institute for Molecular Medicine, Oxford). These proteins were prepared with a similar procedure as described in subsection 4.3.

## 2.5 Microscopy

### 2.5.1 Wide-field fluorescence microscopy

Wide-field Z-stack images of the interaction of B cells with antigen bearing COS-7 cells were acquired with a firewire Orca CCD camera (Hamamatsu, Japan) controlled by OpenLab software (Improvision, UK) on a Zeiss Axiovert LSM 510-META inverted microscope.

Z-stack images were deconvolved using the Volocity software package (Improvision, UK).

### 2.5.2 Scanning electron microscopy

MD4 transgenic B cells in contact with COS-7 cells transfected with a membrane-bound $HEL^{W1}$-GFP construct or in contact with artificial lipid bilayers loaded with HEL antigens were fixed by injecting in the flow chambers 1 ml of pre-warmed freshly prepared 4% paraformaldehyde (Sigma) at selected time-points. The

samples were then processed for scanning electron microscopy by the Electron Microscopy Unit (Cancer Research UK).

All the images were acquired in a JEOL JSM-6700F field emission scanning electron microscope at the Electron Microscopy Unit (Cancer Research UK).

### 2.5.3 Confocal microscopy

The kinetics of interaction of B cells with artificial lipid bilayers was monitored by confocal fluorescence microscopy and interference reflection microscopy (IRM) with a Zeiss Axiovert LSM 510-META inverted microscope equipped with the Zeiss software (Zeiss, Germany). All the images were acquired with a pinhole resulting in an effective optical slice of 1-2 μm. Images were analysed and processed with the Volocity software package (Improvision, UK).

The total number of molecules recruited was obtained by multiplying the accumulated density (molecules/$\mu m^2$) by the selected area ($\mu m^2$) in each cell or time-point. The accumulated density (molecules/$\mu m^2$) was estimated as *[intensity in the selected area (fluorescence units/ $\mu m^2$) - intensity in neighbouring area (fluorescence units/ $\mu m^2$)] / specific activity (fluorescence units/molecule)*. Selected areas were defined as regions in which the fluorescence due to antigen accumulation exceeded the average fluorescence of the lipid bilayer by 120%. Quantifications were done for at least 20 different cells in 3 independent experiments after synchronising the cells for their initial contacts with the lipid bilayer. The error in the total number of molecules recruited calculated is less than 5%, as assessed by the standard error between the independent experiments. The total area comprised inside the perimeter of the antigen signal defined areas of spreading. The error in the areas of spreading measured is less than 7%, as assessed by the standard error between the independent experiments.

### 2.5.4 Total internal reflection fluorescence microscopy

Total internal reflection fluorescence microscopy (TIRFM) images were acquired with a Cascade II CCD camera (Photonics) coupled to an Olympus IX-81 inverted microscope. Images were recorded with the Cell R software (Olympus), and analysed and processed with the Volocity software package (Improvision, UK).

## 2.6 Molecular biology

### 2.6.1 Plasmids and DNA fragments purification

Maxi preparations of plasmids were performed with the Qiagen maxi kit according to manufacturer's instructions (Qiagen).

DNA fragments, PCR amplification products and ligated plasmid DNA were purified from agarose gels. The DNA was visualised in agarose gels by ethidium bromide under low power UV light and the bands of interest were excised using clean scalpels. Agarose fragments were melted and the DNA isolated using a Qiagen gel extraction kit according to manufacturer's instructions (Qiagen).

### 2.6.2 Enzymatic manipulation of DNA fragments

Restriction enzymes, Klenow polymerase and T4 DNA ligase were purchased from NEB and used for restriction digestions, fragment amplification (PCR) and DNA ligations, respectively, according to standard procedures.

### 2.6.3 DNA sequencing

Sequencing reactions were set up using BigDyeTerminator mix according to manufacturer's instructions and purified using DyeEx spin columns (Qiagen). Samples were run on capillary sequencing gels (Prism 3730) by the Equipment Park Facility (CR-UK).

### 2.6.4 Bacterial transformation

Competent *Escherichia coli* bacteria (prepared in our laboratory) were used for cloning of DNA. The transformation was performed by heat shock according to standard protocols.

## 2.7 General methods

### 2.7.1 Cell treatment with inhibitors

B cells were treated with the src kinases inhibitors (PP1 or PP2, Calbiochem) at a concentration of 100 μM in chambers buffer. After 30 minutes of treatment at 37 °C cells were settled on the antigen loaded bilayers without washing.

ML-7 or blebbistatin (Calbiochem) treatment were performed by treating B cells with 100 μM in chamber buffer at 37 °C for 30 min, and injecting the cells without previous washing.

### 2.7.2 Immunostaining on lipid bilayers

Transgenic B cells were incubated with lipid bilayers loaded with their specific antigen at defined densities and then fixed at the indicated time points by injecting 1 ml pre-warmed 4% paraformaldehyde (Sigma) into the FCS2 chamber. After 10 min of incubation at 37°C, the cells were treated with permeabilising buffer (PBS, 0.2% Triton X-100) for 5 min at RT and blocked with PBS 1% BSA, 0.1% goat serum, 0.05% Tween-20, 0.1% $NaN_3$ for at least 1 hour. Cells were then stained for F-actin with 1 ml of Alexa Fluor 543-phalloidin (Molecular Probes, Invitrogen) in blocking buffer. After 20 minutes the chambers were washed with 2 ml of blocking buffer. Phosphotyrosine was revealed with the biotinylated 4G10 anti-pTyr antibody (Upstate Biotechnology) followed by incubation with Alexa Fluor 633-streptavidin (Molecular Probes, Invitrogen).

### 2.7.3 $Ca^{2+}$ influx assays

Intracellular $Ca^{2+}$ influx was measured by confocal microscopy with a fluorometric assay. Cells were labelled with fluo-4FF calcium indicator (Molecular Probes, Invitrogen) (1 μM in culture medium) for 30 min at room temperature, washed, and injected into the FCS2 closed chamber in chamber buffer. The $Ca^{2+}$ flux was monitored by the increase of fluorescence at ≈520 nm with an open pinhole to acquire the total signal.

The total mean fluorescence per cell was quantified as *[intensity in the selected cell – intensity in neighbouring area]* at each time point. Data represent the mean of 20 cells.

### 2.7.4 SDS-PAGE

Protein purification was assessed by SDS-PAGE performed on 4-20% acrylamide pre-cast gels (Pierce). Samples (≈ 5 μg of protein) were mixed with sample buffer (4x stock: 20% sodium dodecyl sulfate (SDS), 4% glycerol, 0.2% bromophenol blue, 5% 2-mercaptoethanol, 1 M Tris, pH = 8.6), heated at 95 °C for 5 min, and

loaded into the gels. The gels were then run according to the manufacturer's instruction. The running buffer (10x stock): 1 M Tris, 1 M HEPES, 10% SDS, pH=8.1.

Gels were stained either with commercial colloidal Coomassie Blue (Pierce) or with a commercial silver staining kit (Invitrogen) according to the manufacturer's instructions.

### 2.7.5 Preparation of Fab fragments of monoclonal antibodies

Fab fragments of purified monoclonal antibodies were prepared by enzymatic digestion with papain (Rousseaux et al., 1986). For this, the antibody was dialysed against phosphate buffer saline (PBS) and concentrated to ≈ 2 mg/ml.

Cysteine (from a freshly prepared 1 M stock solution) was added to a final concentration of 10 mM. The enzyme papain (Sigma) was diluted in PBS containing 10 mM cysteine to a final concentration of 1 mg/ml, and then activated at 37 °C for 10 minutes.

The activated enzyme was then added to the antibody solution (10 µg enzyme/1 mg of antibody), mixed and incubated at 37 °C (water bath). Mouse monclonal antibodies were incubated for 6 hs, and rat monoclonals for 2.5 hs.

The reaction was stopped by the addition of iodoacetamide (final concentration 0.5 mM, Sigma).

The Fab, Fc and intact antibody were isolated by size exclusion chromatography in the case of rat monoclonals. In the case of mouse monoclonal antibodies, the Fab fragments were separated from the Fc fragment and intact antibody molecules with a protein A column that binds the Fc portion of mouse antibodies.

Digestion and purification of the fragments was assessed by SDS-PAGE and Coomassie Blue staining.

# Chapter 3: Recognition of membrane antigens by B cells

## 3.1 Introduction

Recognition of membrane antigens by B cells is a poorly understood process. Batista et al reported for the first time the interaction of antigen specific B cells with cells expressing a membrane-bound form of the antigen (Batista et al., 2001). They observed that B cells accumulate the antigen in a central cluster that is later extracted (Batista et al., 2001). However, nothing is known of the kinetics of the recognition process or the parameters that govern it.

In order to elucidate the early events that take place during membrane antigen recognition, we analysed the interaction of BCR transgenic B cells with their specific antigen tethered on the surface of target cells or on artificial lipid bilayers.

## 3.2 Early events during B cell membrane antigen recognition

We first wanted to elucidate the early events that take place during membrane antigen recognition. To this end, we took advantage of B cells isolated from the spleen of MD4 transgenic mice (Goodnow et al., 1988). These B cells express a B cell receptor (BCR) derived from the HyHel10 antibody that specifically binds an epitope of the model antigen hen egg lysozyme ($HEL^{WT}$) with a very high affinity ($K_a = 2 \times 10^{10}\ M^{-1}$) (Figure 3.1).

In order to visualize the antigen we expressed the $HEL^{WT}$ fused to a transmembrane domain and to green fluorescent protein (GFP) on the plasma membrane of COS-7 cells. We used these cells as they have a large flat surface that allows better visualisation of events in a single focal plane. To follow the B cells, we labelled their plasma membrane with a lipid soluble dye, PKH26.

We then monitored their interaction in real time by fast 3D wide-field fluorescence microscopy.

We observed that 2-4 minutes after contact, most B cells rapidly spread over the target's surface, as assessed by the PKH26 staining (Figure 3.2 A and D). During this period, several small clusters of $HEL^{WT}$-GFP of approximately 0.5 to 1 μm in diameter appeared within the area of interaction. The flattening B cells reached a maximum surface area of contact of approximately 25 $\mu m^2$ and then gradually start to contract (Figure 3.2 A and D). During this second phase, which lasts for

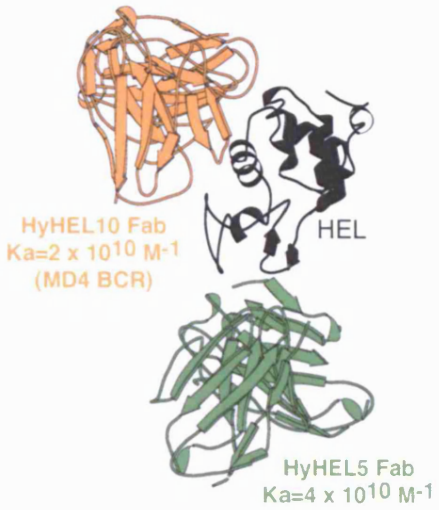


**Figure 3.1. X-ray crystal structure of a complex of HEL with two MAbs.**
This schematic diagram illustrates the X-ray crystal structure of the hen egg lysozyme (HEL) complexed with two monoclonal antibodies, the HyHel10 (expressed as a BCR by the MD4 transgenic line, gold) and the HyHel5 (green). Both antibodies bind the $HEL^{WT}$ antigen in non-overlapping epitopes and with a very high affinity of interaction (taken from Batista and Neuberger, 1998). Note that only the Fv portions are shown.

approximately 5-7 minutes, the antigen is gathered into a central defined cluster, with an eventual area of 10 $\mu m^2$ (Figure 3.2 A, C and D).

In order to determine whether this process is dependent on immunological recognition and not caused simply by cell-to-cell contact, we repeated the experiment with WT B cells with no specificity for the $HEL^{WT}$ antigen. As shown in Figure 3.2 B, C and D, these B cells do not form stable contacts or spread on the surface of COS-7 transfected cells, or aggregate any antigen.

To analyse in more detail the morphological changes of the B cells during the recognition process, we incubated the MD4 B cells with the $HEL^{WT}$-transfected COS-7 cells, fixed them at different time points and analysed them by scanning electron microscopy (SEM). The SEM data showed that indeed the shape of B cells correlates with the observed pattern of antigen accumulation: they initially spread over the target cell correlating with cluster formation, and later contract to collect the initially engaged antigen molecules (Figure 3.2 E).

From these experiments we conclude that membrane antigen recognition in B cells is characterised by a two-phase response. During the early minutes of this process B cells spread over the target surface and engage the antigen molecules in small clusters. During the second phase, B cells contract to aggregate the antigen molecules previously engaged in a central cluster.

What are the parameters that govern this process? Our main objective was to quantitatively analyse the membrane antigen recognition process in order to understand the parameters that drive it. However, one of the consequences of using cell-to-cell systems is the presence of multiple ligand/receptor interactions that cannot be controlled accurately, and therefore, effects due to the different interactions cannot be discriminated. Therefore, we looked for an alternative model system that would allow us to quantitatively study the membrane antigen recognition process.

Glass-supported artificial lipid bilayers constitute a simple and accurate model to mimic cell-to-cell interactions (Groves and Dustin, 2003). Thus, next we decided to set-up a system of glass-supported artificial bilayers to study quantitatively the interaction of B cells with membrane antigens by confocal microscopy.

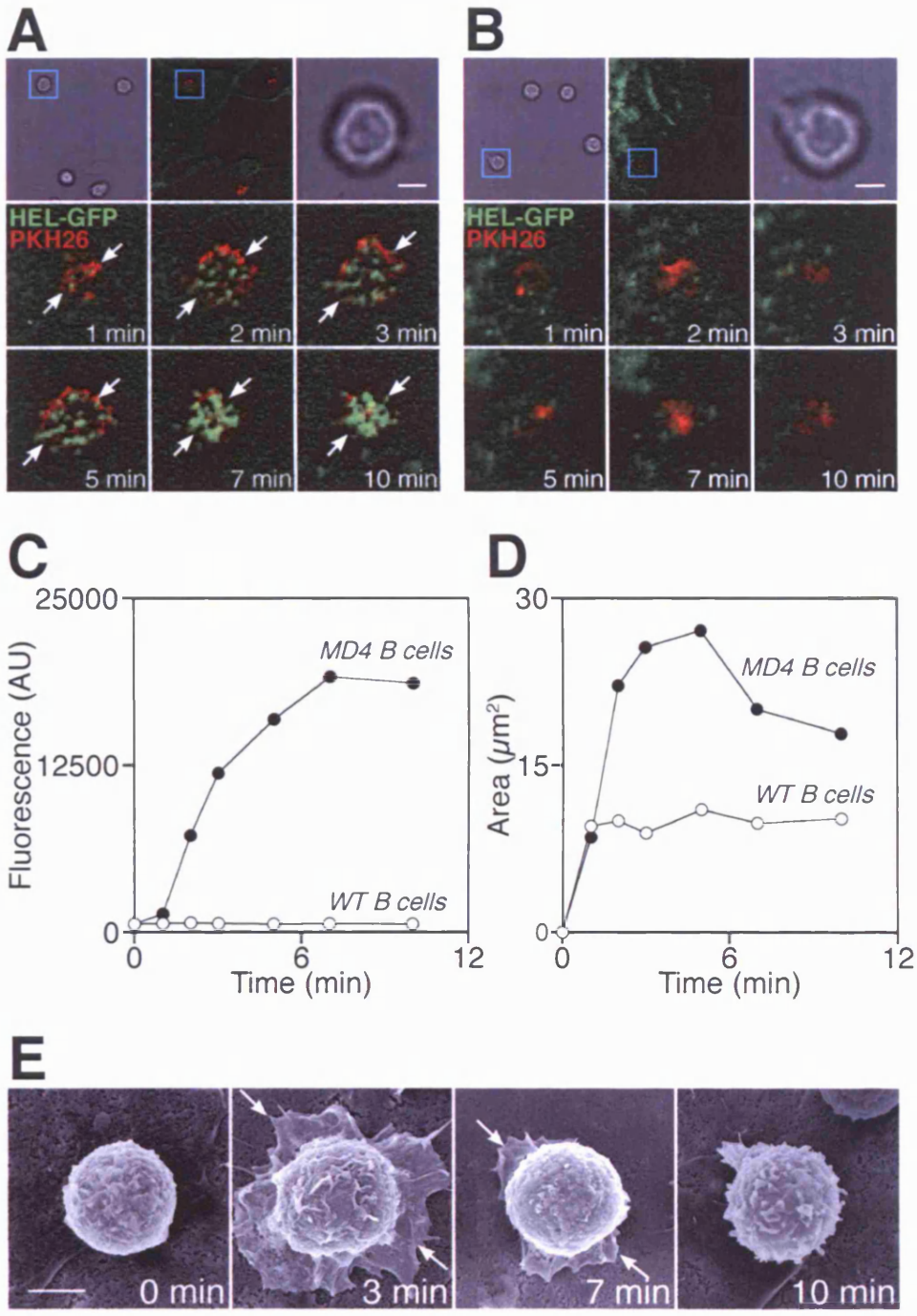


**Figure 3.2. Recognition of membrane antigens by B cells: cell-to-cell interaction.** **(A)** Transgenic MD4 or **(B)** wild-type naive B cells were labelled with PKH26 dye (red) to visualise the cell membrane and incubated with COS-7 cells expressing a membrane-bound form of $HEL^{WT}$-GFP fusion protein (green). Z-stacks images of the cells were acquired every 1 min. The time lapse shows the overlayed antigen (green) and B cell membrane (red) images for the selected cell. A single confocal plane for each time point is pictured. **(C)** Amount of antigen accumulated in total units of fluorescence and **(D)** the area of contact for the antigen recognition process quantified as a function of time. **(E)** SEM analysis of the same process showed in **(A)**. The arrows show the limits of the spreading B cell. Scale bars: 2 μm.

## 3.3 Artificial lipid bilayers system as a model to study cell-to cell interactions

Artificial lipid membranes have been extensively used as simplified models of the plasma membrane for the last 40 years. Bilayers accessible on both sides generated in small apertures ('black lipid bilayers') or on the tip of glass electrodes were initially introduced by electrophysiologists to characterise the electrochemical properties of ion channels incorporated into these artificial membranes (Hladky and Haydon, 1970; Mueller et al., 1962). This model system was later extended to study lymphocyte-mediated lysis of target cells by measuring the changes in the electrical properties of the bilayers due to the secretion of lytic mediators (Henkart and Blumenthal, 1975). A clear breakthrough came with the introduction of glass-supported planar lipid monolayers by Hafeman et al. as it expanded the artificial membrane technology to study cell-membrane interactions by fluorescence microscopy (Hafeman et al., 1981).

Since then artificial lipid bilayers have become an invaluable system model to study the interaction of lymphocytes with membrane ligands (Brian and McConnell, 1984; Groves and Dustin, 2003). The composition of the bilayers as well as the molecular densities can be precisely controlled. Due to the flat surface of the glass support used to generate the bilayers, in combination with confocal microscopy they become a powerful quantitative technique. In order to study quantitatively the interaction of B cells with membrane bound antigens we set-up a glass supported artificial bilayer system. Our idea was to generate bilayers on which freely diffusing and fluorescently labelled ligands could be tethered in order to follow the ligand recognition process by confocal microscopy.

### 3.3.1 Tethering molecules on lipid bilayers: GPI-linked molecules

A major difficulty of the artificial bilayers systems is how to tether ligand molecules on their surface with the characteristics described above. Different ways of tethering molecules to artificial bilayers have been previously used for structural and electrophysiological studies. However, we decided to explore fluorescently labelled GPI-linked molecules, since they have been successfully used to study cell-membrane interactions by confocal microscopy (Chan et al.,

1991; Dustin et al., 1996).

GPI-linked molecules are expressed and purified from the plasma membranes of transfected cells. Once incorporated into artificial lipid bilayers they can freely diffuse, and their interaction with cells can be followed by confocal microscopy (Bromley et al., 2001; Carrasco et al., 2004).

In this study, instead of expressing a GPI-linked form of the antigen, we decided to express a GPI-linked Fab fragment of an anti-HEL antibody, HyHel5, that binds a non-overlapping epitope of the HEL recognised by the HyHel10 BCR expressed by the MD4 transgenic B cells (Figure 3.1). The affinity of the HyHel5/HEL interaction is extremely high, and therefore the complexes should be stable for long periods of time (Figure 3.1). This strategy would result an advantage for our studies.

#### 3.3.1.1 Expression and purification of a GPI-linked HyHEL5 Fab fragment protein

The Fab fragment of the HyHel5 antibody was expressed and purified as a GPI-linked protein on the plasma membrane of the Sp2/0 cell line (see Materials and Methods for a detailed description). Briefly, cell membranes were solubilised in Triton X-100 buffer, and the fusion GPI-linked protein was then captured in a HEL-coupled Sepharose column. To fluorescently label the captured protein, the column was injected with Alexa Fluor 488 reagent and incubated for 30 minutes to allow the reaction to take place. Then the column was extensively washed and the labelled fusion protein eluted with acidic buffer.

We evaluated the presence of the protein in the fractions by FACS with streptavidin-coated beads loaded with biotinylated HEL (see Materials and Methods). As shown in Figure 3.3 A, five of the eight eluted fractions contained intact and biologically active GPI-linked Fab fragment. The protein in these fractions had a high level of purity (>90%) as assessed by SDS-PAGE (Figure 3.3 B).

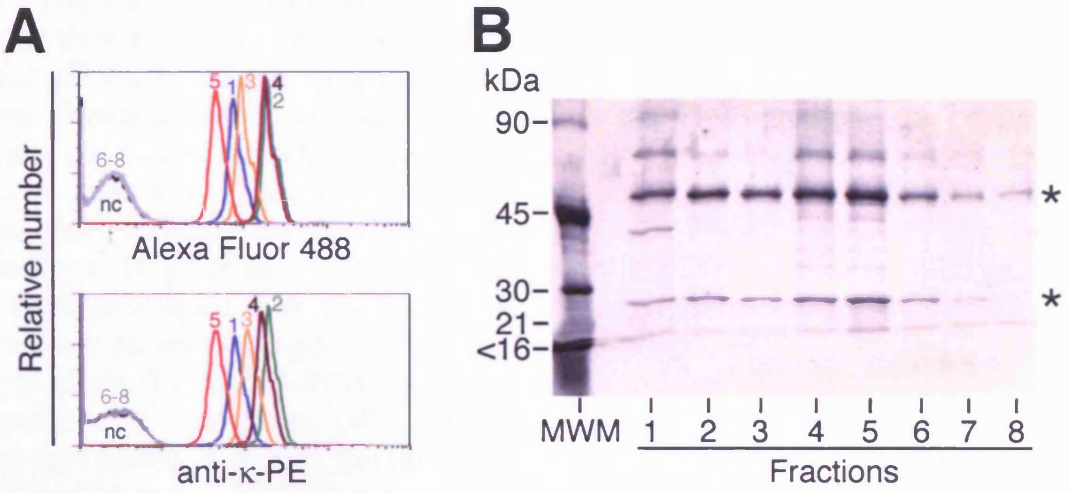
A
Relative number
6-8
nc
5
1
3
4
2
Alexa Fluor 488
anti-κ-PE
B
kDa
90
45
30
21
<16
*
*
MWM
1
2
3
4
5
6
7
8
Fractions

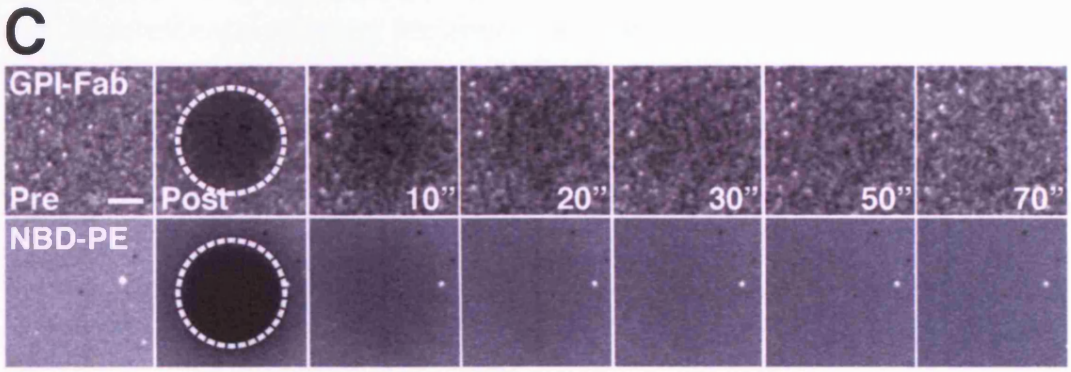
C
GPI-Fab
Pre
Post
10"
20"
30"
50"
70"
NBD-PE

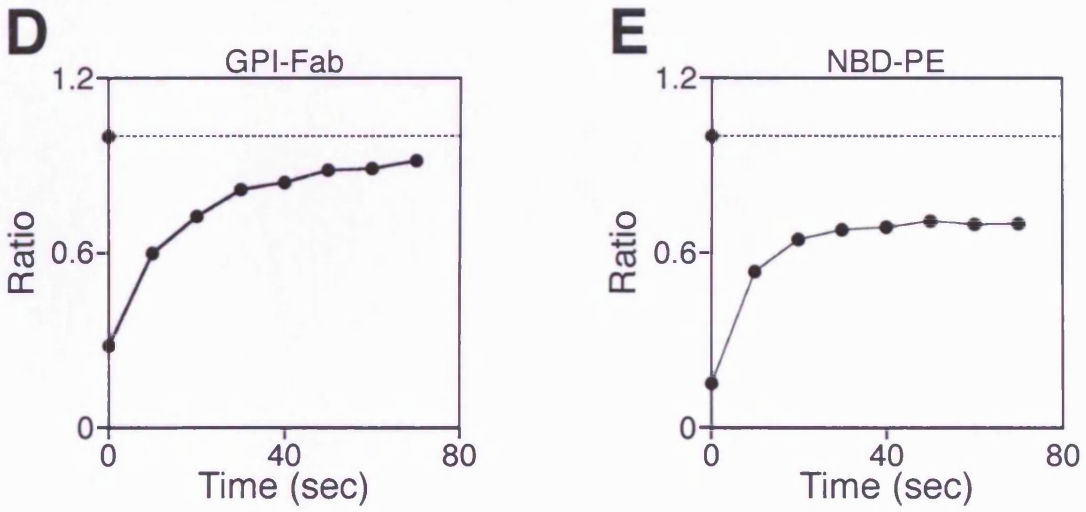
D
GPI-Fab
1.2
0.6
0
Ratio
0
40
80
Time (sec)
E
NBD-PE
1.2
0.6
0
Ratio
0
40
80
Time (sec)

**Figure 3.3. Purification and characterisation of the GPI-linked Fab fragment of the HyHel5 anti-HEL monoclonal antibody.**
**(A)** The GPI-linked Fab protein was detected in the eluted fractions by FACS analysis with HEL-coated beads. HEL-coated beads (1 μl/sample) were incubated with dilutions of each eluted fraction, and the protein bound to the beads was then detected with an anti-kappa-PE antibody and FACS analysis. The histograms show the fluorescence from the labelling reagent used to label the protein (Alexa Fluor 488, top panel) and from the antibody (anti-kappa-PE, bottom panel). Numbers indicate the fraction number. **(B)** SDS-PAGE analysis of the eluted fractions. 10 μl of each fraction were loaded in 4-20% polyacrylamide gel, and the gel developed with silver staining. The asterisks mark the bands of the Fab fragment corresponding to the heavy chain fused to GFP (55 kDa) and the kappa light chain (25 kDa). MWM: molecular weight markers. **(C)** FRAP experiments of lipid bilayers containing GPI-linked Fab fragment (top panel) or NBD-PE lipids (bottom panel). A spot on the lipid bilayer (white dotted circle) was bleached with 25 laser pulses, and the fluorescence recovery was followed for 2 min. Scale bar: 2 μm. Fluorescence recovery (expressed as *ratio = mean intensity at time n after bleaching / mean intensity at t=pre-bleaching*) of lipid bilayers containing **(B)** GPI-linked Fab fragment and **(C)** NBD-PE lipids is represented as a function of time.

### 3.3.1.2 Functional evaluation of the GPI-linked Fab fragment

The purified labelled GPI-linked protein was reconstituted in DOPC liposomes by detergent dialysis according to standard procedures (Mimms et al., 1981) see Materials and Methods for a detailed explanation). Artificial lipid bilayers were then prepared by liposome spreading on the surface of clean glass coverslips in the FCS2 closed chamber system (Brian and McConnell, 1984) (Materials and Methods).

The GPI-linked Fab can freely diffuse, as evidenced by the recovery of the fluorescent signal in a simple fluorescence recovery after photobleaching (FRAP) experiment performed by confocal microscopy (Figure 3.3 C and D). Furthermore, the diffusion rate is comparable to the diffusion rate observed for fluorescently labelled lipid molecules (Figure 3.3 C, D and E).

### 3.3.1.3 Estimation of the density of molecules of GPI-linked Fab fragment protein on the artificial bilayers

In order to study the recognition process in a quantitative way, it was important to estimate the density of antigen on the bilayer. To this end, we generated artificial lipid bilayers on glass coverslips that have a defined area (Figure 3.4 A). We then resuspended the lipid bilayers with detergent buffer and measured the amount of HyHel5 Fab fragment with a capture enzyme-linked immunosorbent assay (ELISA) (Figure 3.4 B, and see Materials and Methods for a detailed explanation). Finally, we estimated the density dividing the number of molecules of HyHel5 Fab fragments measured by ELISA by the area of the bilayers prepared in the glass coverslips.

### 3.3.1.4 Recognition of antigens tethered on lipid bilayers

We next tested the capacity of MD4 B cells to interact with the antigen tethered on the artificial lipid bilayers. As shown in Figure 3.5 A, after 10 minutes of interaction most B cells are able to make contacts with the bilayer as assessed by IRM (interference reflection microscopy), a technique that allows visualising tight contacts between the cell and the bilayer. During the same period, B cells aggregate the freely diffusing antigen in a central cluster (green), as the fluorescence intensity associated with it increases in the point of contact (Figure

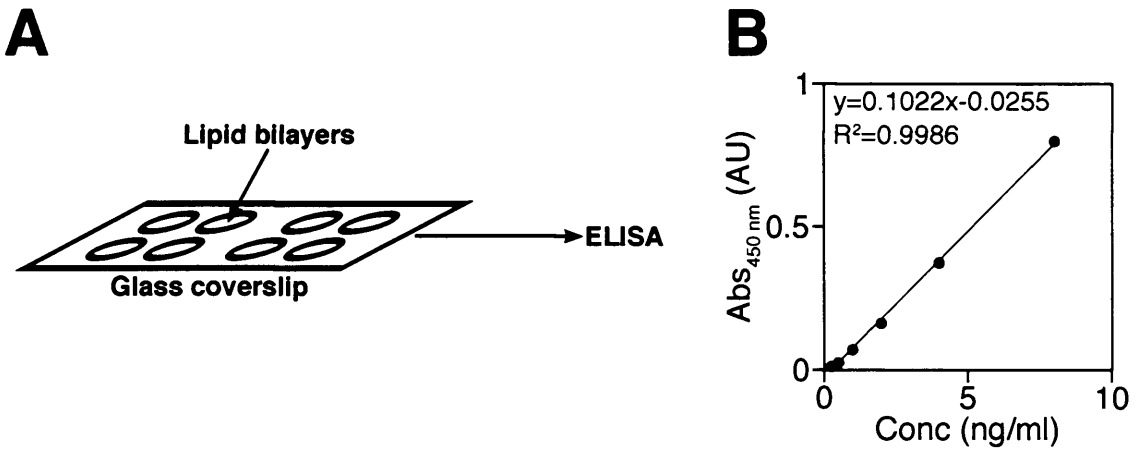


**Figure 3.4. Estimation of the molecular density of the GPI-linked Fab fragment on artificial lipid bilayers.**

**(A)** Artificial lipid bilayers containing the GPI-linked HyHel5 Fab fragment were prepared on glass coverslips that have a defined surface area (Culturewell, Grace Bio-Labs). Then, the lipids were recovered with a buffer containing detergent and the amount of Fab fragment measured by ELISA. **(B)** A calibration curve was obtained with Fab fragments prepared from the HyHel5 monoclonal antibody. The density of antigen was then estimated by dividing the number of molecules of Fab fragment measured by ELISA by the area of the coverslip.

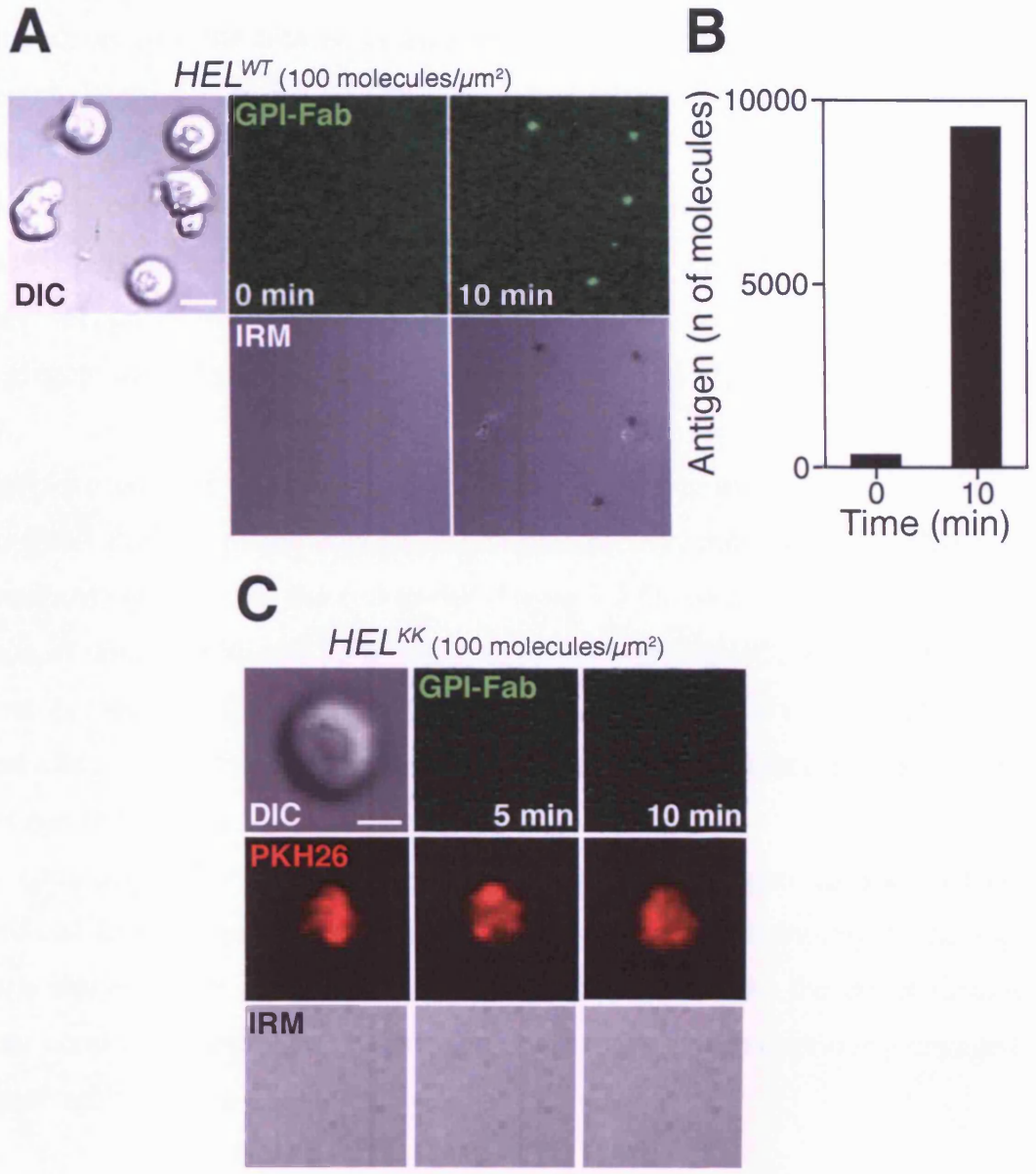


**Figure 3.5. Recognition of the HEL$^{WT}$ antigen tethered on artificial lipid bilayers through the GPI-linked Fab fragment by MD4 B cells.**
**(A)** Confocal images of MD4 B cells settled on artificial bilayers loaded with the HEL$^{WT}$ antigen tethered through the GPI-linked Fab (GPI-Fab, green) at a density of 100 molecules/μm$^2$. The cells efficiently recognise and accumulate the antigen as observed by the increase in the fluorescence intensity at the site of contact. Contacts with the bilayer were assessed by IRM (interference reflection microscopy). Scale bar: 5 μm. **(B)** Shows the amount of antigen aggregated by the MD4 B cells after 10 minutes of interaction. **(C)** Confocal images of MD4 B cells settled on artificial bilayers loaded with HEL$^{KK}$ antigen tethered through the GPI-linked Fab (GPI-Fab, green) at a density of 100 molecules/μm$^2$. Scale bar: 2 μm.

3.5 A and B). When we tested B cells for their capacity to recognise a mutant HEL with no measurable affinity for the BCR ($HEL^{KK}$), we could not detect any interaction with the bilayer as assessed by IRM or non specific GPI-linked Fab accumulation (Figure 3.5 C). This shows that antigen accumulation is dependent on immunological recognition.

The lipid bilayer system was also able to recapitulate what we observed in a cell-to-cell interaction: B cells initially spread over the surface of the bilayer when they recognise the tethered antigens, and after this phase they contract to aggregate the antigen previously engaged in a central cluster (Figure 3.6 A, B and C).

Next, we wanted to understand if the cell spreading and contraction response triggered during antigen recognition correlates with morphological changes, as previously observed in the cell-to-cell (Figure 3.2 E). To this end, we fixed MD4 B cells in contact with the lipid bilayers loaded with the HEL antigens at different time points and then analysed them by SEM. As shown in (Figure 3.6 D), spreading and contraction seems to be a general mechanism during membrane antigen recognition by B cells.

In conclusion, B cells effectively recognise and aggregate antigens tether on artificial lipid bilayers through a GPI-linked anti-HEL Fab fragment. During the early stages of the recognition process B cells spread over the target surface to later contract during which B cells accumulate the antigen previously engaged, as observed in the cell-to-cell system.

### 3.3.1.5 Membrane antigen recognition: dependence on density and affinity

We then wanted to understand what are the parameters that define the thresholds for membrane-antigen recognition. We postulated that the density of antigen on the bilayer should have an impact on the antigen recognition process. To achieve the different antigen densities, the liposomes containing the GPI-linked Fab were diluted with DOPC liposomes.

As shown in Figure 3.7, when we decreased the density of antigen on the artificial membrane, the amount of antigen that B cells accumulated also decreased. We determined that B cells recognise and aggregate $HEL^{WT}$ at densities as low as $\approx 15$ molecules/$\mu m^2$. Below this value B cells do not longer recognise the antigen even

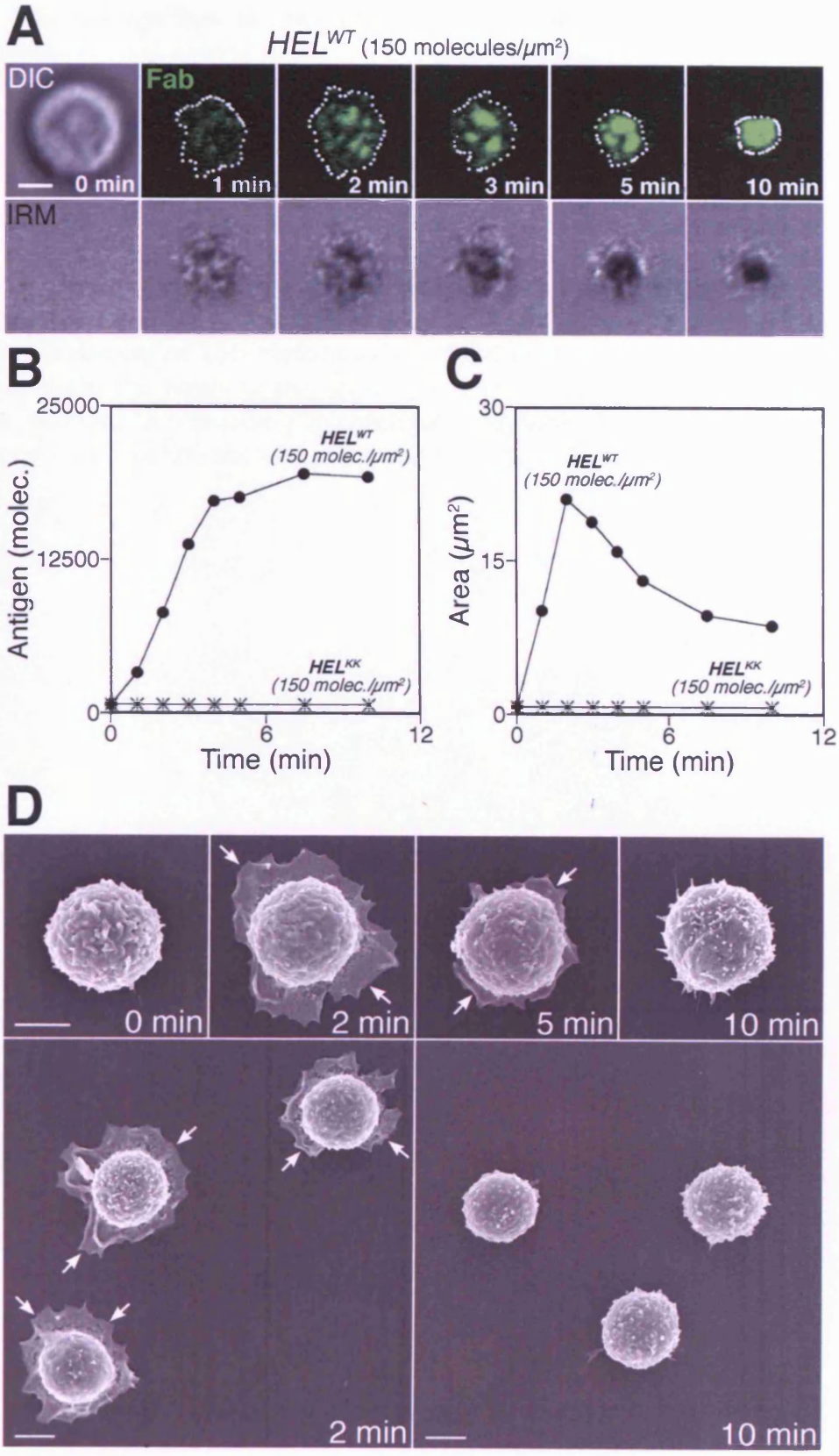
A
HEL^WT (150 molecules/μm²)
DIC
Fab
IRM
0 min
1 min
2 min
3 min
5 min
10 min
B
Antigen (molec.)
25000
12500
0
HEL^WT (150 molec./μm²)
HEL^KK (150 molec./μm²)
0
6
12
Time (min)
C
Area (μm²)
30
15
0
HEL^WT (150 molec./μm²)
HEL^KK (150 molec./μm²)
0
6
12
Time (min)
D
0 min
2 min
5 min
10 min
2 min
10 min

**Figure 3.6. Recognition of membrane antigens on bilayers: spreading and contraction.**

**(A)** The time lapse shows confocal images of transgenic MD4 naïve B cells in contact with an artificial lipid bilayer loaded with $HEL^{WT}$ antigen at a density of 150 molecules/$\mu m^2$. Contacts of the B cells with the bilayer were visualised by IRM (grayscale, lower panels). Dotted lines indicate the perimeter of the spreading cell as assessed by the fluorescent antigen signal. Scale bar: 2 μm. **(B)** Amount of $HEL^{WT}$ antigen aggregated and **(C)** surface area of spreading quantified as a function of time. **(D)** Scanning electron microscopy (SEM) images of transgenic MD4 naïve B cells in contact with artificial lipid bilayer loaded with $HEL^{WT}$ antigen at a density of 150 molecules/$\mu m^2$ fixed at indicated time points. White arrows indicate the limits of the spreading B cell. 65% of cells examined at 2 minutes showed a spreading phenotype (indicated by the presence of a lamellipodia), while 0% showed the same phenotype at 10 minutes. Scale bar: 2 μm.

though the affinity of this interaction is extremely high (Figure 3.7). The amount of antigen aggregated showed an exponential decrease with the density on the bilayer (Figure 3.7).

This finding suggests that a minimum affinity threshold governs the effective recognition and accumulation of antigen. If so, then there should be interplay between antigen density and the strength of the BCR/antigen interaction. But, what is the effect of the affinity on the thresholds of antigen recognition?

To address this question we took advantage of a set of mutant lysozymes obtained by alanine scanning of the $HEL^{WT}$ epitope recognised by the HyHel10 BCR (Batista and Neuberger, 1998). These antigens show a 20,000-fold range of affinities for the BCR mainly due to their off-rates, as measured by surface plasmon resonance (SPR) (Figure 3.8 and Table 1).

We then explored the kinetics of antigen aggregation for the different mutants of HEL displayed on the bilayers at different densities. As shown in Figure 3.9 A and B, a minimum affinity of $1 \times 10^6$ $M^{-1}$ is necessary in order to trigger effective antigen accumulation. Above this affinity threshold, B cells are sensitive to the precise antigen/BCR binding affinity and give a proportional response up to a plateau of $5 \times 10^7$ $M^{-1}$. For example, when we tested the $HEL^{K}$ and $HEL^{RKD}$ mutants that have affinities of $8.7 \times 10^6$ $M^{-1}$ and $8 \times 10^5$ $M^{-1}$ respectively, we observed that B cells discriminated them by the total amount of antigen accumulated as well as by the slower kinetics of their aggregation (Figure 3.9 B). However, when we assessed the $HEL^{RDGN}$ mutant that has an affinity of $5.2 \times 10^7$ $M^{-1}$, we observed that B cells accumulated equivalent amounts of antigen compared to $HEL^{WT}$ (Figure 3.9 B).

In order to understand if the high levels of antigen on the artificial bilayers were responsible for the lack of discrimination in the upper range of affinities, we explored the kinetics of antigen recognition for the different antigens displayed at decreasing densities. As shown in Figure 3.10 A, when we decreased the density of antigen on the bilayer by half from 150 to 75 molecules/$\mu m^2$, HEL mutants with binding affinities lower than $8 \times 10^5$ $M^{-1}$ were no longer accumulated, however, mutants with affinities greater than $5 \times 10^7$ $M^{-1}$ were accumulated at similar amounts. A further 5-fold decrease in the density of antigen did not improve the discrimination of antigen affinities (Figure 3.10 B).

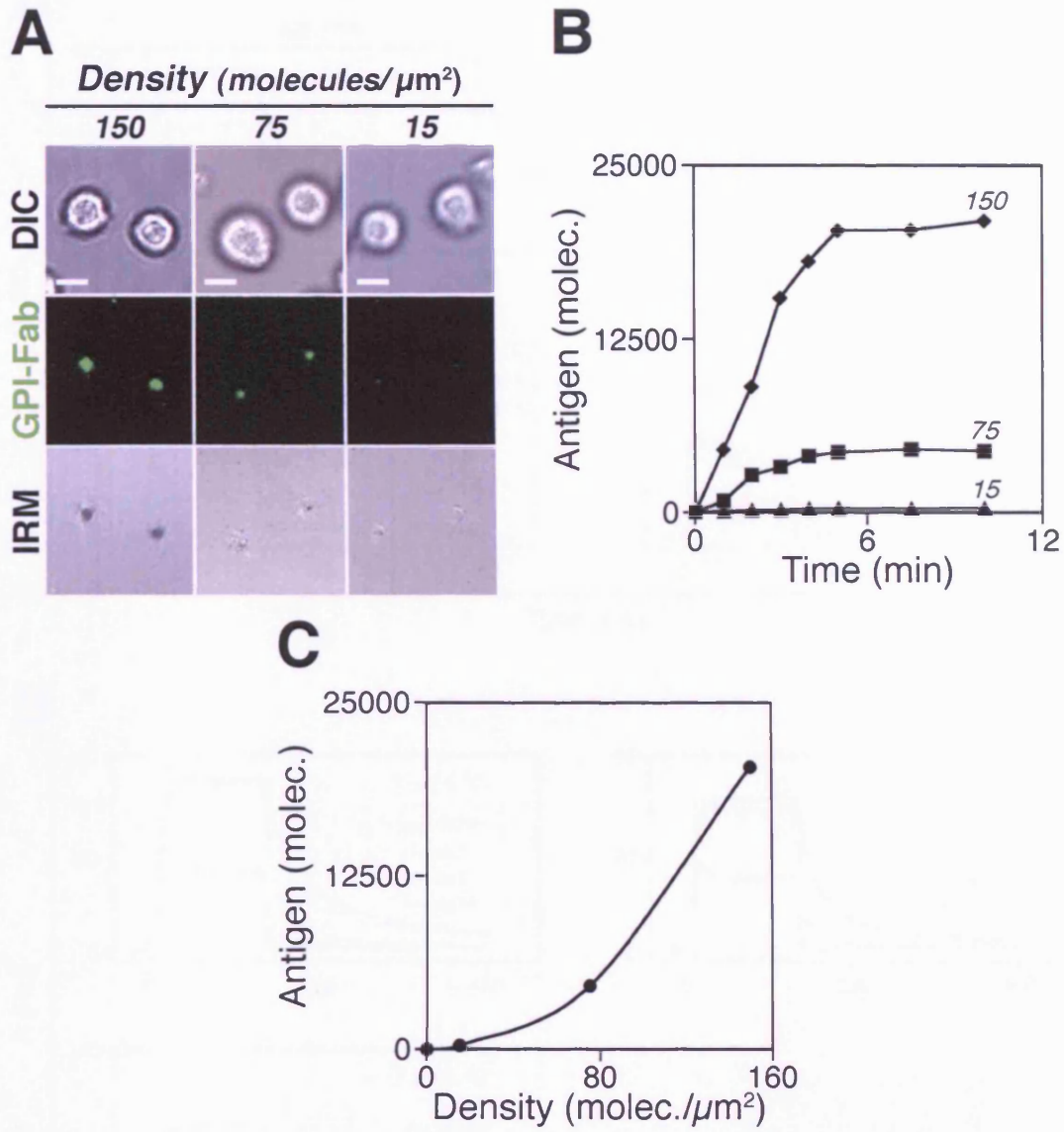


**Figure 3.7. Dependence of B cell membrane antigen recognition on the density of antigen on the target membrane.**

MD4 B cells were settled on artificial bilayers loaded with the $HEL^{WT}$ antigen at the indicated densities, and the kinetics of interaction followed by confocal microscopy. **(A)** Shows representative B cells after 10 minutes of interaction with the antigen loaded bilayers. Contacts with the bilayers were assessed by IRM. Scale bars: 4 μm. **(B)** Shows the kinetics of antigen accumulation for the different densities tested. **(C)** Shows the dependence of the total molecules of antigen accumulated after 10 minutes of contact with the density of antigen displayed on the artificial bilayer.

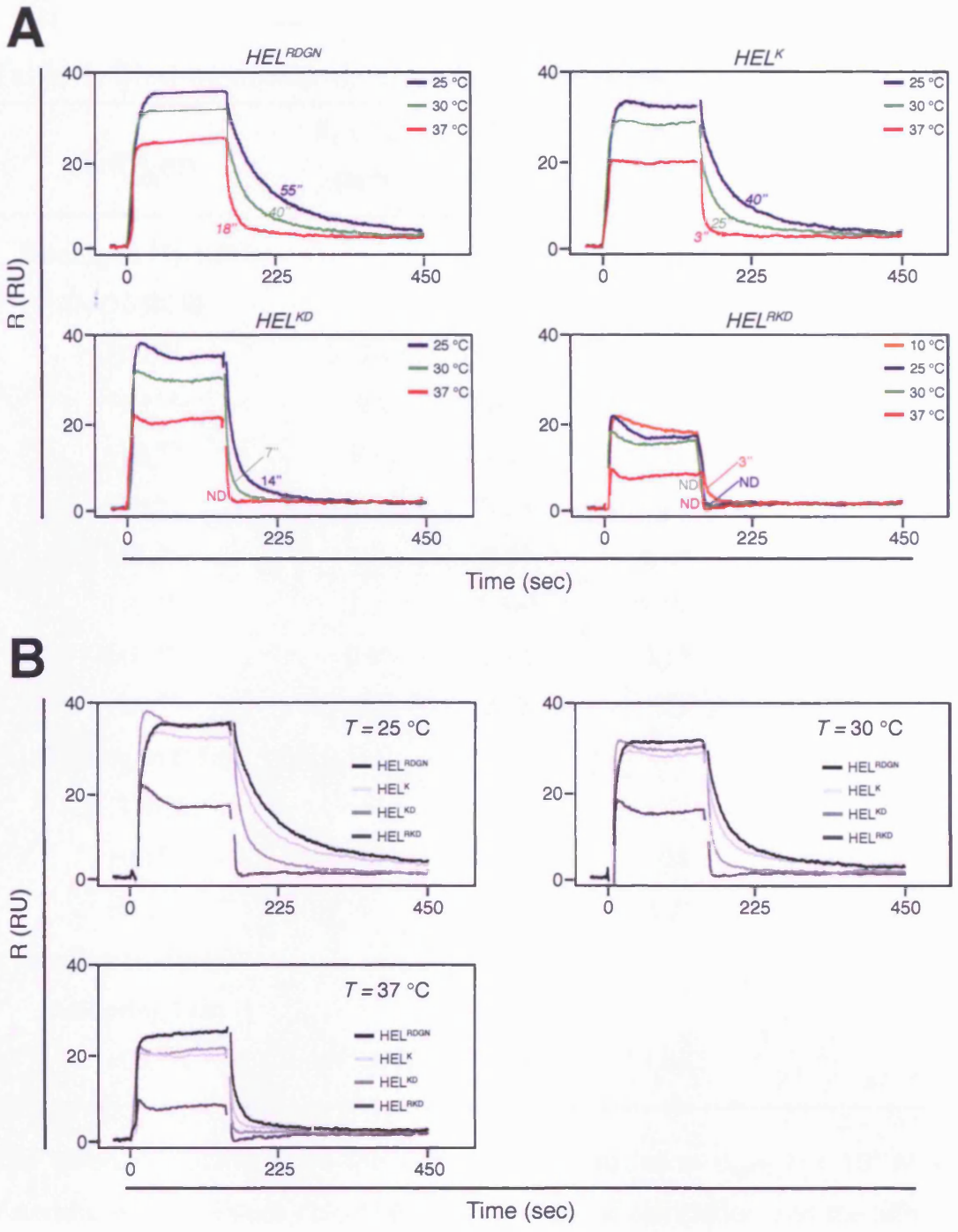


**Figure 3.8. Analysis of the kinetics of binding of the HyHel10 monoclonal antibody with the HEL mutants by surface plasmon resonance.**
**(A)** Shows the overlaid sensorgrams (Resonance Units (RU) as a function of time (sec)) at varying temperatures of the interaction between the HyHel10 monoclonal antibody and the indicated HEL mutants. Values indicate the measured dissociation half-life in seconds. **(B)** Shows the overlaid sensorgrams of the interaction between the HyHel10 monoclonal antibody and different HEL mutants at the indicated temperature. Note the strong dependence of the dissociation half-life with the temperature, while the $k_{on}$ is rather insensitive.

**Table 1. Binding constants of mutant lysozymes.**

| Antigen | $K_a \times 10^6$ ($M^{-1}$) | $k_{off}$ ($sec^{-1}$) | $t_{1/2}$ 37 °C (sec) | $t_{1/2}$ 10 °C (sec) |
|---|---|---|---|---|
| **Binding to HyHel10 (MD4 BCR)** | | | | |
| $HEL^{WT}$ | 20,740 | 0.0001 | 7,187 | 17,000 |
| $HEL^{RD}$ | 793 | 0.0025 | 275 | 720 |
| $HEL^{RDGN}$ | 52 | 0.0385 | 18 | 170 |
| $HEL^{K}$ | 8.7 | 0.23 | 3 | 20 |
| $HEL^{KD}$ | 4 | 0.5* | 1.4* | 12 |
| $HEL^{RK}$ | 1.3 | 1.54* | 0.45* | 5 |
| $HEL^{RKD}$ | 0.8 | 2.5* | 0.3* | 2 |
| $HEL^{KK}$ | <0.4 | ND | ND | ND |
| **Binding to D1.3 (D1.3 BCRs)** | | | | |
| $HEL^{WT}$ | 300 | 0.0067 | 104 | - |
| $HEL^{V}$ | 5 | 0.41 | 1.7 | - |
| **Binding to HyHel5 (tethering Fab)** | | | | |
| $HEL^{WT}$ | 40,000 | 0.00005 | 13,852 | - |

The different mutants share the same rate of association ($k_{on} \approx 2 \times 10^6$ $M^{-1}s^{-1}$). Asterisks indicate values calculated from the rate of association and the affinities measured by SPR.

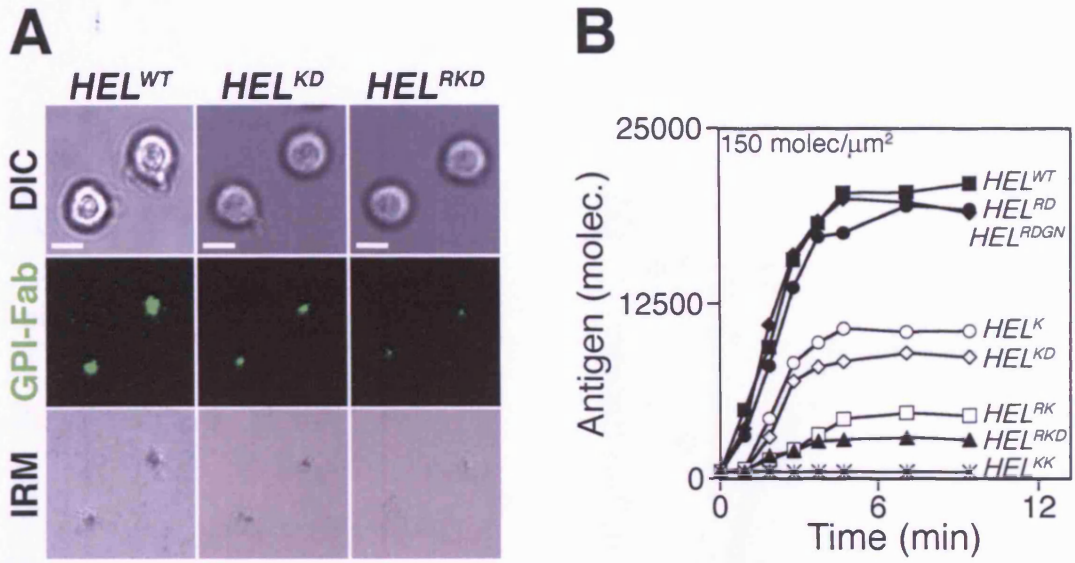


**Figure 3.9. Dependence of B cell membrane antigen recognition on the affinity of the BCR/antigen interaction.**

MD4 B cells were settled on artificial bilayers loaded with the indicated HEL mutant antigen at a density of 150 molecules/$\mu m^2$, and the kinetics of interaction followed by confocal microscopy. **(A)** Shows representative B cells after 10 minutes of interaction with the antigen loaded bilayers. Contacts with the bilayers were assessed by IRM. Scale bar: 4 μm. **(B)** Shows the kinetics of antigen accumulation for the different mutants of HEL.

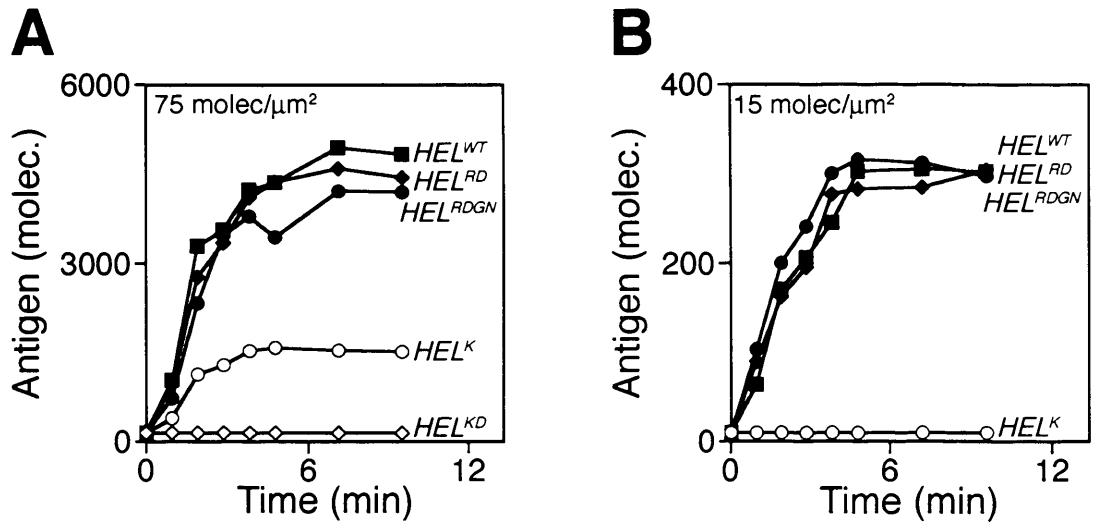


**Figure 3.10. Evidence of an affinity ceiling in membrane antigen recognition.** MD4 B cells were settled on artificial bilayers loaded with the different HEL antigens at the indicated densities, and the kinetics of interaction followed by confocal microscopy. The plots show the kinetics of antigen accumulation for **(A)** 75 molecules/μm² and **(B)** 15 molecules/μm². Note that B cells cannot discriminate $HEL^{RDGN}$ from $HEL^{WT}$ even though their 400-fold difference in affinity.

Thus, the affinity of the antigen for the BCR and the density at which it is displayed are the two parameters that define the thresholds of membrane antigen aggregation. If this avidity threshold is overcome, then the amount of antigen aggregated will be proportional to the affinity. However, once the affinity is greater than 2.5 x $10^8$ $M^{-1}$, a ceiling is achieved and equivalent amounts of antigen are accumulated.

### 3.3.2 Recognition of polyvalent antigens: biotinylated lipids

The HEL tether through the GPI-linked Fab fragment is presented as a monovalent antigen to MD4 B cells. However, it is likely that in vivo antigens are presented to B cells as immunocomplexes, and therefore as polyvalent species (Haberman and Shlomchik, 2003). Avidity effects that arise from this situation are difficult to account for and they can result in changes in thresholds and/or ceilings. Furthermore, affinity values and kinetic parameters of the BCR/antigen interaction obtained by SPR, and therefore as monomeric species, cannot be related in any simple way to multivalent species. Then, we wanted to understand what is the effect of the antigen valency in the recognition process.

To study this we looked for an alternative way of tethering antigens on the bilayers. Bilayers or monolayers containing biotinylated lipids have been extensively used for structural and thermodynamic studies of proteins (Muller et al., 1993; Uzgiris and Kornberg, 1983). We wanted to adapt the same technology to explore the interaction of B cells with polyvalent membrane-bound antigens with the idea that avidin would work as a bridge between the biotinylated lipid on the bilayer and a biotinylated antigen or molecule. A labelled avidin would also provide the fluorescence required for confocal microscopy studies. Furthermore, the high affinity interaction of avidin/biotin would ensure stability for the complexes for very long periods of time ($K_a$>$10^{15}$ $M^{-1}$).

#### 3.3.2.1 Preparation and characterisation of lipid bilayers containing biotinylated lipids

The first step was to prepare and characterise the bilayers. Liposomes containing biotinylated phosphoethanolamine (N-biotinyl Cap-PE) lipids were prepared by sonication and detergent dialysis according to standard procedures (see Materials

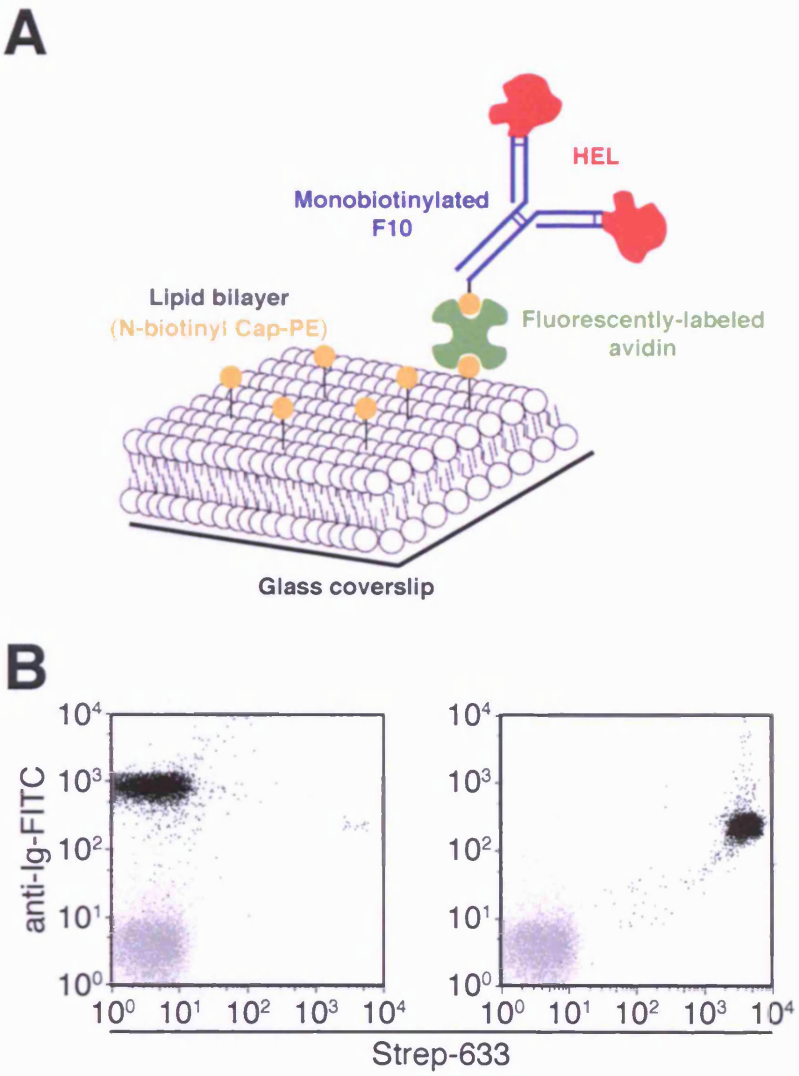


**Figure 3.11. Antigens tethered on artificial lipid bilayers through biotinylated lipids.**

**(A)** Lipid bilayers containing biotinylated lipids (N-biotinyl Cap-PE, yellow) are generated on the surface of glass coverslips. The HEL antigen (red) is tethered through a monobiotinylated F10 antibody (blue) - avidin (bright green) bridge. The avidin is fluorescently labelled and therefore the antigen bound to it. **(B)** Streptavidin-coated beads were used to estimate the degree of biotinylation of the F10 antibody. The beads were coated with the biotinylated F10, and then labelled with an anti-Ig (FITC) and streptavidin-Alexa Fluor 633. The degree of biotinylation can be distinguished by the levels of streptavidin-Alexa Fluor 633 staining as shown by the FACS profiles of beads coated with a monobiotinylated (left panel) or a polybiotinylated F10 antibody (right panel). Uncoated control beads are shown in gray.

and Methods for a detailed explanation). Artificial lipid bilayers were then prepared by liposome spreading on the surface of clean glass coverslips in the FCS2 closed chamber system (Brian and McConnell, 1984).

To avoid the modification of the HEL antigen with the biotin reagent which may interfere with its binding to the receptor, we looked for an alternative way to load it on the fluorescently labelled avidin tethered on the bilayer. This was achieved by generating a monobiotinylated form of a HEL specific antibody to use as a linking molecule (Figure 3.11 A).

The F10 antibody binds HEL with a very high affinity ($K_a$=5 x $10^{10}$ $M^{-1}$) in an epitope overlapping the one recognised by the HyHel5 monoclonal antibody - used for the GPI-linked system - and therefore, it does not affect the binding to the HyHel10 antibody expressed as a BCR by the MD4 transgenic mice strain (Figure 3.1).

The monobiotinylated form of the F10 was obtained by mixing the antibody with limiting amounts of the NHS-sulfolink LC biotin reagent. The degree of biotinylation was assessed by FACS using streptavidin-coated beads (Figure 3.11 B).

We then loaded the artificial bilayers sequentially with Alexa Fluor 488-avidin, the monobiotinylated F10 antibody and $HEL^{WT}$ antigen solutions (Materials and Methods).

In order to assess the diffusion of molecules on the bilayers, we performed FRAP experiments. These showed that antigen molecules tethered on bilayers through an avidin bridge freely diffuse and their diffusion rate is comparable to the diffusion rate of fluorescently labelled lipids (NBD-PE) (Figure 3.12 A, B and C). MD4 B cells can interact with the freely diffusing molecules as assessed by IRM and accumulate the antigen in a central cluster as the fluorescence intensity associated with it increases in the point of contact (Figure 3.12 D and E).

### 3.3.2.2 Determination of the density of antigen

In order to quantitatively study the membrane antigen recognition process, we needed to determine the density of antigen on the bilayers. We initially tried the same approach that we had used to measure the density of the GPI-linked Fab membranes. But as the ELISA employed to measure the concentration of Fab

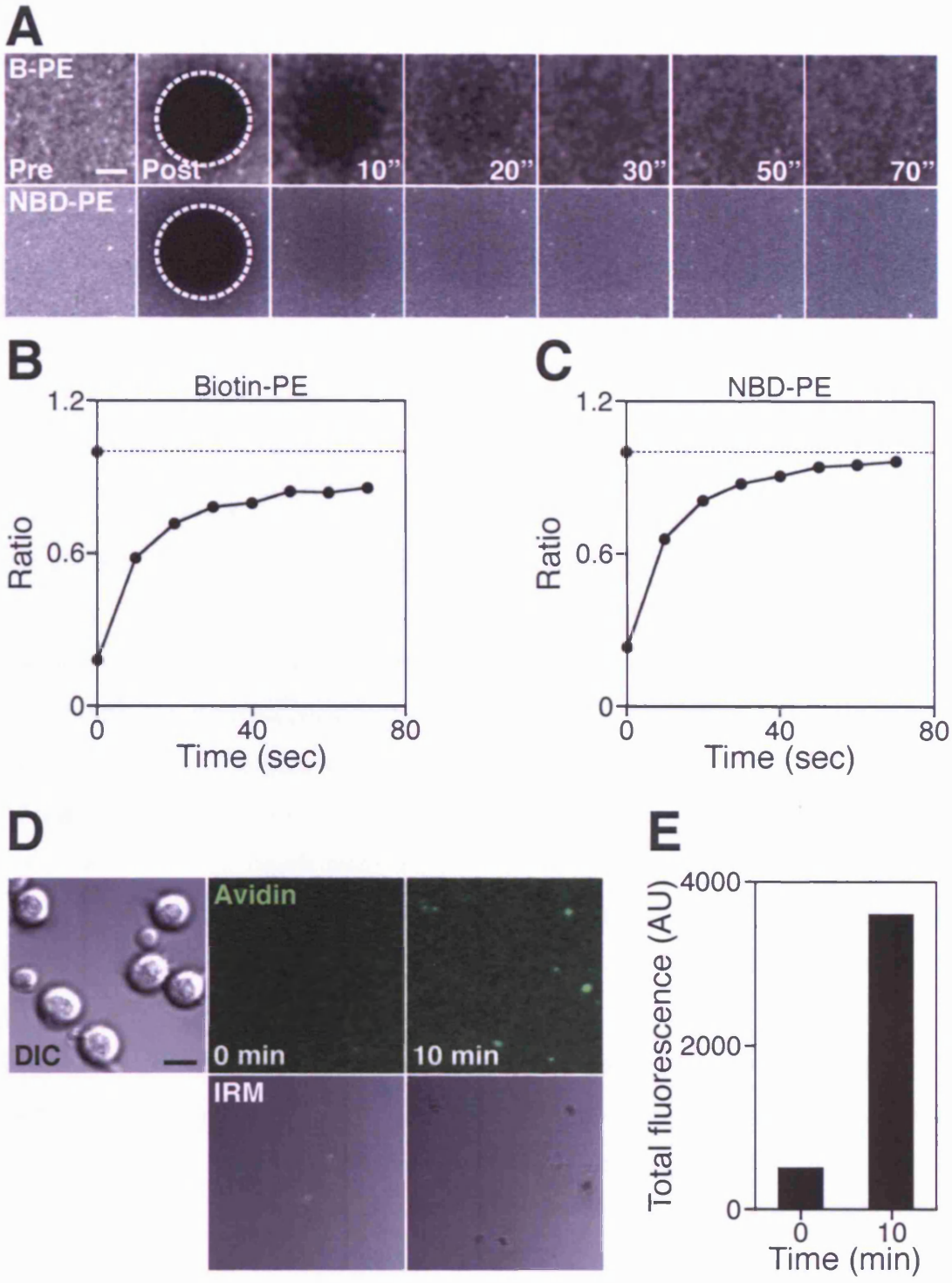


**Figure 3.12. Characterisation of lipid bilayers containing biotinylated lipids.**
**(A)** FRAP experiments of lipid bilayers containing biotin-PE lipids (top panel) or NBD-PE lipids (bottom panel). A spot on the lipid bilayer (white dotted circle) was bleached with 25 laser pulses, and the fluorescence recovery was followed for 2 min. Scale bar: 2 μm. Fluorescence recovery (expressed as ratio = mean intensity at time n after bleaching / mean intensity at t=pre-bleaching) of lipid bilayers containing **(B)** biotin-PE and **(C)** NBD-PE lipids is represented as a function of time. **(D)** Shows the interaction of MD4 B cells with artificial bilayers loaded with $HEL^{WT}$. Scale bar: 4 μm. **(E)** Shows the amount of antigen aggregated (expressed as total fluorescence) by the MD4 B cells in **(D)**.

fragment (or antibody) involves the use of biotin/streptavidin for the development, the biotin and avidin used on the lipid bilayers would interfere with it. Therefore we needed to look for another technique.

We followed two strategies based on fluorometric assays rather than radioactive as previously described for other bilayer systems (Grakoui et al., 1999) (for a detailed description see Materials and Methods). Both approaches used calibrated beads with known antibody binding capacities to compare the densities of F10 antibody (used to tether the antigen) on the artificial bilayers, with the densities on the beads.

#### 3.3.2.2.1 Glass beads

This approach focused on generating artificial lipid bilayers on the surface of glass beads of a defined area. The bilayers are then incubated with fluorescently labelled avidin, the monobiotinylated F10 and a fluorescently labelled anti-mouse Ig antibody. The fluorescent signal associated with the beads is analysed by FACS, and the specific fluorescence (density as molecules/$\mu m^2$) derived with the calibration curve obtained from the calibrated beads (Lauer et al., 2002).

We chose the silica beads from Bangs Laboratories for our assay. We prepared lipid bilayers containing different ratios of biotinylated lipids on the surface of the silica beads and incubated them with Alexa Fluor 488-avidin (or Alexa Fluor 633-streptavidin).

Glass beads proved to be very heterogeneous in size as shown by forward vs size scatter analysis (Figure 3.13 A). When we analysed the associated fluorescence, we observed that it decreased linearly with the dilution factor (Figure 3.13 A and B).

However, the situation was different when we incubated the beads sequentially with avidin, the monobiotinylated F10 antibody and an anti-mouse kappa chain antibody fluorescently labelled with phycoeritrine (PE): no signal from the fluorescently labelled antibody could be detected, indicating that the monobiotinylated F10 antibody did not bind to the avidin.

As a consequence of these results, we discarded this method to measure the density of antigen on the bilayer.

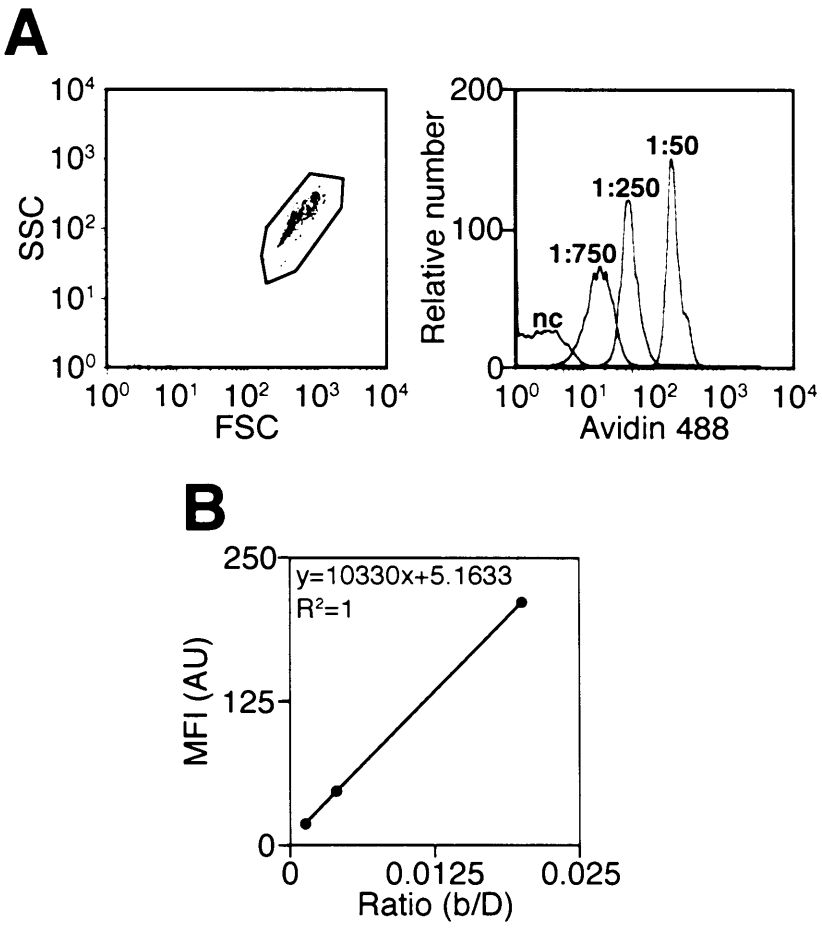


**Figure 3.13. Estimation of the antigen density on lipid bilayers with biotinylated lipids I: glass beads.**

Artificial bilayers with varying ratios of biotinylated lipids were prepared on the surface of silica beads, loaded with Alexa Fluor 488-avidin and analysed by FACS. **(A)** Left panel shows the forward vs size scatter, and the right panel the histogram of the associated fluorescence. Numbers indicate the different biotinylated lipids : DOPC ratios. **(B)** The fluorescence associated to the avidin (MFI) increases linearly with the biotinylated lipids : DOPC ratio (b/D).

#### 3.3.2.2.2 Lipid bilayers

The second approach consisted in comparing the fluorescence of artificial bilayers generated on glass coverslips with the calibration curve by confocal microscopy.

As these beads bind specifically mouse IgG we coated them with the F10 mAb (used to tether the HEL mutants on the bilayers) and then we used an anti-mouse kappa chain antibody labelled with phycoeritrin (PE) to analyse the fluorescence associated with them. A FACS histogram showed five populations with defined levels of fluorescence that comprised a negative control and four different ABCs (Figure 3.14 A).

These five populations were also evident when the beads were visualised by confocal microscopy (Figure 3.14 B). Furthermore, the mean fluorescence of each population of beads is directly proportional to the antibody binding capacity (ABCs) of each population (Figure 3.14 C and D).

We then incubated artificial bilayers loaded with avidin and the monobiotinylated F10 antibody with the anti-mouse kappa chain antibody fluorescently labelled with phycoeritrine (PE), and measured the mean fluorescence of the bilayer at different dilutions of biotin lipids.

We compared these values with the calibration curve obtained with the beads and determined that the density of antigen on a lipid bilayer prepared with a dilution 1:25 of biotinylated lipids in DOPC corresponds to approximately 250 molecules/$\mu m^2$.

This approach to determine the density of antigen allowed us to correlate the density of the antibody used to tether the antigens to the bilayers with the density of antigen itself. This is possible by assuming that the antigen occupies all the binding sites of the antibody, an assumption that is probably correct since the affinity of the interaction is extremely high, and the concentrations of antigens used to incubate the bilayers are high enough to saturate the available antibody.

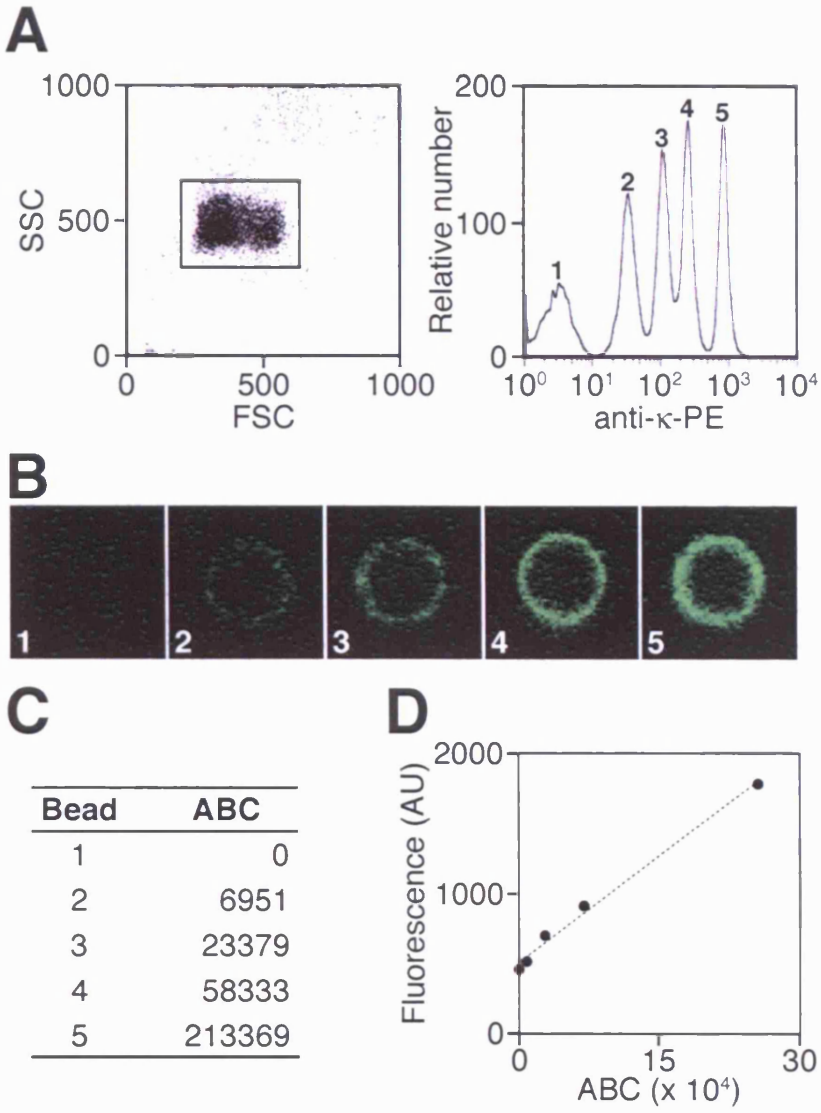


| Bead | ABC |
|---|---|
| 1 | 0 |
| 2 | 6951 |
| 3 | 23379 |
| 4 | 58333 |
| 5 | 213369 |

**Figure 3.14. Estimation of the antigen density on lipid bilayers with biotinylated lipids II: glass beads.**

**(A)** Calibrated beads were loaded with the F10 antibody and labelled with an anti-kappa-PE antibody. FACS analysis showed the five populations with different levels of antibody binding capacity (ABC). **(B)** Images of the different beads observed by confocal microscopy. **(C)** Antibody binding capacities (ABC) of the different calibrated beads used to estimate the density of antigen. **(D)** Calibration curve derived from the mean intensity of the fluorescence measured by confocal microscopy of the different populations of calibrated beads and their respective ABCs.

### 3.3.2.3 Thresholds of membrane antigen recognition

To determine the thresholds for antigen aggregation when the antigen was tethered in a polyvalent way, we explored the interaction of MD4 B cells with bilayers containing the different mutant HEL antigens loaded at different densities (Table 1).

We observed that the avidity threshold necessary to trigger antigen aggregation does not differ significantly compared to antigens tethered through a GPI-linked Fab: a minimum density of 6 molecules/$\mu m^2$ and an affinity higher than $K_d = 8 \times 10^7 M^{-1}$ are necessary to trigger antigen accumulation (Figure 3.15). Similarly, the ceiling for antigen accumulation is maintained: when the affinity of the BCR for the antigen is higher than $K_d = 5 \times 10^7 M^{-1}$ then the HEL mutants are accumulated equally (Figure 3.15).

From these experiments, we concluded that in our system polyvalent antigens do not affect in any significant way the thresholds of antigen recognition or the affinity ceiling observed with a monovalent antigen system.

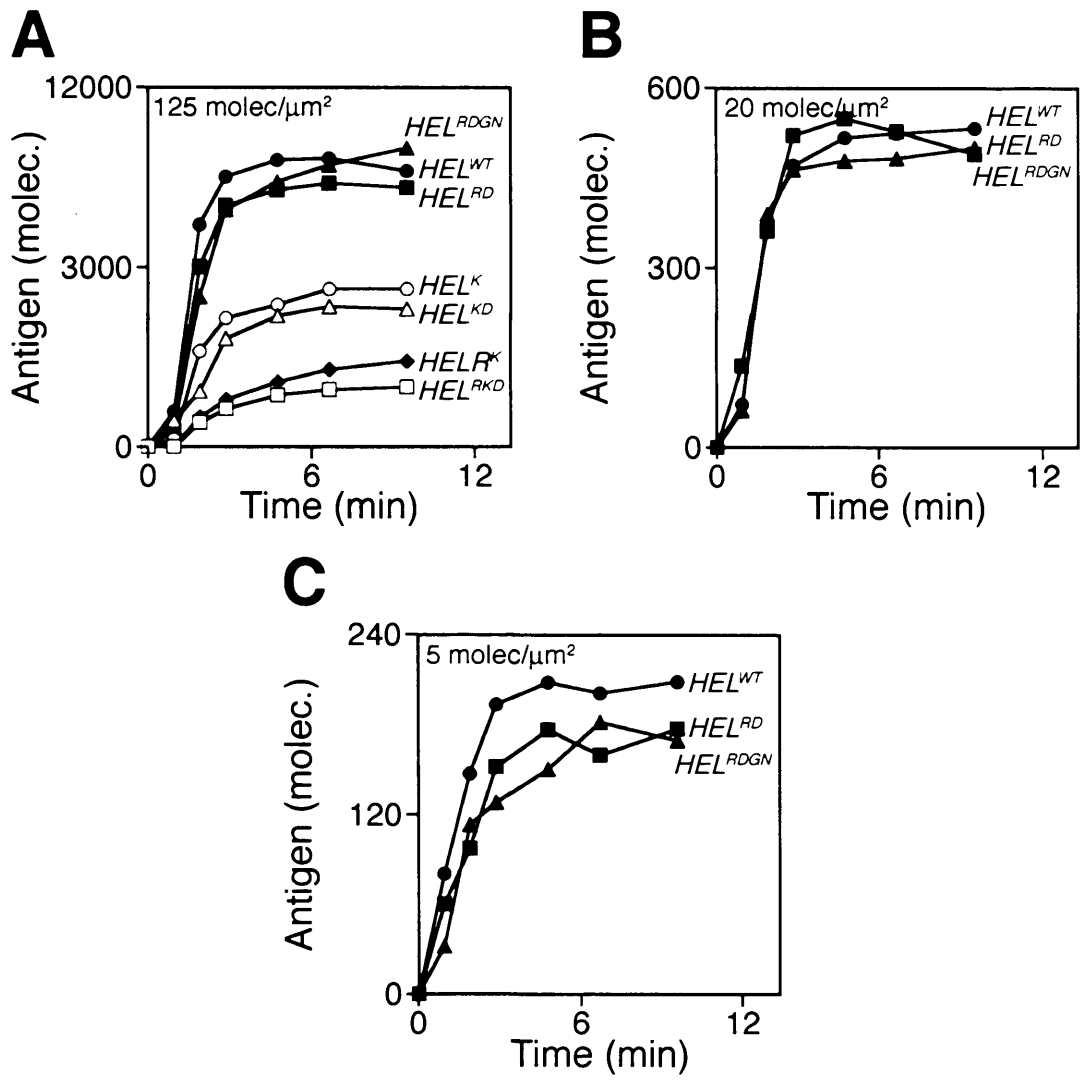


**Figure 3.15. Effect of the valency of the antigen in the recognition process.**
MD4 B cells were settled on artificial bilayers loaded through biotinylated lipids with the different HEL antigens, and the kinetics of interaction followed by confocal microscopy. The plots show the kinetics of antigen accumulation at the different densities **(A)** 125 molecules/μm², **(B)** 20 molecules/μm² and **(C)** 5 molecules/μm². Note that B cells cannot discriminate $HEL^{RDGN}$ from $HEL^{WT}$ even though their 400-fold difference in affinities.

### 3.3.3 Antigen extraction

One of the main functions of the BCR upon antigen recognition is the internalisation of the BCR/antigen complex and targeting of the antigen for processing and presentation in the context of MHC class II molecules to T cells (Lanzavecchia, 1985). When CD4 T cells recognise the specific MHC-peptide complexes on the surface of B cells, these receive T cell help. This event is necessary in order to fully activate antigen specific B cells (Janeway, 2005).

We wanted to determine if B cells were able to extract antigens tethered on artificial lipid bilayers. To this end we settled MD4 B cells on bilayers loaded with an Alexa Fluor 543-labelled $HEL^{W1}$ antigen, and followed the interaction by confocal microscopy. As shown in Figure 3.16 A, B cells aggregated the antigen in a central cluster, and the signal from the GPI-linked and the labelled antigen co-localise.

After 15 minutes the area of contact with the bilayer and the size of the cluster decreased, indicating that dissociation or internalization of the previously engaged antigen had occurred (Figure 3.16 A).

When we analysed the B cells by 3D-confocal microscopy for the presence of intracellular antigen we were surprised to see that MD4 B cells not only extracted the fluorescently labelled antigen, but they also extracted the GPI-linked Fab used to tether the antigen, as the fluorescence associated with both molecules can be observed inside the cell (Figure 3.16 B). Antigen extraction is evident after 10-15 minutes of interaction, and therefore once the accumulation process has finished, although we cannot discard the possibility that it takes place long before it happens at levels that cannot be detected by confocal microscopy.

The presence of intracellular antigen was confirmed by labelling the cells with LysoTracker, a probe that specifically stains lysosomes. A three-dimensional reconstruction showed that antigen and LysoTracker signals co-localise inside the cell (Figure 3.16 C).

As we were able to follow antigen internalisation by confocal microscopy on the artificial bilayers, we wanted to further study the effect of the affinity/BCR interaction in the internalisation process as this process would be a key event during B cell activation. This showed to be more complicated than initially

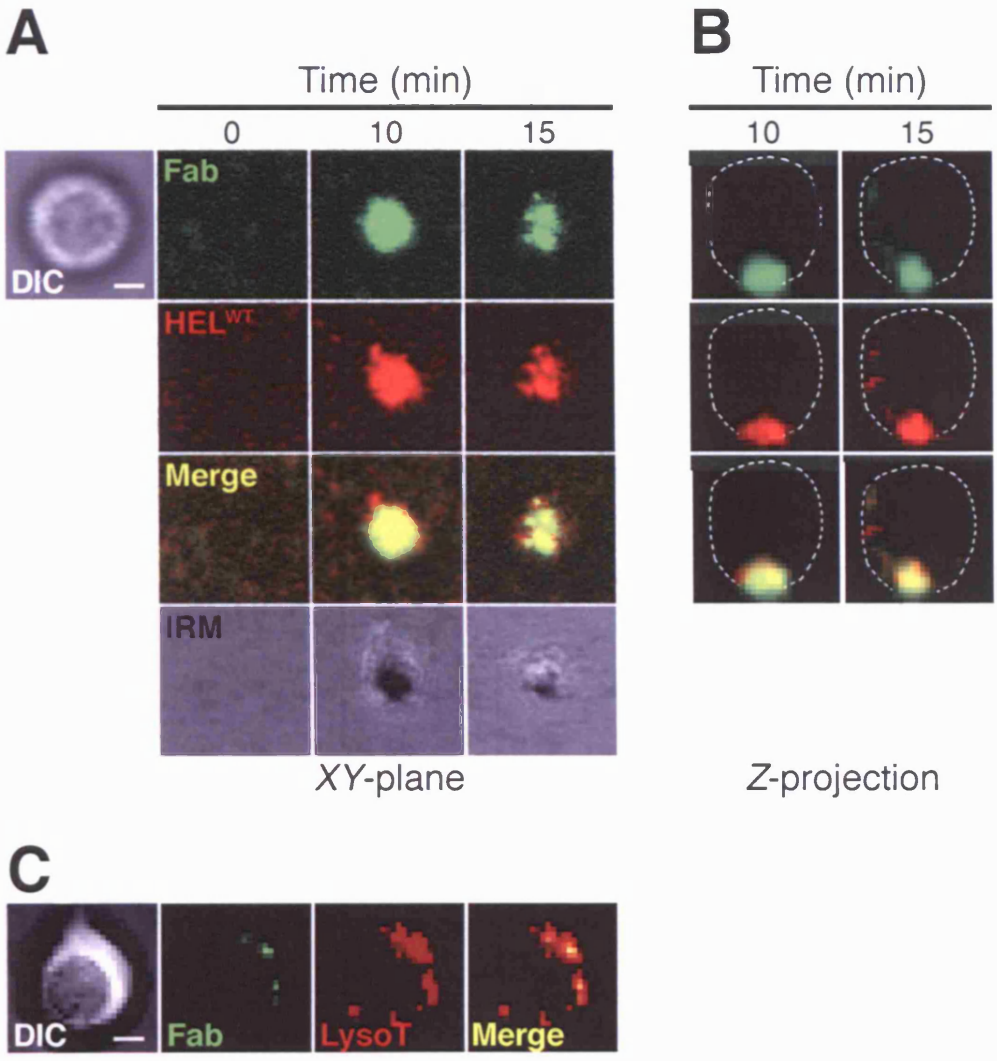


**Figure 3.16. Antigen extraction and internalisation.**
**(A)** Shows the interaction of MD4 naïve B cells with planar lipid bilayers containing GPI-linked Alexa Fluor 488-labelled HyHel5 Fab (Fab, green) loaded with Alexa Fluor 543-labeled hen egg lysozyme ($HEL^{WT}$, red) at a density of 150 molecules/$\mu m^2$ as visualised by confocal microscopy. The antigen is aggregated in a central cluster after 10 minutes of interaction, however, after 15 minutes its size and the area of contact with the bilayer (as assessed by IRM) decrease. **(B)** Shows the axial projection of the process showed in **(A)**. Both the antigen (red) and the GPI-linked Fab (green) are extracted. The Z-stacks were acquired with slices of 0.3 µm. The dashed white line shows the perimeter of the B cell in the Z-projection. **(C)** Shows the co-localisation of the GPI-Fab molecule (green) with the lysosomal marker LysoTracker (red), indicating that the extracted antigen is efficiently internalised. Scale bar: 2 µm.

thought, as it became very difficult to visualise by confocal microscopy the internalisation of antigens of low affinity.

## 3.4 Discussion

The study presented in this chapter deals with the early stages of membrane antigen recognition and describes the parameters that determine this process. In addition it introduces the use of artificial lipid bilayers to quantitatively study the interaction of B cells with membrane antigens.

### 3.4.1 Early events during membrane antigen recognition by B cells

Taking advantage of HEL-specific BCR transgenic B cells and target cells expressing a membrane bound form of the antigen, we showed that the early stages of the recognition process proceeds in two distinct phases: first the B cell spreads quickly over the surface of the target membrane to increase its area of contact and, secondly, it slowly contracts to gather the antigen previously engaged which can then be efficiently extracted by the B cell in order to present to T cells. The spreading is triggered by antigen engagement through the BCR.

While different groups have reported a similar T cell response, our experiments are the first to suggest that this response is associated with antigen engagement and accumulation (Bunnell et al., 2001; Negulescu et al., 1996; Parsey and Lewis, 1993). In a following chapter, we will explore in detail the relevance of this cellular response and we will unveil part of its mechanism.

### 3.4.2 Recognition of membrane antigens by B cells: lipid bilayers

Different groups have analysed the dependence of the B cell response on the BCR/antigen affinity (Batista and Neuberger, 1998; Kouskoff et al., 1998). While these studies were performed with soluble antigens, very little is known of the B cell response to membrane bound antigens (Batista et al., 2001; Batista and Neuberger, 2000).

Thus, we took advantage of artificial lipid bilayers to analyse the interaction of B cells with membrane antigens in a precise quantitative way (Carrasco et al., 2004; Grakoui et al., 1999). In order to do this, we developed two ways of tethering freely diffusing molecules on artificial membranes. We achieved this through an

anti-HEL GPI-linked Fab fragment and by including biotinylated lipids in the bilayers. While GPI-linked molecules have been previously used to study by confocal microscopy the interaction of immune cells with specific ligands, membranes containing biotinylated lipids had only been applied for structural studies (Chan et al., 1991; Dustin, 1997; Uzgiris and Kornberg, 1983).

FRAP experiments showed that ligands freely diffuse on both type of bilayers. This initially surprised us, as the liposome spreading technique used to generate the artificial lipid bilayers should generate bilayers with GPI-linked proteins on both leaflets of the membrane. This would in turn limit the diffusion rate through association of the molecules to the glass coverslip.

However, a certain degree of orientation with the molecules preferentially locating in the upper leaflet takes place when the liposome solutions are incubated with the coverslips to form the bilayers, as the FRAP experiments revealed that the recovery is almost complete. This has been previously reported for transmembrane proteins and presumably a similar process takes place when bilayers with GPI-linked proteins or modified lipids are assembled (Salafsky et al., 1996).

It is likely that slight differences in the diffusion coefficient between the planar bilayers system and the surface of a professional APC such as FDCs or DC may exist as a result of the lack of a target cell cytoskeleton and other membrane proteins. But the supported bilayers system allows precise quantification of the number of ligands while keeping the nature of the stimulus over physiological range of affinities and densities recognised *in vivo* by B cells.

### 3.4.3 Parameters that determine the recognition of membrane antigens

Taking advantage of the artificial bilayers, we determined that the density of antigen and its affinity for the BCR are the two parameters that establish the thresholds of antigen recognition, similar to what has been reported for T cells (Grakoui et al., 1999).

#### 3.4.3.1 Dependence on the antigen density

Our results show that antigen recognition strongly depends on the density of antigen: a two-fold decrease in the density of antigen leads to a four-fold decrease

in the amount of antigen accumulated, showing an exponential dependence on this parameter (Figure 3.7).

Grakoui and colleagues reported similar results in the case of T cells using artificial lipid bilayers as model system (Grakoui et al., 1999). However, a surprising difference is that the density threshold for antigen accumulation appears to be higher in the case of B cells, even though the affinities of the BCR/antigen interaction are several orders of magnitude higher than the TCR/MHC-pepitde interaction affinity (Batista and Neuberger, 1998; Foote and Milstein, 1991; Sykulev et al., 1994). This could be simply due to the different ways in which the densities were estimated (radio immunoassays or fluorometric assays). More tempting, however, is the notion that T cells and B cells may have different sensitivities for antigen.

In this line, Davis et al have shown that helper T cells ($CD4^+$ T cells) respond even to a single MHC-agonist peptide complex displayed on the surface of an antigen presenting cell (APC), while B cells are not as sensitive to antigens presented on the surface of APCs (Irvine et al., 2002)(F.D. Batista data not shown). The authors proposed the pseudodimer theory in order to explain this remarkable sensitivity to antigen, in which non-agonist peptides may be involved together with CD4 in amplifying the signal triggered by the engagement through the TCR of a single agonist peptide (Krogsgaard et al., 2003; Li et al., 2004; Wulfing et al., 2002a). The situation is somehow different for B cells as they recognise intact antigens in isolation without any accessory molecule. Although CD19 may amplify the BCR signalling through a similar mechanism, its cross-linking to the BCR is dependent on the presence of complement, while CD4 interacts directly with the MHC class II molecules in the absence of any other molecule (Dempsey et al., 1996; Sakihama et al., 1995).

### 3.4.3.2 Dependence on the BCR/antigen affinity

From our experiments we concluded that a minimum affinity of $8 \times 10^5$ $M^{-1}$ is necessary to trigger effective antigen accumulation. This value is similar to the affinity of antibodies produced in a primary immune response in vivo, as reported by different groups (Foote and Eisen, 1995; Foote and Milstein, 1991). Above this threshold B cells are sensitive to the precise binding affinity as shown by the

different amounts of antigen aggregated. However, once the affinity is above 5.2 x $10^7$ $M^{-1}$ a ceiling is reached, and B cells are no longer able to discriminate antigens in terms of the amount of molecules accumulated, even though they differ almost 400 times in their binding affinities (Table 1).

The presence of an affinity ceiling in the response of B cells has been previously reported for soluble antigens, and our results show that the same constraint applies to membrane antigens (Batista and Neuberger, 1998).

Foote and Eisen predicted that the affinity maturation of antibodies during immune responses would be also limited by a ceiling, a 'maximal affinity likely to be found in antibodies produced during an immune response' (Foote and Eisen, 1995).

Both reports stressed on the relevance of the single kinetic parameters of interaction - association rate and dissociation rate - in both the triggering of B cells and in the affinity maturation of the humoral immune response, respectively. In the same line, Foote and Milstein showed that the affinity maturation of antibodies is driven by both thermodynamic and kinetic parameters, although other reports arrived to different conclusions (Foote and Milstein, 1991; Goldbaum et al., 1999; Sagawa et al., 2003).

While Foote and Eisen predicted an affinity ceiling of $K_a \approx 10^{10}$ $M^{-1}$, the value reported by us differs by three orders of magnitude ($K_a \approx 10^7$ $M^{-1}$). One question that arises from this is whether this difference is due to the method employed to measure the affinity values, or if other mechanisms are involved. The efficiency of extraction of antigens that are aggregated equally, but have different binding affinities may be one of these mechanisms.

### 3.4.4 Antigen extraction

How does the antigen accumulated influence the subsequent B cell activation process? Antigen extraction is a late event guided by the BCR and necessary for presentation and T cell co stimulation. It is likely that the amount of antigen that a B cell accumulates will have a direct impact in the amount of antigen that the B cell will extract, and therefore in the degree of T cell help that they will eventually receive.

We observed that after accumulating the antigen, B cells are able to extract it from the artificial bilayers. Though, our experiments suggest that the amount of antigen internalised depends on the amount of antigen accumulated, we do not have any data to support the degree of presentation derived from this process so far.

Thus, antigen extraction may account for the difference in the affinity ceiling observed, if we consider that the half-life of the internalisation process ($t_{1/2}$ = 510 minutes) is at least one order of magnitude higher than the dissociation half-life of our affinity ceiling ($t_{1/2}$ = 18 seconds) (Guermonprez et al., 1998; Watts and Davidson, 1988).

In this line, Guermonprez and colleagues have shown that the efficiency of antigen internalisation is dependent on the dissociation half-life of the interaction, although these experiments have been performed with soluble antigens (Guermonprez et al., 1998).

Therefore, antigens that are still aggregated equally will be extracted with different efficiencies, depending on their dissociation half-life from the BCR.

Future experiments addressing this issue will be important, as they will give an insight on the mechanism of selection during the affinity maturation process.

# Chapter 4: Effect of binding kinetics on membrane antigen recognition

## 4.1 Introduction

In the previous chapter, we showed that the recognition of membrane antigens is characterised by the existence of an affinity ceiling: when the affinity of the BCR for the antigen is higher than $5 \times 10^7$ $M^{-1}$, B cells accumulate equivalent amounts of antigen independent of the affinity.

The presence of an affinity ceiling in B cell activation has been previously reported for the recognition of soluble antigens, and different reports suggested that this might be regulated by the kinetic binding parameters, particularly the rate of dissociation (Batista and Neuberger, 1998; Foote and Eisen, 1995). However, nothing was known of the recognition of membrane antigens by B cells.

Grakoui and colleagues have suggested that the aggregation of the T cell receptor (TCR) and MHC-peptide is dependent on the dissociation rate constant ($k_{off}$) of this interaction (Grakoui et al., 1999). From these results, the authors proposed a model based on partial differential equations to explain the recognition of antigens and synapse formation depending on specific kinetic parameters (Lee et al., 2002b). However, the range of affinities and kinetic parameters of antigen/BCR interaction that a B cell may encounter are broader than those recognised by T cells (Foote and Milstein, 1991; Sykulev et al., 1994). Therefore, this model could not be applied to B cells. Thus, we wanted to unveil the relevance of the single kinetic parameters during membrane antigen recognition by B cells.

In an interesting commentary, Foote and Eisen suggested that the affinity ceiling of the antibodies produced during an immune response is determined by limits in the on-rate and off-rate (Foote and Eisen, 1995). The maximum on-rate should be determined by the diffusion of the antigen and the antibody molecules in solution, and therefore this value should be around $10^5$-$10^6$ $M^{-1}s^{-1}$; the maximum off-rate is less precise and defined according to the half-life of endocytosis of BCR/antigen complexes, that is 8.5 minutes (Watts and Davidson, 1988).

Therefore, we reasoned that for membrane antigen recognition, the association phase would be limited by the diffusion rate of molecules on the artificial bilayers, as this value is considerably lower than the association rate of the BCR/antigen interaction (Bell, 1978).

On the other hand, the complexes formed will dissociate according to their dissociation rates and therefore this parameter alone will have a direct impact on the total amount of molecules that a cell can accumulate (Bell, 1978).

However, as the mutant lysozymes used in our studies were generated by alanine scanning, they show similar on-rates ($k_{on}$ = 6 x $10^6$ $M^{-1}$ $s^{-1}$) and the differences in affinities are characterised by differences in their off-rates (Table 1). Therefore, to test our hypothesis we needed to look for alternative transgenic BCR systems in which we could obtain specific antigens with lower on-rates.

## 4.2 Antigens and transgenic systems

In order to tackle this problem we explored two different transgenic BCR mice: the 3-83 transgenic mouse and the HSμ transgenic mouse (Nemazee and Burki, 1989). As it will be shown during this section their kinetic parameters of interaction are adequate to answer the main question posed.

### 4.2.1 3-83 transgenic mouse

B cells from the 3-83 transgenic mouse express a BCR that specifically recognises different H-2K MHC class I molecules with varying affinities ranging from (Table 2). In addition, this BCR also recognise a set of artificial peptides obtained from a phage display library (Kouskoff et al., 1998).

We took advantage of these two different sets of antigens, the H2-K molecules and the phage display antigenic peptides, to elucidate how the kinetic parameters affect the antigen recognition process.

#### 4.2.1.1 Monomeric forms of the peptides recognised by the 3-83 transgenic system

The phage display library generated by Nemazee and colleagues gave rise to peptides that are specifically recognised by the 3-83 BCR (Kouskoff et al., 1998). We selected different peptides: p5, p7, p11 and p31, and designed a random

peptide (p0) with no affinity for the BCR to use as a control (see Materials and Methods). Monobiotinylated versions of each peptide were synthesised and purified by the Protein Synthesis Facility at Cancer Research UK.

We then tested the capacity of 3-83 B cells to recognise the peptides tethered through an avidin bridge on lipid bilayers. As shown in Figure 4.1 A and B, 3-83 B cells recognise and accumulate the four selected peptides with varying efficiencies. For instance, the p5 peptide is poorly recognised even when it is displayed at extremely high densities (at $\delta \approx 1500$ molecules/$\mu m^2$, 25% of the cells accumulate antigen), which suggests that its affinity is extremely low. On the other hand, p7 is aggregated very efficiently, and p31 and p11 are accumulated with intermediate efficiencies (Figure 4.1 B). We discarded p5 for further analysis, as the densities at which it is efficiently accumulated exceed the physiological densities of receptors expressed on the surface of cells.

We next measured the binding properties of the interaction between the 3-83 BCR and the peptides by Surface Plasmon Resonance (SPR) (Figure 4.2 A and Table 2). The amount of antigen accumulated correlates with the affinity of the interaction. However, since the binding kinetics were determined by tethering the monobiotinylated peptides on an SA-chip, and then the 3-83 monoclonal was injected, the affinity parameters may in fact reflect a measurement of avidity (see Materials and Methods).

To test whether this was the case, we prepared Fab fragments of the 3-83 monoclonal antibody, and repeated the measurements. As shown in Figure 4.2 C, we were not able to measure any interaction. This indicates that either the affinity of interaction is extremely low, or that the binding properties of the 3-83 monoclonal antibody are altered when the Fab fragments are prepared.

Therefore, we focused our attention on setting up ways to obtain monomeric forms of the 3-83 peptides. In order to do this we explored two different approaches. The first one consisted of generating fusion proteins with the HEL and each antigenic peptide, and the second of diluting the peptides with an unrelated monobiotinylated molecule to decrease the valency of the antigen tethered on the bilayer.

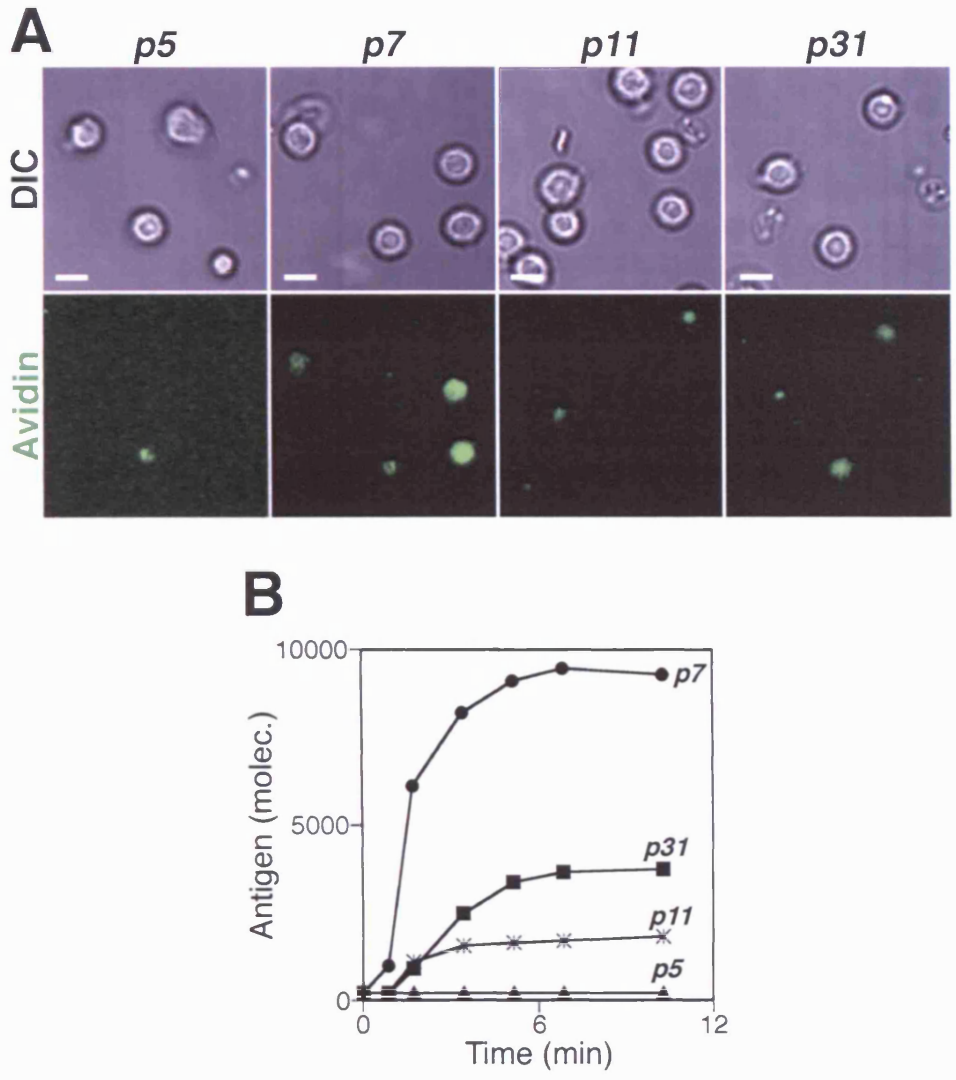


**Figure 4.1. Recognition of antigenic peptides by 3-83 transgenic B cells.**
**(A)** Confocal images of 3-83 B cells after 10 minutes of contact with artificial bilayers loaded with the indicated peptides tethered through an Alexa Fluor 488-conjugated avidin bridge (green) at a density of 250 molecules/$\mu m^2$. The cells recognise and accumulate the antigens with varying efficiencies. Scale bar: 5 μm. **(B)** Shows the kinetics of antigen accumulation for the different peptides. p5 is accumulated only when it is displayed at very high densities.

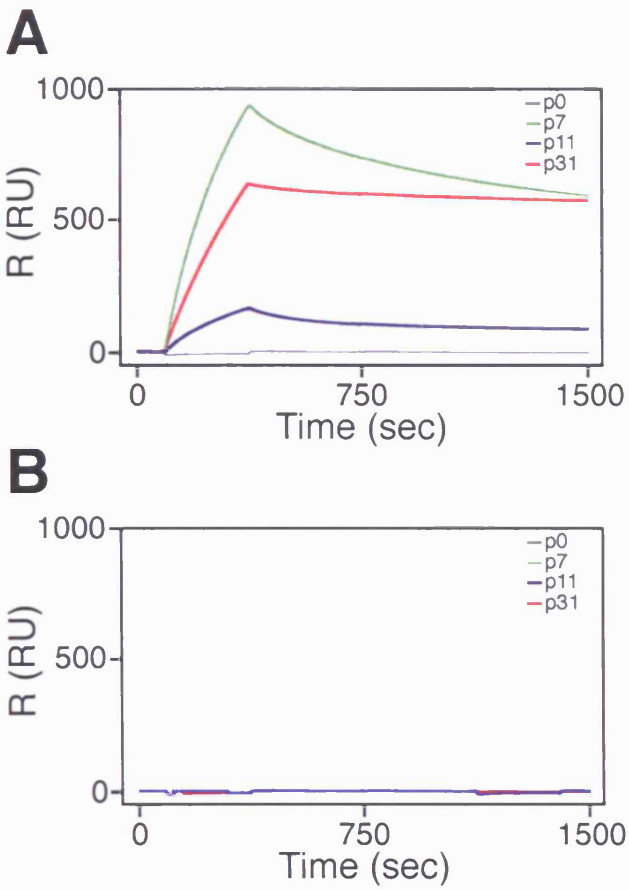


**Figure 4.2. Analysis of the kinetics of binding of the 3-83 monoclonal antibody with the antigenic peptides by surface plasmon resonance.**
**(A)** Shows the overlaid sensorgrams (Resonance Units (RU) as a function of time (sec)) of the interaction of the 3-83 monoclonal antibody with the indicated peptides. The 3-83 antibody was injected at a concentration of 200 nM. **(B)** Shows the overlaid sensorgrams (Resonance Units (RU) as a function of time (sec)) of the interaction of Fab fragments of the 3-83 monoclonal antibody with the indicated peptides. The Fab fragments were injected at a concentration of 200 nM.

**Table 2. Binding constants of antigenic peptides.**

| Antigen | $K_a \times 10^6$ ($M^{-1}$) | $k_{on} \times 10^3$ ($M^{-1}$ $sec^{-1}$) | $k_{off} \times 10$ ($sec^{-1}$) | $t_{1/2}$ 37 °C (sec) |
|---|---|---|---|---|
| **Binding to 3-83** | | | | |
| p7 | 25.8 | 15.3 | 0.0006 | 1155 |
| p11 | 7.13 | 8.51 | 0.0012 | 577 |
| p31 | 64.3 | 9.36 | 0.0001 | 6931 |

#### 4.2.1.2 HEL-peptide fusion proteins

Our approach consisted in fusing the antigenic peptides p11 and p31 to the HEL antigen and to tether the resulting antigens through the GPI-linked Fab fragment as monovalent species. We selected these two peptides as they show similar levels of antigen aggregation.

In order to fuse them with the HEL, we used the vector coding for the $HEL^{RD}$ mutant as the backbone vector. This vector contains the sequence coding for the $HEL^{RD}$ mutant and a histidine tag for purification (Figure 4.3 A). We introduced the sequences coding for the peptides into the construct by PCR, and then expressed them in the J558L cell line. Finally, the protein was purified from the supernatant by affinity chromatography (see Materials and Methods).

We first analysed if the protein was efficiently produced and purified by SDS-PAGE analysis of the fractions eluted from the column. This showed that indeed the fusion protein is produced, and its molecular weight is higher than the $HEL^{WT}$ from which the fusion protein is derived as expected (Figure 4.3 B).

We next tested the capacity of 3-83 B cells to recognise and aggregate the chimeric antigens when these were tethered to the bilayer through the GPI-linked Fab fragment. As shown in Figure 4.3 C, 3-83 B cells did not recognise the chimeric antigens since no increase in the antigen signal was observed at the site of contact. However, MD4 B cells (labelled with the membrane dye PKH26 (red)) efficiently recognised the fusion antigens, confirming that these were in fact tethered on the bilayers (Figure 4.3 C).

We confirmed that the fusion proteins were not recognised by the 3-83 BCR when we attempted to measure the affinity of this interaction by SPR. To this end, we tethered the biotinylated 3-83 monoclonal antibody on an SA-chip, and then injected the fusion proteins. As shown in Figure 4.3 D, the sensorgram did not reveal any specific interaction between the proteins and the monoclonal antibody.

These results showed that the fusion proteins produced are not recognised by the specific 3-83 BCR expressed by the transgenic B cells, therefore we did not follow this strategy any further.

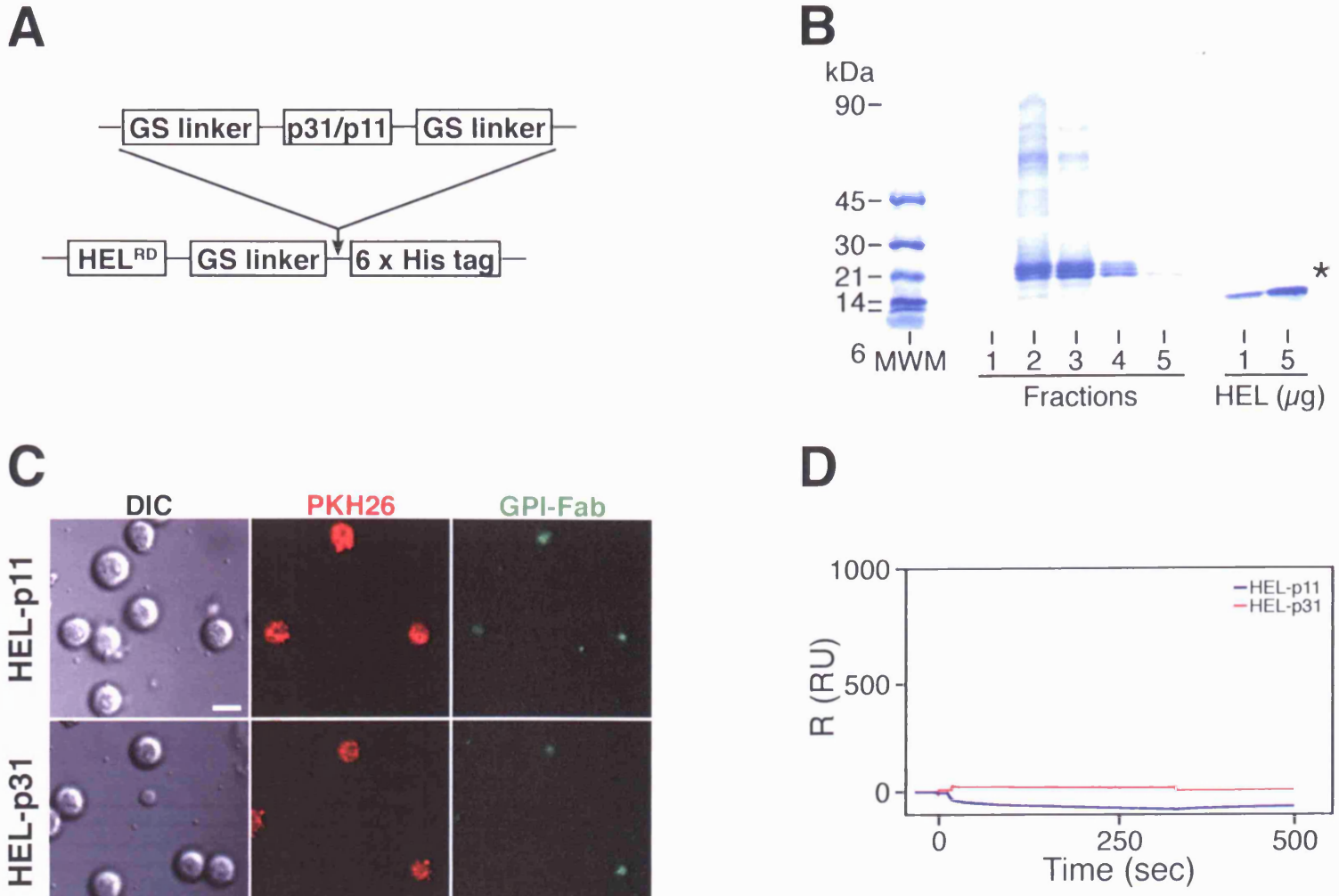
A
GS linker
p31/p11
GS linker
HEL^RD
GS linker
6 x His tag
B
kDa
90
45
30
21
14
6
MWM
1 2 3 4 5
Fractions
1 5
HEL (μg)
*
C
DIC
PKH26
GPI-Fab
HEL-p11
HEL-p31
D
1000
500
0
R (RU)
HEL-p11
HEL-p31
0
250
500
Time (sec)

**Figure 4.3. Purification and characterisation of HEL-peptides fusion proteins.**
**(A)** Diagram of the HEL-peptides fusion proteins generated. Antigenic peptides p11 and p31 flanked by glycine-serine linkers were introduced by PCR into the plasmid coding for the $HEL^{RD}$ mutant. This plasmid contains a 6 x Histidine tag to facilitate the purification. **(B)** Shows the SDS-PAGE of a typical purification of the HEL-p31 fusion protein. 10 µl of each of the five fractions were loaded in a 4-20% polyacrylamide gel and the gel was developed with colloidal Coomassie blue staining. As a control 1 and 5 µg of $HEL^{WT}$ were also loaded. The purified fusion protein (indicated with an asterisk) shows a molecular weight higher than the HEL from which it is derived. The same result was obtained for the HEL-p11 fusion protein. **(C)** Shows confocal images of 3-83 (unlabelled) and MD4 (PKH26-labelled, red) B cells in contact with GPI-linked Fab bilayers (green) loaded with the HEL-p11 (top row) or the HEL-p31 (bottom row) fusion proteins at a density of 200 molecules/$\mu m^2$. The images show the cells after 10 minutes of interaction. 3-83 B cells do not recognise the fusion proteins that are still recognised by the MD4 B cells. Scale bar: 2 µm. **(D)** Shows the sensorgram of the interaction between the 3-83 monoclonal antibody and the indicated HEL-peptide fusion proteins. The biotinylated 3-83 monoclonal antibody was tethered on an SA-chip and then the fusion proteins were injected at a flow rate of 10 µl/min.

#### 4.2.1.3 Dilution with an unrelated monobiotinylated ligand

The avidin molecule that we use to tether antigens on artificial lipid bilayers has four binding sites. Structural studies have shown that two of the binding sites are occupied by biotin when an avidin molecule is in contact with artificial bilayers containing biotinylated lipids (Darst et al., 1991; Qin et al., 1995). Therefore, it is likely that the monobiotinylated peptides tethered on artificial bilayers are present as dimeric species.

We reasoned that by diluting the monobiotinylated peptides with another irrelevant monobiotinylated molecule we should be able to obtain monomeric antigenic species. For this purpose, we selected the p0 peptide, as this has no detectable affinity for the 3-83 BCR (Figure 4.2).

From simple combinatorial calculations we derived a plot that shows the distribution of probabilities of the different species - that is, monomeric, dimeric and null - that would be present in an artificial bilayer if a fixed number of molecules of an antigenic peptide (pN) were mixed with an increasing number of molecules of the irrelevant peptide (p0) (Figure 4.4 A). This shows that with a ratio p0/pN $\geq$ 5 the ratio dimeric/monomeric antigen is $\leq$ 0.1. Clearly, this is not an ideal 100% monomeric antigen, but it should at least allow us to test our main hypothesis.

We initially had to determine the exact molar concentrations of monobiotinylated peptide solutions to prepare the corresponding dilutions. To this end, we developed a FACS analysis method using streptavidin-coated beads and biotin-FITC (see Materials and Methods). We first incubated the streptavidin-coated beads with fixed amounts of biotin-FITC (a saturating solution for all the binding sites available in the beads) and increasing dilutions of the different peptides (p0, p7, p11 and p31), and measured their levels of fluorescence by FACS analysis (Figure 4.4 B). Then, we derived a calibration curve from the mean fluorescence intensity measured by FACS and the corresponding dilution factors of the peptides solutions (Figure 4.4 C). This strategy allowed us to set the correct dilutions of peptides.

Next, we prepared artificial bilayers and loaded them with the different antigenic peptides diluted with the p0 peptide in a 1:6 ratio and tested the capacity of 3-83 B cells to recognise them. As shown in Figure 4.5 A, B cells efficiently

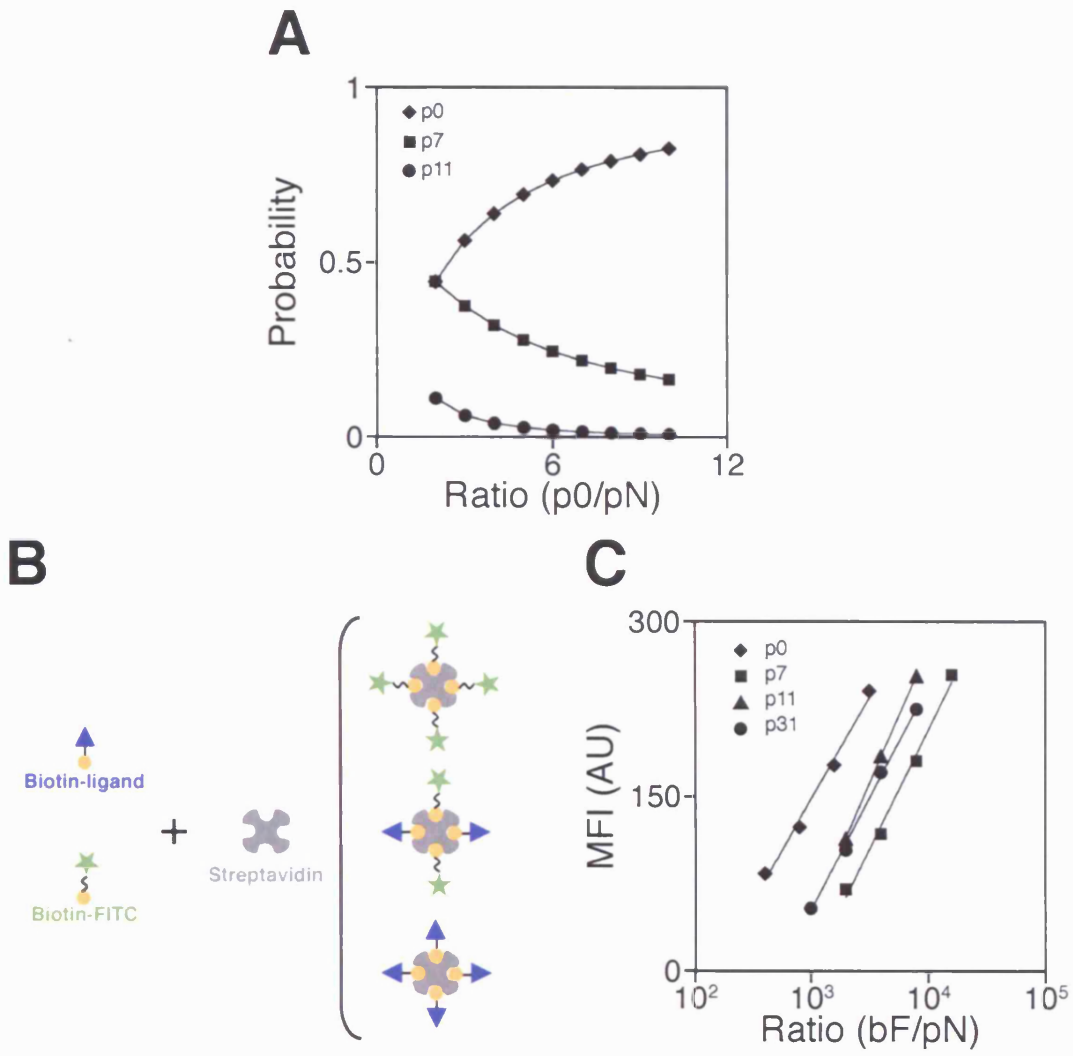


**Figure 4.4. Strategy followed to obtain monomeric forms of the antigenic peptides recognised by the 3-83 BCR.**
**(A)** Probability distribution of species obtained by mixing the antigenic peptides (pN) with the non-antigenic peptide (p0) at varying ratios. **(B)** Species that would be present in a sample of streptavidin mixed with a biotinylated ligand and biotin-FITC. **(C)** Mean fluorescence intensity (MFI) as a function of the biotin-FITC : biotin-peptide (bF/pN) as measured by FACS with streptavidin-coated beads.

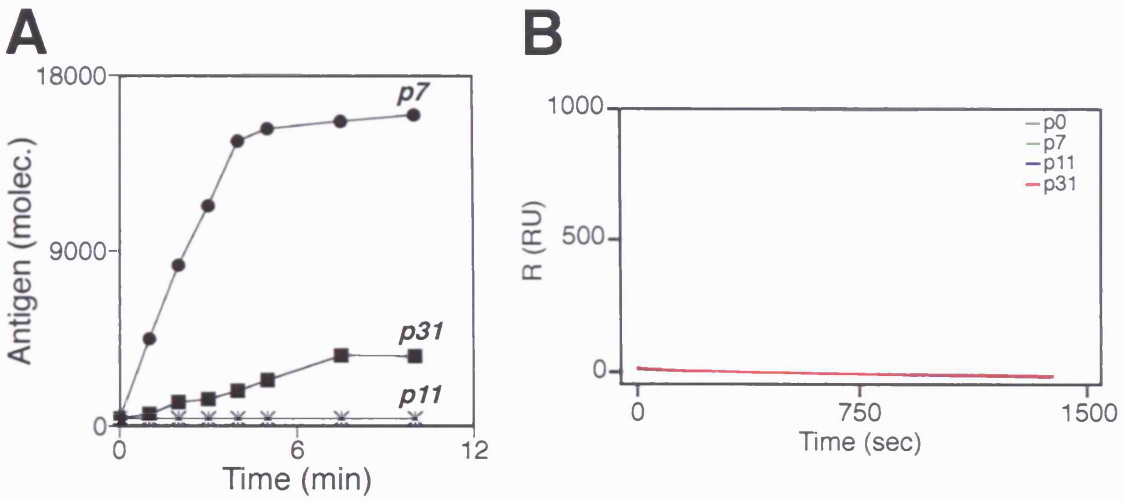


**Figure 4.5. Recognition of monomeric peptides by the 3-83 transgenic B cells.** **(A)** Shows the kinetics of antigen aggregation for the different peptides when these are in a monomeric form on the bilayers at a density of 250 molecules/$\mu m^2$. **(B)** Sensorgram of the interaction between tetramers prepared with mixtures of the peptides, p0 and avidin, and the 3-83 monoclonal antibody. The biotinylated 3-83 monoclonal antibody was immobilised on an SA chip and the indicated tetramers were injected at a concentration of 100 nM.

accumulated the p31 and p7 peptides. However, in these conditions B cells did not recognise the p11 peptide any longer (Figure 4.5 A).

These results were promising, however, we were still lacking kinetic parameters of interaction of monomeric species. In order to obtain these values we prepared tetramers of the different peptides diluted in p0 to obtain a family of tetramers enriched in the monovalent form of the antigenic peptide (see Materials and Methods). We used them to measure the affinity and kinetic parameters of interaction with the 3-83 antibody by SPR. Unfortunately we were not able to detect any interaction between the two (Figure 4.5 B).

After these results we decided to look for alternative approaches to take advantage of the 3-83 transgenic system.

### 4.2.2 H-2K MHC class I molecules

From SPR studies Nemazee and colleagues measured the kinetic parameters of interaction of the 3-83 BCR with the H2-K molecules (Lang et al., 1996). The on rate for the 3-83/H-2K$^{b}$ interaction is around 1.42 x $10^{4}$ $M^{-1}$ $s^{-1}$ which means that it is two orders of magnitude lower than for the HEL/HyHel10 interaction (Table 1). Furthermore, the $t_{1/2}$ is around 18.6 seconds, and therefore it is comprised in the range of the HEL$^{RDGN}$. This antigen constitutes an ideal system to test the effect of the kinetic binding parameters in the membrane antigen recognition process.

MHC molecules loaded with specific peptides are usually used conjugated with fluorescently labelled avidin in the form of tetramers to detect antigen specific T cells by FACS (Cerundolo, 2000; Klenerman et al., 2002; Valmori et al., 2000). We wanted to produce the monomeric biotinylated H2-K molecules in order to tether them on artificial lipid bilayers through an avidin bridge.

Dr Ton Schumacher (The Netherlands Cancer Institute, Netherlands) and Dr Dirk Busch (Institut of Microbiology, Immunology and Hygiene, Munich Technical University, Germany) provided us with the vectors coding for the H2-K$^{k}$ and H2-K$^{b}$ heavy chains, and the β2-microglobulin to generate the MHC class I molecules. The heavy chain of the H-2K molecules contains a target site for the biotin ligase (BirA), an enzyme that specifically binds a biotin to the lysine contained in a short amino acid sequence (O'Callaghan C et al., 1999). Dr Schumacher also generously provided us with the vector coding for this enzyme.

### 4.2.2.1 Expression and purification of monobiotinylated H-2K molecules

We expressed and purified the H-2K molecules from inclusion bodies in bacteria according to a protocol from Dr Dirk Busch (for a detailed explanation see Materials and Methods). Briefly, the vectors were transfected in the BL21 ($RecA^-$) pLysS strain of Escherichia coli by electroporation. Protein production was induced with IPTG and then purified from inclusion bodies with an 8 M urea buffer. This protocol yielded several mgs of protein (Figure 4.6, step 1).

Properly folded MHC molecules containing both the heavy chain and the β2-microglobulin were generated by dialysis against PBS and then purified from the excess non-folded chains by size exclusion chromatography. SDS-PAGE analysis of the peaks isolated showed that the complexes contained only heavy and light chains (Figure 4.6, step 2).

The MHC monomers were biotinylated with the BirA enzyme (Materials and Methods). As shown in Figure 4.6, FACS analysis revealed that the monomers were correctly folded and monobiotinylated as they were recognised by anti-H-2K (k and b) antibodies when they were loaded on streptavidin-coated beads.

### 4.2.2.2 Recognition of the H-2K molecules tethered on artificial bilayers

We next tested the capacity of 3-83 transgenic B cells to recognise the monobiotinylated H-2K molecules tethered through an avidin bridge on bilayers containing biotinylated lipids.

As shown in Figure 4.7 A and B, B cells could not recognise and accumulate these molecules on the bilayers even when they were displayed at high densities ($\delta \approx 250$ molecules/$\mu m^2$). Under the same conditions, B cells recognised and efficiently accumulated large amounts of p31 peptide antigen (Figure 4.7 A and B).

3-83 transgenic B cells bound the monomeric forms of the H-2K proteins when they were sequentially incubated with the proteins and then with fluorescently labelled avidin as shown by FACS analysis (Figure 4.7 B).

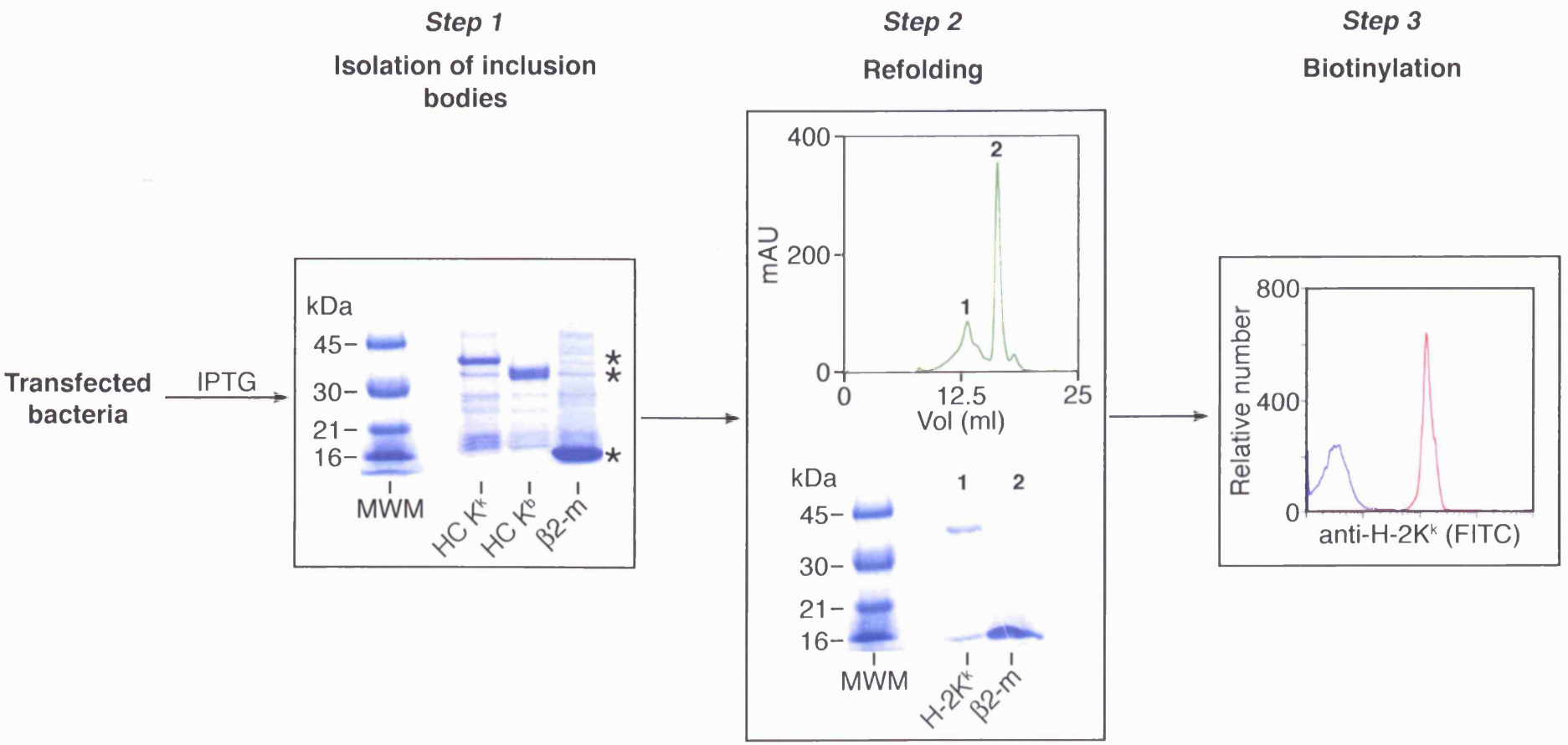
Step 1
Isolation of inclusion bodies
Step 2
Refolding
Step 3
Biotinylation
Transfected bacteria
IPTG
kDa
45–
30–
21–
16–
MWM
HC Kᵏ
HC Kᵇ
β2-m
**
*
400
200
0
mAU
2
1
0
12.5
25
Vol (ml)
kDa
45–
30–
21–
16–
MWM
1
2
H-2Kᵏ
β2-m
800
400
0
Relative number
anti-H-2Kᵏ (FITC)

**Figure 4.6. Stepwise representation of the H-2K proteins purification.**
*Step 1*: the heavy chains (HC $K^k$ and HC $K^b$) and the β2-microglobulin (β2-m) were purified from inclusion bodies isolated from transfected bacteria, and the purification assessed by SDS-PAGE. The asterisks mark the correct molecular weight of the three proteins (β2-m: 12 kDa, $K^b$: 34 kDa, and $K^k$: 35 kDa).
*Step 1*: the complexes were then generated by dialysis, and purified by size exclusion chromatography (top panel). SDS-PAGE analysis of the two isolated peaks (1 and 2) showed that the peak 1 consisted exclusively of heavy and light chain - therefore the folded complexes -, and peak 2 consisted exclusively of free β2-microglobulin (bottom panel). Only an example of one of the two proteins is shown, as the results were the same for both.
*Step 3*: the purified complexes were then biotinylated with the BirA enzyme. The biotinylation and correct folding of the monomers were assessed by FACS. Streptavidin-coated beads were incubated with the biotinylated proteins and then revealed with an anti-H-$2K^{k \text{ or } b}$ specific antibody and analysed by FACS. The histogram of the beads shows that the complexes were correctly folded and biotinylated (red trace). Blue trace shows unstained beads.

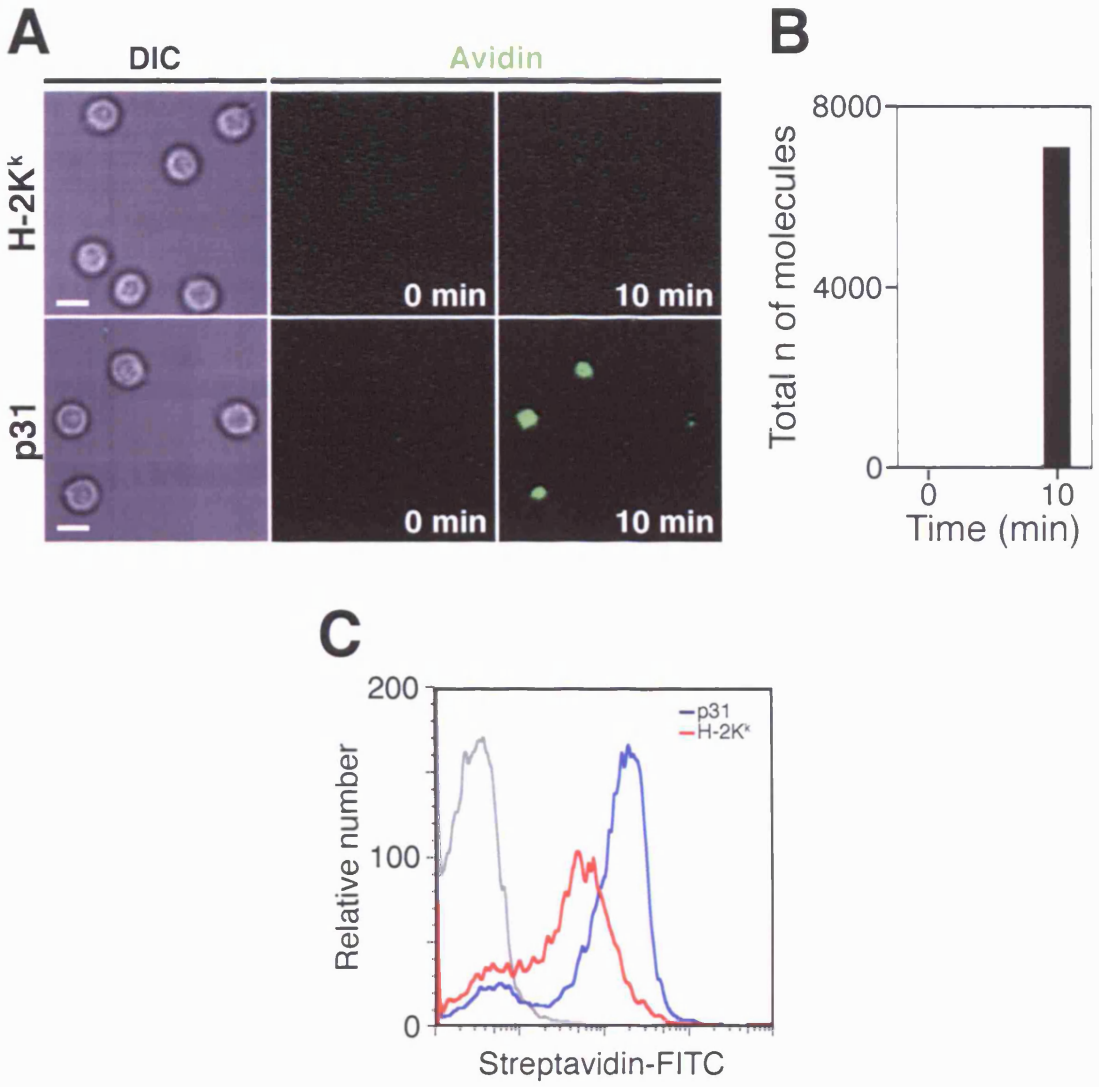


**Figure 4.7. Recognition of the H-2K molecules tethered on artificial lipid bilayers by 3-83 B cells.**

**(A)** Confocal images of 3-83 B cells settled on artificial bilayers containing the monobiotinylated H-2K$^k$ molecule (top) or p31 peptide (bottom) tethered through an Alexa Fluor488-conjugated avidin (green) at a density of 250 molecules/μm$^2$. The antigen-specific B cells did not recognise the H-2K molecules, even though in the same conditions they efficiently accumulated the p31 peptide. Scale bar: 5 μm. **(B)** Shows the amount of p31 accumulated by the 3-83 B cells. **(C)** FACS profile of 3-83 B cells sequentially incubated with either the monobiotinyalted H-2K$^k$ molecule (red trace) or the monobiotinylated p31 peptide (blue trace), and streptavidin-FITC. Gray trace shows the profile of 3-83 B cells incubated with streptavidin-FITC in the absence of the peptides.

Taken together, these results suggest that the proteins are not properly recognised on artificial bilayers when tethered through an avidin bridge, as the affinity of the interaction at least for the H-2K$^k$ has been reported to be very high (Lang et al., 1996).

As a consequence of these results we discarded the H-2K molecules as model antigen for our studies.

### 4.2.3 The HSμ transgenic mouse

HSμ transgenic B cells express a BCR formed by the canonical B1-8 heavy chain and λ1 light chain (Allen et al., 1988). This BCR binds the 4-hydroxy-5-iodo-3-nitrophenyl (NIP) and the 4-hydroxy-3-nitrophenyl (NP) haptens with different affinities (Figure 4.8 A). Therefore, we wanted to test if this transgenic mouse was suitable to test the importance of the kinetic parameters in the antigen recognition process.

We obtained the monobiotinylated forms of the two haptens from Biosearch. To obtain monovalent forms of the antigens tethered through a streptavidin molecule we planned to use the same strategy as the one we used for the p11 and p31 antigenic peptides.

#### 4.2.3.1 Recognition of the NIP/NP haptens by the HSμ transgenic system

We initially tested the capacity of the HSμ B cells to recognise and aggregate the multivalent forms of the NIP and NP haptens tethered on artificial bilayers. As shown in Figure 4.8 B, B cells did not recognise these antigens on the lipid bilayers even at very high densities of antigen ($\delta \approx$ 500-600 molecules/μm$^2$).

As a further control, we explored the interaction of the HSμ B cells with the haptens in solution. To this end, we sequentially incubated the HSμ B cells with the monobiotinylated NP or NIP molecules and Alexa Fluor 488-conjugated streptavidin, and analysed the B cells by FACS. As shown in Figure 4.8 C, we did not detect any binding with this assay.

These results suggest that the binding of the haptens to the avidin-loaded artificial bilayers (or the streptavidin in FACS analysis) impairs their recognition by the 3-83 transgenic B cells. As a consequence of this, we discarded this system for further analysis.

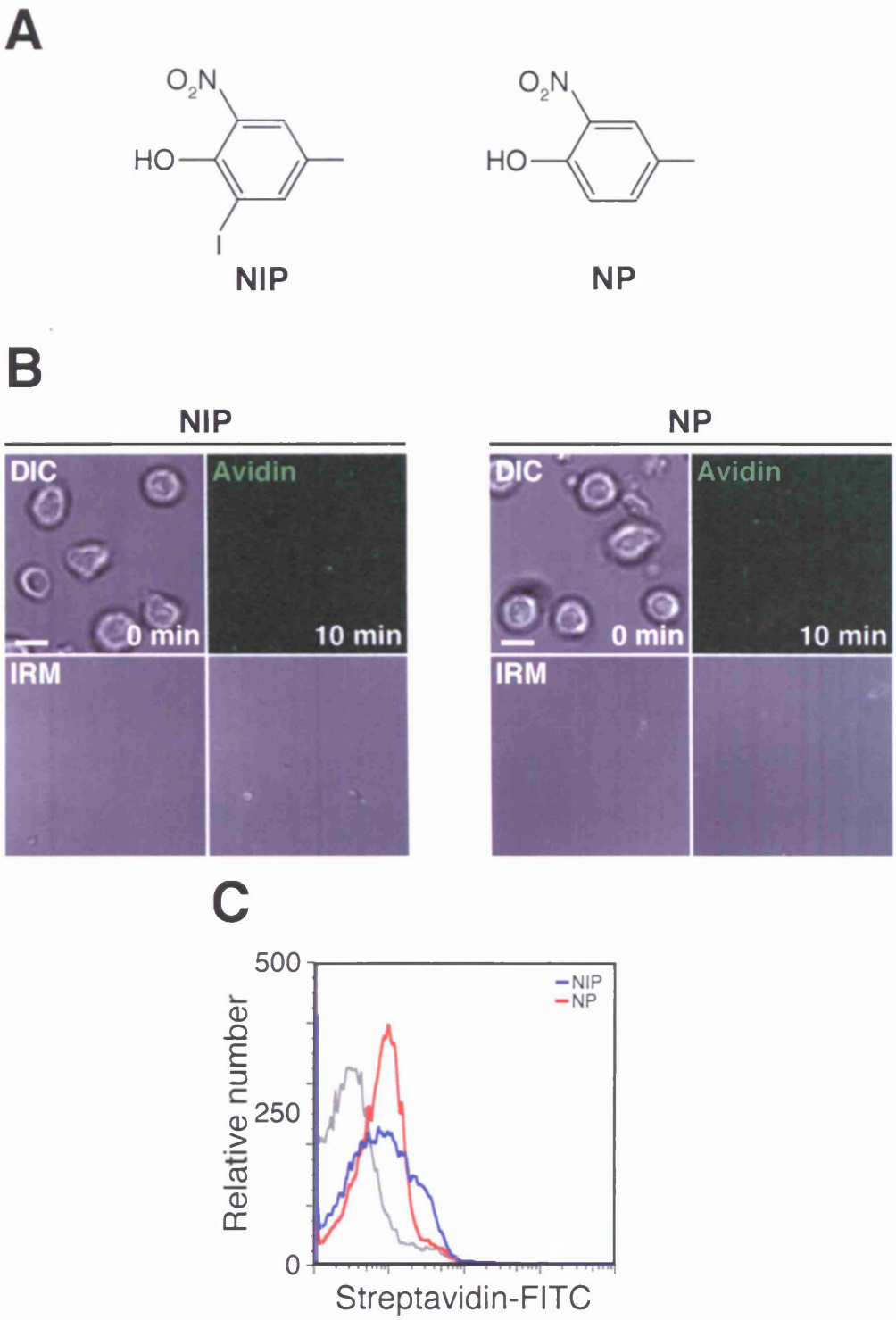


**Figure 4.8. Recognition of NIP and NP haptens tethered on artificial bilayers by HSμ transgenic B cells.**
**(A)** Structures of the NIP (left) and NP (right) haptens recognised by the HSμ B cells. **(B)** Confocal images of HSμ B cells settled on artificial bilayers loaded with the NIP (left panels) or the NP (right panels) haptens at a density of 550 molecules/μm$^2$. **(C)** FACS analysis of HSμ B cells sequentially incubated with the monobiotinylated NIP (blue trace) or NP (red trace) haptens and streptavidin-FITC. Gray trace indicate unstained cells.

## 4.3 Effect of the membrane diffusion in the antigen aggregation process

As discussed earlier, for very fast on-rates measured in solution the diffusion rate of the membrane should be a limiting factor in the association process. However, the dissociation phase is not affected by this. Therefore, we postulated that decreasing the diffusion rate of the bilayer should increase the thresholds of antigen accumulation, as well as the affinity ceiling.

Diffusion properties of artificial bilayers can be altered by the inclusion of phospholipids with saturated chains like DSPC that increase the $T_m$. In addition, the inclusion of cholesterol increases the rigidity of the membrane and has a similar effect (Veatch and Keller, 2002; Veatch and Keller, 2003).

Thus, to test this hypothesis, we prepared liposomes with phospholipids containing saturated fatty acids (such as DSPC) and DOPC including different percentages of cholesterol. We mixed them with liposomes containing NBD-PE phopspholipids and visualised them by confocal microscopy.

The different artificial membranes showed a differential degree of clustering (Figure 4.9). The proportion of cholesterol included in the liposomes appeared to have a key impact in the formation of these clusters, as these increased in size with the proportion of cholesterol included (Figure 4.9). We observed by FRAP experiments that there are two lipid fractions present on the bilayers: one fraction that can freely diffuse and another fraction that is almost immobile and consists mainly of big clusters of lipids (Figure 4.9). These results showed that this approach was not suitable; therefore we discarded their further use.

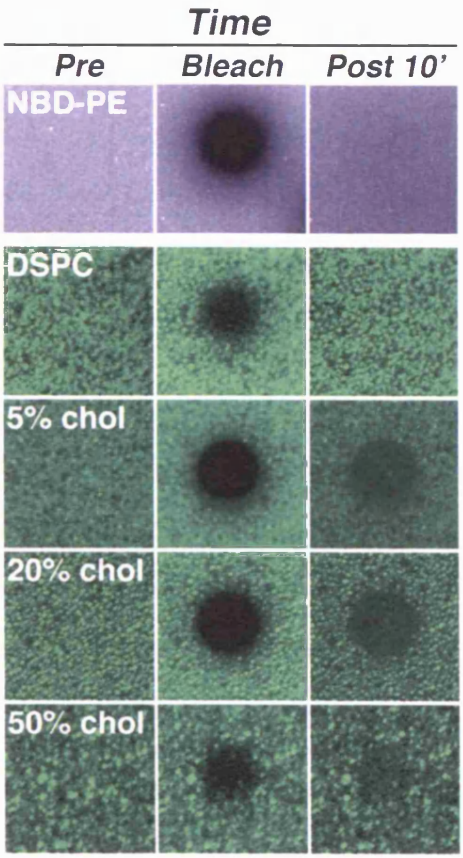


**Figure 4.9. Effect of the lipid bilayer composition in the diffusion rate and antigen recognition process.**
FRAP experiments of artificial lipid bilayers prepared with liposomes of different compositions (indicated in the panels). Pre: pre-bleaching; Post 10': image after 10 minutes of bleaching. The membranes appeared clustered compared to NBD-PE lipid and with two populations of diffusing molecules.

## 4.4 Effect of tethering antigens on a membrane on the dissociation half-life of the antigen/BCR interaction

Our results showed that antigens that have an extremely low affinity are nevertheless efficiently accumulated (Figure 3.9 and Table 1). Therefore, membrane tethering of ligands has a positive effect in the affinity of the interaction and in the recognition process.

We postulated that the positive effect on the affinity of membrane tethering of antigens would be mainly due to a positive effect on the dissociation half-life.

To test this, we performed FRAP experiments of antigen clusters on artificial lipid bilayers. One of the problems that we encountered was that B cells extract the antigens after aggregation, and therefore the system was not suitable for long-term visualisation required for FRAP experiments (Figure 3.16). Thus, we searched for alternative ways of approaching this problem.

### 4.4.1 Polymer beads as surrogate cells

Our first approach consisted in using beads coated with the HyHel10 antibody (MD4 BCR) as surrogate cells. To this end, we took advantage of streptavidin-coated beads and the calibrated beads previously used to estimate the antigen density on the bilayer.

We coated both type of beads with the HyHel10 monoclonal antibody, and then incubated them with artificial bilayers loaded with the $HEL^{WT}$ antigen. As shown in Figure 4.10 A, neither of the two types of beads clustered any antigen. The result was surprising as these beads have a density of antibody that exceed the density of the B cell receptor expressed on the surface of MD4 B cells (Figure 4.10 B).

As previously described in Chapter 3, B cells spread on the target membrane during the initial stages of antigen recognition. Therefore, taken together these results suggest that due to their rigidity the beads cannot expose an appropriate surface of contact (therefore, antibody molecules) with the artificial bilayers.

### 4.4.2 Blocking antigen extraction

The second approach consisted in treating the B cells with src kinase inhibitors (PP1 and PP2) to block the antigen extraction process, as the signalling

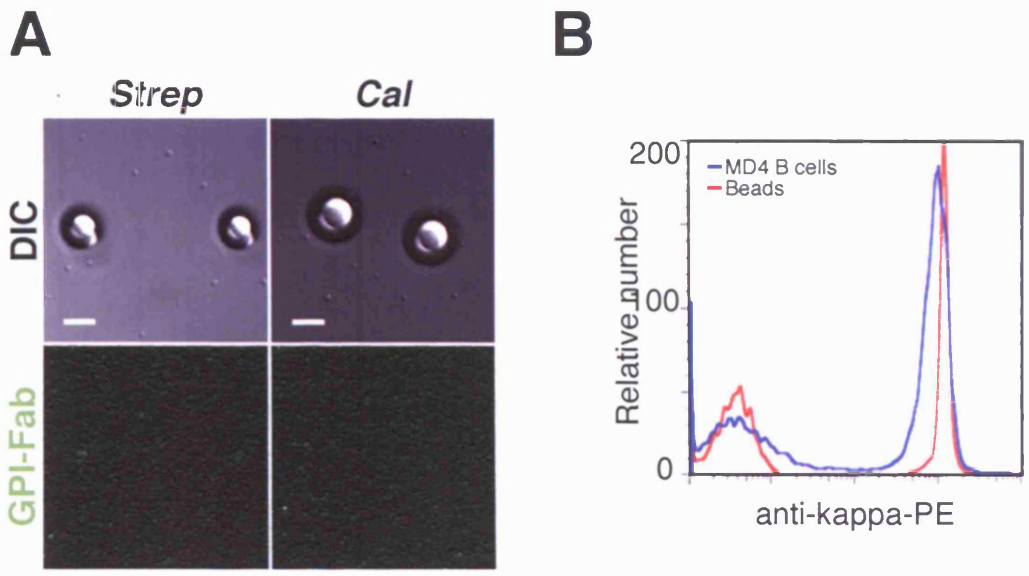


**Figure 4.10. Antibody-coated beads as surrogate cells to study membrane antigen recognition.**

**(A)** Confocal images of streptavidin-coated beads (Strep) or calibrated beads (Cal) coated with the HyHel10 monoclonal antibody settled on artificial bilayers containing the $HEL^{WT}$ antigen tethered through the GPI-linked Fab (GPI-Fab, green) at a density of 150 molecules/$\mu m^2$. Scale bar: 5 μm. **(B)** FACS analysis of MD4 B cells (blue trace) and streptavidin-coated beads coated with the HyHel10 MAb (red trace) stained with a PE-conjugated anti-kappa antibody.

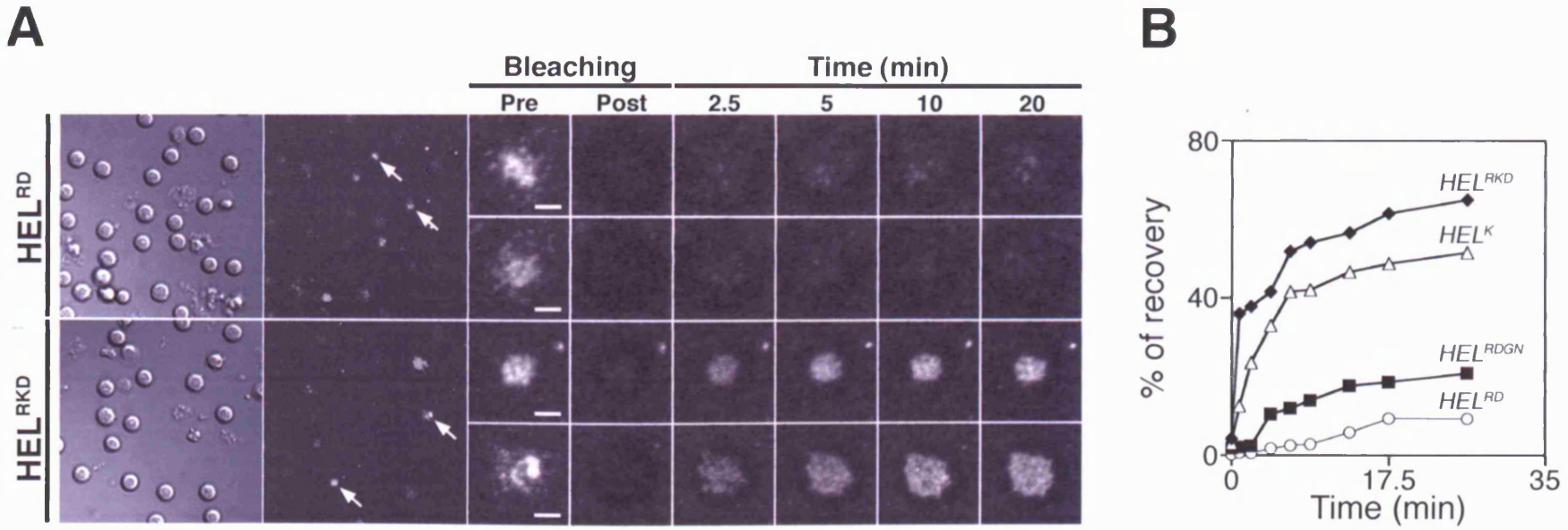


**Figure 4.11. Effect of tethering antigens on a membrane on the dissociation half-life of the BCR/antigen interaction.**
**(A)** MD4 B cells treated with PP2 inhibitor were settled on artificial bilayers loaded with different mutant lysozymes at a density of 150 molecules/$\mu m^2$. After 30 minutes of interaction, selected clusters of antigen were bleached and the recovery of fluorescence followed for 30 minutes. Scale bars: 2 μm. **(B)** Shows the recovery of fluorescence as a function of time for different mutant lysozymes.

component of the BCR is necessary to perform this task (Batista and Neuberger, 2000). Under these conditions, B cells are suitable for long-term FRAP experiments. MD4 B cells were treated with PP2 and settled on artificial bilayers loaded with the different HEL antigens tethered through a GPI-linked Fab (Table 1). We then probed the stability of the antigen/BCR interaction by FRAP experiments.

As shown in Figure 4.11, the recovery rate of fluorescence correlates with the rates of dissociation of the antigen/BCR interactions measured by SPR. However, the half-lives ($t_{1/2}$) increased by several orders of magnitude when both, ligands and receptors are tether on a membrane. For instance, $HEL^{RDGN}$ that in solution has a measured $t_{1/2}$ of 18 seconds, when it is tethered on a membrane this value increases to an apparent $t_{1/2}$ of $\approx$ 120 seconds. Similar results were obtained for other mutant lysozymes.

## 4.5 Discussion

### 4.5.1 Binding kinetics and membrane antigen recognition

In the study presented in this chapter, we explored different strategies to address the relevance of the binding kinetic parameters of the BCR/antigen interaction in the membrane antigen recognition process. To this end, we took advantage of BCR transgenic mice that recognise antigens with varying on-rates and off-rates, something that was not attainable with the MD4 transgenic system.

Unfortunately, the different approaches did not provide any conclusive result. B cells isolated from the 3-83 transgenic mouse did not recognise fusion antigens of HEL and peptides and monobiotinylated H-2K molecules tethered on artificial lipid bilayers. Similar negative results were obtained with the HSμ transgenic mouse.

In the case of the HEL-peptides fusion antigens probably the epitope is hidden due to the fusion itself, and therefore the BCR cannot bind it. A similar mechanism may be involved with the monobiotinylated antigens, but in this case the masking of the epitopes may be due to the tethering through an avidin molecule on the bilayers.

This idea is supported by experiments that showed that transgenic B cells effectively bound some of the antigens (for example the H-2K molecules) when they were incubated in solution with them.

The experiments performed with antigenic peptides recognised by the 3-83 BCR transgenic mouse diluted with an irrelevant monobiotinylated peptide were the only experiments that provided a positive result. They suggest that the off-rate is an important parameter determining the accumulation of antigen. The main problem encountered in this case was that we did not manage to obtain measurements of the binding kinetics for the antigens as the antigenic peptides have a very low molecular weight, and therefore they are not adequate for SPR analysis.

These experiments also showed that for this system the avidity plays an important role in the recognition of membrane antigens, contrary to what we observed with the MD4 system. Structural differences of the two types of antigens may account for this difference, as one consists of small peptides and the other of globular proteins.

The relevance of the dissociation half-life in the recognition of membrane antigens would be in line with previous reports on the recognition of MHC-peptides by T cells (Grakoui et al., 1999). Furthermore, as the range of affinities and kinetic parameters of antigen/BCR interaction that a B cell may encounter are broader than T cells, our results could be extensive to most ligand/receptor interactions. Further experiments will be necessary to solve this question.

### 4.5.2 Membrane diffusion and antigen recognition

Alteration of the composition of the artificial bilayers proved to be a difficult task, since the inclusion of phospholipids with saturated chains or cholesterol altered the structure of the artificial bilayers generating clusters of non-diffusible molecules (Figure 4.9). Thus, we could not use bilayers prepared with these phospholipids to address the effect of membrane diffusion in antigen recognition.

Previous reports have shown that the diffusion of receptors in the postsynaptic membrane is an important parameter controlling the transmission of nerve impulses (Choquet and Triller, 2003). Therefore, it will be interesting to explore if

this is also an important parameter affecting the recognition of membrane antigens by lymphocytes.

This will require a dedicated effort in the development of artificial bilayers with the desired characteristics.

### 4.5.3 Dissociation half-life and membrane tethering

Several groups have attempted to measure two-dimensional affinity constants (2D $K_d$). However, this has proved to be a very difficult task and only a few 2D constants of interaction have been reported (Davis et al., 2003; Dustin et al., 1996; Shaw and Dustin, 1997). What is evident from these studies is that there is no simple relationship between the 2D and the 3D $K_d$ values.

FRAP experiments with cells treated with src kinase inhibitors allowed us to explore the effect of tethering an antigen on a membrane on the dissociation half-life. Although this approach only provides estimated membrane $t_{1/2}$ that are slower than real membrane $t_{1/2}$, it is interesting to remark that they increase by several orders of magnitude compared to solution measurements. This in part explains why B cells efficiently aggregate antigens that have an extremely low $t_{1/2}$ in solution as measured by SPR (Bell, 1978; Dustin, 1997).

Finally, the kind of measurements that we performed may be useful in order to understand how 2D and 3D affinity are related.

# Chapter 5: Spreading and contraction response during membrane antigen recognition

## 5.1 Introduction

As described in the previous chapters, during the early stages of membrane antigen recognition, B cells spread and contract on the target surface. We have also shown that this cellular response correlates with the engagement and accumulation of antigen. Interestingly, we observed that most of the antigen molecules seem to be engaged during the spreading phase as the time point of maximum area of spreading correlates with the time point of maximum amount of antigen engagement (see Figures 3.2 and 3.6). In the same line, the results obtained with the experiments using beads as surrogate cells suggest that the flexibility of the cell membrane may play a role during membrane antigen recognition.

Taken together these results suggest that cell spreading has in fact an important role during antigen accumulation. Therefore, we wanted to explore further its involvement in this process.

## 5.2 Importance of the spreading response

### 5.2.1 Dependence on signalling

Initial experiments support the notion that spreading is triggered by antigen engagement through the BCR and not simply by contact with the bilayer (Figures 3.2 and 3.6). Therefore, we reasoned that B cells that cannot signal through the BCR should not be able to spread.

To test this hypothesis, we took advantage of different lines of transgenic B cells that express the D1.3 BCRs that bind an epitope of the hen egg lysozyme with a very high affinity (Figure 5.1 A) (Teh and Neuberger, 1997). However, the three different lines of transgenic BCRs present altered signalling properties (Figure 5.1 B). B cells from the IgM transgenic line express a canonical BCR, with an antigen-specific membrane immunoglobulin and the signalling components Igα and Igβ. The IgM/$\beta^{Y>L}$ transgenic B cells express a chimeric IgM that consists of the membrane immunoglobulin fused to the cytoplasmic tail of the Igβ chain. The

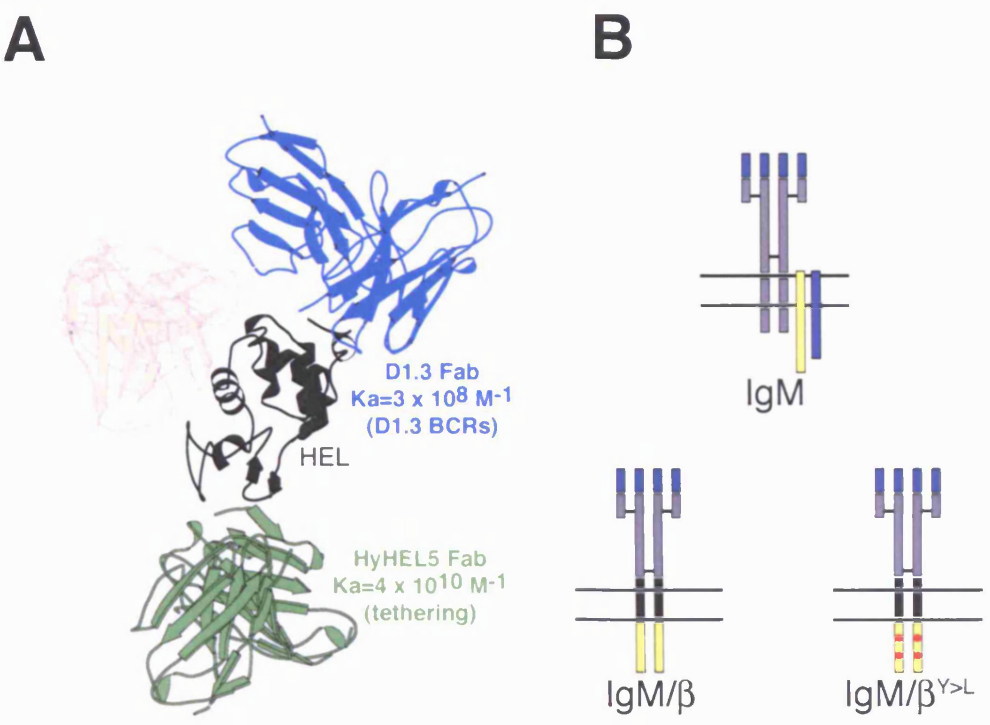


**Figure 5.1. Schematic representation of the D1.3 transgenic lines.**
**(A)** Shows the X-ray crystal structure of HEL complexed with the D1.3 (blue), the HyHel5 (green) and the HyHel10 (light gold) monoclonal antibodies. The affinity of interaction for the D1.3 antibody is very high. **(B)** Diagrams of the different chimeric BCRs with D1.3 binding specificity, but altered signalling properties. IgM is a canonical BCR, while IgM/β is a chimeric receptor that consists of the Igβ tail (yellow) fused directly to the membrane immunoglobulin. The IgM/$\beta^{Y>L}$ receptor is the same chimeric receptor, but is signalling-deficient since the tyrosines on the ITAM motif have been mutated (yellow band with red dots).

transmembrane domain was replaced with the H2 transmembrane domain of the MHC molecules, and therefore this receptor cannot associate with the endogenous signalling components of the BCR (Teh and Neuberger, 1997). Furthermore, the tyrosines of the ITAM motif of the fused Igβ chain were replaced by leucines, thus the BCR of these B cells is signalling deficient (Figure 5.1 B). The third transgenic line (IgM/β) expresses the same chimeric BCR, but with an intact ITAM motif of the fused Igβ chain (Figure 5.1 B).

We first analysed the recognition of the $HEL^{WT}$ antigen tethered on the bilayer by the D1.3 transgenic B cells that express the canonical BCR (IgM). As shown in Figure 5.2 A (top panels) and B, these B cells spread normally and contract to accumulate the antigen previously engaged.

When we tested the behaviour of B cells isolated from the signalling-deficient D1.3 mouse ($IgM/\beta^{Y>L}$), we observed that they have an impaired capacity to spread, and the antigen seems to be accumulated in a passive way, by engagement of the freely diffusing antigen at the point of contact (Figure 5.2 A (middle panels) and B). Signals delivered from the IgM/β chimeric BCR are sufficient to restore this cellular response, as B cells spread normally (Figure 5.2 A (bottom panels) and B).

We then quantified the amount of antigen aggregated by measuring the increase of the associated fluorescence at the site of contact. We observed that signalling deficient B cells ($IgM/\beta^{Y>L}$) have an impaired capacity to accumulate antigen compared to signalling competent B cells (IgM and IgM/β) (Figure 5.2 C).

Similar results were obtained when we tested other signalling deficient B cells, the A20 B cell line transfected with the same HEL-specific BCRs with altered signalling capacity (Figure 5.3 A and B) (Williams et al., 1994). As shown in Figure 5.3 A and B, A20 B cells transfected with signalling deficient BCRs, $IgM/\beta^{Y>L}$ and H2, did not spread and aggregated the antigen in a passive way. A signalling-competent BCR restored their spreading response (Figure 5.3 A and B). This differential response depending on the signalling capacity had a dramatic effect in the amount of antigen that the cells accumulated (Figure 5.3 C).

These results were further confirmed by treatment of MD4 B cells with Src kinase inhibitors (PP1 or PP2) that block the initial signals delivered by the BCR. As shown in Figure 5.4, B cells treated with these inhibitors did not spread compared

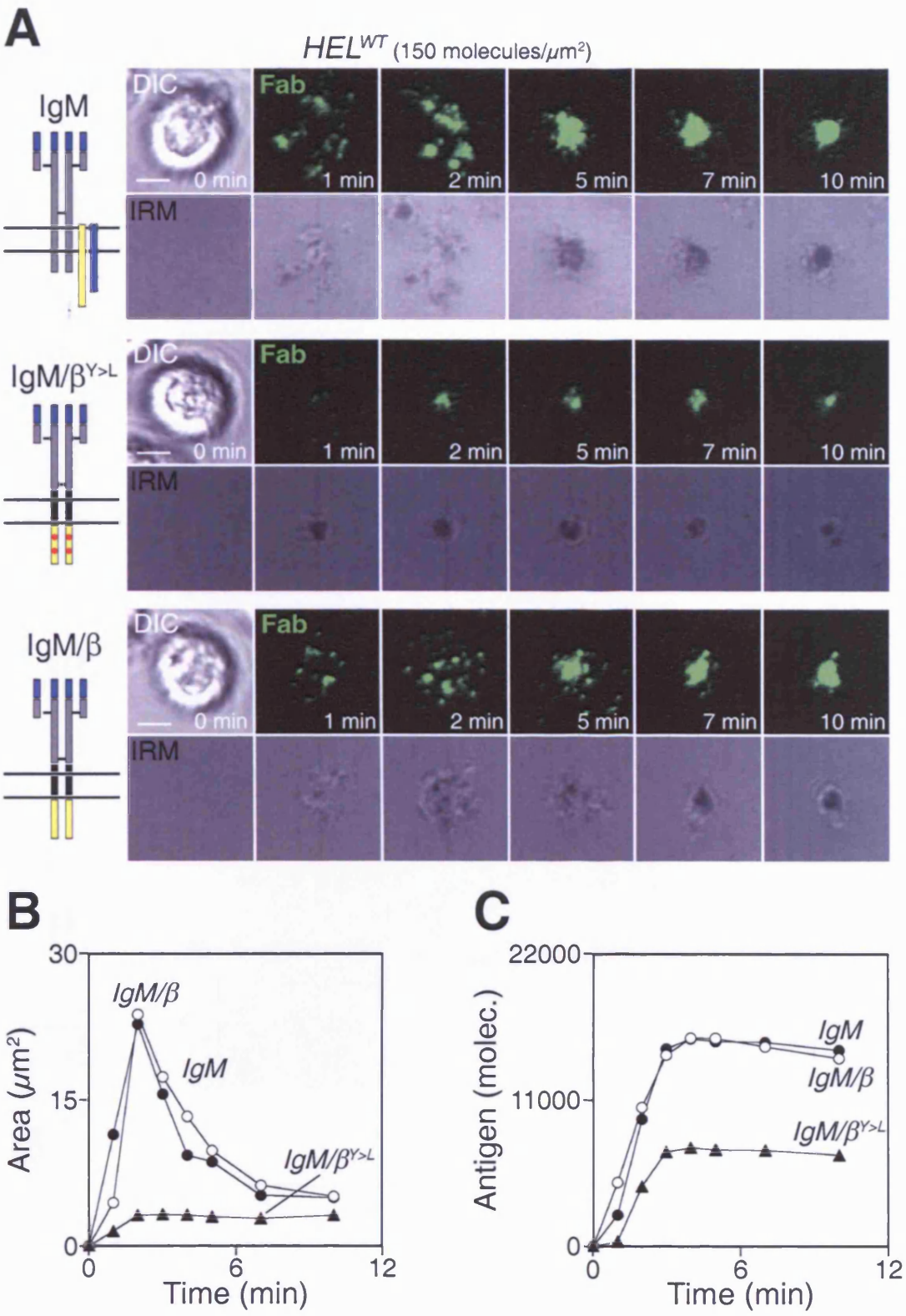


**Figure 5.2. Signalling dependence of the spreading response.**
**(A)** The time lapses show confocal images of IgM (top panels), IgM/$\beta^{Y>L}$ (medium panels) and IgM/β (bottom panel) transgenic D1.3 B cells naïve in contact with artificial lipid bilayers loaded with $HEL^{WT}$ antigen at a density of 150 molecules/μm². Contacts of the B cell with the bilayer were visualised by IRM (grayscale). Scale bars: 2 μm. **(B)** Surface area of spreading and **(C)** amount of $HEL^{WT}$ antigen aggregated for the different transgenic backgrounds as a function of time.

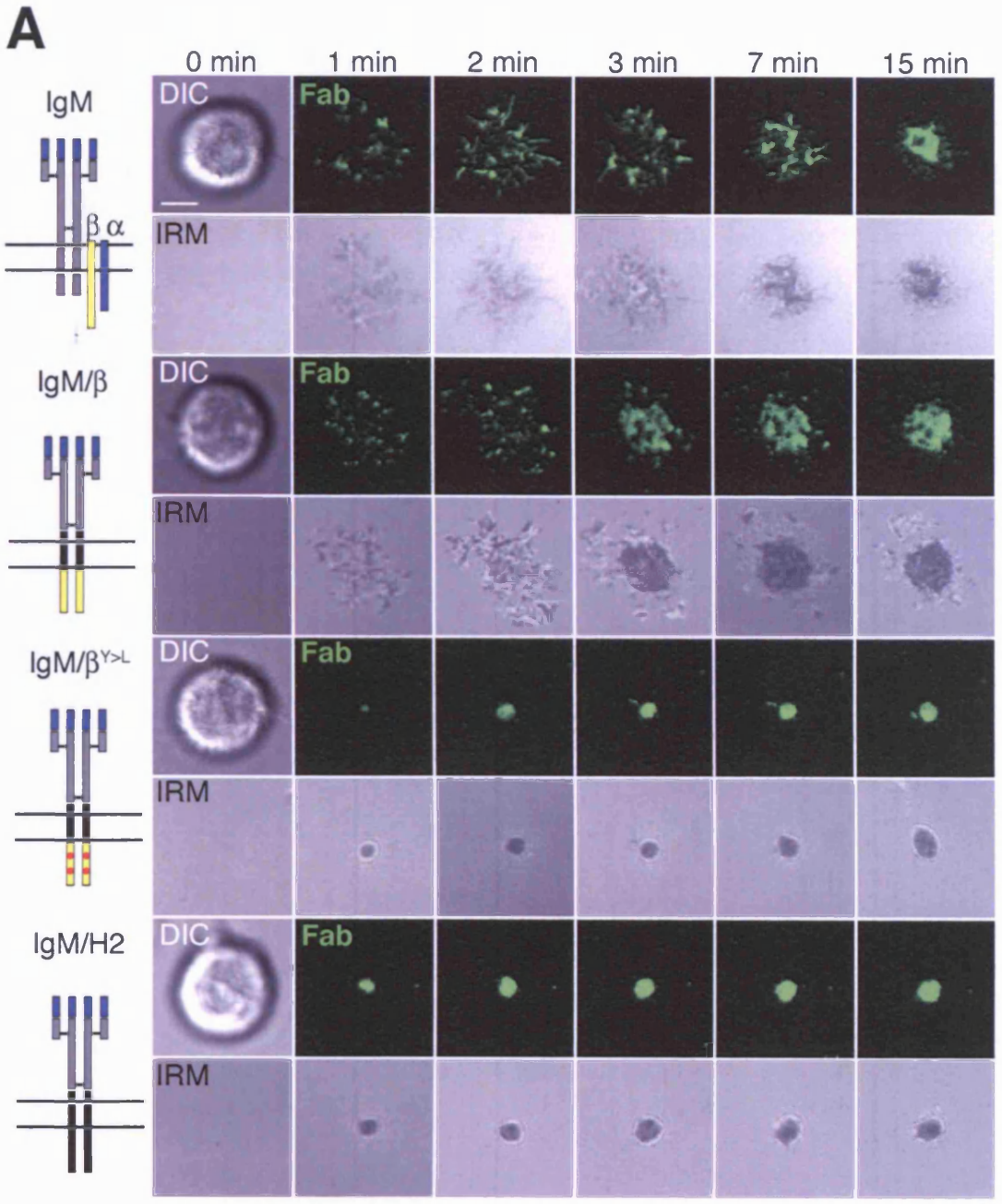
A
0 min
1 min
2 min
3 min
7 min
15 min
IgM
β α
IgM/β
IgM/β^Y>L
IgM/H2
DIC
Fab
IRM

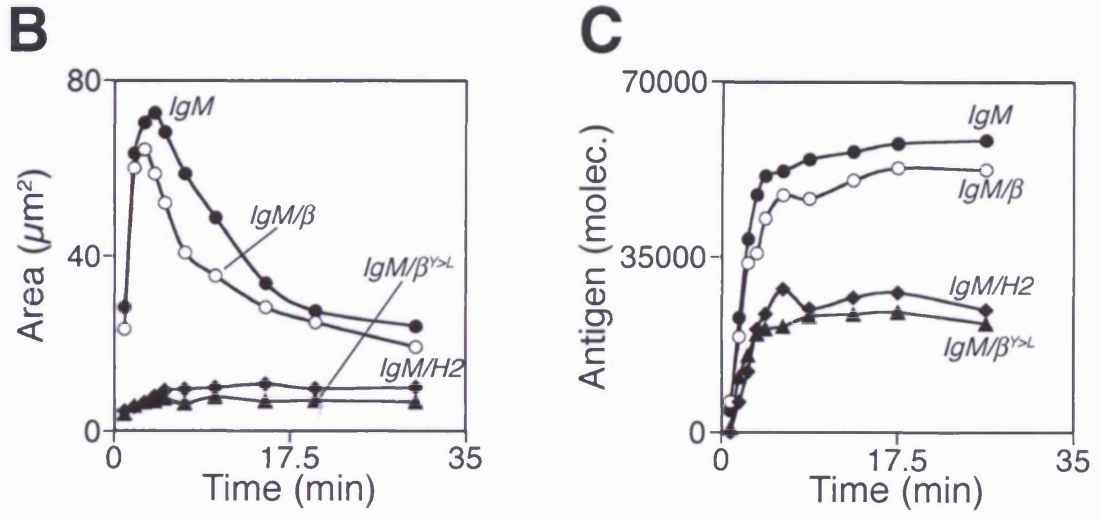
B
Area (μm²)
80
40
0
IgM
IgM/β
IgM/β^Y>L
IgM/H2
0
17.5
35
Time (min)


C
Antigen (molec.)
70000
35000
0
IgM
IgM/β
IgM/H2
IgM/β^Y>L
0
17.5
35
Time (min)

**Figure 5.3. Signalling dependence of the spreading response: A20 B cell line.**
**(A)** A20 B cells expressing a canonical IgM (top panel), IgM/β (second panel), IgM/$\beta^{Y>L}$ (third panel) or IgM/H2 (bottom panel) BCR were allowed to settle onto artificial lipid bilayers loaded with $HEL^{WT}$ antigen at a density of 150 molecules/$\mu m^2$ (green, top rows). Individual cells were followed by confocal microscopy for 30 minutes. Contacts of the B cell with the bilayer were visualised by IRM (grayscale, bottom rows). **(B)** Surface area of spreading and **(C)** amount of $HEL^{WT}$ antigen aggregated for the different transgenic backgrounds as a function of time.

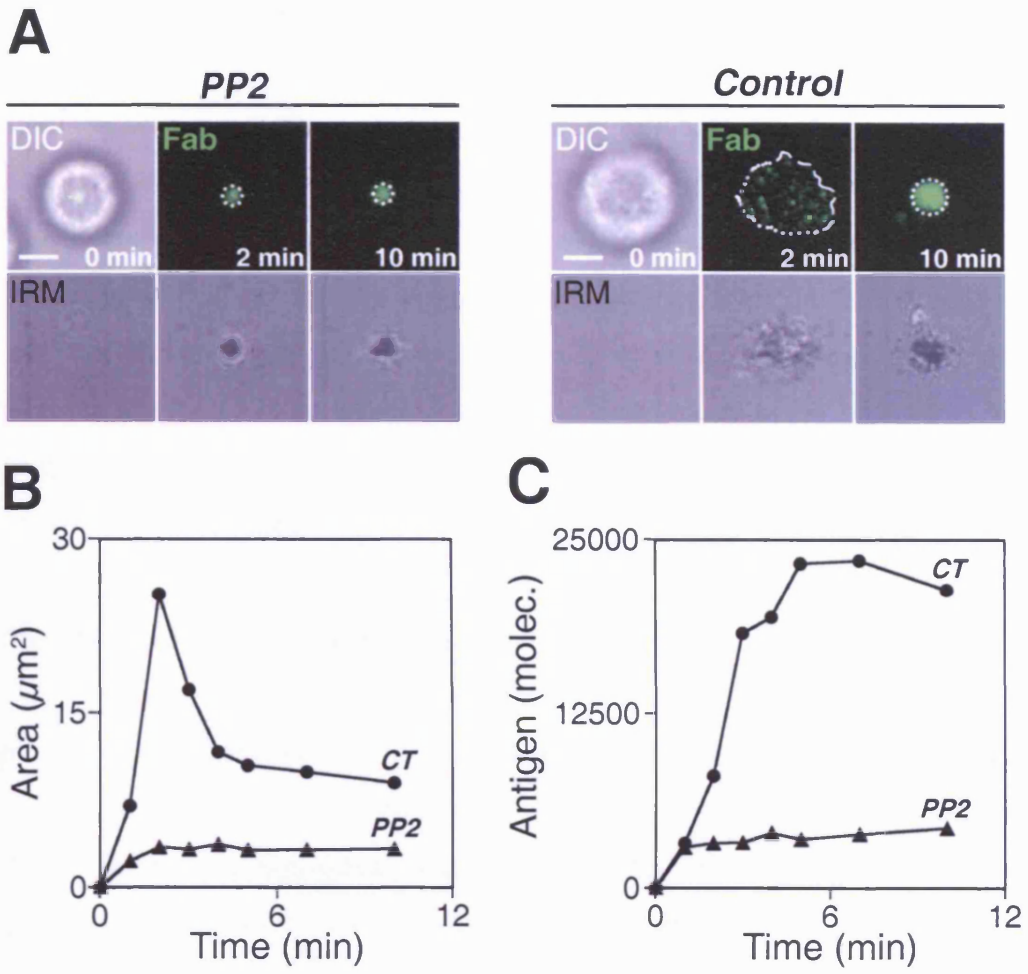


**Figure 5.4. Inhibition of cell spreading by Src kinases inhibitor PP2.**
**(A)** Confocal images of MD4 B cells treated (left panels) or untreated (right panels) with the Src kinase inhibitor PP2 in contact with artificial bilayers loaded with the $HEL^{WT}$ antigen at a density of 150 molecules/μm². Dotted white lines delimit the area of contact as assessed by the antigen fluorescence. Scale bar: 2 μm. **(B)** Area of spreading and **(C)** amount of antigen accumulated as a function of time for the processes described in **(A)**.

to untreated cells when they encounter the $HEL^{WT}$ on artificial lipid bilayers. Their capacity to accumulate antigen was also impaired and the aggregation process resembled the one of signalling deficient B cells (Figure 5.4).

In conclusion, these results show that B cell spreading is triggered by signals delivered through the BCR and not only by antigen binding. In fact, B cells that express a BCR with an extremely high affinity for the antigen but are signalling-deficient cannot spread. In addition, when we performed the experiments with the IgM/β transgenic line, in which the BCR is fused to only the Igβ chain, the spreading response was normal. This result indicates that this single signalling component of the BCR complex is sufficient to trigger this cellular response.

### 5.2.2 Signal localisation and spreading

We next wanted to understand if signals bypassing the localised triggering through the BCR on the lipid bilayer could eventually promote cell spreading. For this purpose, we settled signalling-deficient B cells on lipid bilayers loaded with HEL and allow them to aggregate the antigen passively for 15 minutes. After that, we injected into the chambers ionomycin or an anti-kappa antibody to trigger cell signalling through two different pathways. Ionomycin is an ionophore that causes the entry of calcium through the plasma membrane. Calcium is an important second messenger responsible of several of the effects of BCR mediated signalling (Niiro and Clark, 2002). The anti-kappa antibody has a high capability to crosslink the endogenous non-transgenic BCR expressed by the signalling-deficient B cells (Teh and Neuberger, 1997).

As shown in Figure 5.5, B cells did not spread on the target membrane by overcoming the signals delivered by local contact through the BCR. This suggest that signals delivered locally through the BCR as a consequence of membrane antigen recognition are responsible for the oriented spreading response on the antigen bearing membrane.

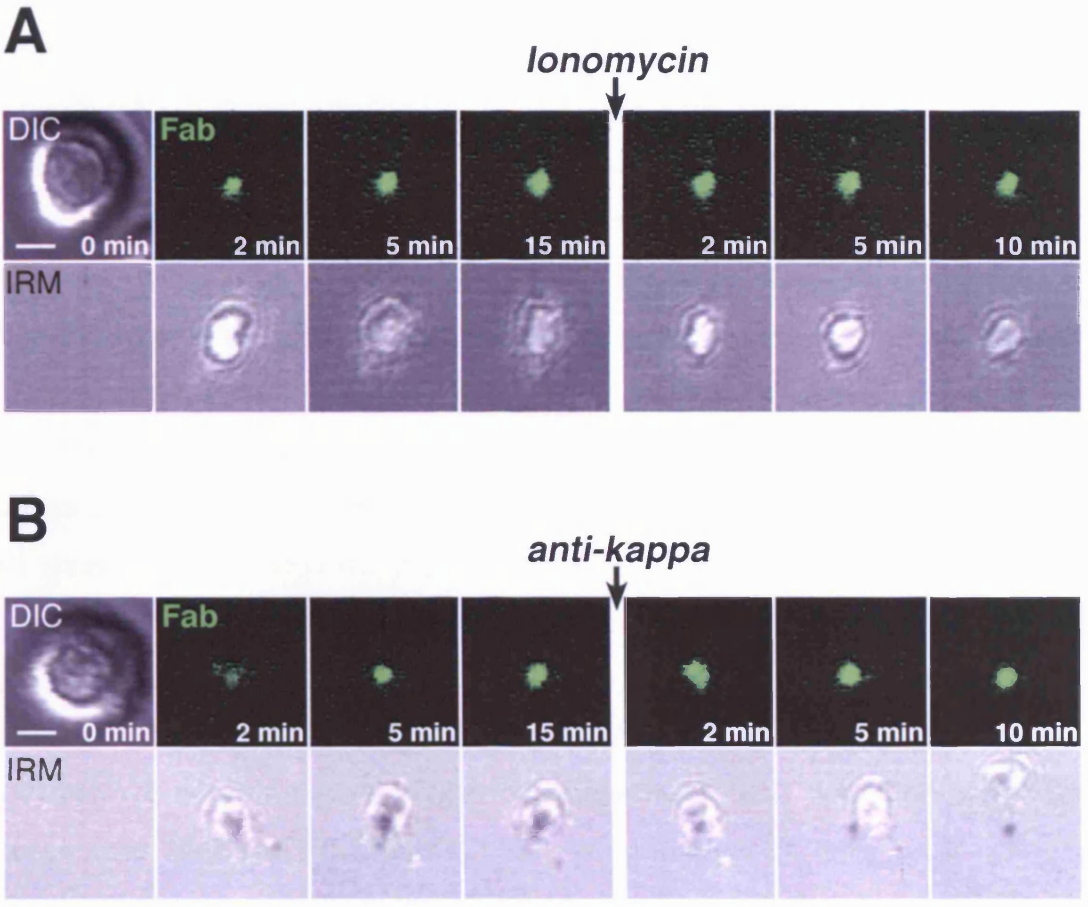


**Figure 5.5. Effect of bypassing the BCR signalling cascade.**
Transgenic IgM/$\beta^{Y>L}$ D1.3 B cells were allowed to interact with the $HEL^{WT}$ antigen loaded on artificial bilayers at a density of 150 molecules/$\mu m^2$. After 15 minutes of interaction, the chambers were injected with **(A)** ionomycin or **(B)** an anti-kappa antibody and the response of the B cells followed for another 15 minutes.
The signals delivered by the ionophore or by the cross-linking of the endogenous BCR expressed by the IgM/$\beta^{Y>L}$ D1.3 B cells were not sufficient to trigger the cell spreading response of B cells.

### 5.2.3 Dependence of the spreading response on the affinity and the density of antigen on the target membrane

Our results showed that cell spreading is important for antigen accumulation; therefore we postulated that the extent of this response should be sensitive to the affinity of the BCR/antigen interaction as well as to the density of antigen on the bilayer. This would in turn have an impact on the amount of antigen accumulated at the end of the process. To test this hypothesis, we analysed the interaction of MD4 B cells with the different HEL antigens tethered on artificial bilayers through the GPI-linked HyHel5 Fab fragment. To follow changes in morphology by confocal microscopy, we labelled the cell membranes with the PKH26 dye.

As expected, PKH26 fluorescence images showed that the maximum area of B cell spreading depended on the affinity of the interaction (Figure 5.6 A). For example, B cells exhibited an increased area of spreading on bilayers loaded with $HEL^{RD}$ compared to those loaded with $HEL^{RKD}$, which has a 1000-fold decreased in its affinity for the HyHel10 BCR (Figure 5.6 A).

However, we could not observe any difference in the area delimited by PKH26 fluorescence between $HEL^{RD}$ and $HEL^{K}$, even though B cells were able to discriminate them efficiently in terms of number of molecules accumulated (Figure 5.6 A). Since the dye is homogeneously distributed in the plasma membrane, we reasoned that confocal images might not be accurate enough to discriminate morphological changes that take place at the level of the artificial bilayer from morphological changes in other sections of the cell body.

We then measured the area defined by the surface of antigen engagement (see Materials and Methods). In this case, we observed that in fact the maximum area of spreading depended precisely on the affinity of the BCR/antigen interaction (Figure 5.6 A and B). Differences in the spreading response to the different antigens were also evident when we analysed MD4 B cells by SEM (Figure 5.7).

We also tested the effect of the density in the spreading response, and we found a similar dependence: the extent of the spreading area decreases when the density of antigen on the bilayer decreases (Figure 5.8). In fact, cell spreading showed a sharp decrease when the density was decreased, as we have previously shown for the antigen accumulation process (Figure 5.8).

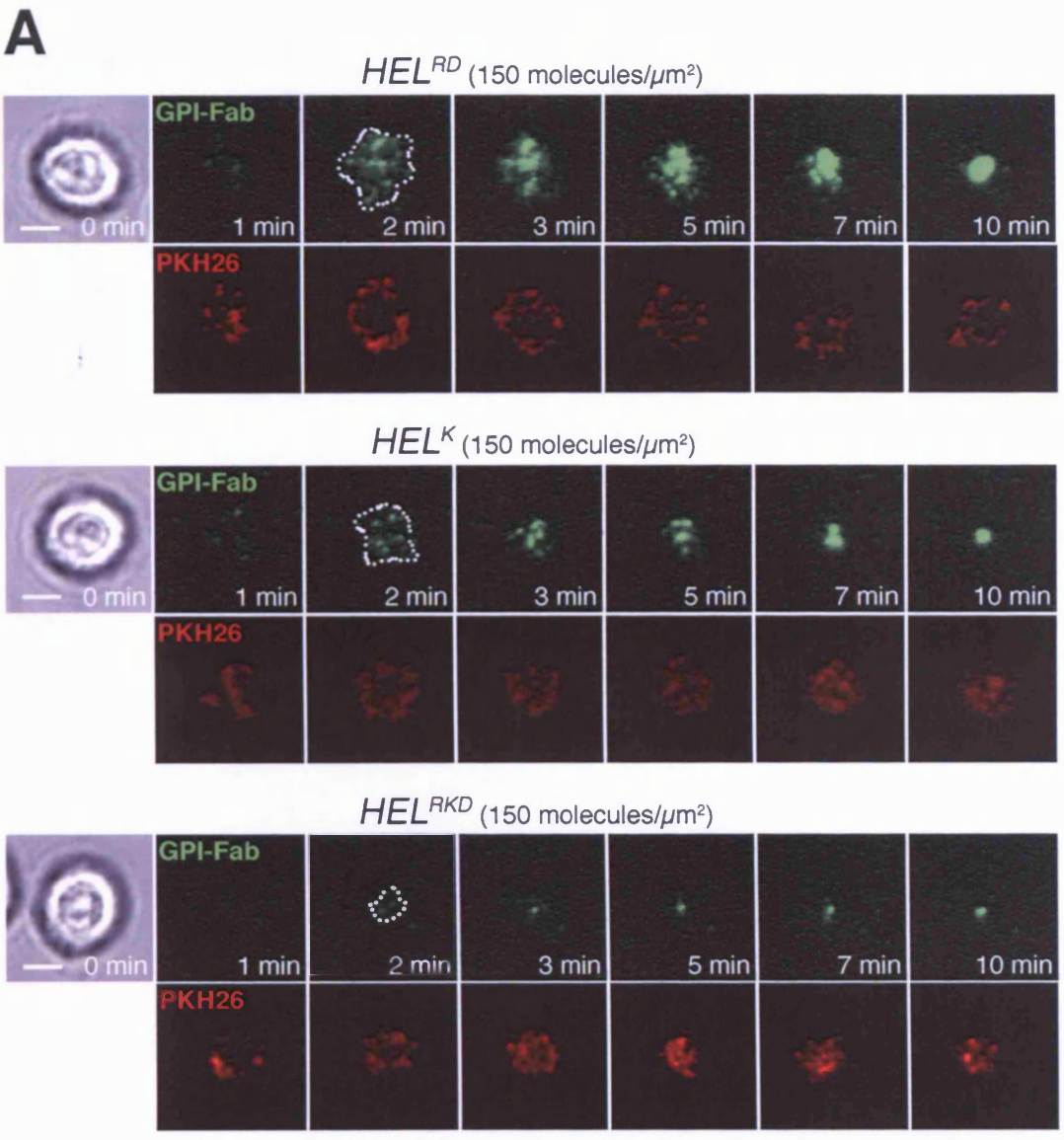
A
HEL^RD (150 molecules/μm²)
GPI-Fab
PKH26
0 min
1 min
2 min
3 min
5 min
7 min
10 min
HEL^K (150 molecules/μm²)
GPI-Fab
PKH26
0 min
1 min
2 min
3 min
5 min
7 min
10 min
HEL^RKD (150 molecules/μm²)
GPI-Fab
PKH26
0 min
1 min
2 min
3 min
5 min
7 min
10 min

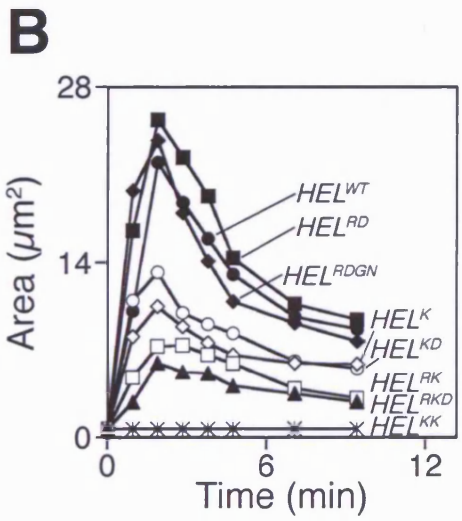
B
28
14
0
Area (μm²)
0
6
12
Time (min)
HEL^WT
HEL^RD
HEL^RDGN
HEL^K
HEL^KD
HEL^RK
HEL^RKD
HEL^KK

**Figure 5.6. Dependence of the spreading response on the affinity of the BCR/antigen interaction.**
**(A)** The time lapses show confocal images of transgenic MD4 naïve B cells in contact with artificial lipid bilayers loaded with $HEL^{RD}$ (top panels), $HEL^{K}$ (middle panels) and $HEL^{RKD}$ (bottom panels) antigens at a density of 150 molecules/$\mu m^2$. Cell membranes were visualised by PKH26 staining (red). Dotted line shows the maximum area of spreading as assessed by the antigen fluorescence. Scale bars: 2 μm. **(B)** Surface area of spreading of MD4 B cells for the different HEL mutant antigens as a function of time.

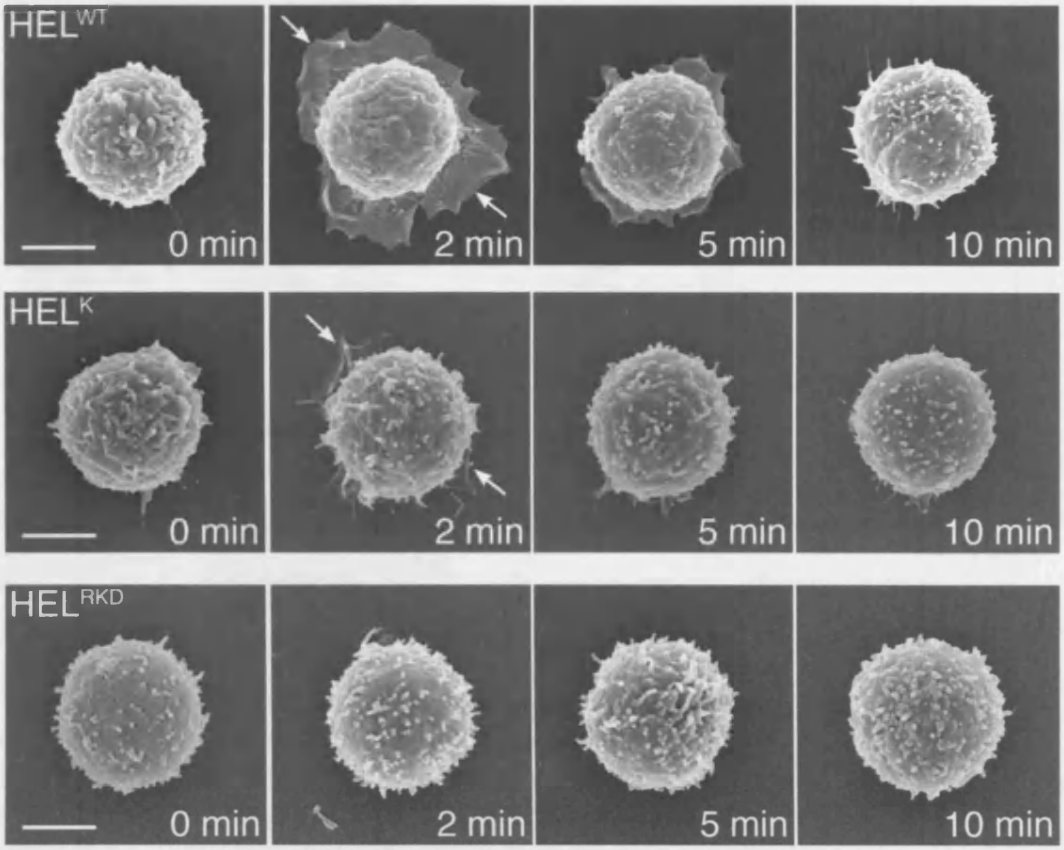


**Figure 5.7. Dependence of the spreading response on the affinity of the BCR/antigen interaction: SEM analysis of B cell morphology.**
MD4 B cells were settled on artificial bilayers loaded with $HEL^{WT}$ (top lane), $HEL^{K}$ (middle lane) and $HEL^{RKD}$ (bottom lane) at a density of 150 molecules/$\mu m^2$ and fixed at different time points. Cell morphology was then analysed by SEM. Arrows mark the limits of the spreading cell membrane. Scale bars: 2 μm.

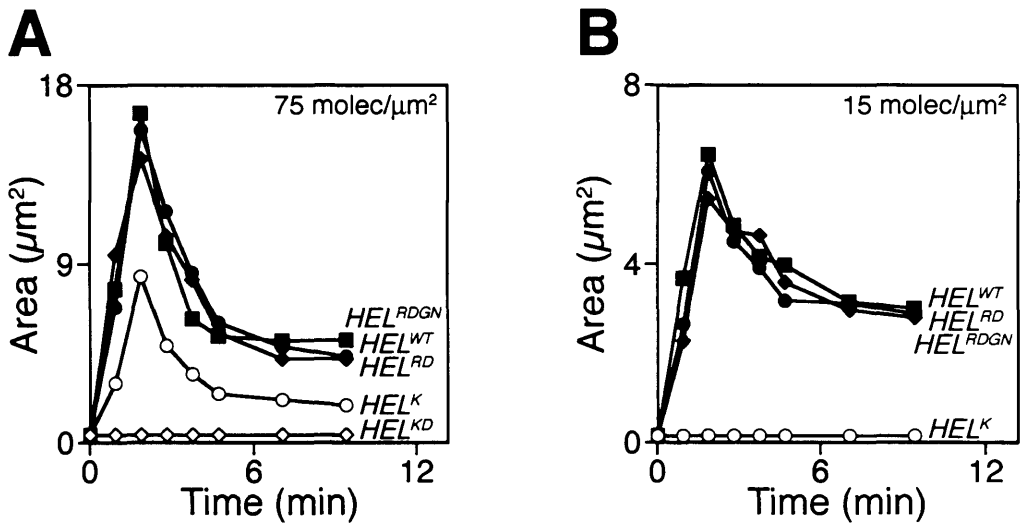


**Figure 5.8. Dependence of the spreading response on the density of antigen on the artificial bilayer: evidence for an affinity ceiling.**
MD4 B cells were settled on artificial bilayers loaded with the different HEL antigens at the indicated densities, and the kinetics of interaction followed by confocal microscopy. The plots show the area of spreading accumulation for **(A)** 75 molecules/μm² and **(B)** 15 molecules/μm². Note that B cells spread to the same extent when they encounter either $HEL^{RDGN}$ or $HEL^{WT}$ even though their 400-fold difference in affinity.

In this case we also observed a ceiling in the maximum area of spreading coincident with the affinity ceiling observed for the antigen accumulation process (Figure 5.8).

Taken together, these results suggest that a minimum membrane avidity, that is affinity and density, is necessary not only to trigger the cell spreading, but also to sustain it. Therefore, the extent of this response has a direct impact on the amount of antigen that is accumulated at the end of the antigen recognition process.

### 5.2.4 Effect of LFA-1/ICAM-1 interaction in the spreading response

When B cells recognise antigens tethered on a cell membrane, a structure known as immunological synapse (IS) is formed (Batista et al., 2001; Carrasco et al., 2004). This structure is characterised by a central cluster of BCR/antigen complexes (known as cSMAC), and a peripheral ring of ICAM-1/LFA-1 adhesion molecules (known as pSMAC) (Figure 5.9 A). We reproduced the IS on artificial bilayers by including GPI-linked ICAM-1 together with the antigen (Figure 5.9 B). Using this system we previously showed that the presence of ICAM-1 on the bilayers decreases the thresholds for antigen recognition and B cell activation (Carrasco et al., 2004). Therefore, we wondered whether the ICAM-1/LFA-1 interaction plays a role during the spreading response and in antigen accumulation.

To test this, we prepared lipid bilayers with GPI-linked Fab fragments together with GPI-linked Alexa Fluor 543-ICAM-1 and then analysed the effect of this adhesion molecule in the spreading and contraction response of MD4 B cells. As shown in Figure 5.9 C, the presence of ICAM-1 on the bilayer did not significantly affect the maximum area of spreading of the B cells in contact with a high affinity mutant ($HEL^{RD}$). But, we observed a small increase in the area of spreading of the B cells when the bilayers were loaded with a HEL antigen ($HEL^{RKD}$) that has a low affinity for the BCR (Figure 5.9 C). These results are in agreement with our previous report in which we showed that the ICAM-1/LFA-1 interaction during membrane antigen recognition decreases the threshold of activation by increasing adhesion (Carrasco et al., 2004).

SEM analysis of B cells in contact with bilayers loaded with the $HEL^{WT}$ antigen in the presence or in the absence of ICAM-1 revealed that spreading B cells adhere

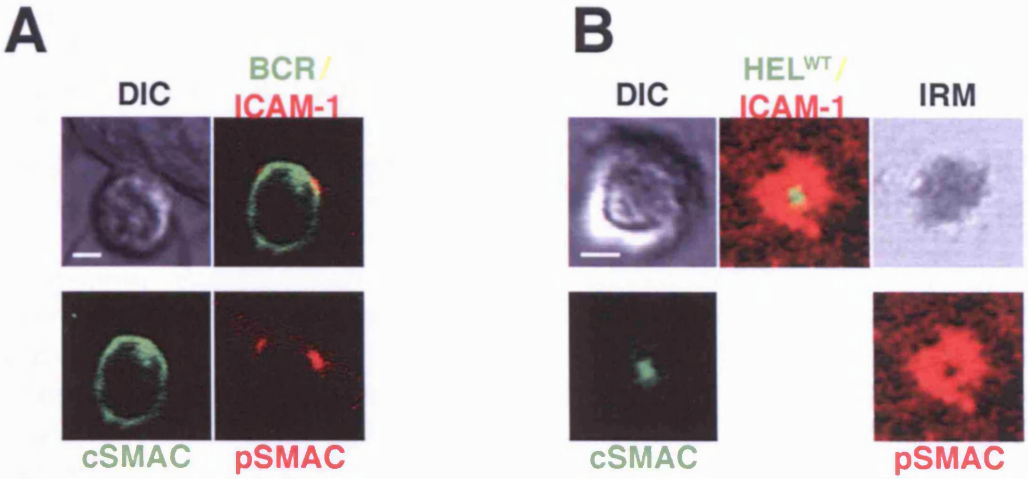
A
DIC
BCR/
ICAM-1
cSMAC
pSMAC
B
DIC
HEL^WT/
ICAM-1
IRM
cSMAC
pSMAC

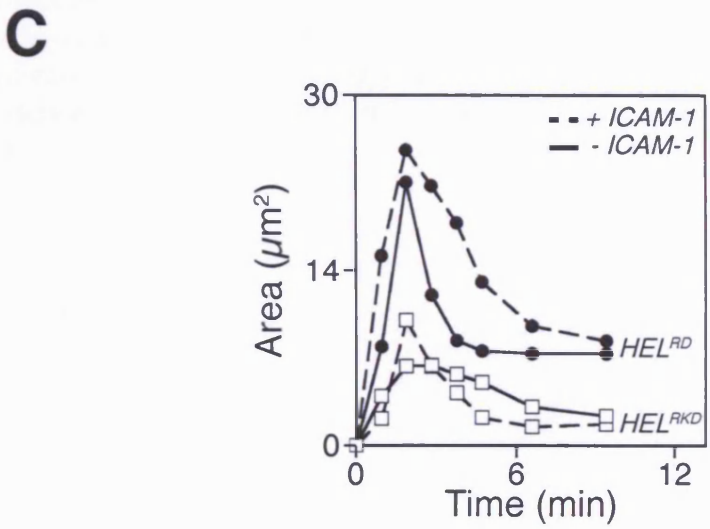
C
30
14
0
Area (μm²)
+ ICAM-1
- ICAM-1
HEL^RD
HEL^RKD
0
6
12
Time (min)

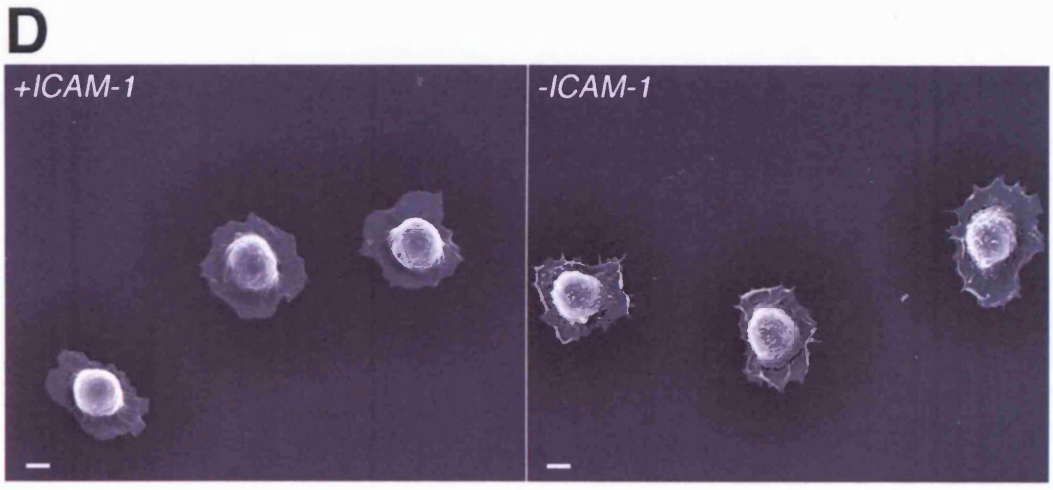
D
+ICAM-1
-ICAM-1

**Figure 5.9. Effect of ICAM-1 in the spreading response.**
**(A)** 3-83 transgenic B cells labelled with a Cy3-conjugated Fab fragment of an anti-IgM monoclonal antibody (green) were incubated with L-cells transfected with a GPI-linked ICAM-1 molecules fused to GFP (red). The L-cells express the H-2K$^{k}$ molecule, recognised specifically by the 3-83 B cells. The confocal images show an immunological synapse established between the two cells evidenced by the accumulation of the BCR in the centre (cSMAC) and the exclusion of the ICAM-1 molecule to the periphery (pSMAC). **(B)** Shows confocal images of a mature immunological synapse formed by an MD4 B cell in contact with artificial bilayers containing HEL antigen (green) and an Alexa Fluor 543-conjugated GPI-linked ICAM-1 molecule (red). Note the enlarged surface of contact evidenced by the large IRM signal (grayscale). Scale bars: 2 μm. **(C)** Area of spreading as a function of time of MD4 B cells in contact with artificial lipid bilayers loaded with either HEL$^{RD}$ (closed circles) or HEL$^{RKD}$ (open squares) at a density of 150 molecules/μm$^2$ in the presence (full trace) or in the absence (dashed trace) of ICAM-1. **(D)** SEM analysis of MD4 B cells fixed at 2 minutes of contact with artificial lipid bilayers loaded with HEL$^{WT}$ at a density of 150 molecules/μm$^2$ in the presence (left picture) or in the absence (right picture) of ICAM-1. Scale bars: 2 μm.

more strongly to the membrane in the presence of ICAM-1, as revealed by the flat surface of the lamellipodia structure, compared to a rough surface in the absence of the adhesion molecule (Figure 5.9 D).

These results support the notion that cell spreading is driven mainly by the BCR.

### 5.2.5 Spreading and affinity discrimination

Our results show that cell spreading is triggered by signals delivered through the BCR upon antigen engagement: B cells that express a signalling deficient BCR or treated with signalling inhibitors do not spread. The membrane antigen avidity, that is the density at which it is displayed and its affinity for the BCR, affect the extent of the spreading response mainly by affecting the signalling through the BCR. The extent of the B cell spreading response determines in turn the amount of antigen that B cells accumulate at the end of the process.

With this in mind, we wanted to understand if cell spreading plays a role in the capacity of B cells to discriminate between antigens with different affinities.

To this end, we took advantage of the D1.3 transgenic system and mutant HEL antigens that show a 60-fold difference in their affinity for the BCR (Table 1). B cells isolated from the signalling competent IgM D1.3 transgenic mouse spread normally and discriminated between the two antigens in terms of number of molecules accumulated (Figure 5.10 A, left plot). However, signalling deficient B cells showed an impaired capacity to discriminate antigens and both were aggregated to a similar extent (Figure 5.10 A, right plot).

Similar results were obtained when we tested the transfected A20 B cell line. Cells transfected with the canonical IgM were able to discriminate the different antigens, while cells transfected with the signalling impaired BCR lost this capacity (Figure 5.10 B).

From this results we concluded that cell spreading is not only important for antigen accumulation, but it also plays an important role in affinity discrimination.

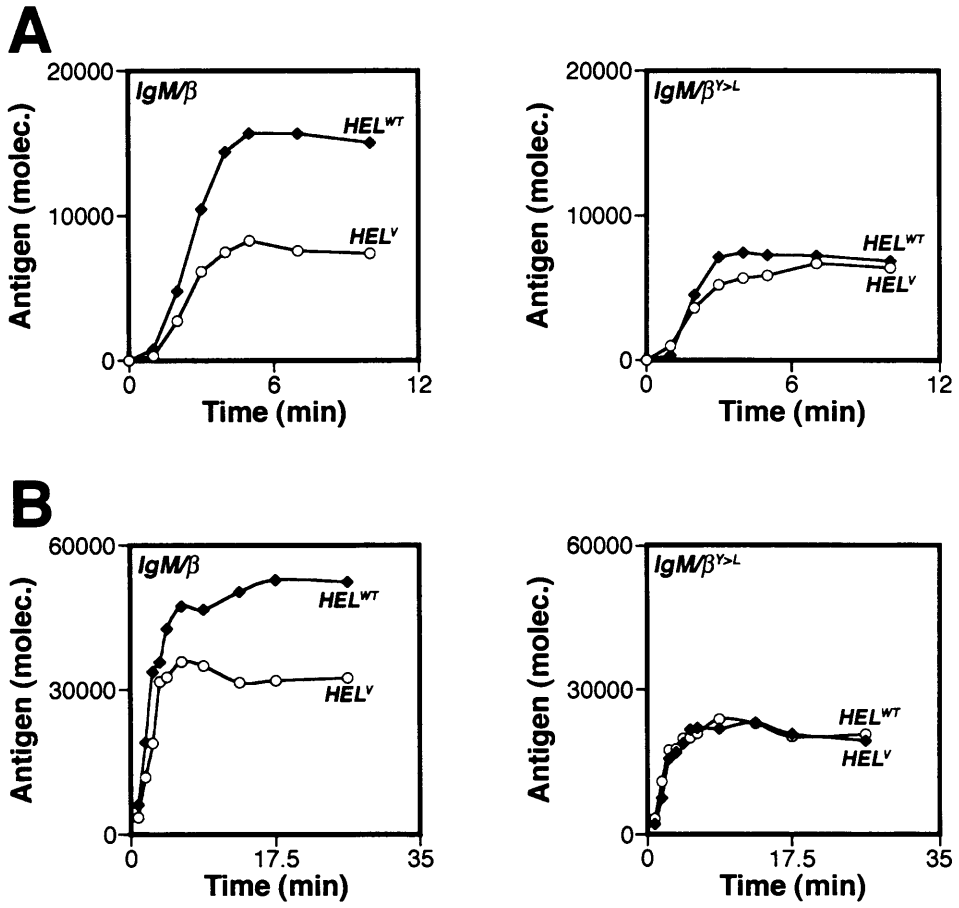


**Figure 5.10. Spreading response and affinity discrimination.**
**(A)** Kinetics of antigen accumulation of IgM/β (left panel) and IgM/$\beta^{Y>L}$ (right panel) transgenic B cells in contact with lipid bilayers loaded with $HEL^{WT}$ (triangles) or $HEL^{V}$ (triangles) antigens at a density of 150 molecules/$\mu m^2$. Signalling deficient IgM/$\beta^{Y>L}$ B cells show an impaired capacity to discriminate antigens compare to signalling competent IgM/β B cells. **(B)** Similar results were obtained with A20 B cells transfected with the same BCRs.

## 5.3 Insights into the mechanism of cell spreading and contraction

We showed that cell spreading is triggered by antigen engagement through the BCR. A minimum avidity is necessary to trigger it, but probably it is also necessary to sustain it. Therefore, to dissect its mechanism we focused on two aspects of the spreading process: the force that drives the cell spreading, and how cell spreading is sustained.

### 5.3.1 Driving force of cell spreading: actin polymerization

Previous reports have shown that synapse formation in B cells leads to F-actin polarisation (Batista et al., 2001). Therefore, we reasoned that polarised actin polymerisation may be the driving force of the spreading response.

To test this hypothesis, we incubated MD4 B cells with $HEL^{WT}$ antigen loaded bilayers for 10 minutes and fixed them (Materials and Methods). To visualise F-actin, we stained them with fluorescently labelled phalloidin and analysed them by confocal microscopy.

We observed a polarisation of the F-actin towards the antigen recognition site (artificial membrane) in the form of an actin ring surrounding the antigen/BCR cluster in agreement with previous reports (Figure 5.11).

When we analysed B cells fixed at different time points, we observed that F-actin is initially present at the site of cell contact with the bilayer (antigen engagement site) and then localises in a peripheral ring throughout the spreading phase (Figure 5.11). The F-actin ring is maintained even during the contraction phase, coordinating the antigen accumulation process (Figure 5.11). Thus, actin polymerisation appears to be the driving force that guides cell spreading.

Michele Weber (a PhD student in the lab) further confirmed this result by treating B cells with actin polymerisation inhibitors (latrunculin and cytochalasin D). The inhibitor treatment abolished the capacity of B cells to spread.

These results suggest that signals delivered through the BCR trigger local actin polymerisation that drives the cell spreading. To test this hypothesis, we fixed MD4 B cells at different time points and looked for the pattern of tyrosine phophorylation by immunostaining. As shown in Figure 5.11, tyrosine phosphorylation shows a similar pattern of distribution as F-actin, and they partially co-localise.

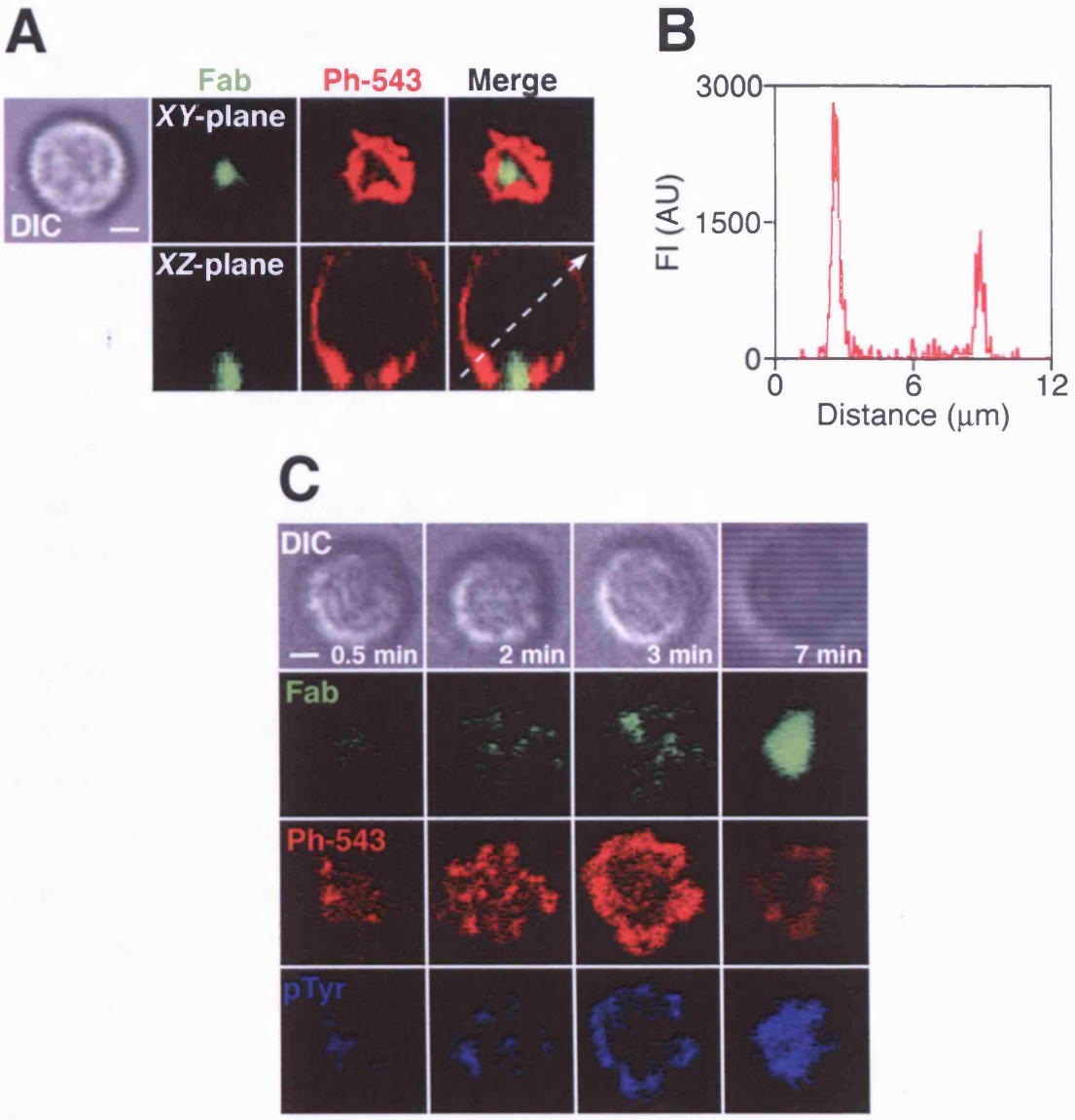


**Figure 5.11. Localisation of F-actin and pTyr during membrane antigen recognition.**

**(A)** Confocal images of a representative MD4 B cell fixed after 10 minutes of contact with an artificial membrane loaded with $HEL^{WT}$ antigen (green) at a density of 150 molecules/μm² and stained with Alexa Fluor 543-phalloidin (red). **(B)** Shows the profile of the actin staining shown in **(A)** defined by the dashed arrow. **(C)** Confocal images of representative MD4 B cells fixed at the indicated time of contact with an artificial membrane loaded with $HEL^{WT}$ antigen (green) at a density of 150 molecules/μm² and stained with Alexa Fluor 543-phalloidin (red) and a fluorescently labelled anti-pTyr antibody (blue). Scale bars: 2 μm.

These results support the notion that signals delivered through the BCR upon antigen engagement trigger a local actin polymerisation that drives cell spreading.

### 5.3.2 BCR/cytoskeleton connections

The next aspect we investigated was how the signals of the BCR are transmitted to the cytoskeleton. Bunnell and colleagues have shown that the adaptor protein LAT is fundamental for the spreading response of T cells, presumably linking the TCR to the cytoskeleton (Bunnell et al., 2001). Another protein that has been involved in TCR-mediated cytoskeletal reorganization is the guanosine exchange factor Vav (Fischer et al., 1998a; Fischer et al., 1998b; Wulfing et al., 2000). As LAT is not expressed in B cells, we focused on the Vav protein.

### 5.3.3 Role of Vav proteins

Vav is a guanine nucleotide exchange factor for the Rho family of GTP-ases (Hornstein et al., 2004). In B cells, Vav has been shown to play an important role in diverse aspects of BCR-mediated signalling and B cell development, but very little is known of its involvement in cytoskeletal modifications (Turner, 2002a; Turner, 2002b).

B cells express three isoforms of the Vav proteins, Vav1, Vav2 and Vav3 (Turner, 2002b). To explore the function of the Vav exchange factors in the spreading response of B cells, we took advantage of B cells isolated from mice deficient in Vav1 and Vav2 proteins ($Vav1^{-/-}/Vav2^{-/-}$). Dr Martin Turner (Barbaham Institute, Cambridge) provided us with the mice and we crossed the $Vav1^{-/-}/Vav2^{-/-}$ with the MD4 transgenic mice, therefore we could analyse the spreading response on artificial bilayers loaded with HEL antigen.

We observed that $Vav1^{-/-}/Vav2^{-/-}$ knockout MD4 B cells have a marked impairment in cell spreading (Figure 5.12 A, B and C). Surprisingly, these B cells aggregate as much antigen as MD4 WT B cells, but at a much lower rate (Figure 5.12 D). In order to clarify this discrepancy, we analysed the morphology of the Vav deficient B cells in contact with artificial bilayers loaded with the HEL antigen. SEM analysis revealed that these cells appeared deformed and flattened compared to WT MD4 B cells, thus showing a change in morphology (Figure 5.12 E and F).

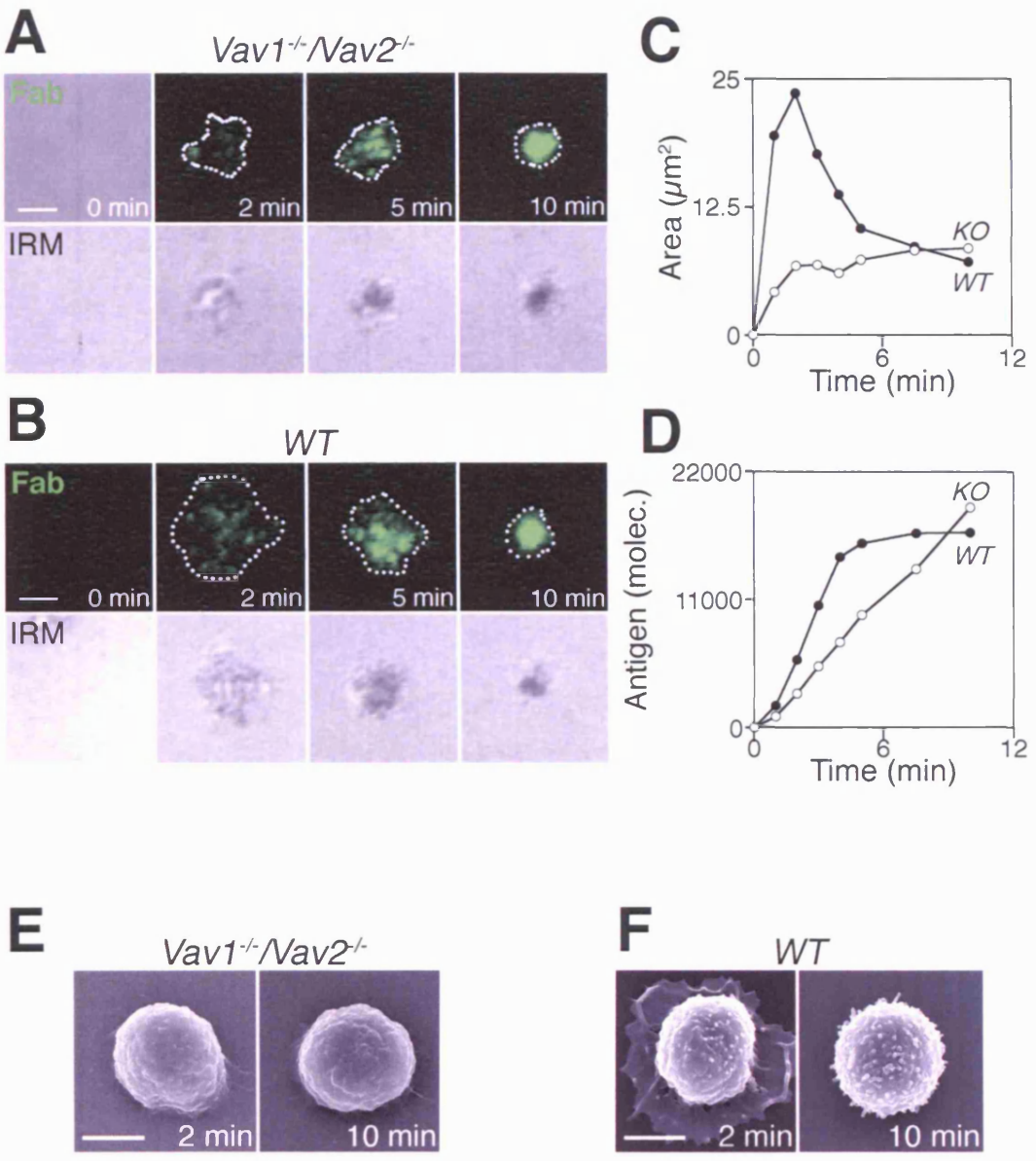


**Figure 5.12. Role of Vav proteins in B cell spreading.**
**(A)** Vav1/Vav2-deficient or **(B)** WT MD4 B cells were settled on artificial bilayers loaded with $HEL^{WT}$ antigen at a density of 150 molecules/μm², and the kinetics of interaction followed by confocal microscopy. Contacts with the bilayer were followed by IRM (greyscale). Dotted white line limits the spreading area as assessed by antigen fluorescence. Scale bars: 2 μm. **(C)** Area of spreading and **(D)** amount of antigen accumulated as a function of time (closed circles: WT MD4 B cells; open circles: Vav1/Vav2-deficient MD4 B cells). **(E)** Vav1/Vav2-deficient or **(F)** WT MD4 B cells were settled on artificial bilayers loaded with $HEL^{WT}$ antigen at a density of 150 molecules/μm², and fixed at different time points. Cell morphology was analysed by SEM. Scale bars: 2 μm.

The results presented in this section suggest that Vav1 and/or Vav2 are the proteins that link the BCR with the cytoskeleton. Further experiments will be needed to address the importance of the individual Vav isoforms in the spreading response.

### 5.3.4 Role of Rac proteins

Next we addressed the mechanism by which Vav proteins are able to trigger the localised actin polymerisation guided by the BCR. Rho GTP-ases are one of the main downstream effectors of Vav adaptor proteins (Turner, 2002b). This family of GTP-ases includes Rho, Rac and Cdc42 proteins, and each one of these proteins has been involved in triggering actin polymerization leading to the formation of particular cellular structures during cell movement (Jaffe and Hall, 2005). For instance, Rho has been associated to the formation of stress fibers, Cdc42 to the formation of filopodia and Rac is involved in the formation of lamellipodia during migration (Jaffe and Hall, 2005).

Since the cell spreading that we observed in B cells involves the formation of a lamellipodia-like structure, we decided to investigate the function of Rac during this cellular response.

B cells express two isoforms of Rac proteins, Rac1 and Rac2, which are involved in development and signalling (Walmsley et al., 2003). In order to test the relevance of the Rac proteins in the cell spreading response, we took advantage of B cells isolated from Rac1 and Rac2 deficient mice (Walmsley et al., 2003).

We first analysed the spreading response of Rac1 and Rac2-deficient B cells. Since the Rac deficient lines do not express an antigen-specific transgenic BCR, we used artificial bilayers with biotinylated lipids loaded with an anti-kappa antibody as a surrogate antigen. As shown in Figure 5.13 A, $Rac1^{-/-}$ and $Rac2^{-/-}$ B cells did not show any evident compromise in cell spreading.

When we next analysed the cell morphology by SEM, we observed that Rac deficient B cells presented a smooth surface with the loss of microvilli compared to WT B cell (Figure 5.13 B). However, they did not show any major abnormality contrary to Vav deficient B cells (Figures 5.13 B and 5.12 E and F).

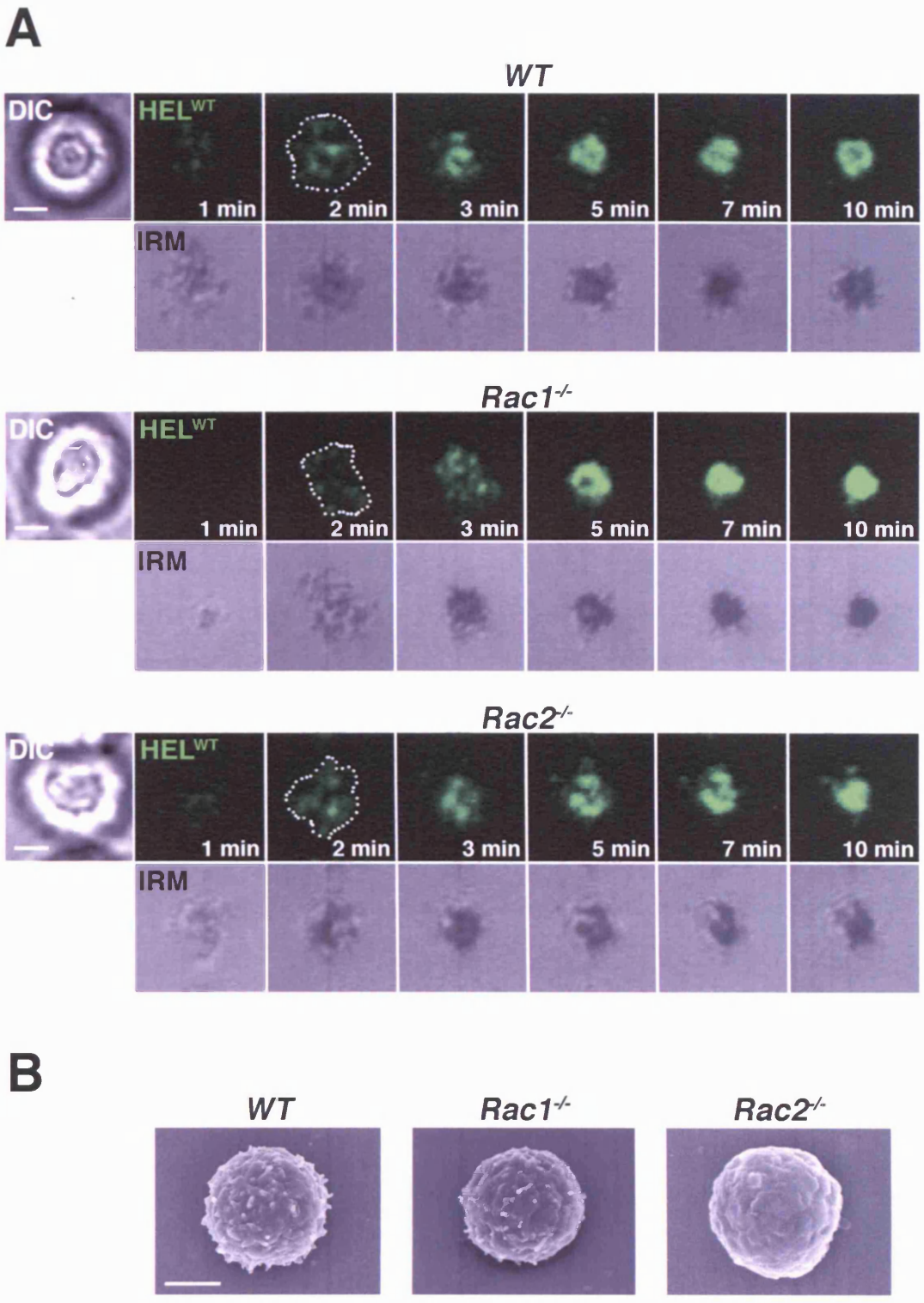


**Figure 5.13. Role of Rac proteins in B cell spreading.**
**(A)** WT (top panels), Rac1-deficient (middle panels) and Rac2-deficient (bottom panels) B cells were settled on artificial bilayers loaded with an anti-kappa antibody as a surrogate antigen, and the kinetics of interaction followed by confocal microscopy. Contacts with the bilayer were followed by IRM (grayscale). Dotted line shows the maximum area of spreading. Scale bars: 2 μm. **(B)** SEM analysis of fixed B cells after 10 minutes of interaction with antigen-loaded bilayers. Scale bar: 2 μm.

### 5.3.5 Contraction phase

We have shown that cell spreading is triggered by signals delivered through the BCR and is an active mechanism dependent on actin reorganisation. Thus, next we wanted to get an insight into the mechanism of the contraction phase. Several reports suggest that myosin proteins are involved in the contraction phase during cell migration (Jacobelli et al., 2004; Small and Resch, 2005).

As an initial approach to test this hypothesis, we tested the capacity of MD4 B cells treated with myosin light chain kinase inhibitors to contract. B cells were treated with either ML-7 or blebbistatin inhibitors and settled on artificial bilayers without previous washing. This was performed so that the inhibitors would be present throughout the whole experiment.

In both cases the capacity of B cells to accumulate antigen was severely impaired (Figure 5.14). In fact, cells treated with the ML-7 inhibitor did not establish any contact with the artificial bilayer, nor aggregated any antigen (Figure 5.14). In the case of cells treated with blebbistatin, we observed that some cells ($\approx$ 40%) were still able to established weak contacts with the bilayers and to spread (Figure 5.14). However, they seemed to have a delayed contraction phase as well as an impaired capacity to accumulate antigen (Figure 5.14). Although these results seemed promising they did not provide any insight of the contraction mechanism.

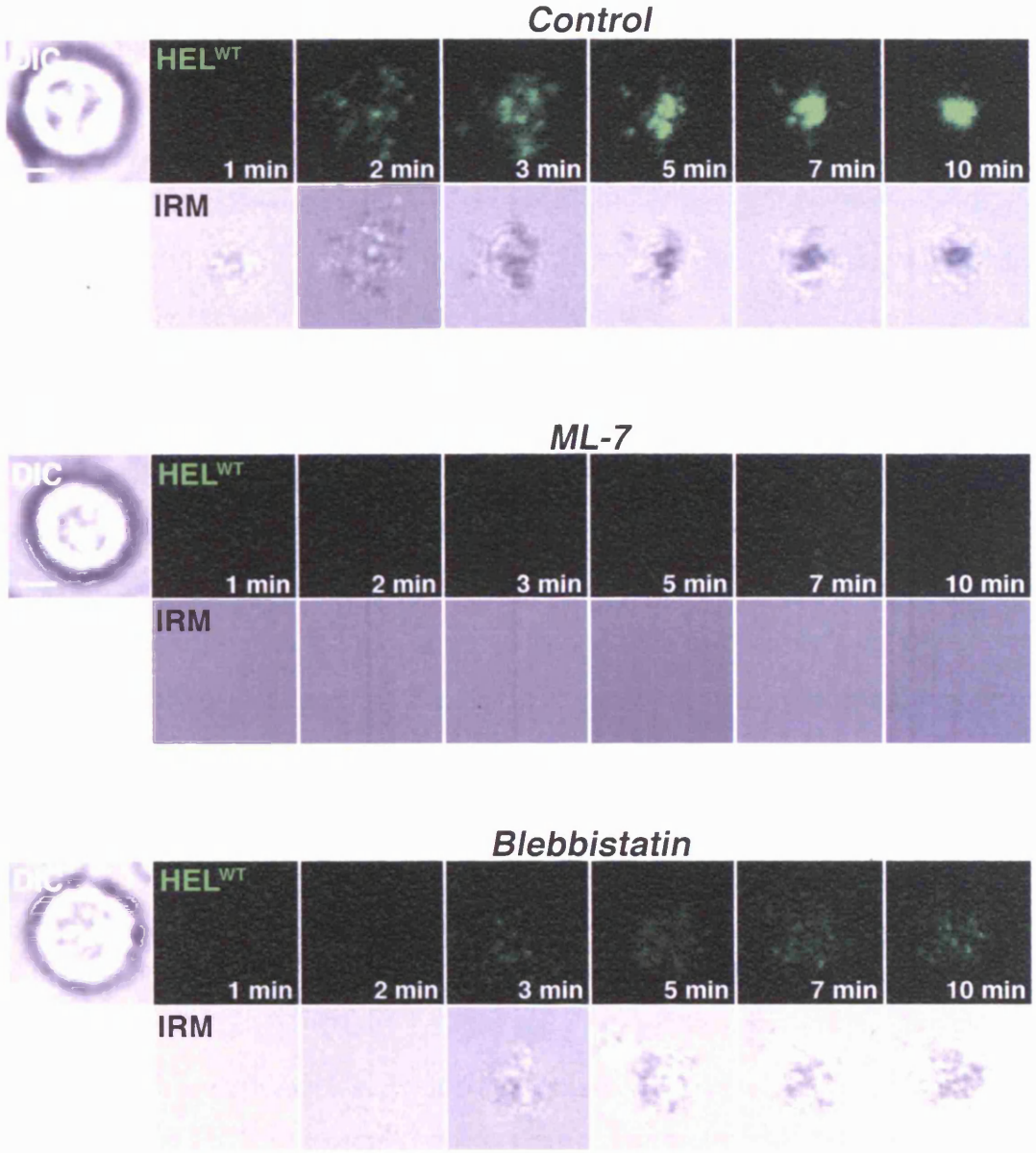


**Figure 5.14. Contraction phase.**
MD4 B cells were treated with vehicle (DMSO, top panels), ML-7 (middle panels) and blebbistatin (bottom panels) for 20 minutes and settled on artificial bilayers loaded with $HEL^{WT}$ antigen at a density of 150 molecules/$\mu m^2$ and the interaction followed by confocal microscopy. Contacts with the bilayer were followed by IRM (grayscale) Scale bars: 4 μm.

## 5.4 Proposing a model of the cell spreading and contraction response

In this chapter we showed that the spreading response is triggered by antigen engagement through the BCR and it only takes place when the binding avidity of the B cell for the antigen bearing membrane is above a minimum threshold. This avidity threshold is determined by both the affinity of the BCR for the antigen and its density in the two-dimensional plane of the membrane. The maximum area of spreading is also dependent on these two parameters.

With these results in mind, we proposed a model for the spreading phase of the membrane antigen recognition process (Figure 5.15). Initially, the B cell will expose a certain number of antigen receptors to the antigen bearing membrane; if a minimum percentage of these receptors engage the freely diffusing antigen molecules, the cell spreading response will be triggered (Figure 5.15). The degree of receptor occupancy will depend exclusively on the membrane avidity.

After the initial spreading event, the cell will expose a new set of receptors to the antigen bearing membrane. These new receptors will be subject to the same stringent avidity conditions in order to trigger a new round of cell spreading. In this way, this response will proceed in a series of spreading events until the contraction phase is triggered (Figure 5.15). Which are the signals that trigger the contraction phase are unknown at the moment, but it seems a tightly controlled response as cells looked coordinated during the entire response. Moreover, our results using inhibitors of the myosin light chain (blebbistatin and ML-7) suggest that myosin proteins are involved in this cellular response.

Finally, the spreading response enhances the discrimination of antigens of different affinities.

This model is supported by the results obtained by immunostaining of B cells fixed on the artificial lipid bilayers. These results show that both signalling, as evaluated by phosphotyrosine immunostaining, and actin polymerisation take place in progressive rings in the periphery.

But, we wanted to test if the proposed model was a possible explanation for our quantitative results. To further address this we set out to setup a fluorescence resonance energy transfer (FRET) live microscopy technique.

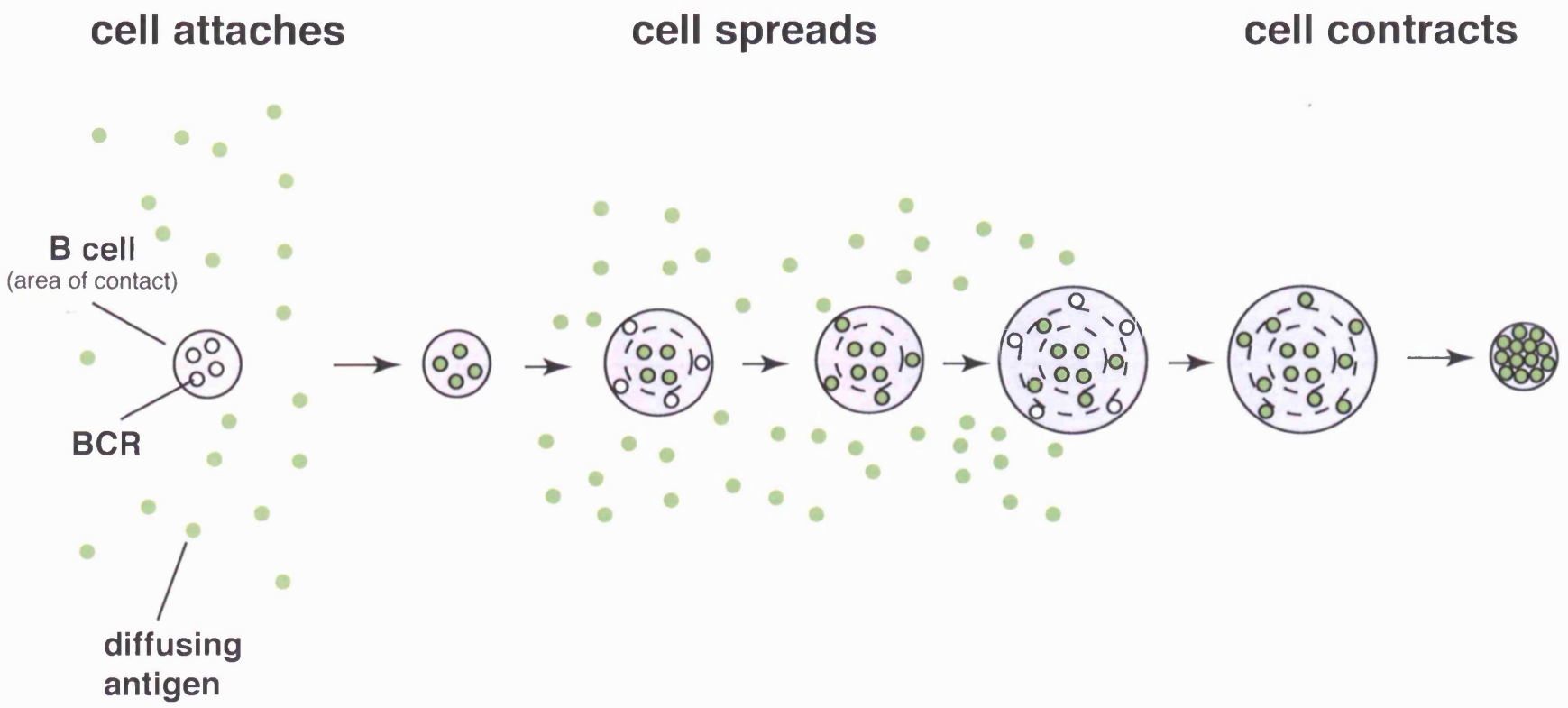


**Figure 5.15. Model of spreading and contraction of B cells.**
This diagram illustrates a B cell in contact with a membrane carrying antigen (green). The B cell exposes a certain number of BCRs (white circles). The B cell will sense the antigen only if the avidity of the interaction is above a certain threshold. Then, if the avidity is high enough, a critical number of B cell receptors will be occupied and that will trigger a spreading event. This will expose a new set of receptors that will be subject to the same stringent condition to sustain the spreading or to stop. The sustained spreading will continue until the cell starts to contract. At present the mechanism is not fully understood, and it is the focus of major research (adapted from Fleire et al., 2006).

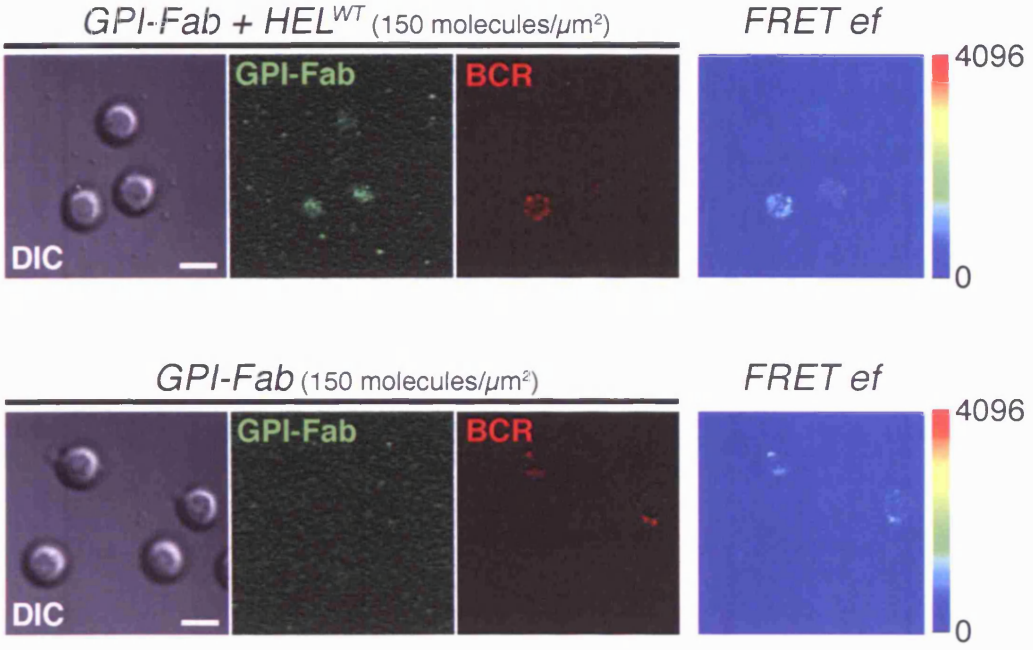


**Figure 5.16. Fluorescence resonance energy transfer (FRET) and spreading mechanism.**
MD4 B cells were labelled with a Cy3-conjugated Fab fragment of an anti-IgM antibody (red) and settled on artificial bilayers containing the Alexa Fluor 488-conjugated GPI-linked Fab fragment (green) loaded with $HEL^{WT}$ antigen (top panels) or in the absence of it (bottom panels) at a density of 150 molecules/$\mu m^2$. The FRET signal between Cy3 and Alexa Fluor 488 (shown in a pseudo color scale) was then measured over the time. A single time point (5 minutes) of each condition is shown. FRET ef: FRET efficiency. Scale bars: 5 μm.

Our idea was to measure a progressive increase in the area of positive FRET signal between the BCR, labelled with an Alexa Fluor 543-labelled Fab, and the antigen on the bilayer labelled with Alexa Fluor 488. This increase should be proportional to the serial spreading mechanism postulated.

We observed efficient FRET signal between the two fluorescent molecules which was very encouraging initially (Figure 5.16). However, we also observed an efficient FRET signal when the cells were settled on artificial bilayers in the absence of antigen (Figure 5.16). Furthermore, the difference between the two was extremely small. Therefore, part of the signal is due to the contact of the B cells with the bilayer, even in the absence of antigen.

As a consequence of this, we discarded the FRET technique.

## 5.5 Discussion

In this chapter we analysed in detail the spreading and contraction response of B cells when they encounter antigens tethered on a membrane. We showed that this process is triggered by signals delivered through the BCR upon antigen engagement, and is guided by actin polymerisation. Furthermore, our quantitative results show the dependence of the spreading process extent on both the affinity of the BCR/antigen interaction and the density of the antigen on the target membrane.

### 5.5.1 Cell spreading: its relevance

Bunnell et al have previously described a spreading response of T cells in contact with rigid surfaces (coverslips) coated with anti-TCR antibodies (Bunnell et al., 2001). In the same line, Negulescu and colleagues described a similar behaviour when T cells encounter APCs that carry specific antigens on their surface (Negulescu et al., 1996). In the case of B cells, spreading has been described when integrins are activated through anti-CD44 and anti-CD38 antibodies bound to coverslips (Santos-Argumedo et al., 1997; Sumoza-Toledo and Santos-Argumedo, 2004). However, our experiments show for the first time that the spreading and contraction response triggered by antigen engagement through the BCR described here is a dynamic mechanism that B cells employ to collect antigen molecules. Our results also suggest that the affinity of the BCR/antigen

interaction and the density of the antigen on the target membrane regulate the extent of the spreading response. This in turn determines the amount of antigen that B cells collect at the end of the process.

Furthermore, our results revealed an important function of the spreading response in the affinity discrimination of antigens, as we showed that B cells that cannot spread have an impaired capacity to discriminate antigens in terms of the amount accumulated. In this line, it is interesting to cite the model of affinity maturation proposed by Tarlinton and Smith (Tarlinton and Smith, 2000). This model proposed that the selection of B cells that express BCRs with high affinity for a specific antigen is based on the competition for limiting amounts of this antigen presented on the surface of follicular dendritic cells (Tarlinton and Smith, 2000).

Thus, it is tempting to speculate that by spreading on the target membrane, B cells expressing BCRs with varying affinities for a particular antigen can compete for limiting amounts of this based fundamentally in the affinity of the BCR/antigen interaction. B cells that express BCRs with a higher affinity for the antigen will accumulate more antigen and they will be favoured in the selection process.

Although affinity maturation is a poorly understood process, it is well documented that the selection process is guided by the BCR/antigen interaction, and this could be a possible description of the mechanism involved in this process (Shih et al., 2002).

It will be important to dissect this model and to unveil the mechanism of spreading and contraction in vivo. Hopefully, technical improvements in microscopy, such as two-photon microscopy, will allow us to follow in detail the process of antigen recognition in intact lymph nodes.

Currently, the information available is scarce and limited to measure the encounters.

### 5.5.2 Cell spreading: its mechanism

Bunnell et al have previously described the cell spreading response in Jurkat T cells (Bunnell et al., 2001). This report shows the dependence of the spreading response on signals delivered through the TCR and calcium; but more important, it shows its dependence on the adaptor protein LAT (Bunnell et al., 2001).

As B cells do not express the LAT adaptor protein, we looked for an alternative protein that may be involved in the spreading response. Vav proteins have been involved in cytoskeletal rearrangements in T cells, therefore we tested their involvement in B cell spreading (Fischer et al., 1998a; Fischer et al., 1998b).
While the spreading capacity is severely impaired in Vav-deficient B cells, their capacity to accumulate antigen is not (though the process is delayed). This was initially surprising, as signalling deficient B cells (IgM/$\beta^{Y>L}$), that do not spread, do not accumulate antigen as efficiently as signalling competent B cells. However, when we analysed the cell morphology of Vav1/2 deficient B cells in contact with artificial bilayers by SEM, we observed that they looked deformed (Figure 5.12 E).
Interestingly, it has recently been reported that stimulation through the BCR induces a rapid global actin de-polymerisation in a BCR signal-strength dependent manner, followed by polarised actin re-polymerisation (Hao and August, 2005).
This result may explain why we observed deformed cell morphology when we analysed Vav1/2 deficient B cells by SEM: while these cells have a signalling-competent BCR, its engagement to the cytoskeleton is impaired. Therefore, the BCR would still be able to trigger the initial actin de-polymerisation event, but not to coordinate and direct the active polarised actin polymerisation that guides the cell spreading response.

B cells deficient in Rac1 or Rac2 proteins did not show any marked phenotype in the spreading response in our system. This result seems contradictory; however, one possibility is that any difference in the spreading response might be masked due to the strong nature of the stimulus (monobiotinylated anti-kappa antibody tethered on artificial bilayers through an avidin bridge). Alternatively, Rac1 and Rac2 may have a partially redundant role in B cell cytoskeletal rearrangements. The normal morphology revealed by SEM supports this last idea.
Recent reports have suggested that the WAVE/Abi proteins are important for this process and this may help in trying to understand the pathways that guide it (Nolz et al., 2006; Zipfel et al., 2006).

Taken together, these results suggest that cell spreading and contraction response will involve two coordinated mechanisms: a fast actin de-polymerisation on one hand, followed by a localised actin polymerisation triggered and guided by the B cell receptor on the other.

In the same line, Delon and colleagues have shown that membrane relaxation promotes the conjugation between T cells and APCs that express a specific antigen (Faure et al., 2004). In this study, the authors showed that the inactivation of ezrin-radexin-moesin (ERM) proteins triggered by the TCR is important for membrane relaxation and conjugates formation (Faure et al., 2004). The authors also showed that ERM proteins are rapidly inactivated through a Vav1-Rac1 pathway.

Based on our results and those of other groups it is clear that the BCR is the key organizer of the spreading and contraction mechanism; however, its linkage with the cytoskeleton is poorly understood (Braun et al., 1982; Hartwig et al., 1995; Jugloff and Jongstra-Bilen, 1997; Park and Jongstra-Bilen, 1997). From previous reports and our own results it seems intuitive that Vav proteins play a key role in directing and coordinating the cytoskeletal changes triggered by the BCR (Hornstein et al., 2004).

It will be important to understand how the different cytoskeletal rearrangements guided by the BCR are coordinated. Particularly, it will be important to understand how the initial actin de-polymerisation is triggered and how this is coordinated with the membrane relaxation promoted by the Vav proteins.

### 5.5.3 Cell spreading: a lymphocyte response

Based on our experiments and previous reports on T cells we can conclude that cell spreading is a general mechanism of antigen recognition for lymphocytes. It's an early response to membrane antigen recognition that is triggered by signals delivered through the antigen receptor. The precise mechanism of spreading and contraction is clearly very complex and further experiments will be necessary in order to unveil it.

# Chapter 6: Recognition of lipidic antigens by natural killer T cells

## 6.1 Introduction

Most T cells recognise antigenic peptides presented by MHC class I or class II molecules, but certain subset of T cells are able to respond to antigenic lipids (Godfrey et al., 2004). These lipidic antigens are presented by the CD1 family of non-canonical MHC class IB molecules (Gumperz, 2006). A particular subset of human T cells that recognise lipidic antigens in the context of CD1 molecules is known as NKT cells.

Following antigen stimulation, NKT cells rapidly release large amounts of both Th1 and Th2 cytokines, including TNF-α, IFN-γ and IL-4, which stresses their importance as regulators of immune responses.

While the recognition of antigenic peptides by canonical CD4 and CD8 T cells have been extensively characterised, very little is known about the recognition of lipidic antigens by NKT cells (Grakoui et al., 1999; Irvine et al., 2002; Wulfing et al., 2002a).

In the following chapter, we analysed the parameters that govern this process. In order to understand what are, we took advantage of the artificial lipid bilayers to mimic the interaction of NKT cells with specific antigens.

### 6.1.1 CD1 antigenic system and natural killer T cells

The CD1 family of non-canonical MHC class IB molecules has a limited polymorphism and it can be divided into two types: type I that consist of CD1a, CD1b and CD1c, (and CD1e in humans), and type II that includes the CD1d molecule. While type I CD1 molecules present mammalian and mycobacterial lipids to both CD4 and CD8 T cells, it is currently unknown which antigens present the CD1d molecule (Godfrey et al., 2004; Gumperz, 2006). It has been shown that the CD1d molecule can bind specifically a broad range of lipids that can in turn stimulate CD1d-restricted T cells (Fischer et al., 2004; Rauch et al., 2003; Wu et al., 2005). The marine sponge derived α-galactosylceramide (α-

GalCer) is the most extensively studied ligand for CD1d-restricted T cells (Godfrey et al., 2004).

CD1d-restricted T cells are characterised by the expression of a semi invariant αβ T cell receptor (TCR). In mice, the TCR is composed of the Vα14Jα28 α-chain paired to the Vβ8.2, Vβ7 or Vβ2 β-chains, whereas in humans it is exclusively composed of the Vα24JαQ α-chain and the Vβ11 β-chain.

Though the physiological relevance of a lipid derived from a marine sponge is unclear, it provides a model antigen to study the recognition of lipid antigens by CD1d-restricted T cells.

The work presented in this chapter is part of a collaboration that we established with Dr Vincenzo Cerundolo and Dr Corinna McCarthy to understand the parameters that govern the recognition of lipidic antigens by NKT cells (Institute of Molecular Medicine, Oxford - United Kingdom).

## 6.2 Results

### 6.2.1 Antigen recognition and synapse formation by NKT cells

In order to characterise the antigen recognition process, we followed by confocal microscopy the interaction of NKT cells with artificial lipid bilayers, loaded with a monobiotinylated CD1d-α-GalCer molecule tethered through an Alexa Fluor 488-avidin bridge (Figure 6.1). We also included in the bilayers an Alexa Fluor 543-conjugated GPI-linked ICAM-1 molecule, as it has been previously shown that T cells need ICAM-1 to effectively recognise antigens (Grakoui et al., 1999).

We observed that NKT cells quickly spread on the target membrane as evidenced by the antigen and the large IRM signal (Figure 6.2 A). Simultaneously, they efficiently accumulated ICAM-1 and the CD1d-α-GalCer monomer in the area of contact, as observed by their fluorescent signal (Figure 6.2 A, B and C). After 5 minutes, NKT cells formed a classical mature immunological synapse, characterised by a central cluster of the CD1d-α-GalCer monomer surrounded by a ring of ICAM-1 (Figure 6.2 A). This structure was stable for at least 30 minutes (Figure 6.2 A).

To determine if the immunological synapse formation process is dependent on antigen recognition, we settled NKT cells on lipid bilayers loaded with the GPI-linked ICAM-1 molecule and an monobiotinylated CD1d molecule loaded with

α-GalCer ($K_a$=7.7 x $10^5$ $M^{-1}$)

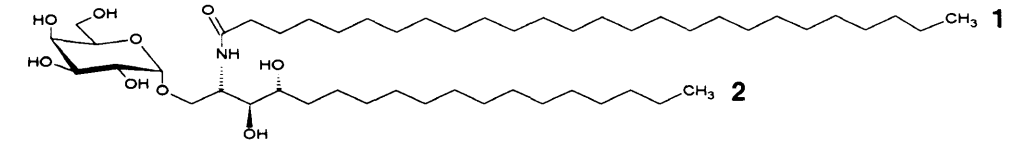


β-GalCer

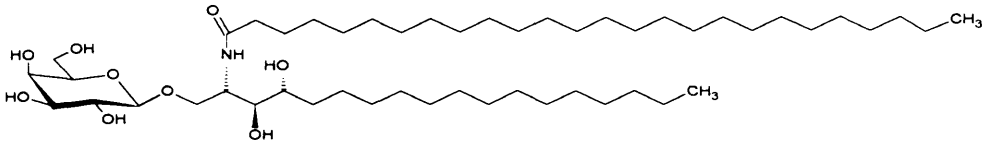


C20:0 ($K_a$=3.6 x $10^5$ $M^{-1}$)

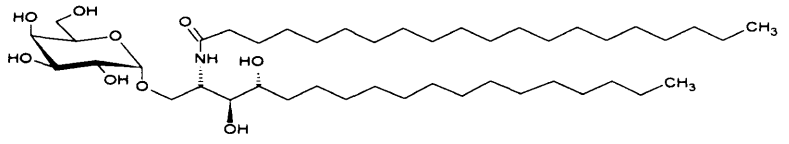


OCH ($K_a$=8.1 x $10^3$ $M^{-1}$)

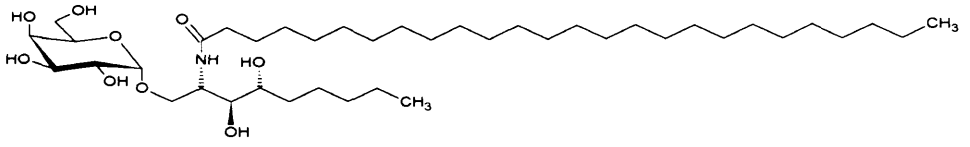


**Figure 6.1. Ceramide analogues used as antigens for NKT cells.**
Structure of the analogues of the ceramide used in this study. Affinity values ($K_a$) for the TCR are indicated next to the analogues' names. The numbers indicate the alkyl chain (1) and the phytosphingosine chain (2) of ceramides.

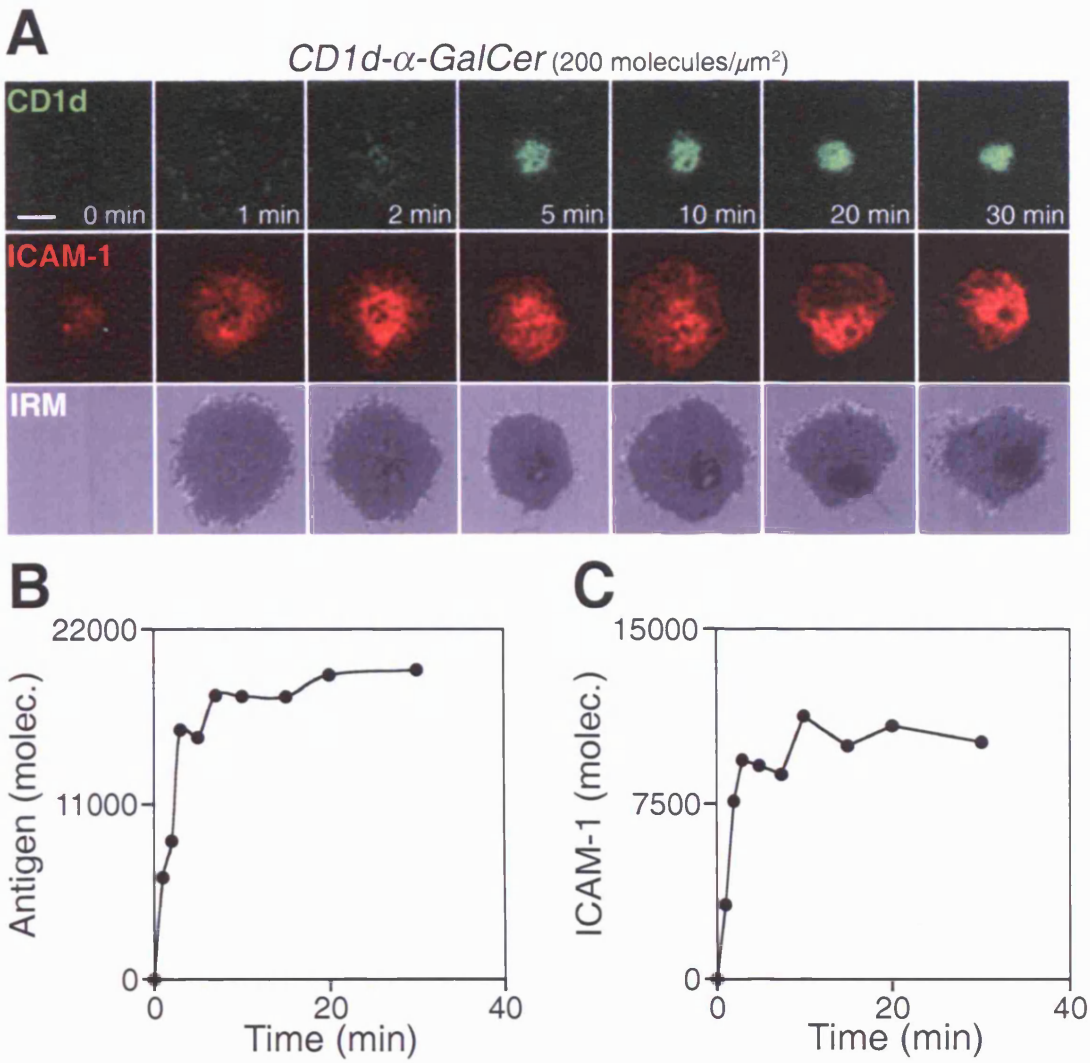


**Figure 6.2. Recognition of the CD1d-α-GalCer antigen tethered on lipid bilayers: formation of the NK T cell immunological synapse.**

Kinetics of the NK T cell immunological synapse formation. **(A)** Time lapse of the interaction of an NK T cell with an artificial lipid bilayer loaded with the CD1d-α-GalCer antigen (green) at a density of 200 molecules/μm² and ICAM-1 (red) at a density of 80 molecules/μm² as visualised by confocal microscopy. Contacts of the NK T cell with the bilayer were visualised by IRM (grayscale, lower panels). The amount of **(B)** CD1d-ligand and **(C)** ICAM-1 aggregated were quantified as a function of time. Scale bars: 5 μm.

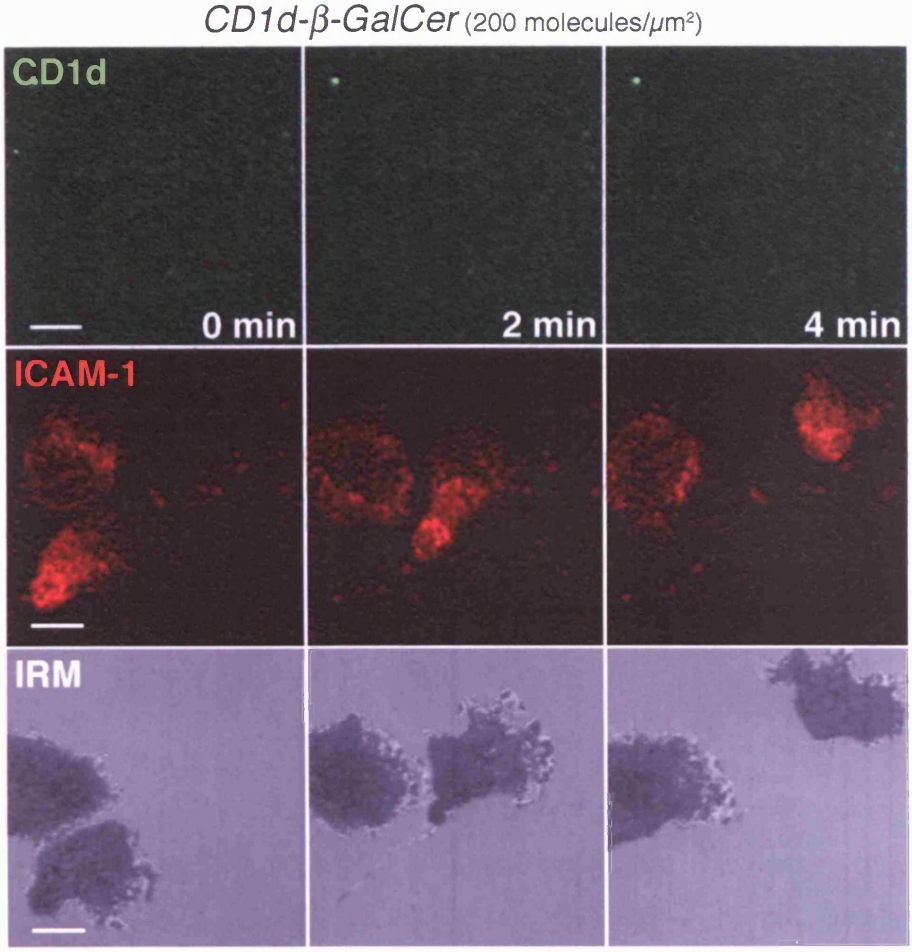


**Figure 6.3. Immunological recognition and immunological synapse formation.** Short time lapse of the interaction of NK T cells with an artificial lipid bilayer loaded with CD1d-β-GalCer antigen (green) at a density of 200 molecules/μm² and ICAM-1 (red) at a density of 80 molecules/μm² as visualised by confocal microscopy. Contacts of the NK T cell with the bilayer were visualised by IRM (grayscale, lower panels). In the absence of a specific immunological recognition NK T cells continue to migrate and do not form an immunological synapse. Scale bars: 4 μm.

the β-GalCer analogue that is an epimer of α-GalCer (Figure 6.1). The TCR has no affinity for this CD1d-analogue complex. As shown in Figure 6.3, NKT cells did not recognise this antigen. Instead, NKT cells efficiently accumulated ICAM-1 molecules and migrated on the bilayer, without any detectable accumulation of CD1d monomer (Figure 6.3). The NKT cells migrated with a mean speed of 10 μm/s, which is similar to previously reported values for T cells in vitro and in vivo (Miller et al., 2004; Stoll et al., 2002).

These results show that NKT cells recognise the specific antigens tether on artificial bilayers and the antigen recognition process leads to the formation of an immunological synapse.

### 6.2.2 Effect of affinity and density: thresholds for antigen recognition

We next examined the effect of the affinity of the TCR/CD1d-ligand interaction in the antigen recognition process by NKT cells. To this end, we loaded in the bilayer an analogue of the α-GalCer, the OCH that has an affinity that is 100 times lower (Figure 6.1).

As shown in Figure 6.4 A, the NKT cells also recognised efficiently this antigen and they formed an immunological synapse with similar kinetics as when the membranes were loaded with the α-GalCer analogue. However, quantitative analysis revealed that the number of CD1d-OCH molecules accumulated was lower than for the CD1d-α-GalCer analogue (Figure 6.4 B). Furthermore, after 20-30 minutes of interaction the NKT cells started to migrate disrupting the structure of the immunological synapse (Figure 6.4 A).

To analyse the effect of the antigen density in the recognition process, we followed by confocal microscopy the interaction of NKT cells with artificial lipid bilayers containing decreasing concentrations of antigen. The data showed that CD1d-α-GalCer is efficiently accumulated to form a mature immunological synapse up to densities of antigen as low as 10 molecules/$\mu m^2$, while CD1d-OCH is no longer recognised when its density is lower than 100 molecules/$\mu m^2$ (Figure 6.5).

In conclusion, these results show that the affinity of the TCR for the CD1d-analogue complex and the density of this on the target membrane are key parameters that determine the effective recognition of antigens by the NKT cells.

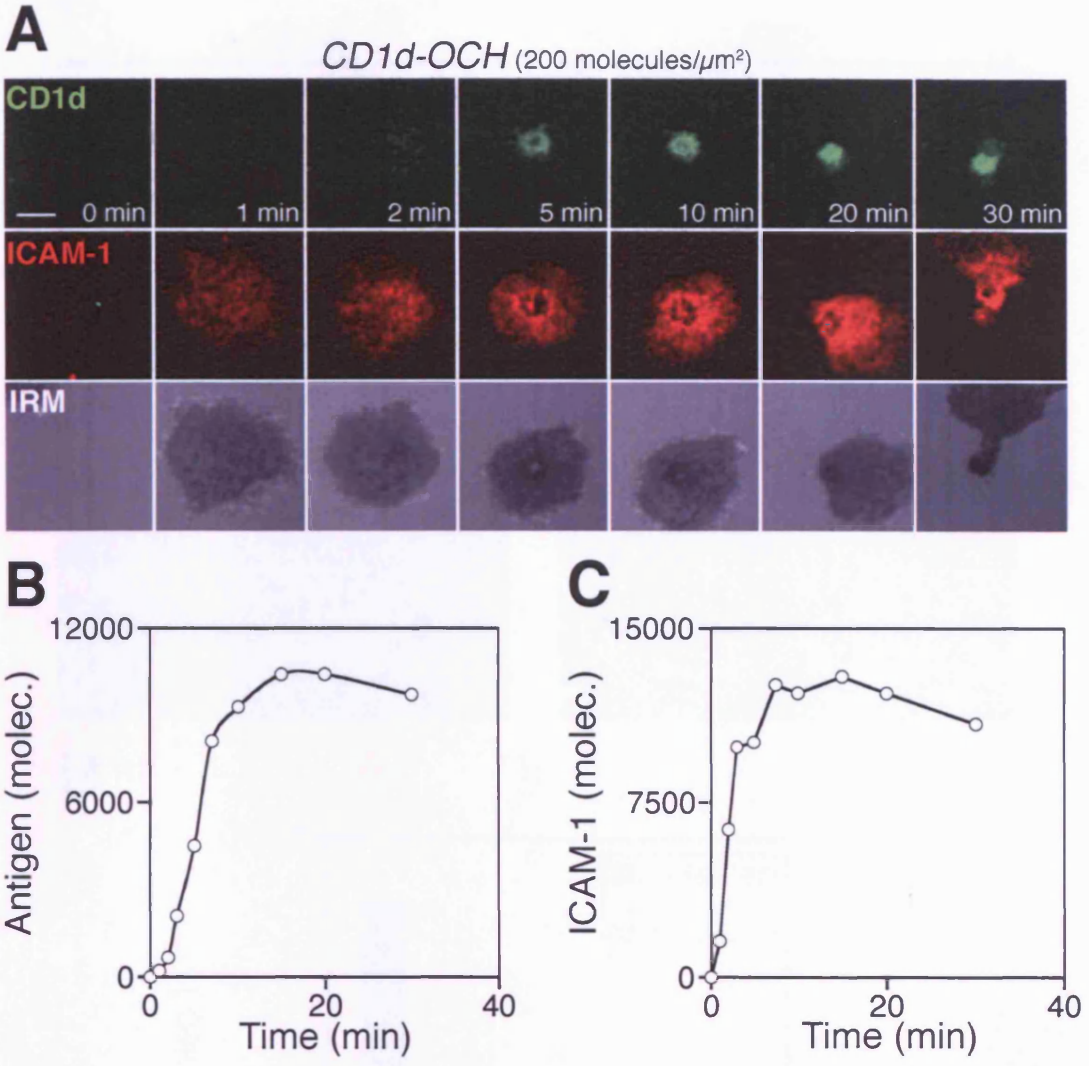


**Figure 6.4. Dependence of the antigen recognition on the affinity of the TCR/CD1d-ligand interaction.**

**(A)** Time lapse of the interaction of an NK T cell with an artificial lipid bilayer loaded with the CD1d-OCH antigen (green) at a density of 200 molecules/μm² and ICAM-1 (red) at a density of 80 molecules/μm² as visualised by confocal microscopy. Contacts of the NK T cell with the bilayer were visualised by IRM (grayscale, lower panels). The amount of **(B)** CD1d-ligand and **(C)** ICAM-1 aggregated were quantified as a function of time. Note that after 20-30 minutes of interaction the synapse is disrupted as the cell starts to migrate. Scale bars: 5 μm.

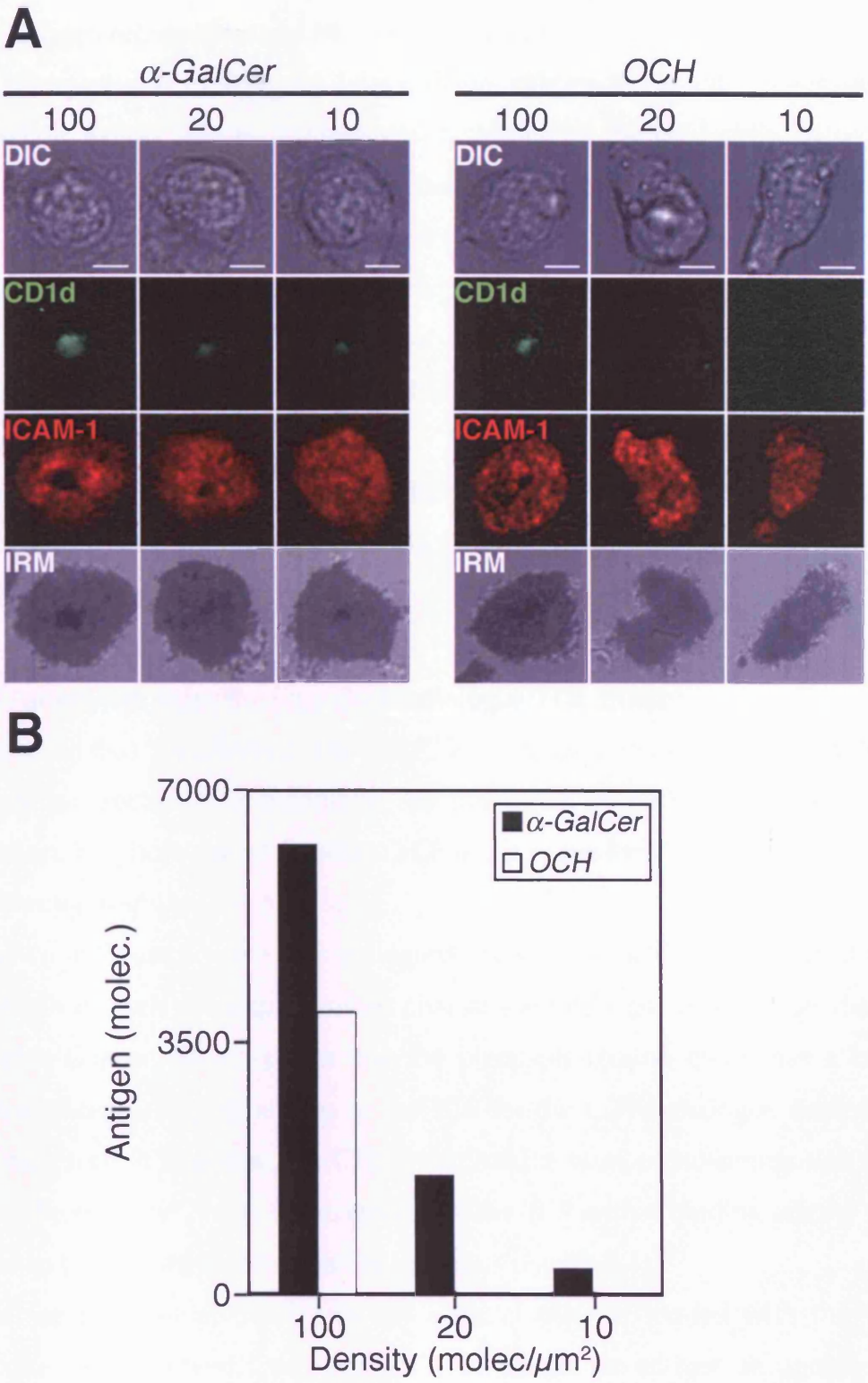


**Figure 6.5. Thresholds of immunological synapse formation for different ligands.** **(A)** Synapse formation for the indicated ligands (α-GalCer and OCH) displayed at varying densities (top number in molecules/$\mu m^2$) in the presence of ICAM-1 (density=80 molecules/$\mu m^2$) as visualised by confocal microscopy. A representative single cell after 15 minutes of interaction with the bilayer is shown in each column. **(B)** Shows the amount of antigen accumulated for the different ligands and densities after the formation of the mature immunological synapse (10-15 minutes). ICAM-1 accumulation levels are equivalent in all the cases (data not shown). Scale bars: 5 μm.

### 6.2.3 Antigen recognition and NKT cell activation

Next, we wanted to understand if the different efficiencies in antigen engagement and accumulation lead to a differential activation of the NKT cells. In order to study this, we labelled NKT cells with the Fluo4-FF calcium sensitive probe, and then settled them on artificial bilayers loaded with the CD1d-α-GalCer and CD1d-OCH, and followed the kinetics of calcium signalling by confocal microscopy. As shown in Figure 6.6, the levels of intracellular calcium is proportional to the amount of antigen that the NKT cells accumulate at the end of the process.

These experiments indicate that activation of NKT cells is dependent as shown for B cells and T cells, on the density of the CD1d-analogue on the target membrane and on the affinity of the CD1d-analogue/TCR interaction.

### 6.2.4 Parameters that affect the CD1d-analogue/TCR affinity

We showed that the affinity of the TCR/CD1d-analogue interaction and its density are key parameters that determine the thresholds of NKT cell triggering and activation. But, how can an invariant TCR and a single MHC molecule give rise to a differential response to antigens?

As shown in Figure 6.1, the two analogues analysed, α-GalCer and OCH, differ in the length of their phytosphingosine chains: the OCH chain is shorter than the one of α-GalCer. This suggests that the phytosphingosine chain has a critical effect in determining the affinity of the TCR for the CD1d-analogue complex. In this line a second analogue, the C20:0, that has the same phytosphingosine chain, but a different alkyl chain, is recognised by the TCR with a binding affinity that is similar to the affinity of the α-GalCer analogue (Figure 6.1).

When we then settled NKT cells on artificial bilayers loaded with the C20:0 analogue, we observed that the density threshold for antigen recognition and synapse formation is comparable to the density threshold observed for α-GalCer (Figure 6.7).

These results show that the CD1d presentation system takes advantage of different structural features of the antigens to extend the range of affinities at which the NKT cells are responsive.

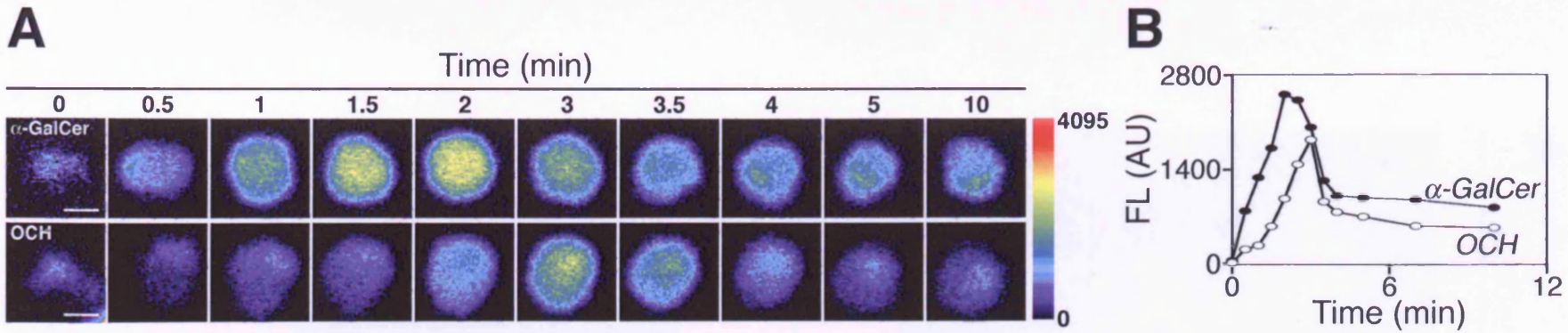


**Figure 6.6. Calcium influx for the CD1d-ligands.**
**(A)** Kinetics of calcium influx of NK T cells in contact with bilayers loaded with CD1d-α-GalCer (top panels) or CD1d-OCH (bottom panels) at a density of 200 molecules/μm² in the presence of ICAM-1 (density=80 molecules/μm²) as visualised by confocal microscopy. Fluorescence is shown in a pseudocolor scale. **(B)** The level of the intracellular calcium influx in fluorescence units (AU) for α-GalCer (closed circles) and OCH (open circles) were quantified over a period of 10 minutes. Scale bars: 5 μm.

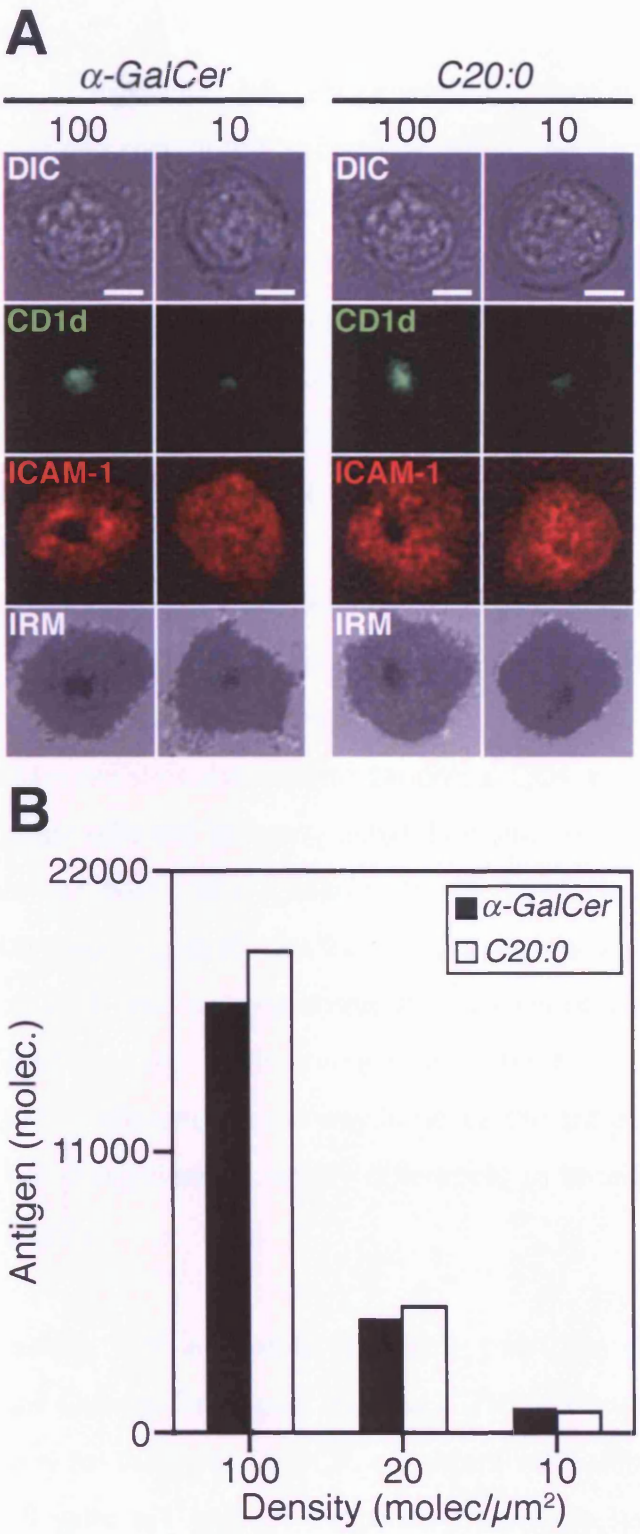


**Figure 6.7. Structural parameters of the analogue affecting the affinity of interaction.**

**(A)** Synapse formation for the indicated ligands (α-GalCer and C20:0) displayed at varying densities (top number in molecules/μm²) in the presence of ICAM-1 (density=80 molecules/μm²) as visualised by confocal microscopy. A representative single cell after 30 minutes of interaction with the bilayer is shown in each column. **(B)** Shows the amount of antigen accumulated for the different ligands and densities after the formation of the mature immunological synapse (10-15 minutes). Scale bars: 5 μm.

## 6.3 Discussion

Taking advantage of artificial bilayers containing biotinylated lipids we characterised the antigen recognition process of human NKT cells (Dr Vincenzo Cerundolo, unpublished results). The early stages of this event are characterised by a spreading and contraction response that leads to the formation of a classical mature immunological synapse (Grakoui et al., 1999; Monks et al., 1998).

By using a set of CD1d-analogue complexes, we determined that the affinity of the TCR/CD1d-analogue interaction and the density at which the antigen is displayed on the target membrane are key parameters that determine the efficiency of antigen recognition.

Furthermore, we established that the efficiency of antigen accumulation leads to a differential activation of the NKT cells, as shown by the measurement of calcium signals, and by the production of cytokines.

While these are characteristics shared with canonical CD4 and CD8 T cells, the density thresholds for efficient antigen recognition and synapse formation are surprisingly higher for NKT cells (Grakoui et al., 1999; Irvine et al., 2002; Purbhoo et al., 2004; Wulfing et al., 2002a). In fact, reports from different groups have shown that CD4 T cells are responsive to densities of antigen as low as 1 molecule/$\mu m^2$ (Grakoui et al., 1999; Irvine et al., 2002). This could reflect as previously discussed, a difference in the way in which the antigen densities on the artificial bilayers are determined or simply differences in sensitivity between the different types of T cells.

How can an invariant TCR and MHC molecule pair give rise to differential antigen recognition? Our results suggest that the CD1d molecule/lipid interaction determines its affinity for the invariant TCR, consistent with affinity measurements obtained by SPR (Figure 6.1 and Dr Vincenzo Cerundolo, unpublished data). Surprisingly, both the polar head and the phytosphingosine chain seem to be responsible of this effect, even though only the polar head is exposed to the interface in contact with the TCR. However, this correlates with the recently solved crystallographic structure of the CD1d molecule with and without α-GalCer (Koch et al., 2005). In this reports, the authors showed that there are conformational differences between lipid bound and non-lipid bound CD1d

molecules (Koch et al., 2005). Our results suggest the involvement of the phytosphingosine chain in fine-tuning the affinity of the CD1d-lipid/TCR interaction.

In this line, the expression of an invariant αβ T cell receptor (TCR) and the recognition of antigens in the context of CD1d molecules could suggest that NKT cells may function as cells of the innate immune system. Therefore, NKT cells could have evolved to recognize a particular set of antigenic lipids, and the sophisticated mechanisms proposed for the affinity discrimination of antigenic peptides would result redundant in this case.

# Chapter 7: Molecular events during B cell activation

## 7.1 Introduction

Recognition of membrane antigens by B cells leads to the formation of an immunological synapse (see Chapter 5). In this process, antigen and BCR aggregate in the centre forming the cSMAC and a ring of ICAM-1/LFA-1 surround the central cluster forming the pSMAC (see Figure 1.7). Concomitantly, other co-receptors on the B cell surface are differentially segregated (Batista et al., 2001). Several of these co-receptors take part in triggering the signalling cascade downstream of the BCR (Niiro and Clark, 2002). Thus, we wanted to study the kinetics of distribution of co-receptors during membrane antigen recognition by using several microscopy techniques.

## 7.2 B cell activation and co-receptors

The signalling events taking place downstream of the BCR are very complex and not fully understood (Niiro and Clark, 2002). The available information is based on biochemical data that only helps to unveil general mechanisms of action of receptors and co-receptors. However, their localisation and kinetics are not known. Moreover, research on BCR signalling process has only been performed with soluble antigens, therefore nothing is known of this during the process of membrane antigen recognition.

Understanding the spatiotemporal segregation of molecules involved in BCR signalling is a key issue to understand how membrane antigen recognition leads to B cell activation and to unveil the mechanism that regulates this process.

In order to address this, we prepared fluorescently labelled Fab fragments of monoclonal antibodies that recognise some key receptors, including CD45 and CD19. We then labelled MD4 B cells with these antibodies and followed the kinetics of interaction with artificial lipid bilayers loaded with the HEL antigen by confocal microscopy.

## 7.3 Reorganisation of CD45

To study the kinetics of distribution of CD45, we labelled MD4 transgenic B cells with Alexa Fluor 543-conjugated Fab fragments of the 14.8 antibody (anti B220) and settled them on artificial lipid bilayers loaded with the $HEL^{WT}$ antigen. We observed that CD45 is initially aggregated in the contact area and then is rapidly excluded from the centre (Figure 7.1 A). At the end of the antigen accumulation process, a small proportion of CD45 seemed to be maintained in the central cluster of antigen (Figure 7.1 A).

The fast exclusion of CD45 from the central cluster of antigen takes place during the spreading phase, and therefore during this phase CD45 co-localises in the periphery with the newly engaged antigen molecules where we have previously shown that phosphotyrosine is detected (see Figure 5.11).

## 7.4 Reorganisation of CD19

Next, we looked at the distribution of the BCR co-receptor CD19. To this end, we labelled the MD4 B cells with fluorescently labelled Fab fragments of the 1D3 antibody and settled them on artificial lipid bilayers loaded with the $HEL^{WT}$ antigen. We observed that CD19 is co-localising throughout the antigen recognition process with the accumulated antigen clusters (Figure 7.1 B). At the end of the aggregation process CD19 seemed to disappear form the contact area (Figure 7.1 B).

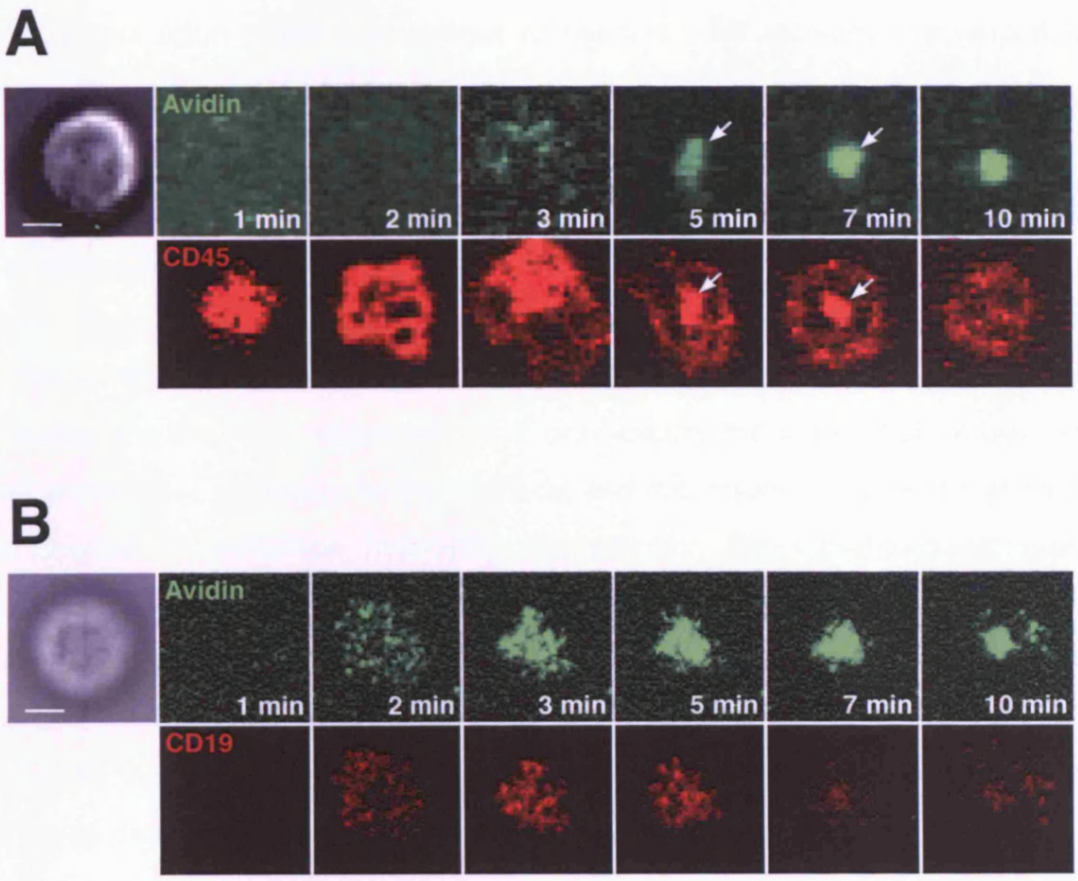


**Figure 7.1. Kinetics of reorganisation of co-receptors.**
MD4 B cells were labelled with fluorescent Fab fragments of monoclonal antibodies directed against **(A)** CD45 or **(B)** CD19, and the kinetics followed by confocal microscopy. The white arrows indicate the clusters of CD45 molecules that co-localises with the antigen cluster. Scale bars: 2 μm.

## 7.5 TIRF (total internal reflection fluorescence) microscopy

Although, confocal microscopy analysis allowed us to follow the reorganisation of co-receptors upon membrane antigen recognition, this technique is limited in time and spatial resolution.

Total internal reflection fluorescence microscopy (TIRFM) is a microscopy technology that allows the visualisation of single molecules in real time (Douglass and Vale, 2005).

This technology takes advantage of the reflection of an incident collimated beam at the interface of two mediums of different refraction indexes to generate an evanescent wave. The evanescent wave only excites the fluorophore molecules that are in close proximity to the interface, and this results in the elimination of background fluorescence improving dramatically the signal-to-noise ratio. Furthermore, acquisition of images with a sensitive CCD camera allows a very fast recording of events. As a consequence of this, the spatiotemporal resolution is increased to the molecular level.

Thus, the visualisation of artificial lipid bilayers by TIRF microscopy is an ideal set-up to dissect at the molecular level the interaction of B cells with membrane antigens. Although, the initial reports using these two technologies date from the early '80s, only in the past year they have been merged successfully (Varma et al., 2006; Watts et al., 1986; Yokosuka et al., 2005).

In order to dissect at the molecular level the reorganisation of co-receptors that take place upon membrane-antigen recognition by B cells, we followed the process by TIRF microscopy.

## 7.6 Setting-up the TIRF microscopy technique with lipid bilayers

We wanted to set-up a system with enough sensitivity and speed of acquisition to visualise single molecules or small clusters of molecules in real time. The first step involved adjusting the different technical specifications to fit the microscope to our experiments. After that, we prepared artificial lipid bilayers containing the Alexa Fluor 488-conjugated GPI-linked Fab fragments and set-up the conditions to visualise single molecules.

As shown in Figure 7.2 A, the bilayers appeared as surface scattered with small bright dots of heterogeneous fluorescence intensity.

A fast time-lapse movie showed that consistent with our previous FRAP experiments on bilayers, most of the small dots on the bilayers (≈ 90%) can freely diffuse and the diffusion is characterised by a Brownian motion as expected for freely diffusing molecules (Figure 7.2 A).

We interpreted that these dots represented single molecules or small clusters of few molecules. However, the real nature of the spots remains open, as we did not set-up a technique to prove this yet.

We obtained similar results when we visualised artificial lipid bilayers containing biotin lipids loaded with Alexa Fluor 488-avidin. However, in this case the percentage of freely diffusing molecules was lower (≈ 70%).

## 7.7 Antigen recognition process

To get more insight on antigen recognition by B cells, we monitored the early events by TIRFM. To this end we prepared artificial bilayers loaded with $HEL^{WT}$. Interestingly, we observed that the spreading response of B cells is characterised by the formation of small clusters that are later accumulated during the contraction phase (Figure 7.2 B).

The spatiotemporal resolution appears to be higher than for confocal microscopy, as the small clusters of molecules could be distinguished clearly from the background fluorescence and tracked in time, contrary to the fuzzy images acquired with a confocal microscope (Figure 7.2 B and compare with Figure 3.6).

Taken together, these results validate the TIRF microscope as an adequate tool to follow the rearrangement of receptors on the membrane of B cells in detail.

## 7.8 Kinetics of receptors reorganisation

We next investigated the kinetics of reorganisation of co-receptors on the cell membrane of B cells during the recognition of membrane antigens by TIRF microscopy.

In order to analyse in greater detail what we observed by confocal microscopy, we selected CD45 and CD19 as the co-receptors to study. When we investigated the kinetics of distribution, we observed similar results as those obtained by confocal microscopy, with similar kinetics of reorganisation (Figure 7.3 A and B).

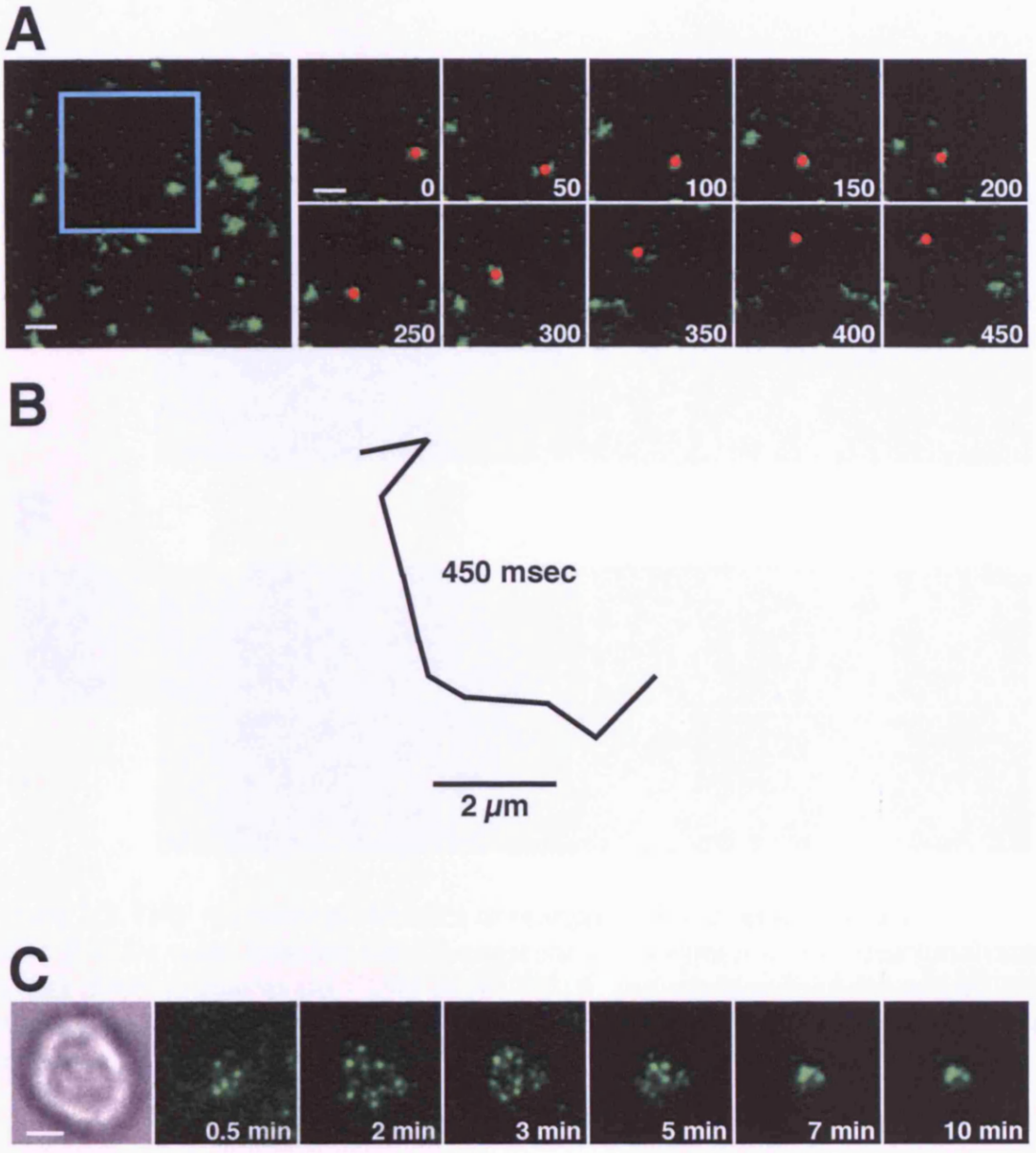


**Figure 7.2. Single molecule tracking on lipid bilayers by TIRF microscopy.**
**(A)** Bilayers visualised under the TIRF microsocope show bright spots of varying intensities scattered throughout the surface. Fast time lapse imaging allows to track freely diffusing molecules; one such example is marked with a red dot. **(B)** Shows the trajectory of the marked molecule tracked for 450 msec. **(C)** Shows a time lapse of the antigen recognition process as visualised by TIRF microscopy. Note the small antigen cluster that can be tracked during the entire process. Scale: 2 μm.

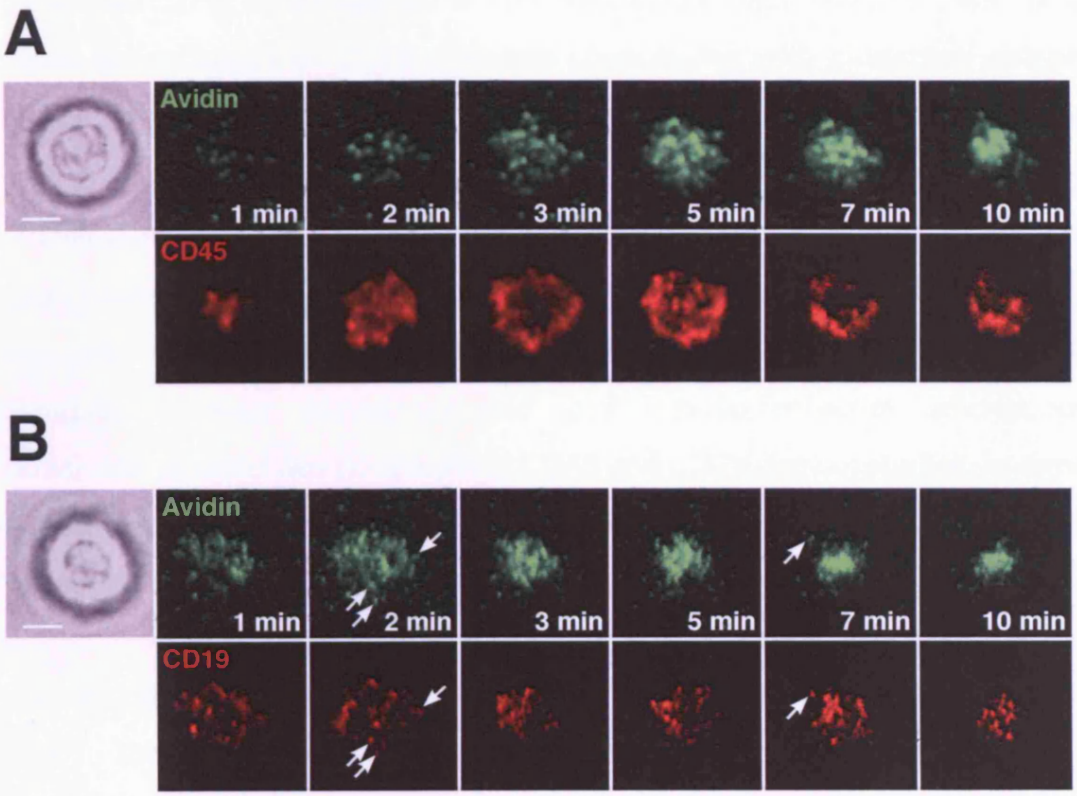


**Figure 7.3. TIRF microscopy: kinetics of reorganisation of co-receptors.**
MD4 B cells were labelled with fluorescent Fab fragments of monoclonal antibodies directed against **(A)** CD45 or **(B)** CD19, and the kinetics followed by TIRF microscopy. White arrows indicate clusters where CD19 and antigen co-localise. Scale bars: 2 μm.

However, we did not observe any accumulation of CD45 by TIRF, contrary to what we observed by confocal microscopy (Figure 7.3 A).

While images of co-receptors appear homogeneous under the confocal microscope, taking advantage of the TIRF microscope high resolution, we could observe some clusters of CD19 molecule co-localising with clusters of antigen molecules (Figure 7.3 B).

## 7.9 Discussion

In this chapter we analysed the kinetics of reorganisation of co-receptors that take place upon membrane antigen recognition by B cells by two different microscopy techniques, confocal microscopy and total internal reflection microscopy (TIRFM). We selected two co-receptors, CD45 and CD19, for our studies, as these are involved in the early signalling events that take place upon antigen engagement through the BCR (Niiro and Clark, 2002).

Our results obtained by both microscopy techniques are consistent with previous reports on the kinetics of distribution of CD45 (Johnson et al., 2000; Varma et al., 2006). In the case of CD19, the information on its signalling properties is vast; however, nothing is known on its kinetics of distribution (Carter and Fearon, 1992; Fearon and Carroll, 2000).

Though, both microscopy techniques gave overall similar results, the TIRF microscope clearly increases the spatiotemporal resolution. In this line, recently different groups have analysed the interaction of T cells with antigens displayed either on bilayers or immobilised on plastic plates by TIRF microscopy (Douglass and Vale, 2005; Varma et al., 2006; Yokosuka et al., 2005). These reports have stressed the importance of resolving the kinetics of distribution of receptors in an effort to unveil the molecular events that lead to T cell activation.

Clearly, our results are preliminary; however, we strongly believe that TIRF microscopy together with artificial membrane technology will become the technique of choice to study the interaction of lymphocytes with antigen, and their subsequent activation process. Our idea is to study in detail this process in B cells.

# Chapter 8: Discussion

The recognition of membrane antigens by lymphocytes is a key event in the initiation of the adaptive immune response. In this Thesis, we have quantitatively characterised in detail the process of membrane ligand recognition by lymphocytes, focusing mainly on B cells and NKT cells. In this final Chapter, we will summarise our main findings and discuss the major issues raised by this Thesis and suggest directions for future research.

## 8.1 Glass supported artificial lipid bilayers are a simple and powerful system to mimic cell-to-cell interactions

Although artificial membranes have been previously used to analyse the interaction of T cells with membrane ligands, we extended this method to dissect quantitatively the interaction of B cells with membrane antigens (Brian and McConnell, 1984; Bromley et al., 2001; Grakoui et al., 1999). We have described two systems that allowed us to dissect the interaction of B cells with membrane antigens. One based on cell-to-cell interactions and the second one based on artificial lipid bilayers to mimic a cell membrane.

To this end we have first developed a new and simple way of tethering antigens on bilayers using biotinylated lipids. This proved to be a simple and reliable method that could be applied to study other ligand/receptor interactions.

The work presented in this Thesis shows that artificial lipid bilayers are an extremely powerful tool to study quantitatively the interaction of lymphocytes with membrane antigens by combining a variety of microscopy techniques including confocal microscopy (CM), scanning electron microscopy (SEM), and more recently total internal reflection microscopy (TIRFM).

The use of artificial membranes is a very versatile technique as we were able to extend the system to analyse the interaction of different antigen-specific lymphocytes with their respective antigens. This shows that this system could be easily employed to analyse other cell-to-cell interactions, this is, the interaction of any pair of membrane-bound ligands and receptors, and even follow the dynamics of this interaction at the molecular level.

## 8.2 B cell spreading: a cellular response that regulates the recognition of membrane antigens

Our results described a novel dynamic cellular response in which B cells spread and contract when they encounter membrane antigens. This is a key process as it may equip B cells with an enhanced capacity to discriminate the affinities of membrane antigen ligands that they encounter displayed on a membrane, determining an efficient accumulation of antigen.

The experiments that we presented in Chapter 5 show that the degree of spreading is determined by two factors: the amount of antigen that the B cells encounters and the affinity of the BCR for the antigen.

It has been shown that T cells show a similar spreading response, however the biological significance of this process in defining the fate of T cells has not been unveiled yet (Bunnell et al., 2001; Negulescu et al., 1996). It will be interesting in the future to test if the spreading mechanism described for B cells is a general mechanism for other lymphocyte interactions.

## 8.3 Parameters that determine membrane ligand/receptor interactions: a look into the future

It will be important to elucidate the mechanism of spreading and contraction and to get further insights on its influence on B cell activation. In order to understand these processes we will have to focus on the parameters that we will discuss in this section.

As we previously discussed in Chapter 1, interactions of membrane ligands and receptors are better described by the density of ligand on the target membrane and the two dimensional affinity (2D $K_d$). Moreover, membrane ligand/receptor interactions on a cell-to-cell contact are influenced by different parameters, such as diffusion rates of molecules on the membranes, the presence of other molecules than the receptor and mechanical properties of the membranes.

Biological membranes display a complex structure that affects the mobility of proteins included in them by different mechanisms (Kusumi et al., 2005). In this line, Choquet and Triller recently proposed a role for receptor diffusion in the organisation of the postsynaptic membrane in neurons (Choquet and Triller, 2003). Clustering of receptors due to a limited mobility or through interaction

with the cytoskeleton increase their avidity for the ligand, as observed for adhesion molecules like integrins (Hughes and Pfaff, 1998). It would be very interesting if this mechanism in neurons applies to lymphocytes, in particular to B cells.

On the other hand, the available knowledge on the diffusion rates of receptors on lymphocytes is very limited; therefore, exploring this will be of great importance to address the impact of this parameter in the interaction with membrane antigens (Axelrod et al., 1976; Dragsten et al., 1979; Londo et al., 1986). In particular, the use of the fluorescence microscopy techniques Fluorescence Resonance Energy Transfer (FRET) and Fluorescence Recovery After Photobleaching (FRAP) will prove extremely useful to this end.

A second parameter to take into account is the presence of other molecules that can interfere with the interaction process. Models of formation of the immunological synapse in T cells have explained the differential segregation of ligand/receptor pairs based on the equilibrium thermodynamics of relevant physicochemical parameters, including bond lengths between molecule pairs (Burroughs and Wulfing, 2002; Lee et al., 2002a; Lee et al., 2002b; Qi et al., 2001). Moreover, the dimension of the TCR relative to other abundant cell membrane molecules such as CD43 and CD45 is relatively small, and therefore it would not be accessible to the MHC-peptide (Shaw and Dustin, 1997). In this line, van der Merwe and colleagues have shown that triggering through the T cell receptor is critically dependent on the length of the MHC-peptide complex (Choudhuri et al., 2005; Wild et al., 1999).

Although a similar phenomenon has been described for natural killer cells (NK cells), nothing is known yet in the case of B cells (McCann et al., 2003).

A third parameter to consider is the mechanical properties of the cell membrane. In this line, Delon and colleagues pointed out the importance of membrane relaxation in promoting the formation of conjugates between T cells and APCs (Faure et al., 2004). Clearly, cell spreading and contraction will be included in this third group, since this response implies morphological changes of the cell body.

Understanding the cytoskeletal modifications that take place in B cells upon antigen engagement will be very important to unveil the mechanisms of antigen recognition and lymphocyte activation. The family of ERM proteins are likely to play an important role, since recent evidence suggest that they are involved in cell membrane modifications during antigen recognition in B cells (Gupta et al., 2006).

## 8.4 A step forward for understanding membrane antigen recognition and lymphocyte activation

Quantitative analysis revealed that the density thresholds of antigen recognition are higher for B cells than for T cells; this is, higher densities of antigen are necessary for effective recognition in B cells compared to T cells (Carrasco et al., 2004; Grakoui et al., 1999). Dustin and colleagues reported that CD4 T cells efficiently recognise agonist MHC-peptides displayed at densities lower than 1 molecule/$\mu m^2$ (Grakoui et al., 1999). In the same line, Davis and colleagues suggested that CD4 T cells are sensitive to a single MHC-agonist peptide expressed on an APC (Irvine et al., 2002). These results are surprising considering that B cells are responsive to a much wider range of affinities than T cells.

What is the mechanism that makes T cells more sensitive to lower doses of antigen than B cells? The most likely explanation is that this difference relies on downstream signalling of the antigen receptors (the TCR for T cells and the BCR for B cells).

For instance, T cells have CD4 and CD8 as co-receptors, enhancing the signals delivered through the TCR. Chakraborty and colleagues suggested that this synergy is mediated by the recruitment of Lck to the synapse by the CD4 molecule (Li et al., 2004). Furthermore, different groups have suggested that also MHC-endogenous peptides may enhance the sensitivity of T cells (Krogsgaard et al., 2005; Stefanova et al., 2002; Yachi et al., 2005).

In the case of B cells, they are able to recognise antigens in the absence of any co-receptor. Even though co-receptors such as CD19 have been recently described as amplifiers of BCR signalling and has been shown to associate with the BCR, its function relies in the recognition of antigens along with proteins of

the complement system (Carter and Fearon, 1992; Fearon and Carroll, 2000). These results point out also at the importance of the context in which membrane-tethered ligands are recognised, and therefore, co-receptors can exquisitely regulate BCR signalling depending on this context (Carrasco and Batista, 2006a). These studies taken together show that although B cells and T cells share many biological mechanisms, it is important to remember the differences.

Future research will be focused in trying to understand the spatial reorganisation of co-receptors and how this regulates intracellular signalling cascade in B cells. To this end, total internal reflection fluorescence microscopy together with artificial lipid bilayers will be an invaluable tool, as shown by our preliminary results.

## 8.5 Mathematical models in the immune system

Mathematical models have become a very useful tool in helping to understand complex biological systems (Chakraborty et al., 2003; Goldstein et al., 2004). Indeed, just by looking at the array of co-receptors present in the structure of the IS, one can say that the study of membrane ligand recognition is indeed a complex problem.

In recent years, the effort was focused in understanding the basic features of TCR signalling to explain concepts such as sensitivity and specificity (Altan-Bonnet and Germain, 2005). However, at the time when this Thesis was started no models were available for the membrane antigen recognition process of B cells.

### 8.5.1 Mathematical simulation of B cell antigen recognition

In this line, we decided to model our results and use them to generate a computer simulation. Our collaborators, Dr Jacki Goldman and Dr Dennis Bray (Cambridge University, UK) generated the model. This stochastic mathematical model implemented the method of Brownian dynamics to simulate the spreading and contraction response of B cells when they encounter a membrane antigen.

The spreading phase is simulated as described in Figure 5.15, as a series of lamellipodia extensions on the antigen loaded bilayer. In these conditions, the

BCR sequentially probes the density and the affinity of the antigen to sustain or to abort accordingly the spreading phase.

This 'kinetic model' for membrane antigen recognition by B cells leads us to make specific predictions on the behavior of B cells upon certain situations. From these predictions, we designed the experiments shown in Figure 5.10.

The implementation of this model gives an insight on the mechanism of the spreading phase; however, further research will be needed in order to address the molecular details.

A complete different approach was implemented in the case of the contraction phase: our experiments did not provide any information on its molecular mechanism. Therefore, this phase was empirically implemented according to the time scale determined by our experiments.

## 8.6 Concluding remarks

It is clear that membrane antigens play a critical role in B cell activation and development. We believe that the *in vitro* system of lipid bilayers described in this Thesis, in particular exploiting the TIRFM technology will shed light into the steps that lead to B cell IS formation and activation.

Until recently, most studies in lymphocyte biology had addressed the early events of membrane antigen recognition by B cells. This Thesis describes a novel response of spreading and contraction that allows B cells to discriminate antigens with different affinities. It will be important to elucidate its mechanism.

Finally, combining this *in vitro* method with *in vivo* studies will be an important step. Two-photon technology has allowed to follow how B cells interact with membrane bound antigen on dendritic cells in the lymph nodes (Qi et al., 2006). In the future, we will have to test how parameters elucidated from combining *in vitro* and *in silico* studies translate in vivo to understand how B cell fate is determined by its affinity for antigen and the context in which B cells encounter antigens.

Finally, the range of affinities of antigens that B cells recognise comprises all the possible affinities of interaction between ligand and receptors, therefore, we hope that our studies will help not only in the understanding of antigen recognition by lymphocytes, but also to understand other membrane ligand/receptor interactions.

## Publications

The work presented in this Thesis has contributed to the following publications:

McCarthy, C., Shepherd, D., **Fleire, S.J.**, Stronge, V., Koch, M., Illarionov, P.A., Bossi, G., Salio, M., Denkberg, G., Mathew, B., Schmidt, R.R., Reiter, Y., Griffiths, G., van der Merwe, A., Besra, G.S., Jones, Y.E., Batista, F.D., Cerundolo, V. "The length of lipids bound to human CD1d molecules modulates the affinity of the NKT Cell Receptor and NKT cell activation". Journal of Experimental Medicine. In press.

**Fleire, S.J.** and Batista, F.D. "Studying cell-to-cell interactions: an easy method of tethering ligands on artificial membranes". Methods in Molecular Biology book series, Humana Press. In press.

**Fleire, S.J.**, Goldman, J.P., Carrasco, Y.R., Weber, M., Bray, D., Batista, F.D. (2006). "B cell ligand discrimination through a spreading and contraction response". Science 312 (5774): 738-741.

Carrasco, Y.R., **Fleire, S.J.**, Cameron, T., Dustin, M.L., Batista, F.D. (2004). "LFA-1/ICAM-1 interaction lowers the threshold of B cell activation by facilitating B cell adhesion and synapse formation". Immunity 20(5): 589-599.

## References


Allen, D., Simon, T., Sablitzky, F., Rajewsky, K., and Cumano, A. (1988). Antibody engineering for the analysis of affinity maturation of an anti-hapten response. Embo J *7*, 1995-2001.

Altan-Bonnet, G., and Germain, R. N. (2005). Modeling T cell antigen discrimination based on feedback control of digital ERK responses. PLoS Biol *3*, e356.

Axelrod, D., Koppel, D. E., Schlessinger, J., Elson, E., and Webb, W. W. (1976). Mobility measurement by analysis of fluorescence photobleaching recovery kinetics. Biophys J *16*, 1055-1069.

Balazs, M., Martin, F., Zhou, T., and Kearney, J. (2002). Blood dendritic cells interact with splenic marginal zone B cells to initiate T-independent immune responses. Immunity *17*, 341-352.

Bassing, C. H., Swat, W., and Alt, F. W. (2002). The mechanism and regulation of chromosomal V(D)J recombination. Cell *109 Suppl*, S45-55.

Batista, F. D., Iber, D., and Neuberger, M. S. (2001). B cells acquire antigen from target cells after synapse formation. Nature *411*, 489-494.

Batista, F. D., and Neuberger, M. S. (1998). Affinity dependence of the B cell response to antigen: a threshold, a ceiling, and the importance of off-rate. Immunity *8*, 751-759.

Batista, F. D., and Neuberger, M. S. (2000). B cells extract and present immobilized antigen: implications for affinity discrimination. Embo J *19*, 513-520.

Bell, G. I. (1978). Models for the specific adhesion of cells to cells. Science *200*, 618-627.

Bergtold, A., Desai, D. D., Gavhane, A., and Clynes, R. (2005). Cell surface recycling of internalized antigen permits dendritic cell priming of B cells. Immunity *23*, 503-514.

Berney, C., Herren, S., Power, C. A., Gordon, S., Martinez-Pomares, L., and Kosco-Vilbois, M. H. (1999). A member of the dendritic cell family that enters B cell follicles and stimulates primary antibody responses identified by a mannose receptor fusion protein. J Exp Med *190*, 851-860.

Braun, J., Hochman, P. S., and Unanue, E. R. (1982). Ligand-induced association of surface immunoglobulin with the detergent-insoluble cytoskeletal matrix of the B lymphocyte. J Immunol *128*, 1198-1204.

Brian, A. A., and McConnell, H. M. (1984). Allogeneic stimulation of cytotoxic T cells by supported planar membranes. Proc Natl Acad Sci U S A *81*, 6159-6163.

Bromley, S. K., Iaboni, A., Davis, S. J., Whitty, A., Green, J. M., Shaw, A. S., Weiss, A., and Dustin, M. L. (2001). The immunological synapse and CD28-CD80 interactions. Nat Immunol *2*, 1159-1166.

Bunnell, S. C., Kapoor, V., Trible, R. P., Zhang, W., and Samelson, L. E. (2001). Dynamic actin polymerization drives T cell receptor-induced spreading: a role for the signal transduction adaptor LAT. Immunity *14*, 315-329.

Burroughs, N. J., and Wulfing, C. (2002). Differential segregation in a cell-cell contact interface: the dynamics of the immunological synapse. Biophys J *83*, 1784-1796.

Carrasco, Y. R., and Batista, F. D. (2006a). B cell recognition of membrane-bound antigen: an exquisite way of sensing ligands. Curr Opin Immunol *18*, 286-291.

Carrasco, Y. R., and Batista, F. D. (2006b). B-cell activation by membrane-bound antigens is facilitated by the interaction of VLA-4 with VCAM-1. Embo J *25*, 889-899.

Carrasco, Y. R., Fleire, S. J., Cameron, T., Dustin, M. L., and Batista, F. D. (2004). LFA-1/ICAM-1 interaction lowers the threshold of B cell activation by facilitating B cell adhesion and synapse formation. Immunity *20*, 589-599.

Carter, R. H., and Fearon, D. T. (1992). CD19: lowering the threshold for antigen receptor stimulation of B lymphocytes. Science *256*, 105-107.

Cerundolo, V. (2000). Use of major histocompatibility complex class I tetramers to monitor tumor-specific cytotoxic T lymphocyte response in melanoma patients. Cancer Chemother Pharmacol *46 Suppl*, S83-85.

Chakraborty, A. K., Dustin, M. L., and Shaw, A. S. (2003). In silico models for cellular and molecular immunology: successes, promises and challenges. Nat Immunol *4*, 933-936.

Chan, P. Y., Lawrence, M. B., Dustin, M. L., Ferguson, L. M., Golan, D. E., and Springer, T. A. (1991). Influence of receptor lateral mobility on adhesion strengthening between membranes containing LFA-3 and CD2. J Cell Biol *115*, 245-255.

Cheng, P. C., Brown, B. K., Song, W., and Pierce, S. K. (2001). Translocation of the B cell antigen receptor into lipid rafts reveals a novel step in signaling. J Immunol *166*, 3693-3701.

Choquet, D., and Triller, A. (2003). The role of receptor diffusion in the organization of the postsynaptic membrane. Nat Rev Neurosci *4*, 251-265.

Choudhuri, K., Wiseman, D., Brown, M. H., Gould, K., and van der Merwe, P. A. (2005). T-cell receptor triggering is critically dependent on the dimensions of its peptide-MHC ligand. Nature *436*, 578-582.

Colino, J., Shen, Y., and Snapper, C. M. (2002). Dendritic cells pulsed with intact Streptococcus pneumoniae elicit both protein- and polysaccharide-specific immunoglobulin isotype responses in vivo through distinct mechanisms. J Exp Med *195*, 1-13.

Darst, S. A., Ahlers, M., Meller, P. H., Kubalek, E. W., Blankenburg, R., Ribi, H. O., Ringsdorf, H., and Kornberg, R. D. (1991). Two-dimensional crystals of streptavidin on biotinylated lipid layers and their interactions with biotinylated macromolecules. Biophys J *59*, 387-396.

Davis, S. J., Ikemizu, S., Evans, E. J., Fugger, L., Bakker, T. R., and van der Merwe, P. A. (2003). The nature of molecular recognition by T cells. Nat Immunol *4*, 217-224.

Dempsey, P. W., Allison, M. E., Akkaraju, S., Goodnow, C. C., and Fearon, D. T. (1996). C3d of complement as a molecular adjuvant: bridging innate and acquired immunity. Science *271*, 348-350.

Douglass, A. D., and Vale, R. D. (2005). Single-molecule microscopy reveals plasma membrane microdomains created by protein-protein networks that exclude or trap signaling molecules in T cells. Cell *121*, 937-950.

Dragsten, P., Henkart, P., Blumenthal, R., Weinstein, J., and Schlessinger, J. (1979). Lateral diffusion of surface immunoglobulin, Thy-1 antigen, and a lipid probe in lymphocyte plasma membranes. Proc Natl Acad Sci U S A *76*, 5163-5167.

Dustin, M. L. (1997). Adhesive bond dynamics in contacts between T lymphocytes and glass-supported planar bilayers reconstituted with the immunoglobulin-related adhesion molecule CD58. J Biol Chem *272*, 15782-15788.

Dustin, M. L., Ferguson, L. M., Chan, P. Y., Springer, T. A., and Golan, D. E. (1996). Visualization of CD2 interaction with LFA-3 and determination of the two-dimensional dissociation constant for adhesion receptors in a contact area. J Cell Biol *132*, 465-474.

Dustin, M. L., Golan, D. E., Zhu, D. M., Miller, J. M., Meier, W., Davies, E. A., and van der Merwe, P. A. (1997). Low affinity interaction of human or rat T cell adhesion molecule CD2 with its ligand aligns adhering membranes to achieve high physiological affinity. J Biol Chem *272*, 30889-30898.

Eisen, H. N., and Siskind, G. W. (1964). Variations in Affinities of Antibodies During the Immune Response. Biochemistry *3*, 996-1008.

Faure, S., Salazar-Fontana, L. I., Semichon, M., Tybulewicz, V. L., Bismuth, G., Trautmann, A., Germain, R. N., and Delon, J. (2004). ERM proteins regulate cytoskeleton relaxation promoting T cell-APC conjugation. Nat Immunol *5*, 272-279.

Fearon, D. T., and Carroll, M. C. (2000). Regulation of B lymphocyte responses to foreign and self-antigens by the CD19/CD21 complex. Annu Rev Immunol *18*, 393-422.

Fischer, K., Scotet, E., Niemeyer, M., Koebernick, H., Zerrahn, J., Maillet, S., Hurwitz, R., Kursar, M., Bonneville, M., Kaufmann, S. H., and Schaible, U. E. (2004). Mycobacterial phosphatidylinositol mannoside is a natural antigen for CD1d-restricted T cells. Proc Natl Acad Sci U S A *101*, 10685-10690.

Fischer, K. D., Kong, Y. Y., Nishina, H., Tedford, K., Marengere, L. E., Kozieradzki, I., Sasaki, T., Starr, M., Chan, G., Gardener, S., *et al.* (1998a). Vav is a regulator of cytoskeletal reorganization mediated by the T-cell receptor. Curr Biol *8*, 554-562.

Fischer, K. D., Tedford, K., and Penninger, J. M. (1998b). Vav links antigen-receptor signaling to the actin cytoskeleton. Semin Immunol *10*, 317-327.

Foote, J., and Eisen, H. N. (1995). Kinetic and affinity limits on antibodies produced during immune responses. Proc Natl Acad Sci U S A *92*, 1254-1256.

Foote, J., and Milstein, C. (1991). Kinetic maturation of an immune response. Nature *352*, 530-532.

Gluzman, Y. (1981). SV40-transformed simian cells support the replication of early SV40 mutants. Cell *23*, 175-182.

Godfrey, D. I., MacDonald, H. R., Kronenberg, M., Smyth, M. J., and Van Kaer, L. (2004). NKT cells: what's in a name? Nat Rev Immunol *4*, 231-237.

Goldbaum, F. A., Cauerhff, A., Velikovsky, C. A., Llera, A. S., Riottot, M. M., and Poljak, R. J. (1999). Lack of significant differences in association rates and affinities of antibodies from short-term and long-term responses to hen egg lysozyme. J Immunol *162*, 6040-6045.

Goldstein, B., Faeder, J. R., and Hlavacek, W. S. (2004). Mathematical and computational models of immune-receptor signalling. Nat Rev Immunol *4*, 445-456.

Goodnow, C. C., Crosbie, J., Adelstein, S., Lavoie, T. B., Smith-Gill, S. J., Brink, R. A., Pritchard-Briscoe, H., Wotherspoon, J. S., Loblay, R. H., Raphael, K., and et al. (1988). Altered immunoglobulin expression and functional silencing of self-reactive B lymphocytes in transgenic mice. Nature *334*, 676-682.

Grakoui, A., Bromley, S. K., Sumen, C., Davis, M. M., Shaw, A. S., Allen, P. M., and Dustin, M. L. (1999). The immunological synapse: a molecular machine controlling T cell activation. Science *285*, 221-227.

Groves, J. T., and Dustin, M. L. (2003). Supported planar bilayers in studies on immune cell adhesion and communication. J Immunol Methods *278*, 19-32.

Guermonprez, P., England, P., Bedouelle, H., and Leclerc, C. (1998). The rate of dissociation between antibody and antigen determines the efficiency of antibody-mediated antigen presentation to T cells. J Immunol *161*, 4542-4548.

Gumperz, J. E. (2006). The ins and outs of CD1 molecules: bringing lipids under immunological surveillance. Traffic *7*, 2-13.

Gupta, N., Wollscheid, B., Watts, J. D., Scheer, B., Aebersold, R., and DeFranco, A. L. (2006). Quantitative proteomic analysis of B cell lipid rafts reveals that ezrin regulates antigen receptor-mediated lipid raft dynamics. Nat Immunol *7*, 625-633.

Haberman, A. M., and Shlomchik, M. J. (2003). Reassessing the function of immune-complex retention by follicular dendritic cells. Nat Rev Immunol *3*, 757-764.

Hafeman, D. G., von Tscharner, V., and McConnell, H. M. (1981). Specific antibody-dependent interactions between macrophages and lipid haptens in planar lipid monolayers. Proc Natl Acad Sci U S A *78*, 4552-4556.

Hao, S., and August, A. (2005). Actin depolymerization transduces the strength of B-cell receptor stimulation. Mol Biol Cell *16*, 2275-2284.

Hartley, S. B., Crosbie, J., Brink, R., Kantor, A. B., Basten, A., and Goodnow, C. C. (1991). Elimination from peripheral lymphoid tissues of self-reactive B lymphocytes recognizing membrane-bound antigens. Nature *353*, 765-769.

Hartwig, J. H., Jugloff, L. S., De Groot, N. J., Grupp, S. A., and Jongstra-Bilen, J. (1995). The ligand-induced membrane IgM association with the cytoskeletal matrix of B cells is not mediated through the Ig alpha beta heterodimer. J Immunol *155*, 3769-3779.

Henkart, P., and Blumenthal, R. (1975). Interaction of lymphocytes with lipid bilayer membranes: a model for lymphocyte-mediated lysis of target cells. Proc Natl Acad Sci U S A *72*, 2789-2793.

Hladky, S. B., and Haydon, D. A. (1970). Discreteness of conductance change in bimolecular lipid membranes in the presence of certain antibiotics. Nature *225*, 451-453.

Hombach, J., Tsubata, T., Leclercq, L., Stappert, H., and Reth, M. (1990). Molecular components of the B-cell antigen receptor complex of the IgM class. Nature *343*, 760-762.

Hornstein, I., Alcover, A., and Katzav, S. (2004). Vav proteins, masters of the world of cytoskeleton organization. Cell Signal *16*, 1-11.

Hughes, P. E., and Pfaff, M. (1998). Integrin affinity modulation. Trends Cell Biol *8*, 359-364.
Irvine, D. J., Purbhoo, M. A., Krogsgaard, M., and Davis, M. M. (2002). Direct observation of ligand recognition by T cells. Nature *419*, 845-849.

Itano, A. A., and Jenkins, M. K. (2003). Antigen presentation to naive CD4 T cells in the lymph node. Nat Immunol *4*, 733-739.

Jacobelli, J., Chmura, S. A., Buxton, D. B., Davis, M. M., and Krummel, M. F. (2004). A single class II myosin modulates T cell motility and stopping, but not synapse formation. Nat Immunol *5*, 531-538.

Jaffe, A. B., and Hall, A. (2005). Rho GTPases: biochemistry and biology. Annu Rev Cell Dev Biol *21*, 247-269.

Janeway, C. A. T., P.; Walport, M.; Shlomchik, M.J. (2005). Immunobiology: Garland Science).

Johnson, K. G., Bromley, S. K., Dustin, M. L., and Thomas, M. L. (2000). A supramolecular basis for CD45 tyrosine phosphatase regulation in sustained T cell activation. Proc Natl Acad Sci U S A *97*, 10138-10143.

Jugloff, L. S., and Jongstra-Bilen, J. (1997). Cross-linking of the IgM receptor induces rapid translocation of IgM-associated Ig alpha, Lyn, and Syk tyrosine kinases to the membrane skeleton. J Immunol *159*, 1096-1106.

Kim, K. J., Kanellopoulos-Langevin, C., Merwin, R. M., Sachs, D. H., and Asofsky, R. (1979). Establishment and characterization of BALB/c lymphoma lines with B cell properties. J Immunol *122*, 549-554.

Klenerman, P., Cerundolo, V., and Dunbar, P. R. (2002). Tracking T cells with tetramers: new tales from new tools. Nat Rev Immunol *2*, 263-272.

Koch, M., Stronge, V. S., Shepherd, D., Gadola, S. D., Mathew, B., Ritter, G., Fersht, A. R., Besra, G. S., Schmidt, R. R., Jones, E. Y., and Cerundolo, V. (2005). The crystal structure of human CD1d with and without alpha-galactosylceramide. Nat Immunol *6*, 819-826.

Kosco-Vilbois, M. H. (2003). Are follicular dendritic cells really good for nothing? Nat Rev Immunol *3*, 764-769.

Kouskoff, V., Famiglietti, S., Lacaud, G., Lang, P., Rider, J. E., Kay, B. K., Cambier, J. C., and Nemazee, D. (1998). Antigens varying in affinity for the B cell receptor induce differential B lymphocyte responses. J Exp Med *188*, 1453-1464.

Krogsgaard, M., Huppa, J. B., Purbhoo, M. A., and Davis, M. M. (2003). Linking molecular and cellular events in T-cell activation and synapse formation. Semin Immunol *15*, 307-315.

Krogsgaard, M., Li, Q. J., Sumen, C., Huppa, J. B., Huse, M., and Davis, M. M. (2005). Agonist/endogenous peptide-MHC heterodimers drive T cell activation and sensitivity. Nature *434*, 238-243.

Kusumi, A., Nakada, C., Ritchie, K., Murase, K., Suzuki, K., Murakoshi, H., Kasai, R. S., Kondo, J., and Fujiwara, T. (2005). Paradigm shift of the plasma membrane concept from the two-dimensional continuum fluid to the partitioned fluid: high-speed single-molecule tracking of membrane molecules. Annu Rev Biophys Biomol Struct *34*, 351-378.

Lang, J., Jackson, M., Teyton, L., Brunmark, A., Kane, K., and Nemazee, D. (1996). B cells are exquisitely sensitive to central tolerance and receptor editing induced by ultralow affinity, membrane-bound antigen. J Exp Med *184*, 1685-1697.

Lanzavecchia, A. (1985). Antigen-specific interaction between T and B cells. Nature *314*, 537-539.

Lauer, S., Goldstein, B., Nolan, R. L., and Nolan, J. P. (2002). Analysis of cholera toxin-ganglioside interactions by flow cytometry. Biochemistry *41*, 1742-1751.

Lee, S. J., Hori, Y., Groves, J. T., Dustin, M. L., and Chakraborty, A. K. (2002a). Correlation of a dynamic model for immunological synapse formation with effector functions: two pathways to synapse formation. Trends Immunol *23*, 492-499.

Lee, S. J., Hori, Y., Groves, J. T., Dustin, M. L., and Chakraborty, A. K. (2002b). The synapse assembly model. Trends Immunol *23*, 500-502.

Li, Q. J., Dinner, A. R., Qi, S., Irvine, D. J., Huppa, J. B., Davis, M. M., and Chakraborty, A. K. (2004). CD4 enhances T cell sensitivity to antigen by coordinating Lck accumulation at the immunological synapse. Nat Immunol *5*, 791-799.

Londo, T. R., Peacock, J. S., Roess, D. A., and Barisas, B. G. (1986). Lateral diffusion of antigen receptors artificially incorporated onto B lymphocytes. J Immunol *137*, 1924-1931.

McCann, F. E., Vanherberghen, B., Eleme, K., Carlin, L. M., Newsam, R. J., Goulding, D., and Davis, D. M. (2003). The size of the synaptic cleft and distinct distributions of filamentous actin, ezrin, CD43, and CD45 at activating and inhibitory human NK cell immune synapses. J Immunol *170*, 2862-2870.

Miller, M. J., Safrina, O., Parker, I., and Cahalan, M. D. (2004). Imaging the single cell dynamics of CD4+ T cell activation by dendritic cells in lymph nodes. J Exp Med *200*, 847-856.

Mimms, L. T., Zampighi, G., Nozaki, Y., Tanford, C., and Reynolds, J. A. (1981). Phospholipid vesicle formation and transmembrane protein incorporation using octyl glucoside. Biochemistry *20*, 833-840.

Monks, C. R., Freiberg, B. A., Kupfer, H., Sciaky, N., and Kupfer, A. (1998). Three-dimensional segregation of supramolecular activation clusters in T cells. Nature *395*, 82-86.

Mueller, P., Rudin, D. O., Tien, H. T., and Wescott, W. C. (1962). Reconstitution of cell membrane structure in vitro and its transformation into an excitable system. Nature *194*, 979-980.

Muller, W., Ringsdorf, H., Rump, E., Wildburg, G., Zhang, X., Angermaier, L., Knoll, W., Liley, M., and Spinke, J. (1993). Attempts to mimic docking processes of the immune system: recognition-induced formation of protein multilayers. Science *262*, 1706-1708.

Negulescu, P. A., Krasieva, T. B., Khan, A., Kerschbaum, H. H., and Cahalan, M. D. (1996). Polarity of T cell shape, motility, and sensitivity to antigen. Immunity *4*, 421-430.

Nemazee, D. A., and Burki, K. (1989). Clonal deletion of B lymphocytes in a transgenic mouse bearing anti-MHC class I antibody genes. Nature *337*, 562-566.

Niiro, H., and Clark, E. A. (2002). Regulation of B-cell fate by antigen-receptor signals. Nat Rev Immunol *2*, 945-956.

Nolz, J. C., Gomez, T. S., Zhu, P., Li, S., Medeiros, R. B., Shimizu, Y., Burkhardt, J. K., Freedman, B. D., and Billadeau, D. D. (2006). The WAVE2 complex regulates actin cytoskeletal reorganization and CRAC-mediated calcium entry during T cell activation. Curr Biol *16*, 24-34.

O'Callaghan C, A., Byford, M. F., Wyer, J. R., Willcox, B. E., Jakobsen, B. K., McMichael, A. J., and Bell, J. I. (1999). BirA enzyme: production and application in the study of membrane receptor-ligand interactions by site-specific biotinylation. Anal Biochem *266*, 9-15.

Odegard, V. H., and Schatz, D. G. (2006). Targeting of somatic hypermutation. Nat Rev Immunol *6*, 573-583.

Park, J. Y., and Jongstra-Bilen, J. (1997). Interactions between membrane IgM and the cytoskeleton involve the cytoplasmic domain of the immunoglobulin receptor. Eur J Immunol *27*, 3001-3009.

Parsey, M. V., and Lewis, G. K. (1993). Actin polymerization and pseudopod reorganization accompany anti-CD3-induced growth arrest in Jurkat T cells. J Immunol *151*, 1881-1893.

Purbhoo, M. A., Irvine, D. J., Huppa, J. B., and Davis, M. M. (2004). T cell killing does not require the formation of a stable mature immunological synapse. Nat Immunol *5*, 524-530.

Qi, H., Egen, J. G., Huang, A. Y., and Germain, R. N. (2006). Extrafollicular activation of lymph node B cells by antigen-bearing dendritic cells. Science *312*, 1672-1676.

Qi, S. Y., Groves, J. T., and Chakraborty, A. K. (2001). Synaptic pattern formation during cellular recognition. Proc Natl Acad Sci U S A *98*, 6548-6553.

Qin, H., Liu, Z., and Sui, S. F. (1995). Two-dimensional crystallization of avidin on biotinylated lipid monolayers. Biophys J *68*, 2493-2496.

Rauch, J., Gumperz, J., Robinson, C., Skold, M., Roy, C., Young, D. C., Lafleur, M., Moody, D. B., Brenner, M. B., Costello, C. E., and Behar, S. M. (2003). Structural features of the acyl chain determine self-phospholipid antigen recognition by a CD1d-restricted invariant NKT (iNKT) cell. J Biol Chem *278*, 47508-47515.

Reth, M. (1989). Antigen receptor tail clue. Nature *338*, 383-384.

Rock, K. L., Benacerraf, B., and Abbas, A. K. (1984). Antigen presentation by hapten-specific B lymphocytes. I. Role of surface immunoglobulin receptors. J Exp Med *160*, 1102-1113.

Rousseaux, J., Rousseaux-Prevost, R., and Bazin, H. (1986). Optimal conditions for the preparation of proteolytic fragments from monoclonal IgG of different rat IgG subclasses. Methods Enzymol *121*, 663-669.

Sagawa, T., Oda, M., Ishimura, M., Furukawa, K., and Azuma, T. (2003). Thermodynamic and kinetic aspects of antibody evolution during the immune response to hapten. Mol Immunol *39*, 801-808.

Sakihama, T., Smolyar, A., and Reinherz, E. L. (1995). Oligomerization of CD4 is required for stable binding to class II major histocompatibility complex proteins but not for interaction with human immunodeficiency virus gp120. Proc Natl Acad Sci U S A *92*, 6444-6448.

Salafsky, J., Groves, J. T., and Boxer, S. G. (1996). Architecture and function of membrane proteins in planar supported bilayers: a study with photosynthetic reaction centers. Biochemistry *35*, 14773-14781.

Santos-Argumedo, L., Kincade, P. W., Partida-Sanchez, S., and Parkhouse, R. M. (1997). CD44-stimulated dendrite formation ('spreading') in activated B cells. Immunology *90*, 147-153.

Schamel, W. W., and Reth, M. (2000). Monomeric and oligomeric complexes of the B cell antigen receptor. Immunity *13*, 5-14.

Shaw, A. S., and Dustin, M. L. (1997). Making the T cell receptor go the distance: a topological view of T cell activation. Immunity *6*, 361-369.

Shih, T. A., Meffre, E., Roederer, M., and Nussenzweig, M. C. (2002). Role of BCR affinity in T cell dependent antibody responses in vivo. Nat Immunol *3*, 570-575.

Shulman, M., Wilde, C. D., and Kohler, G. (1978). A better cell line for making hybridomas secreting specific antibodies. Nature *276*, 269-270.

Small, J. V., and Resch, G. P. (2005). The comings and goings of actin: coupling protrusion and retraction in cell motility. Curr Opin Cell Biol *17*, 517-523.

Stefanova, I., Dorfman, J. R., and Germain, R. N. (2002). Self-recognition promotes the foreign antigen sensitivity of naive T lymphocytes. Nature *420*, 429-434.

Stoll, S., Delon, J., Brotz, T. M., and Germain, R. N. (2002). Dynamic imaging of T cell-dendritic cell interactions in lymph nodes. Science *296*, 1873-1876.

Sumoza-Toledo, A., and Santos-Argumedo, L. (2004). The spreading of B lymphocytes induced by CD44 cross-linking requires actin, tubulin, and vimentin rearrangements. J Leukoc Biol *75*, 233-239.

Sykulev, Y., Brunmark, A., Jackson, M., Cohen, R. J., Peterson, P. A., and Eisen, H. N. (1994). Kinetics and affinity of reactions between an antigen-specific T cell receptor and peptide-MHC complexes. Immunity *1*, 15-22.

Tarlinton, D. M., and Smith, K. G. (2000). Dissecting affinity maturation: a model explaining selection of antibody-forming cells and memory B cells in the germinal centre. Immunol Today *21*, 436-441.

Teh, Y. M., and Neuberger, M. S. (1997). The immunoglobulin (Ig)alpha and Igbeta cytoplasmic domains are independently sufficient to signal B cell maturation and activation in transgenic mice. J Exp Med *185*, 1753-1758.

Turner, M. (2002a). B-cell development and antigen receptor signalling. Biochem Soc Trans *30*, 812-815.

Turner, M. (2002b). The role of Vav proteins in B cell responses. Adv Exp Med Biol *512*, 29-34.

Uzgiris, E. E., and Kornberg, R. D. (1983). Two-dimensional crystallization technique for imaging macromolecules, with application to antigen--antibody--complement complexes. Nature *301*, 125-129.

Valmori, D., Dutoit, V., Lienard, D., Lejeune, F., Speiser, D., Rimoldi, D., Cerundolo, V., Dietrich, P. Y., Cerottini, J. C., and Romero, P. (2000). Tetramer-guided analysis of TCR beta-chain usage reveals a large repertoire of melan-A-specific CD8+ T cells in melanoma patients. J Immunol *165*, 533-538.

Varma, R., Campi, G., Yokosuka, T., Saito, T., and Dustin, M. L. (2006). T cell receptor-proximal signals are sustained in peripheral microclusters and terminated in the central supramolecular activation cluster. Immunity *25*, 117-127.

Veatch, S. L., and Keller, S. L. (2002). Organization in lipid membranes containing cholesterol. Phys Rev Lett *89*, 268101.

Veatch, S. L., and Keller, S. L. (2003). Separation of liquid phases in giant vesicles of ternary mixtures of phospholipids and cholesterol. Biophys J *85*, 3074-3083.

Walmsley, M. J., Ooi, S. K., Reynolds, L. F., Smith, S. H., Ruf, S., Mathiot, A., Vanes, L., Williams, D. A., Cancro, M. P., and Tybulewicz, V. L. (2003). Critical roles for Rac1 and Rac2 GTPases in B cell development and signaling. Science *302*, 459-462.

Watts, C., and Davidson, H. W. (1988). Endocytosis and recycling of specific antigen by human B cell lines. Embo J *7*, 1937-1945.

Watts, T. H., Gaub, H. E., and McConnell, H. M. (1986). T-cell-mediated association of peptide antigen and major histocompatibility complex protein detected by energy transfer in an evanescent wave-field. Nature *320*, 179-181.

Weigert, M. G., Cesari, I. M., Yonkovich, S. J., and Cohn, M. (1970). Variability in the lambda light chain sequences of mouse antibody. Nature *228*, 1045-1047.

Wild, M. K., Cambiaggi, A., Brown, M. H., Davies, E. A., Ohno, H., Saito, T., and van der Merwe, P. A. (1999). Dependence of T cell antigen recognition on the dimensions of an accessory receptor-ligand complex. J Exp Med *190*, 31-41.

Williams, G. T., Peaker, C. J., Patel, K. J., and Neuberger, M. S. (1994). The alpha/beta sheath and its cytoplasmic tyrosines are required for signaling by the B-cell antigen receptor but not for capping or for serine/threonine-kinase recruitment. Proc Natl Acad Sci U S A *91*, 474-478.

Wu, D., Xing, G. W., Poles, M. A., Horowitz, A., Kinjo, Y., Sullivan, B., Bodmer-Narkevitch, V., Plettenburg, O., Kronenberg, M., Tsuji, M., *et al.* (2005). Bacterial glycolipids and analogs as antigens for CD1d-restricted NKT cells. Proc Natl Acad Sci U S A *102*, 1351-1356.

Wulfing, C., Bauch, A., Crabtree, G. R., and Davis, M. M. (2000). The vav exchange factor is an essential regulator in actin-dependent receptor translocation to the lymphocyte-antigen-presenting cell interface. Proc Natl Acad Sci U S A *97*, 10150-10155.

Wulfing, C., and Davis, M. M. (1998). A receptor/cytoskeletal movement triggered by costimulation during T cell activation. Science *282*, 2266-2269.

Wulfing, C., Sumen, C., Sjaastad, M. D., Wu, L. C., Dustin, M. L., and Davis, M. M. (2002a). Costimulation and endogenous MHC ligands contribute to T cell recognition. Nat Immunol *3*, 42-47.

Wulfing, C., Tskvitaria-Fuller, I., Burroughs, N., Sjaastad, M. D., Klem, J., and Schatzle, J. D. (2002b). Interface accumulation of receptor/ligand couples in lymphocyte activation: methods, mechanisms, and significance. Immunol Rev *189*, 64-83.

Wykes, M., Pombo, A., Jenkins, C., and MacPherson, G. G. (1998). Dendritic cells interact directly with naive B lymphocytes to transfer antigen and initiate class switching in a primary T-dependent response. J Immunol *161*, 1313-1319.

Yachi, P. P., Ampudia, J., Gascoigne, N. R., and Zal, T. (2005). Nonstimulatory peptides contribute to antigen-induced CD8-T cell receptor interaction at the immunological synapse. Nat Immunol *6*, 785-792.

Yokosuka, T., Sakata-Sogawa, K., Kobayashi, W., Hiroshima, M., Hashimoto-Tane, A., Tokunaga, M., Dustin, M. L., and Saito, T. (2005). Newly generated T cell receptor microclusters initiate and sustain T cell activation by recruitment of Zap70 and SLP-76. Nat Immunol *6*, 1253-1262.

Zipfel, P. A., Bunnell, S. C., Witherow, D. S., Gu, J. J., Chislock, E. M., Ring, C., and Pendergast, A. M. (2006). Role for the Abi/wave protein complex in T cell receptor-mediated proliferation and cytoskeletal remodeling. Curr Biol *16*, 35-46.